

Arthritis & Rheumatology

An Official Journal of the American College of Rheumatology
www.arthritisrheum.org and wileyonlinelibrary.com

GENERAL INFORMATION

TO SUBSCRIBE

Institutions and Non-Members

Email: wileyonlinelibrary.com
Phone: (201) 748-6645
Write: Wiley Periodicals LLC
Attn: Journals Admin Dept
UK
111 River Street
Hoboken, NJ 07030

Volumes 74, 2022:
Institutional Print Only:

Institutional Online Only:
Institutional Print and
Online Only:

Arthritis & Rheumatology and Arthritis Care & Research:
\$2,603 in US, Canada, and Mexico
\$2,603 outside North America

\$2,495 in US, Canada, Mexico, and outside North America
\$2,802 in US, Canada, and Mexico; \$2,802 outside
North America

For submission instructions, subscription, and all other information visit: wileyonlinelibrary.com.

Arthritis & Rheumatology accepts articles for Open Access publication. Please visit <https://authorservices.wiley.com/author-resources/Journal-Authors/open-access/hybrid-open-access.html> for further information about OnlineOpen.

Wiley's Corporate Citizenship initiative seeks to address the environmental, social, economic, and ethical challenges faced in our business and which are important to our diverse stakeholder groups. Since launching the initiative, we have focused on sharing our content with those in need, enhancing community philanthropy, reducing our carbon impact, creating global guidelines and best practices for paper use, establishing a vendor code of ethics, and engaging our colleagues and other stakeholders in our efforts.

Follow our progress at www.wiley.com/go/citizenship.

Access to this journal is available free online within institutions in the developing world through the HINARI initiative with the WHO. For information, visit www.healthinternetwork.org.

Disclaimer

The Publisher, the American College of Rheumatology, and Editors cannot be held responsible for errors or any consequences arising from the use of information contained in this journal; the views and opinions expressed do not necessarily reflect those of the Publisher, the American College of Rheumatology and Editors, neither does the publication of advertisements constitute any endorsement by the Publisher, the American College of Rheumatology and Editors of the products advertised.

Members:

American College of Rheumatology/Association of Rheumatology Professionals

For membership rates, journal subscription information, and change of address, please write:

American College of Rheumatology
2200 Lake Boulevard
Atlanta, GA 30319-5312
(404) 633-3777

ADVERTISING SALES AND COMMERCIAL REPRINTS

Sales: Kathleen Malseed, National Account Manager
E-mail: kmalseed@pminy.com
Phone: (215) 852-9824
Pharmaceutical Media, Inc.
30 East 33rd Street, New York, NY 10016

Production: Patti McCormack
E-mail: pmccormack@pminy.com
Phone: (212) 904-0376
Pharmaceutical Media, Inc.
30 East 33rd Street, New York, NY 10016

Publisher: Arthritis & Rheumatology is published by Wiley Periodicals LLC, 101 Station Landing, Suite 300, Medford, MA 02155

Production Editor: Ramona Talantor, artprod@wiley.com

ARTHRITIS & RHEUMATOLOGY (Print ISSN 2326-5191; Online ISSN 2326-5205 at Wiley Online Library, wileyonlinelibrary.com) is published monthly on behalf of the American College of Rheumatology by Wiley Periodicals LLC, a Wiley Company, 111 River Street, Hoboken, NJ 07030-5774. Periodicals postage paid at Hoboken, NJ and additional offices. POSTMASTER: Send all address changes to Arthritis & Rheumatology, Wiley Periodicals LLC, c/o The Sheridan Press, PO Box 465, Hanover, PA 17331. **Send subscription inquiries care of** Wiley Periodicals LLC, Attn: Journals Admin Dept UK, 111 River Street, Hoboken, NJ 07030, (201) 748-6645 (nonmember subscribers only; American College of Rheumatology/Association of Rheumatology Health Professionals members should contact the American College of Rheumatology). **Subscription Price:** (Volumes 74, 2022: Arthritis & Rheumatology and Arthritis Care & Research) Print only: \$2,603.00 in U.S., Canada and Mexico, \$2,603.00 rest of world. For all other prices please consult the journal's website at wileyonlinelibrary.com. All subscriptions containing a print element, shipped outside U.S., will be sent by air. Payment must be made in U.S. dollars drawn on U.S. bank. Prices are exclusive of tax. Asia-Pacific GST, Canadian GST and European VAT will be applied at the appropriate rates. For more information on current tax rates, please go to www.wileyonlinelibrary.com/tax-vat. The price includes online access to the current and all online backfiles to January 1st 2018, where available. For other pricing options including access information and terms and conditions, please visit <https://onlinelibrary.wiley.com/library-info/products/price-lists>. Terms of use can be found here: <https://onlinelibrary.wiley.com/terms-and-conditions>. **Delivery Terms and Legal Title:** Where the subscription price includes print issues and delivery is to the recipient's address, delivery terms are Delivered at Place (DAP); the recipient is responsible for paying any import duty or taxes. Title to all issues transfers Free of Board (FOB) our shipping point, freight prepaid. We will endeavor to fulfill claims for missing or damaged copies within six months of publication, within our reasonable discretion and subject to availability. **Change of Address:** Please forward to the subscriptions address listed above 6 weeks prior to move; enclose present mailing label with change of address. **Claims** for undelivered copies will be accepted only after the following issue has been received. Please enclose a copy of the mailing label or cite your subscriber reference number in order to expedite handling. Missing copies will be supplied when losses have been sustained in transit and where reserve stock permits. Send claims care of Wiley Periodicals LLC, Attn: Journals Admin Dept UK, 111 River Street, Hoboken, NJ 07030. If claims are not resolved satisfactorily, please write to Subscription Distribution c/o Wiley Periodicals LLC, 111 River Street, Hoboken, NJ 07030. **Cancellations:** Subscription cancellations will not be accepted after the first issue has been mailed. **Journal Customer Services:** For ordering information, claims and any enquiry concerning your journal subscription please go to <https://wolsupport.wiley.com/s/contactsupport?tabset-a7d10=2> or contact your nearest office. **Americas:** Email: cs-journals@wiley.com; Tel: +1 877 762 2974. **Europe, Middle East and Africa:** Email: cs-journals@wiley.com; Tel: +44 (0) 1865 778315; 0800 1800 536 (Germany). **Asia Pacific:** Email: cs-journals@wiley.com; Tel: +65 6511 8000. **Japan:** For Japanese speaking support, Email: cs-japan@wiley.com. **Visit our Online Customer Help** at <https://wolsupport.wiley.com/s/contactsupport?tabset-a7d10=2>. **Back Issues:** Single issues from current and prior year volumes are available at the current single issue price from csjournals@wiley.com. Earlier issues may be obtained from Periodicals Service Company, 351 Fairview Avenue-Ste 300, Hudson, NY 12534, USA. Tel: +1 518 822-9300, Fax: +1 518 822-9305, Email: psc@periodicals.com. Printed in the USA by The Sheridan Group.

Arthritis & Rheumatology

An Official Journal of the American College of Rheumatology
www.arthritisrheum.org and wileyonlinelibrary.com

Editor

Daniel H. Solomon, MD, MPH, *Boston*

Deputy Editors

Richard J. Bucala, MD, PhD, *New Haven*

Mariana J. Kaplan, MD, *Bethesda*

Peter A. Nigrovic, MD, *Boston*

Co-Editors

Karen H. Costenbader, MD, MPH, *Boston*

David T. Felson, MD, MPH, *Boston*

Richard F. Loeser Jr., MD, *Chapel Hill*

Social Media Editor

Paul H. Sufka, MD, *St. Paul*

Journal Publications Committee

Amr Sawalha, MD, *Chair, Pittsburgh*

Susan Boackle, MD, *Denver*

Aileen Davis, PhD, *Toronto*

Deborah Feldman, PhD, *Montreal*

Donnamarie Krause, PhD, OTR/L, *Las Vegas*

Wilson Kuswanto, MD, PhD, *Stanford*

Michelle Ormseth, MD, *Nashville*

R. Hal Scofield, MD, *Oklahoma City*

Editorial Staff

Kimberly M. Murphy, *Managing Editor, Atlanta*

Lesley W. Allen, *Assistant Managing Editor, Atlanta*

Ilani S. Lorber, MA, *Assistant Managing Editor, Atlanta*

Rasa G. Hamilton, *Manuscript Editor, Atlanta*

Stefanie L. McKain, *Manuscript Editor, Atlanta*

Sara Omer, *Manuscript Editor, Atlanta*

Christopher Reynolds, MA, *Editorial Coordinator, Atlanta*

Brittany Swett, MPH, *Assistant Editor, Boston*

Associate Editors

Marta Alarcón-Riquelme, MD, PhD, *Granada*

Heather G. Allore, PhD, *New Haven*

Neal Basu, MD, PhD, *Glasgow*

Edward M. Behrens, MD, *Philadelphia*

Bryce Binstadt, MD, PhD, *Minneapolis*

Nunzio Bottini, MD, PhD, *San Diego*

John Carrino, MD, MPH, *New York*

Lisa Christopher-Stine, MD, MPH,
Baltimore

Andrew Cope, MD, PhD, *London*

Adam P. Croft, MBChB, PhD, MRCP,
Birmingham

Nicola Dalbeth, MD, FRACP, *Auckland*

Brian M. Feldman, MD, FRCPC, MSc, *Toronto*

Richard A. Furie, MD, *Great Neck*

J. Michelle Kahlenberg, MD, PhD,
Ann Arbor

Benjamin Leder, MD, *Boston*

Yvonne Lee, MD, MMSc, *Chicago*

Katherine Liao, MD, MPH, *Boston*

Bing Lu, MD, DrPH, *Boston*

Stephen P. Messier, PhD,

Winston-Salem

Rachel E. Miller, PhD, *Chicago*

Janet E. Pope, MD, MPH, *FRCPC,
London, Ontario*

Christopher T. Ritchlin, MD, MPH,
Rochester

William Robinson, MD, PhD, *Stanford*

Carla R. Scanzello, MD, PhD, *Philadelphia*

Georg Schett, MD, *Erlangen*

Sakae Tanaka, MD, PhD, *Tokyo*

Maria Trojanowska, PhD, *Boston*

Betty P. Tsao, PhD, *Charleston*

Fredrick M. Wigley, MD, *Baltimore*

Edith M. Williams, PhD, MS, *Charleston*

Advisory Editors

Ayaz Aghayev, MD, *Boston*

Joshua F. Baker, MD, MSCE,
Philadelphia

Bonnie Bermas, MD, *Dallas*

Jamie Collins, PhD, *Boston*

Kristen Demoruelle, MD, PhD, *Denver*

Christopher Denton, PhD, FRCP, *London*

Anisha Dua, MD, MPH, *Chicago*

John FitzGerald, MD, *Los Angeles*

Lauren Henderson, MD, MMSc, *Boston*

Monique Hinchcliff, MD, MS, *New Haven*

Hui-Chen Hsu, PhD, *Birmingham*

Mohit Kapoor, PhD, *Toronto*

Seouyoung Kim, MD, ScD, MSCE, *Boston*

Vasileios Kyttaris, MD, *Boston*

Carl D. Langefeld, PhD,
Winston-Salem

Dennis McGonagle, FRCPI, PhD, *Leeds*

Julie Paik, MD, MHS, *Baltimore*

Amr Sawalha, MD, *Pittsburgh*

Julie Zikherman, MD, *San Francisco*

AMERICAN COLLEGE OF RHEUMATOLOGY

Kenneth G. Saag, MD, MSc, *Birmingham*, **President**

Douglas White, MD, PhD, *La Crosse*, **President-Elect**

Carol Langford, MD, MHS, *Cleveland*, **Treasurer**

Deborah Desir, MD, *New Haven*, **Secretary**

Steven Echard, IOM, CAE, *Atlanta*, **Executive Vice-President**

© 2022 American College of Rheumatology. All rights reserved. No part of this publication may be reproduced, stored or transmitted in any form or by any means without the prior permission in writing from the copyright holder. Authorization to copy items for internal and personal use is granted by the copyright holder for libraries and other users registered with their local Reproduction Rights Organization (RRO), e.g. Copyright Clearance Center (CCC), 222 Rosewood Drive, Danvers, MA 01923, USA (www.copyright.com), provided the appropriate fee is paid directly to the RRO. This consent does not extend to other kinds of copying such as copying for general distribution, for advertising or promotional purposes, for creating new collective works or for resale. Special requests should be addressed to: permissions@wiley.com.

Access Policy: Subject to restrictions on certain backfiles, access to the online version of this issue is available to all registered Wiley Online Library users 12 months after publication. Subscribers and eligible users at subscribing institutions have immediate access in accordance with the relevant subscription type. Please go to onlinelibrary.wiley.com for details.

The views and recommendations expressed in articles, letters, and other communications published in Arthritis & Rheumatology are those of the authors and do not necessarily reflect the opinions of the editors, publisher, or American College of Rheumatology. The publisher and the American College of Rheumatology do not investigate the information contained in the classified advertisements in this journal and assume no responsibility concerning them. Further, the publisher and the American College of Rheumatology do not guarantee, warrant, or endorse any product or service advertised in this journal.

Cover design: Todd Machen

©This journal is printed on acid-free paper.

Arthritis & Rheumatology

An Official Journal of the American College of Rheumatology
www.arthritisrheum.org and wileyonlinelibrary.com

VOLUME 74 • August 2022 • NO. 8

In This Issue	A11
Journal Club	A12
Clinical Connections	A13
Special Articles	
Expert Perspectives on Clinical Challenges: Expert Perspective: Management of Antineutrophil Cytoplasmic Antibody-Associated Vasculitis <i>Naomi J. Patel and John H. Stone</i>	1305
Editorial: Complement C4, the Major Histocompatibility Complex, and Autoimmunity <i>Timothy J. Vyse and Betty P. Tsao</i>	1318
COVID-19	
Immunogenicity and Safety of Standard and Third-Dose SARS-CoV-2 Vaccination in Patients Receiving Immunosuppressive Therapy <i>Silje W. Syversen, Ingrid Jyssum, Anne T. Tveter, Trung T. Tran, Joseph Sexton, Sella A. Provan, Siri Mjaaland, David J. Warren, Tore K. Kvien, Gunnveig Grødeland, Lise S. H. Nissen-Meyer, Petr Ricanek, Adity Chopra, Ane M. Andersson, Grete B. Kro, Jørgen Jahnsen, Ludvig A. Munthe, Espen A. Haavardsholm, John T. Vaage, Fridtjof Lund-Johansen, Kristin K. Jørgensen, and Guro L. Goll.</i>	1321
Clinical Images	
Clinical Images: Hydroxyurea-Induced Dermatomyositis-Like Rash <i>Sweta Subhadarshani, Susie Min, Kathryn Holloway, and Matthew Steadmon</i>	1332
Osteoarthritis	
Five-Year Structural Changes in the Knee Among Patients With Meniscal Tear and Osteoarthritis: Data From a Randomized Controlled Trial of Arthroscopic Partial Meniscectomy Versus Physical Therapy <i>Jamie E. Collins, Swastina Shrestha, Elena Losina, Robert G. Marx, Ali Guermazi, Mohamed Jarraya, Morgan H. Jones, Bruce A. Levy, Lisa A. Mandl, Emma E. Williams, Rick W. Wright, Kurt P. Spindler, and Jeffrey N. Katz, on behalf of the METEOR Investigator Group</i>	1333
Do Glucocorticoid Injections Increase the Risk of Knee Osteoarthritis Progression Over 5 Years? <i>Augustin Latourte, Anne-Christine Rat, Abdou Omorou, Willy Nguenon-Sime, Florent Eymard, Jérémie Sellam, Christian Roux, Hang-Korng Ea, Martine Cohen-Solal, Thomas Bardin, Johann Beaudreuil, Francis Guillemin, and Pascal Richette</i>	1343
Clinical Images	
Clinical Images: Intraosseous Calcification Migration: Journey to the Center of the Bone <i>Clément Cholet, Justine Mugnier, Anne Miquel, Juliette Petit, Jérémie Sellam, and Lionel Arrivé</i>	1351
Spondyloarthritis	
Vertebral Bone Mineral Density, Vertebral Strength, and Syndesmophyte Growth in Ankylosing Spondylitis: The Importance of Bridging <i>Sovira Tan, Hadi Bagheri, David Lee, Ahmad Shafiei, Tony M. Keaveny, Lawrence Yao, and Michael M. Ward</i>	1352
Erratum	
Addition of Corresponding Author's Email Address to the Letter by Wang et al (Arthritis Rheumatol, June 2022)	1362
Systemic Lupus Erythematosus	
Small Molecule Inhibitors of Nuclear Export and the Amelioration of Lupus by Modulation of Plasma Cell Generation and Survival <i>Javier Rangel-Moreno, Maria de la Luz Garcia-Hernandez, Teresa Owen, Jennifer Barnard, Enrique Becerril-Villanueva, Trinayan Kashyap, Christian Argueta, Armando Gamboa-Dominguez, Sharon Tamir, Yosef Landesman, Bruce I. Goldman, Christopher T. Ritchlin, and Jennifer H. Anolik</i>	1363
Vasculitis	
Global Transcriptomic Profiling Identifies Differential Gene Expression Signatures Between Inflammatory and Noninflammatory Aortic Aneurysms <i>Benjamin Hur, Matthew J. Koster, Jin Sung Jang, Cornelia M. Weyand, Kenneth J. Warrington, and Jaeyun Sung</i>	1376

Systemic Sclerosis

- Driving Role of Interleukin-2–Related Regulatory CD4+ T Cell Deficiency in the Development of Lung Fibrosis and Vascular Remodeling in a Mouse Model of Systemic Sclerosis
Camelia Frantz, Anne Cauvet, Aurélie Durand, Virginie Gonzalez, Rémi Pierre, Marcio Do Cruzeiro, Karine Bailly, Muriel Andrieu, Cindy Orvain, Jérôme Avouac, Mina Ottaviani, Raphaël Thuillet, Ly Tu, Christophe Guignabert, Bruno Lucas, Cédric Auffray, and Yannick Allanore.1387

- Adipose-Derived Regenerative Cell Transplantation for the Treatment of Hand Dysfunction in Systemic Sclerosis: A Randomized Clinical Trial
Dinesh Khanna, Paul Caldron, Richard W. Martin, Suzanne Kafaja, Robert Spiera, Shadi Shahouri, Ankoor Shah, Vivien Hsu, John Ervin, Robert Simms, Robyn T. Domsic, Virginia Steen, Laura K. Hummers, Chris Derk, Maureen Mayes, Soumya Chatterjee, John Varga, Steven Kesten, John K. Fraser, and Daniel E. Furst.1399

Pediatric Rheumatology

- A Comparison of International League of Associations for Rheumatology and Pediatric Rheumatology International Trials Organization Classification Systems for Juvenile Idiopathic Arthritis Among Children in a Canadian Arthritis Cohort
Jennifer J. Y. Lee, Simon W. M. Eng, Jaime Guzman, Ciáran M. Duffy, Lori B. Tucker, Kiem Oen, Rae S. M. Yeung, and Brian M. Feldman, on behalf of the ReACCh-Out Investigators.1409

- Identification of Novel Loci Shared by Juvenile Idiopathic Arthritis Subtypes Through Integrative Genetic Analysis
Jin Li, Yun R. Li, Joseph T. Glessner, Jie Yang, Michael E. March, Charly Kao, Courtney N. Vaccaro, Jonathan P. Bradfield, Junyi Li, Frank D. Mentch, Hui-Qi Qu, Xiaohui Qi, Xiao Chang, Cuiping Hou, Debra J. Abrams, Haijun Qiu, Zhi Wei, John J. Connolly, Fengxiang Wang, James Snyder, Berit Flatø, Susan D. Thompson, Carl D. Langefeld, Benedicte A. Lie, Jane E. Munro, Carol Wise, Patrick M. A. Sleiman, and Hakon Hakonarson.1420

- Racial Disparities in Renal Outcomes Over Time Among Hospitalized Children With Systemic Lupus Erythematosus
Joyce C. Chang, Cora Sears, Veronica Torres, and Mary Beth F. Son.1430

Autoimmune Disease

- Complement C4 Copy Number Variation is Linked to SSA/Ro and SSB/La Autoantibodies in Systemic Inflammatory Autoimmune Diseases
Christian Lundtoft, Pascal Pucholt, Myriam Martin, Matteo Bianchi, Emeli Lundström, Maija-Leena Eloranta, Johanna K. Sandling, Christopher Sjöwall, Andreas Jönsen, Iva Gunnarsson, Solbritt Rantapää-Dahlqvist, Anders A. Bengtsson, Dag Leonard, Eva Baecklund, Roland Jonsson, Daniel Hammenfors, Helena Forsblad-d'Elia, Per Eriksson, Thomas Mandl, Sara Magnusson Bucher, Katrine B. Norheim, Svein Joar Auglænd Johnsen, Roald Omdal, Marika Kvarnström, Marie Wahren-Herlenius, Antonella Notarnicola, Helena Andersson, Øyvind Molberg, Louise Pyndt Diederichsen, Jonas Almlöf, Ann-Christine Syvänen, Sergey V. Kozyrev, Kerstin Lindblad-Toh, the DISSECT Consortium, the ImmunoArray Development Consortium, Bo Nilsson, Anna M. Blom, Ingrid E. Lundberg, Gunnel Nordmark, Lina Marcela Diaz-Gallo, Elisabet Svenungsson, and Lars Rönnblom.1440

Letters

- On the Perils of Peeking Into the Future: Comment on the Article by Rosenthal et al
Melek Yalcin Mutlu and Koray Tascilar.1451

- Reply
Yael Shalev Rosenthal, Naama Schwartz, Iftach Sagy, and Lev Pavlovsky.1451

- No Evidence of Leptin Mediating the Effect of Body Mass Index on Hand Pain and Its Duration in the Chingford 1000 Women Study: Original Research Supplementing the Study by Gløersen et al
Romain S. Perera, Malvika Gulati, Karishma Shah, Deborah J. Hart, Tim D. Spector, Nigel K. Arden, and Maja R. Radojčić.1452

- Reply
Marthe Gløersen, Tuhina Neogi, S. Reza Jafarzadeh, Joe Sexton, and Ida K. Haugen.1454

- Very Limited Data in the Global Burden of Disease Study 2019 to Estimate the Prevalence of Osteoarthritis in 204 Countries Over 30 years: Comment on the Article by Long et al
Qizhe Chen, Christopher G. Maher, and Gustavo C. Machado.1455

- Reply
Huibin Long, Ai Guo, Yuqing Zhang, Qiang Liu, and Jianhao Lin.1456

- Report of the American College of Rheumatology Fellows-in-Training Subcommittee: Experiences of Rheumatology Fellows Early in the COVID-19 Pandemic
ACR Fellows-in-Training Subcommittee, Didem Saygin, Jean Lin, Noelle A. Rolle, and Mary Mamut.1457

Cover image: The figure on the cover (from Rangel-Moreno et al, pages 1363–1375) shows histologic analysis of a section of spleen tissue from a lupus patient stained with antibodies against CD20 (red; surface B cell marker), exportin 1 (green; nuclear location) (target of Selective Inhibitors of Nuclear Export [SINE]), and CD21 (white; stromal cell surface marker). The image illustrates the presence of exportin+ B cells (cells with green nuclei and red surface) in the mantle zone and inside a germinal center with an organized CD21+ follicular dendritic cell network (white stain on stromal cells), supporting the use of SINE to modulate exportin 1–dependent pathologic mechanisms in lupus (such as NF- κ b activation).

In this Issue

Highlights from this issue of *A&R* | By Lara C. Pullen, PhD

Glucocorticoid Injections May Not Increase the Risk of Knee OA Progression

Steroids have a time- and dose-dependent effect on cartilage, and, when injected into joints, glucocorticoids target synovitis, a key driver of pain and subsequent structural

p. 1343 damage in knee osteoarthritis (OA). Rheumatologists thus use intraarticular (IA) glucocorticoid injections as a treatment for pain in patients with knee OA, while acknowledging the potential for adverse events associated with IA glucocorticoid injections. These adverse effects include an increase in blood glucose level in patients with diabetes mellitus as well as the very rare occurrence of local sepsis after injections. Recently, results from several conflicting studies have addressed the potential adverse

effect of IA glucocorticoids on joints in knee OA. Although the results of some studies have suggested that IA glucocorticoid injections in patients with knee OA may be associated with deleterious effects to the joint, findings from other open-label studies and randomized controlled trials have found no impact of long-term IA glucocorticoid injections on joint structure as assessed on radiographs.

In this issue, Latourte et al (p. 1343) report the result of their effort to use real-world data to inform the risks associated with IA glucocorticoid injections as performed in routine care. The investigators used a well-phenotyped cohort of knee and hip OA patients treated in primary care to identify prognostic factors of OA course

as measured by Kellgren/Lawrence (K/L) grade worsening of knee OA progression. They then used marginal structural modeling to investigate the causality between IA glucocorticoid injections and an outcome such as total knee replacement (TKR) as well as radiographic progression.

The researchers found that IA glucocorticoid injections for symptomatic knee OA did not significantly increase the 5-year risk of incident TKR or radiographic worsening. They emphasize in their discussion that their findings should be interpreted with caution and replicated in other cohorts. They also note that treatment rates and use of TKR can vary substantially by region and depend upon local guidelines and the health care system.

Racial Disparities Remain in Hospitalized Children with SLE

In this issue, Chang et al (p. 1430) report that, across all racial and ethnic groups, children with systemic lupus erythematosus (SLE) experienced significant reductions in

p. 1430 end-stage renal disease (ESRD) and dialysis. The US population-based study is the largest to date to describe renal outcomes over time among children with lupus. The researchers' results indicate that, while renal outcomes improved at the population level, the heterogeneous effects were not sufficient to achieve a reduction in relative Black/White disparities over time.

An analysis of health systems data revealed that the overall burden of severe renal outcomes associated with pediatric SLE hospitalizations decreased from 2006 to 2019 by nearly half. During this time, the use of B cell-depleting therapies became increasingly common, such that 25% of lupus

nephritis patients in the Childhood Arthritis and Rheumatology Research Registry's contemporary pediatric lupus cohort had received rituximab. The analysis of the cohort of 20,893 admissions for 7,434 SLE patients revealed that Hispanic ethnicity was not associated with worse outcomes among hospitalized children with SLE. Moreover, while Asian patients had the highest probability of a new dialysis requirement during hospitalization compared to any other racial or ethnic group, they were not at increased risk of ESRD.

The authors conclude that the lack of corresponding reductions in Black/White racial disparities highlights the need for targeted interventions to achieve greater treatment benefit among higher risk groups. They explain that while advances in pediatric lupus care appear to have reached groups that have been historically marginalized, the advances have not resulted in greater benefit

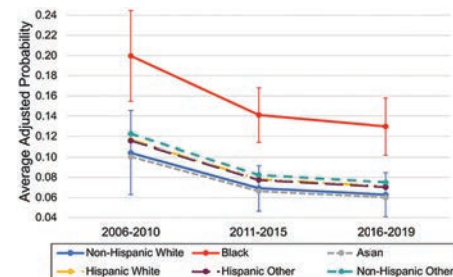


Figure 1. Marginal predictions from a mixed logit model by race, ethnicity, and calendar period, representing the average adjusted probability of the composite adverse renal outcome at any given hospital admission.

for Black children with lupus. The team calls for researchers to provide specific attention to identify the care processes or interventions that can preferentially improve renal outcomes among the highest risk groups.

Complement C4 Copy Number Linked to SLE and SS

Autoantibodies generally appear several years before clinical onset of systemic lupus erythematosus (SLE) and primary Sjögren's syndrome (SS), a finding which suggests a slow progression from asymptomatic autoimmunity to clinical manifestations. Moreover, several studies have suggested that copy number variation of the C4 complement components — C4A and C4B — may play a central role in systemic inflammatory autoimmune diseases.

Lundtoft et al (p. 1440) report that a low C4A copy number is more strongly associated with the autoantibody repertoire than

with the clinically defined disease entities (SLE, primary SS, and myositis). In their study, the investigators analyzed patients with these 3 systemic inflammatory autoimmune diseases and found a strong dose-dependent association between low C4A copy number and the presence of anti-SSA/SSB autoantibodies. This relationship between C4A copy numbers and autoantibody status was similar in SLE, primary SS, and myositis. The researchers' results indicate that a low copy number of C4A is a major risk factor for systemic inflammatory autoimmune disease and that C4B copy number makes only a minor contribution to risk.

The investigators acknowledge that the study was performed using data from a Scandinavian study population and that the relative homogeneity of the population may limit the generalizability of the findings. Nevertheless, they conclude that the presence of anti-SSA/SSB autoantibodies may be largely dependent on genetic predisposition and that rheumatologists may find it useful to consider this subset of autoimmune patients as a specific diagnostic entity. Their findings may have implications for understanding the etiopathogenetic mechanisms of systemic inflammatory autoimmune diseases and for patient stratification that considers genetic profile.

Journal Club

A monthly feature designed to facilitate discussion on research methods in rheumatology.

A Comparison of ILAR and PRINTO Classification Systems for JIA Among Children in a Canadian Arthritis Cohort

Lee et al, *Arthritis Rheumatol* 2022;74:1409-1419

Juvenile idiopathic arthritis (JIA) describes a heterogeneous group of inflammatory conditions characterized by chronic joint inflammation in children. The optimal way to subdivide JIA patients into specific homogeneous groups is debatable and challenging. Lee et al examined the proposed Paediatric Rheumatology International Trials Organization (PRINTO) classification system and compared it to the more universally recognized 2001 International League of Associations for Rheumatology (ILAR) classification system. The primary objective was to examine the agreement of classification groups between the PRINTO and ILAR systems. Second, authors evaluated the agreement of both the PRINTO and ILAR systems with a proposed clinicobiologic classification system and with 4 adult classification systems (rheumatoid arthritis, spondyloarthritis, adult-onset Still's disease, and psoriatic arthritis).

ILAR subtypes and PRINTO disorders were computed for 1,228 JIA patients from a large multicentered inception cohort. Both ILAR and PRINTO classification systems were applied as strictly as possible to generate a fair, data-driven comparison. Several assumptions had to be incorporated for PRINTO classification when dealing with uncaptured data (i.e., anti-cyclic citrullinated peptide or imaging criteria). The proportions of patients in each ILAR and PRINTO subtype/disorder were compared using Pearson's chi-square tests, with relationships visualized using Circos charts. Sensitivity analyses primarily focused on handling missing data, particularly missing antinuclear antibody, rheumatoid

factor, and HLA-B27 serologies. For the proportion of patients with missing serologies, authors simulated how classifications would change according to the percentage of missing data that was considered positive. Similarly, clinicobiologic subtypes were computed for 131 patients, and the adult classification systems were applied to all 1,228 patients. The relationships and associations between ILAR and PRINTO systems and these classification systems were evaluated with Pearson's chi-square tests.

Questions

1. What are the current advantages and disadvantages of the more well-accepted ILAR classification system?
2. How should homogeneous groups be defined within JIA classification systems? How important is it for the JIA classification system to have biologic homogeneity and/or alignment with adult classification systems?
3. How else could relationships between various classification systems be visually represented?
4. A particular limitation that the authors of this study tried to address was the handling of missing data on the classification of JIA patients with the PRINTO system. How else could the authors have attempted to address this concern?
5. Based on the results of the study, what areas of additional refinement do you think are required for the PRINTO classification system, if any?

In this Issue

Highlights from this issue of *A&R* | By Lara C. Pullen, PhD

Glucocorticoid Injections May Not Increase the Risk of Knee OA Progression

Steroids have a time- and dose-dependent effect on cartilage, and, when injected into joints, glucocorticoids target synovitis, a key driver of pain and subsequent structural

p. 1343

damage in knee osteoarthritis (OA). Rheumatologists thus use intraarticular (IA) glucocorticoid injections as a treatment for pain in patients with knee OA, while acknowledging the potential for adverse events associated with IA glucocorticoid injections. These adverse effects include an increase in blood glucose level in patients with diabetes mellitus as well as the very rare occurrence of local sepsis after injections. Recently, results from several conflicting studies have addressed the potential adverse

effect of IA glucocorticoids on joints in knee OA. Although the results of some studies have suggested that IA glucocorticoid injections in patients with knee OA may be associated with deleterious effects to the joint, findings from other open-label studies and randomized controlled trials have found no impact of long-term IA glucocorticoid injections on joint structure as assessed on radiographs.

In this issue, Latourte et al (p. 1343) report the result of their effort to use real-world data to inform the risks associated with IA glucocorticoid injections as performed in routine care. The investigators used a well-phenotyped cohort of knee and hip OA patients treated in primary care to identify prognostic factors of OA course

as measured by Kellgren/Lawrence (K/L) grade worsening of knee OA progression. They then used marginal structural modeling to investigate the causality between IA glucocorticoid injections and an outcome such as total knee replacement (TKR) as well as radiographic progression.

The researchers found that IA glucocorticoid injections for symptomatic knee OA did not significantly increase the 5-year risk of incident TKR or radiographic worsening. They emphasize in their discussion that their findings should be interpreted with caution and replicated in other cohorts. They also note that treatment rates and use of TKR can vary substantially by region and depend upon local guidelines and the health care system.

Racial Disparities Remain in Hospitalized Children with SLE

In this issue, Chang et al (p. 1430) report that, across all racial and ethnic groups, children with systemic lupus erythematosus (SLE) experienced significant reductions in

p. 1430

end-stage renal disease (ESRD) and dialysis. The US population-based study is the largest to date to describe renal outcomes over time among children with lupus. The researchers' results indicate that, while renal outcomes improved at the population level, the heterogeneous effects were not sufficient to achieve a reduction in relative Black/White disparities over time.

An analysis of health systems data revealed that the overall burden of severe renal outcomes associated with pediatric SLE hospitalizations decreased from 2006 to 2019 by nearly half. During this time, the use of B cell-depleting therapies became increasingly common, such that 25% of lupus

nephritis patients in the Childhood Arthritis and Rheumatology Research Registry's contemporary pediatric lupus cohort had received rituximab. The analysis of the cohort of 20,893 admissions for 7,434 SLE patients revealed that Hispanic ethnicity was not associated with worse outcomes among hospitalized children with SLE. Moreover, while Asian patients had the highest probability of a new dialysis requirement during hospitalization compared to any other racial or ethnic group, they were not at increased risk of ESRD.

The authors conclude that the lack of corresponding reductions in Black/White racial disparities highlights the need for targeted interventions to achieve greater treatment benefit among higher risk groups. They explain that while advances in pediatric lupus care appear to have reached groups that have been historically marginalized, the advances have not resulted in greater benefit

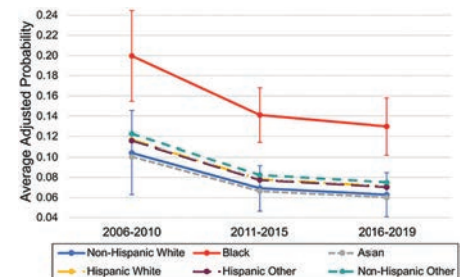


Figure 1. Marginal predictions from a mixed logit model by race, ethnicity, and calendar period, representing the average adjusted probability of the composite adverse renal outcome at any given hospital admission.

for Black children with lupus. The team calls for researchers to provide specific attention to identify the care processes or interventions that can preferentially improve renal outcomes among the highest risk groups.

Complement C4 Copy Number Linked to SLE and SS

Autoantibodies generally appear several years before clinical onset of systemic lupus erythematosus (SLE) and primary Sjögren's syndrome (SS), a finding which suggests a slow progression from asymptomatic autoimmunity to clinical manifestations. Moreover, several studies have suggested that copy number variation of the C4 complement components — C4A and C4B — may play a central role in systemic inflammatory autoimmune diseases.

Lundtoft et al (p. 1440) report that a low C4A copy number is more strongly associated with the autoantibody repertoire than

with the clinically defined disease entities (SLE, primary SS, and myositis). In their study, the investigators analyzed patients with these 3 systemic inflammatory autoimmune diseases and found a strong dose-dependent association between low C4A copy number and the presence of anti-SSA/SSB autoantibodies. This relationship between C4A copy numbers and autoantibody status was similar in SLE, primary SS, and myositis. The researchers' results indicate that a low copy number of C4A is a major risk factor for systemic inflammatory autoimmune disease and that C4B copy number makes only a minor contribution to risk.

The investigators acknowledge that the study was performed using data from a Scandinavian study population and that the relative homogeneity of the population may limit the generalizability of the findings. Nevertheless, they conclude that the presence of anti-SSA/SSB autoantibodies may be largely dependent on genetic predisposition and that rheumatologists may find it useful to consider this subset of autoimmune patients as a specific diagnostic entity. Their findings may have implications for understanding the etiopathogenetic mechanisms of systemic inflammatory autoimmune diseases and for patient stratification that considers genetic profile.

p. 1440

Journal Club

A monthly feature designed to facilitate discussion on research methods in rheumatology.

A Comparison of ILAR and PRINTO Classification Systems for JIA Among Children in a Canadian Arthritis Cohort

Lee et al, *Arthritis Rheumatol* 2022;74:1409-1419

Juvenile idiopathic arthritis (JIA) describes a heterogeneous group of inflammatory conditions characterized by chronic joint inflammation in children. The optimal way to subdivide JIA patients into specific homogeneous groups is debatable and challenging. Lee et al examined the proposed Paediatric Rheumatology International Trials Organization (PRINTO) classification system and compared it to the more universally recognized 2001 International League of Associations for Rheumatology (ILAR) classification system. The primary objective was to examine the agreement of classification groups between the PRINTO and ILAR systems. Second, authors evaluated the agreement of both the PRINTO and ILAR systems with a proposed clinicobiologic classification system and with 4 adult classification systems (rheumatoid arthritis, spondyloarthritis, adult-onset Still's disease, and psoriatic arthritis).

ILAR subtypes and PRINTO disorders were computed for 1,228 JIA patients from a large multicentered inception cohort. Both ILAR and PRINTO classification systems were applied as strictly as possible to generate a fair, data-driven comparison. Several assumptions had to be incorporated for PRINTO classification when dealing with uncaptured data (i.e., anti-cyclic citrullinated peptide or imaging criteria). The proportions of patients in each ILAR and PRINTO subtype/disorder were compared using Pearson's chi-square tests, with relationships visualized using Circos charts. Sensitivity analyses primarily focused on handling missing data, particularly missing antinuclear antibody, rheumatoid

factor, and HLA-B27 serologies. For the proportion of patients with missing serologies, authors simulated how classifications would change according to the percentage of missing data that was considered positive. Similarly, clinicobiologic subtypes were computed for 131 patients, and the adult classification systems were applied to all 1,228 patients. The relationships and associations between ILAR and PRINTO systems and these classification systems were evaluated with Pearson's chi-square tests.

Questions

1. What are the current advantages and disadvantages of the more well-accepted ILAR classification system?
2. How should homogeneous groups be defined within JIA classification systems? How important is it for the JIA classification system to have biologic homogeneity and/or alignment with adult classification systems?
3. How else could relationships between various classification systems be visually represented?
4. A particular limitation that the authors of this study tried to address was the handling of missing data on the classification of JIA patients with the PRINTO system. How else could the authors have attempted to address this concern?
5. Based on the results of the study, what areas of additional refinement do you think are required for the PRINTO classification system, if any?

Clinical Connections

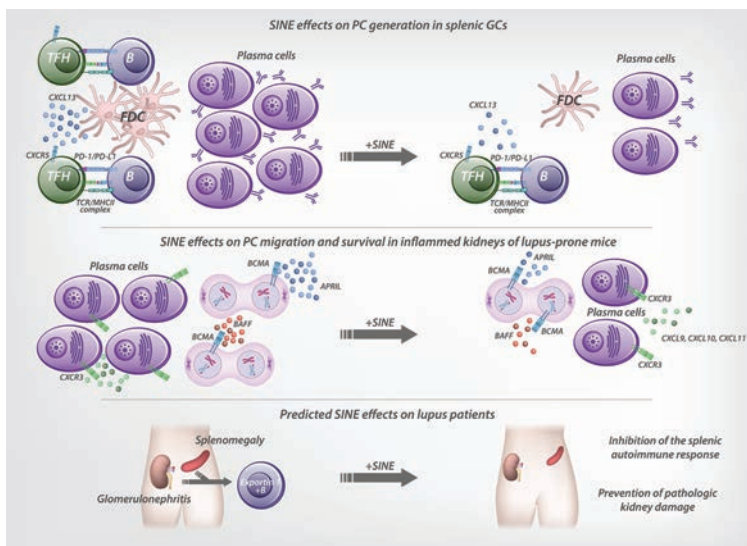
Small Molecule Inhibitors of Nuclear Export and the Amelioration of Lupus

Rangel-Moreno et al, *Arthritis Rheumatol* 2022;74:1363–1375

CORRESPONDENCE

Jennifer H. Anolik, MD, PhD: Jennifer_anolik@urmc.rochester.edu

Javier Rangel-Moreno, PhD: Javier_rangel-moreno@urmc.rochester.edu



KEY POINTS

- Autoreactive GC B cells and PCs are a key feature of lupus and are generated and maintained by NF- κ B–dependent immunologic pathways that are inhibited by SINEs, a therapeutic strategy recently approved in multiple myeloma.
- SINEs rapidly inhibit production of autoreactive PCs in splenic GCs and their migration and survival in inflamed kidneys of lupus-prone mice by decreasing chemokines (CXCL9, CXCL10) and survival factors (BAFF, APRIL, and IL-6).
- Exportin 1, the target of SINEs, was strongly expressed in tonsillar GCs, spleens, and kidneys of lupus patients, supporting the translational potential of this novel therapeutic approach in lupus.

SUMMARY

Although advances in lupus management have improved patient survival, many patients do not respond to available therapies. Lupus nephritis is one of the most severe complications, affecting $\geq 35\%$ of patients depending on ethnicity and with a probability of achieving complete or partial remission of $< 70\%$. B cells, central players in lupus pathogenesis, are activated in germinal centers (GCs) to generate autoreactive plasma cells (PCs) and pathogenic autoantibodies. However, PCs remain an elusive target despite the emergence of targeted biologic therapies including B cell depletion.

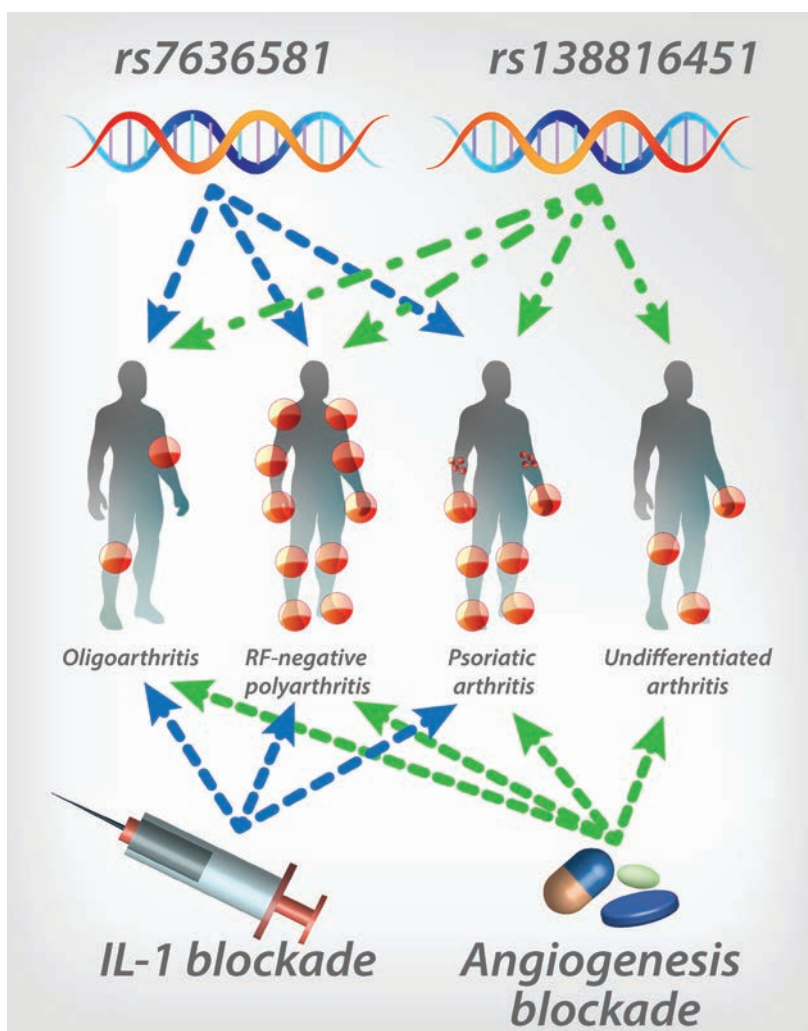
Selective inhibitors of nuclear export (SINEs) are oral agents that inhibit exportin 1, a protein critical for the export of cargo molecules (protein, mRNA) from the nucleus to the cytoplasm. SINEs sequester tumor suppressor proteins in the nucleus and were recently approved by the US Food and Drug Administration for the treatment of multiple myeloma. They also have anti-inflammatory effects (NF- κ B signaling inhibition). Rangel-Moreno et al demonstrate that SINEs abrogate lupus nephritis via strong modulation of splenic GCs, which significantly decreases GC B cells, T follicular helper cells (TFH) and PCs. CXCL13, a chemokine produced by follicular dendritic cells (FDCs), was reduced due to exportin 1–targeted disruption of NF- κ B signaling, altering T and B cell positioning and B cell–TFH interactions. In addition, SINE treatment decreased interferon- γ –induced chemokines and survival factors (BAFF, APRIL, and interleukin-6 [IL-6]) implicated in the migration and survival of autoreactive PCs in the inflamed lupus kidneys. These data suggest that inhibition of nuclear export represents a novel approach for the treatment of lupus, via multipronged effects on autoreactive PCs and other inflammatory cells in multiple organs.

Identification of Novel Loci Shared by Juvenile Idiopathic Arthritis Subtypes Through Integrative Genetic Analysis

Li et al, *Arthritis Rheumatol* 2022;74:1420–1429

CORRESPONDENCE

Hakon Hakonarson, MD, PhD: hakonarson@chop.edu



SUMMARY

Juvenile idiopathic arthritis (JIA) is the most common immune-mediated joint disease among children, yet it is highly heterogenous, encompassing 7 subtypes based on clinical presentations. Some JIA subtypes share serologic and molecular markers with overlapping clinical features. With an optimized methodology of heterogeneity-sensitive meta-analysis and integrative genetic analysis, Li et al systematically investigated the genetic architecture of JIA subtypes in a cohort of 1,245 JIA cases and 9,250 age-, sex-, and ethnicity-matched controls. Their identification of 15 genome-wide significant loci outside of the HLA region highlights the shared genetic underpinnings of JIA subtypes.


Functional annotation of the genome-wide significant loci revealed several genes at these loci known to be targets of existing drugs presenting potential repurposing opportunities for autoimmune or autoinflammatory conditions. The identification of the candidate target genes, *IL1RAP* and *SCUBE1*, associated with multiple JIA subtypes, highlights particularly the likely involvement of interleukin-1 (IL-1) signaling and the importance of angiogenesis in the JIA etiology. This patient-based genomic study provides novel information about the disease etiology, which in turn suggests opportunities of therapeutic strategies, for instance, the potential clinical application of IL-1 blockade and drugs targeting angiogenesis/vascularization for JIA.

KEY POINTS

- Fifteen loci demonstrated significant associations with different subtypes of JIA.
- Genes at these loci include both known and putative drug targets.
- Therapeutics targeting of IL-1, IL-6, or angiogenesis signaling pathways may be repositioned toward specific JIA subtypes.

EXPERT PERSPECTIVES ON CLINICAL CHALLENGES

Expert Perspective: Management of Antineutrophil Cytoplasmic Antibody–Associated Vasculitis

Naomi J. Patel and John H. Stone 

The antineutrophil cytoplasmic antibody (ANCA)–associated vasculitides (AAV) comprise a major subset of diseases that cause destructive inflammation of small and medium-sized blood vessels. Although these conditions have a predilection for pulmonary and renal involvement, they are in fact protean diseases that can involve essentially any organ system. AAV is among the most difficult rheumatic diseases to diagnose and treat. Therapy for AAV has evolved over the past two decades. Rituximab, an anti-CD20 monoclonal antibody, is now the preferred agent for remission induction in conjunction with a reduced-dose glucocorticoid taper. Rituximab is also often a key therapy for remission maintenance. Glucocorticoid toxicity reduction has become a major priority for treatment regimens. Avacopan, an important new adjunct to remission induction therapy, may reduce glucocorticoid use and its resulting toxicity. The role of avacopan as a remission maintenance agent requires further study. The duration of immunosuppression following remission is guided by a number of factors, including the patient’s overall clinical state, the degree of damage from previous disease activity, the tolerability of remission maintenance medications, and SARS–CoV-2 vaccination and immunity status. Certain features, including history of previous relapse, the presence of ANCA directed against proteinase 3, and a diagnosis of granulomatosis with polyangiitis, favor prolonged remission maintenance therapy. The interval between rituximab doses can usually be lengthened over time during the maintenance phase.

THE CLINICAL CHALLENGE

A 56-year-old man developed sinus pain, nasal congestion with crusty, bloody discharge, and difficulty breathing through his nose. Maxillary sinus surgery was planned, but a preoperative chest radiograph demonstrated a pulmonary mass, characterized further by computed tomography (CT) (Figure 1A). A core needle biopsy revealed granulomatous inflammation, multinucleated giant cells (Figure 1B), and broad swaths of “geographic” necrosis (Figure 1C). The patient was referred to the Rheumatology Department. Physical examination was notable for an intense polyarthritis; dusky, cyanotic fingers (Figure 1D); and splinter hemorrhages. He had a painful 1.5-cm left lateral tongue ulcer (Figure 1E). Laboratory results were notable for 2+ proteinuria and urinary red blood cell (RBC) casts. The serum creatinine level was 1.3 mg/dl (normal ≤ 1.2 mg/dl), and blood cultures were negative. The patient was

positive for antineutrophil cytoplasmic antibody (ANCA) with a cytoplasmic staining pattern. Enzyme immunoassay testing confirmed the presence of proteinase 3 (PR3) antibodies, with a PR3-ANCA titer of 194 units (normal <20 units). The patient was diagnosed as having granulomatosis with polyangiitis (GPA).

BACKGROUND

The ANCA-associated vasculitides (AAV) include two major diseases—GPA and microscopic polyangiitis (MPA). Eosinophilic granulomatosis with polyangiitis is also sometimes considered to be part of this disease spectrum, but the prominent role of eosinophils in that condition sets it apart from GPA and MPA. This review will focus on GPA and MPA and on the treatment and management of these diseases’ systemic presentations. Localized, organ-specific features (e.g., subglottic stenosis, bronchial

Dr. Patel’s work was supported by the National Institutes of Health Ruth L. Kirschstein Institutional National Research Service Award (award T32-AR-007258).

Naomi J. Patel, MD, John H. Stone, MD, MPH: Massachusetts General Hospital, Boston.

Author disclosures are available at <https://onlinelibrary.wiley.com/action/downloadSupplement?doi=10.1002%2Fart.42114&file=art42114-sup-0001-Disclosureform.pdf>.

Address correspondence to John H. Stone, MD, MPH, Massachusetts General Hospital, 55 Fruit Street, Yawkey 2, Boston, MA 02114. Email: jhstone@mg.harvard.edu.

Submitted for publication November 10, 2021; accepted in revised form March 9, 2022.

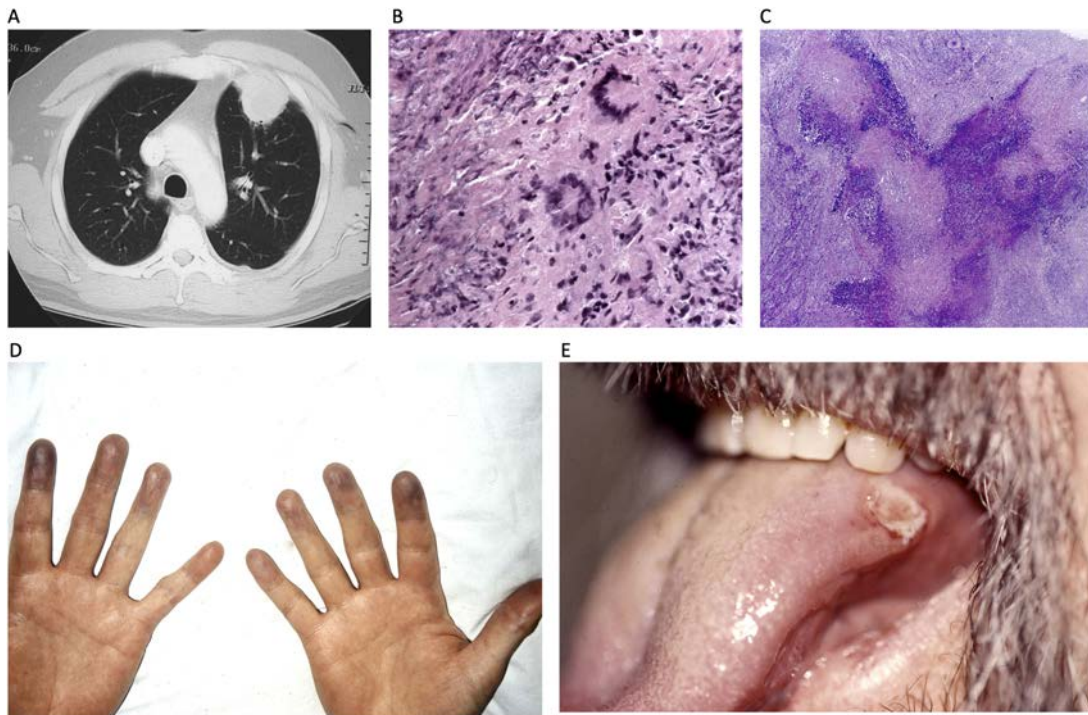


Figure 1. Clinical presentation of the featured patient with granulomatosis with polyangiitis. **A**, Mass-like consolidation on computed tomography of the chest. **B**, Lung nodule biopsy showing broad swaths of geographic necrosis. **C**, Lung nodule biopsy revealing necrotic tissue, granulomatous inflammation, and multinucleated giant cells. **D**, Peripheral cyanosis of multiple fingers. **E**, Ulceration on lateral tongue.

narrowing) that often require procedure-based interventions are not addressed.

GPA and MPA are small- to medium-vessel vasculitides that have a particular predilection for pulmonary and renal involvement but can involve essentially any organ (Table 1). These diseases are also characterized in ~90% of cases by antibodies to either PR3 (PR3-ANCA) or myeloperoxidase (MPO-ANCA)—but not both. Data from Europe indicate a prevalence of ~25–160 GPA cases per million people, and ~25–65 MPA cases per million people (1). The patient described above, with his highly symptomatic upper respiratory tract involvement, granulomatous inflammation, and PR3-ANCA positivity, fits the Chapel Hill Consensus definition of GPA (2). By contrast, MPA includes neither significant upper respiratory tract disease nor granulomatous inflammation and is more likely to be associated with MPO-ANCA. Both GPA and MPA, however, can be associated with pulmonary-renal syndromes, cutaneous vasculitis, vasculitic neuropathy, and a host of other organ manifestations. They are much more than simply pulmonary-renal syndromes.

Current clinical challenges in the treatment of AAV include identifying the optimal approach to remission induction; predicting who is at risk of relapse; determining the optimal remission maintenance strategy; and the longitudinal monitoring of disease activity. This review will address the optimal remission induction therapy, treatment regimens for remission maintenance, the role of ANCA testing and predictors of relapse, and considerations for treatment in the era of SARS-CoV-2.

APPROACH TO MANAGEMENT AND MONITORING

What is the optimal remission induction regimen for this patient with severe AAV?

The combination of rituximab with glucocorticoids has been the cornerstone of remission induction therapy used by the majority of rheumatologists for more than a decade (Figure 2). However, a significant number of clinicians continue to use cyclophosphamide. Multiple trials have found similar rates of remission with rituximab versus cyclophosphamide. One trial showed glucocorticoid-free remission at 6 months among patients with severe GPA or MPA in 64% of the rituximab group compared with 53% of the oral cyclophosphamide group ($P < 0.001$ for noninferiority) (3). Another trial found similar rates of remission at 12 months with rituximab (in conjunction with 2 doses of intravenous cyclophosphamide) versus cyclophosphamide (4). It is important to note that neither of those trials included maintenance therapy in the rituximab arms (3,4). A subgroup analysis of data from one trial found that rituximab was superior to cyclophosphamide among patients who were PR3-ANCA positive (5). A recent study provided the first randomized, controlled trial data to support the use of rituximab in severe renal disease (6). The 2021 American College of Rheumatology (ACR) guidelines recommend rituximab over cyclophosphamide for severe, active disease (7). Rituximab can be

Table 1. Characteristics of GPA and MPA*

Characteristic	GPA	MPA
Demographic characteristics	More common than MPA in Western countries; predominantly European ancestry; higher incidence in White population; men and women affected similarly	More common than GPA in Asian countries; predominantly found in Asian countries (China and Japan); men and women affected similarly
Population prevalence	25–160 cases per million people	25–65 cases per million people
ANCA pattern and type	PR3-ANCA in 80% of patients MPO-ANCA in 5–10% ANCA-negative in 5–10%	MPO-ANCA in >90% of patients PR3-ANCA or ANCA-negative in <10%
Vessel sizes involved	Small to medium vessels; arterial and venous circulation	Small to medium vessels; arterial and venous circulation
Organ systems most commonly involved	Upper and lower respiratory tract; retrobulbar disease; oral/nasal ulcers; conductive hearing loss; subglottic stenosis; renal involvement common; cutaneous (palpable purpura)	Renal (necrotizing glomerulonephritis) and pulmonary (pulmonary capillaritis) involvement common; cutaneous (palpable purpura); vasculitic neuropathy
Histopathologic features	Necrotizing granulomatous inflammation; multinucleated giant cells; abundant neutrophil infiltration; pauci-immune glomerulonephritis	Necrotizing glomerulonephritis; granulomatous inflammation is absent; abundant neutrophil infiltration; pauci-immune glomerulonephritis
Treatment response	Higher risk of relapse in PR3-ANCA GPA; better response with rituximab than cyclophosphamide; 65% achieved complete remission with rituximab compared with 48% with cyclophosphamide ($P = 0.04$) in the RAVE trial (3)	Lower risk of relapse compared to GPA; 61% achieved complete remission with rituximab compared with 64% with cyclophosphamide ($P = 0.8$) in the RAVE trial (3)
Risk of relapse	Higher risk of relapse than MPA (~1.6 times the risk)	Lower risk of relapse than GPA

* GPA = granulomatosis with polyangiitis; MPA = microscopic polyangiitis; ANCA = antineutrophil cytoplasmic antibody, PR3 = proteinase 3; MPO = myeloperoxidase; RAVE = Rituximab in ANCA-Associated Vasculitis.

dosed either at 375 mg/m² weekly for 4 doses or at 1,000 mg on days 1 and 15. A recent systematic review found similar efficacy and safety between these two regimens (3,7,8).

Before the introduction of rituximab, cyclophosphamide (plus glucocorticoids) was the standard of care for remission induction for severe AAV for 40 years (9,10). Either daily oral or intermittent intravenous cyclophosphamide regimens can be used. One trial found similar times to remission and death among patients who received intravenous cyclophosphamide and those who received oral cyclophosphamide (11). Patients treated with oral cyclophosphamide had a higher cumulative dose and greater incidence of leukopenia but also a higher likelihood of sustained remission during the limited follow-up period of that trial. The classic cyclophosphamide regimen developed at the National Institutes of Health beginning in the late 1960s involved oral daily cyclophosphamide (9,10,12,13). More recent approaches to the use of cyclophosphamide in AAV have employed intravenous regimens adapted from the treatment of lupus nephritis (14,15). Many have now moved away from cyclophosphamide as part of remission induction strategies. However, cyclophosphamide may be considered in the minority of patients who continue to experience relapse despite treatment with rituximab or when rituximab access is limited. Relatively little experience and essentially no controlled trials exist with regard to the use of rituximab and cyclophosphamide together during remission induction (16,17). Such data that exist suggest that hypogammaglobulinemia is more prevalent among patients who have been treated with both agents, and many experts have significant concerns about the risk of infection with this treatment combination. A rigorous, placebo-

controlled trial that evaluates the value of this combination regimen would be helpful (18).

What dose and duration of glucocorticoids should be used?

Reduction of glucocorticoid toxicity has become a major priority in treating AAV. The durations of glucocorticoid treatment employed in remission induction efforts have declined substantially since the late 1990s (Table 2). Glucocorticoid tapers of 12 months or longer were used in many studies from that time, typically starting at a dose of 1 mg/kg (or up to 60–80 mg per day). Trials of etanercept and rituximab in AAV, designed to test new therapies, used tapers of 6.0 and 5.5 months, respectively (3,19). Two recent trials were designed specifically to evaluate glucocorticoid dosing (6,20). We favor a reduced-dose glucocorticoid taper along the lines used in those trials and in a recent trial of plasma exchange in AAV, which tapered the dosage to 5 mg of prednisone per day by 4 months (6). For an average-sized adult, a starting prednisone dosage of 40–60 mg daily should be considered, tapering to 20 mg daily by 4 weeks, to 10 mg daily by 12 weeks, to 5 mg daily by 16 weeks, and discontinuing altogether by 5–6 months. Achieving disease control as quickly as possible is the paramount aim in remission induction and some patients will require higher doses at various time points or longer treatment courses. On the other hand, more rapid tapers should be considered in patients with poorly controlled diabetes, obesity, severe osteoporosis, and in those with prior glucocorticoid-induced depression, anxiety, or psychosis. Patients must be monitored carefully for breakthrough disease (6,7).



Figure 2. Algorithm for systemic therapeutic approach to patients with active antineutrophil cytoplasmic antibody-associated vasculitis (AAV). A reduced-dose glucocorticoid (GC) taper is favored; for an average-sized adult, consider starting prednisone at a dosage of 40–60 mg daily, tapering down to 20 mg daily by 4 weeks, to 10 mg daily by 12 weeks, to 5 mg daily by 16 weeks, and discontinuing by 5–6 months. Factors contributing to a high risk of relapse include proteinase 3–ANCA positivity, diagnosis of granulomatosis with polyangiitis (GPA), or prior relapse. Consider intravenous immunoglobulin in cases where there are contraindications to all immunosuppression. MPA = microscopic polyangiitis; RTX = rituximab; MTX = methotrexate; AZA = azathioprine; MMF = mycophenolate mofetil; CYC = cyclophosphamide.

When should pulse-dose intravenous glucocorticoids be used?

There are no randomized clinical trials to guide the use of “pulse-dose” intravenous glucocorticoids (methylprednisolone up to a total of 3,000 mg over 3 days). However, “pulse” glucocorticoid regimens are used routinely in both clinical trials and practice. Retrospective data as well as post hoc analyses from

trials have suggested no difference in survival, renal recovery, or relapse according to whether or not pulse-dose glucocorticoid regimens are used, but such analyses suffer from confounding from a variety of sources (16,17). Increased risks of infection and diabetes have been reported with pulse-dose glucocorticoids (21,22). There are currently no recommendations either for or against the use of pulse-dose glucocorticoids (7). In the critical early stage of treating an AAV patient with severe disease, pulse-

Table 2. Glucocorticoid regimens used in clinical trials of AAV over the years*

Author, year (ref.)	Trial name and randomization arm	Glucocorticoid type and starting daily dosage†	Glucocorticoid daily dosage at 3–6 months	Glucocorticoid daily dosage at 12 months	Duration of taper	Cumulative dose received (in prednisone or prednisolone equivalents)
Jayne et al, 2003 (47)	CYCAZAREM	Prednisolone 1 mg/kg	0.25 mg/kg by 12 weeks	7.5 mg	12 months followed by investigator discretion	Not reported
WGET Research Group, 2005 (19)	WGET	Prednisone up to 80 mg/day	0 mg at 24 weeks	None	6 months	Not reported
De Groot et al, 2005 (26)	NORAM	Prednisolone 1 mg/kg	15 mg at 12 weeks; 7.5 mg at 6 months	None	12 months	6.2–8.8 gm over 18 months
Harper et al, 2012 (11)	CYCLOPS	Prednisolone 1 mg/kg	12.5 mg at 3 months	Between 5 mg and 12.5 mg	18 months followed by investigator discretion	7.6 gm over 9 months
Hiemstra et al, 2010 (46)	IMPROVE	Prednisolone 1 mg/kg	0.25 mg/kg by 13 weeks	5 mg	24 months	8.4–8.5 gm over 39 months of follow-up time
Stone et al, 2010 (3)	RAVE	Prednisolone 1 mg/kg	None by 5 months	None	5 months	6.2–6.9 gm over 6 months
Guillevin et al, 2014 (43)	MAINRITSAN	Prednisone 1 mg/kg	Gradual taper from 1 mg/kg to 5 mg	Minimum of 5 mg	18 months followed by investigator discretion	Not reported
Jones et al, 2019 (22)	EUVAS	Prednisolone 1 mg/kg	5 mg at 6 months	5 mg	>6 months	5.8–6.2 gm over 6 months
Walsh et al, 2020 (6)	PEXIVAS, standard-dose arm	Prednisone 50–75 mg/day depending on weight	15–25 mg by week 12	5 mg	52 weeks followed by investigator discretion	Not reported
Walsh et al, 2020 (6)	PEXIVAS, reduced-dose arm	Prednisone 50–75 mg/day depending on body weight	7.5–12.5 mg by week 12	5 mg	52 weeks followed by investigator discretion	Not reported
Jayne et al, 2021 (20)	ADVOCATE, placebo arm	Prednisone 60 mg	10 mg by week 12	None	21 weeks	3.3 gm over 12 months
Jayne et al, 2021 (20)	ADVOCATE, avacopan arm	None	None	None	NA	0.9 gm over 12 months

* AAV = antineutrophil cytoplasmic antibody-associated vasculitis; CYCAZAREM = Cyclophosphamide versus Azathioprine for Early Remission phase of vasculitis; WGET = Wegener's Granulomatosis Efficacy Trial; NORAM = Nonrenal Wegener's Granulomatosis Treated Alternatively with Methotrexate; CYCLOPS = Pulse Versus Daily Oral Cyclophosphamide for Induction of Remission in Antineutrophil Cytoplasmic Antibody-Associated Vasculitis; IMPROVE = International Mycophenolate Mofetil Protocol to Reduce Outbreaks of Vasculitides; RAVE = Rituximab in ANCA-Associated Vasculitis; MAINRITSAN = Rituximab versus Azathioprine in ANCA-Associated Vasculitis; EUVAS = European Vasculitis Study Group; PEXIVAS = Plasma Exchange and Glucocorticoids in Severe ANCA-Associated Vasculitis; ADVOCATE = Avacopan for the Treatment of ANCA-Associated Vasculitis; NA = not applicable. † Pulse doses of glucocorticoids, i.e., 1–3 gm total of methylprednisolone in daily doses of 1 gm each, were permitted in many trials.

dose intravenous glucocorticoids are still deemed crucial to achieving disease control quickly and to avoiding the complications of overwhelming vasculitis. For patients as severely ill as the one presented here, we recommend erring on the side of overtreatment at the start of therapy and often order up to 3 daily pulses of methylprednisolone in patients whose disease has the potential to deteriorate rapidly. Clinical discretion to use fewer than 3 pulse-doses, lower pulse-doses, or to forgo pulse-dose glucocorticoids altogether in patients with nonsevere disease, however, is appropriate.

What new options are there for remission induction?

More recently, avacopan, a C5a receptor antagonist, was shown to be effective in remission induction as an adjunct to glucocorticoids and either rituximab or cyclophosphamide for the treatment of severe AAV (20). The use of avacopan reduced glucocorticoid toxicity as measured by the Glucocorticoid Toxicity Index at both 13 and 26 weeks (20,23–25). Avacopan, an oral drug administered twice daily, now has an important role to play as part of remission induction regimens (in conjunction with background rituximab or cyclophosphamide) and should lead to even shorter courses of glucocorticoids than used in prior trials. The US Food and Drug Administration stated clearly, however, that avacopan is not a replacement for glucocorticoids. Avacopan may be used most effectively in severe AAV in combination with rituximab or cyclophosphamide, with a principal aim of reducing the quantity of glucocorticoids required to achieve stable sustained disease remission. Its role for the induction of remission in nonsevere disease and in remission maintenance requires further investigation.

What treatment regimen is best for those with nonsevere disease?

“Nonsevere disease” describes GPA patients with disease localized primarily to the upper respiratory tract and no evidence of rapidly progressive glomerulonephritis, vasculitic neuropathy, severe inflammatory ocular disease, alveolar hemorrhage, or other such disease manifestations that pose an immediate threat to organ function or life. Patients with nonsevere GPA may be treated with methotrexate (up to 25 mg/week) and glucocorticoids, principally in the interest of sparing exposure to cyclophosphamide. This regimen induces remission in approximately two-thirds of patients (7,9,26,27). In our experience, rituximab is more effective than methotrexate in exerting full disease control and reducing glucocorticoid exposure, but methotrexate remains an appropriate and sometimes preferred choice when access to rituximab is limited by cost, concerns about COVID-19 infection or vaccine response, or other factors. Methotrexate is less

effective than cyclophosphamide for remission induction in patients with severe disease and should not be used in that setting (26).

Mycophenolate mofetil, a highly effective agent in lupus nephritis, likely also has a role in some AAV patients with nonsevere disease. One trial found that mycophenolate mofetil plus glucocorticoids was noninferior to cyclophosphamide plus glucocorticoids for remission induction (22). Because this trial found higher relapse rates over 6 months with methotrexate (33% compared to 19% with cyclophosphamide), it is not recommended for patients with severe AAV or for those at high risk of relapse. Mycophenolate mofetil can be considered, however, in patients with nonsevere disease at low risk of relapse (22). Azathioprine was shown to be more effective than mycophenolate mofetil for remission maintenance and can also be considered as a maintenance agent in those with nonsevere disease (7).

What adjunct therapies should be used to prevent treatment-related adverse effects?

All patients starting on high doses of glucocorticoids combined with other agents for remission induction should receive prophylaxis against *Pneumocystis* pneumonia. There are few data to guide the duration of *Pneumocystis* prophylaxis. This decision should be informed by the patient’s clinical picture and overall risk profile. Our practice is to consider discontinuing *Pneumocystis* prophylaxis once the daily prednisone dosage is <15 mg, but longer courses may be appropriate in patients treated with therapies likely to produce prolonged lymphopenia (e.g., concomitant rituximab or cyclophosphamide).

Measures designed to mitigate glucocorticoid-induced osteoporosis—calcium, vitamin D, and consideration of a bisphosphonate—are important (28). The routine use of antiviral prophylaxis is not recommended presently, even though patients treated with the immunosuppression regimens used in AAV are at an increased risk of viral infections and reactivation. Patients should receive the varicella-zoster virus, SARS-CoV-2, and seasonal influenza vaccines, as well as the pneumococcal conjugate vaccine (Pneumovax 13) followed by the pneumococcal polysaccharide vaccine (Pneumovax 23) at least 2 months later (29,30).

Our patient. Our patient was started on methylprednisolone 1 gm intravenously daily for 3 days, followed by prednisone 60 mg daily and oral cyclophosphamide 150 mg daily. He was also started on *Pneumocystis jirovecii* prophylaxis with trimethoprim/sulfamethoxazole. He felt dramatically better following his first methylprednisolone infusion. His arthritis resolved promptly and the pain from his tongue ulcer subsided quickly. He was discharged from the hospital after 3 days, but 5 days after discharge, his serum creatinine level had risen to 2.7 mg/dl (normal <1.3 mg/dl). A repeat urinalysis revealed 1+ proteinuria, 80–100 RBCs per high-power field, and multiple RBC casts. The patient

was then admitted to our hospital due to worsening renal function. The decision was made to transition him to rituximab 1 gm intravenously with a plan for 2 loading doses administered 15 days apart. This decision was made not because cyclophosphamide was judged to have failed, but rather out of practice style and the consideration of using rituximab as the cornerstone of remission induction as well as long-term remission maintenance therapy. The possibility of instituting plasma exchange was also suggested at this time.

Is there a role for plasma exchange?

The question of whether plasma exchange has a role in the treatment of AAV remains a subject of controversy. Plasma exchange, in theory, is designed to remove pathologic antibodies (i.e., ANCA) as well as other proinflammatory factors. Early observational studies suggested a short-term benefit of plasma exchange for subsets of AAV patients in the prevention of end-stage renal disease but failed to demonstrate a mortality difference (31). A nonblinded study published in 2007 randomized patients with AAV and severe, biopsy-proven glomerulonephritis to receive either 7 days of plasma exchange or 3 days of pulse-dose methylprednisolone in addition to cyclophosphamide and conventional glucocorticoid doses. The investigators reported that a lower proportion of patients randomized to receive plasma exchange had end-stage renal disease at both 3 and 12 months (32). A meta-analysis of plasma exchange studies, however, did not demonstrate a mortality benefit of plasma exchange even though it confirmed the reduction of end-stage renal disease with plasma exchange at both 3 and 12 months (31).

In a recent trial of plasma exchange in AAV, patients with GPA or MPA and renal or pulmonary involvement were randomized in a nonblinded manner to receive either plasma exchange or placebo. The patients were also randomized a second time to receive either a standard or reduced-dose glucocorticoid taper. The primary outcome in the trial was a composite of time to end-stage renal disease or death. The outcome of all-cause mortality or end-stage renal disease was not significantly different between those who received plasma exchange versus those who received placebo (hazard ratio [HR] 0.86; 95% confidence interval [95% CI] 0.65, 1.13) (6). The lower-dose glucocorticoid treatment regimen was noninferior to the higher-dose regimen for remission induction and was associated with fewer severe infections.

These results suggest that the routine use of plasma exchange for AAV is not indicated. It is worth noting, however, that plasma exchange was seldom considered appropriate for all such disease presentations before this trial, and its implications for the treatment of certain important disease subsets remain unclear. The strongest rationale for the use of plasma exchange in AAV is in the early period of active disease in which there is an imminent threat to major organ function or life (e.g., early, aggressive glomerulonephritis or diffuse alveolar hemorrhage). Current

remission induction regimens are quite effective at inducing remission in most patients within 3–6 months. When either end-stage renal disease or death occurs in AAV, they are generally late events, often happening only after years of treatment, multiple disease relapses, and prolonged or repeated treatments with different immunosuppressive regimens. Some AAV experts therefore continue to believe that plasma exchange should remain part of the regimen for patients with severe, diffuse alveolar hemorrhage or with early, aggressive renal disease (6,33). Nevertheless, the 2021 ACR guidelines indicate that plasma exchange should not be included as part of the induction therapy regimen in AAV (7).

Our patient. Plasma exchange was not pursued in our patient. His renal function worsened despite treatment with glucocorticoids, 1 week of oral cyclophosphamide, and 2 doses of rituximab. Although his GPA appeared to be controlled in every organ system except his kidneys, 2 months after presentation he required renal replacement therapy with hemodialysis, which—it was hoped—would be temporary. Fortunately, he required hemodialysis for only 6 weeks and then regained independent renal function, achieving a new baseline serum creatinine level of 1.8 mg/dl. He received a remission maintenance dose of rituximab 4 months after his loading doses and discontinued prednisone completely at 5 months. Seven months after the start of treatment, he was negative for ANCA.

Are there known risk factors for disease relapse?

Remission and relapse of AAV are both defined clinically, and there is significant variation in the severity of relapses. Disease relapses are the rule rather than the exception in AAV. Data indicate that only 39% of patients treated for remission induction with rituximab and three 1-gram pulses of methylprednisolone and a 5.5-month prednisone course achieved and maintained disease remission through 18 months (compared with 31% of cyclophosphamide-treated patients) (34). Thus, development of a clear remission maintenance strategy in every patient—whether it involves active treatment or not—is important to avoid mounting cumulative damage from the effects of active disease, to obviate potential complications from repeated induction regimens, and to reduce mortality from both the underlying disease and its management (5,35). Surveillance for the possibility of relapse needs to be maintained in all AAV patients, and the majority of patients need some active treatment at least early in the remission maintenance period.

Certain baseline characteristics predict a higher risk of future relapse. History of a previous relapse is perhaps the strongest predictor of future relapse (34). The diagnosis of GPA as opposed to MPA is associated with a lower probability of achieving complete remission—defined as no evidence of clinical disease activity while off treatment—and a higher risk of relapse (3). Similarly, PR3-ANCA positivity as opposed to MPO-ANCA positivity is also

independently associated with a higher risk of relapse (subhazard ratio 1.6; 95% CI 1.4, 1.9) (35).

Higher creatinine level at diagnosis is associated with a lower risk of relapse (35). One potential explanation is that patients with MPO-ANCA are more likely to present with advanced renal dysfunction but also have a lower likelihood of relapse compared to their PR3-ANCA-positive counterparts. Treatment with rituximab as opposed to cyclophosphamide is also associated with a lower risk of relapse, particularly among PR3-ANCA-positive patients (5). In contrast, longer duration (>2 years) of persistent ANCA positivity poses a higher risk of relapse (discussed more below) (36), and shorter duration (≤ 2 years) of maintenance immunosuppression is associated with a greater risk of relapse (5,36). Active, ongoing remission maintenance therapy should be considered for patients at highest risk of relapse as well as for patients with disease-related damage in whom a relapse might have significant long-term implications. Because nearly all data pertaining to the risk of relapse are from ANCA-positive patients, it is not clear if these data also apply to those who are ANCA negative.

What laboratory features should be monitored following diagnosis?

We monitor the complete blood cell count, comprehensive metabolic panel, urinalysis with microscopic evaluation, spot urine protein:creatinine ratio, erythrocyte sedimentation rate, and C-reactive protein level. These tests may need to be performed every week during the treatment of active disease. The frequency of testing can be decreased as disease activity decreases. Once remission is achieved, the interval between laboratory assessments can be increased, to every month for several months, then to every 3 months for the next 2 years, and then to every 4–6 months. However, patient-specific modifications based on tissues at risk (e.g., renal injury) are important for the detection of any disease relapse as early as possible. Some clinicians have patients perform weekly dipstick urine analyses that, if positive, trigger more formal evaluation. We also check ANCA every 3–6 months. Recurrent ANCA positivity or rising titers should trigger closer subsequent monitoring. The role of ANCA testing is discussed further below.

It is also important to monitor for signs of treatment toxicity, including intermittent hemoglobin A1c, lipid profile, and serum protein electrophoresis, with quantitative immunoglobulins. A bone mineral density study at intervals dictated by the patient's age, glucocorticoid exposure, and other risk factors is also important.

We perform a CT scan of the chest at diagnosis and follow any abnormal thoracic findings with a repeat CT scan during or after remission induction therapy. Other imaging studies at similar intervals may also be appropriate, depending on the organ involved. For example, CT scans of the orbits and sinuses are often crucial for tracking disease in those areas when present.

Magnetic resonance imaging is critical in following up patients with meningeal disease.

What is the utility of ANCA titer as a predictor of relapse?

The value of ANCA in the management of AAV can be summarized by 3 primary points. First, the finding of ANCA positivity is highly specific for the diagnosis of AAV. Positive ANCA testing from a reliable laboratory sometimes obviates the need for tissue biopsy when the clinical presentation is highly consistent with AAV. Second, persistent ANCA positivity after remission induction therapy is associated with a higher likelihood of disease relapse compared with ANCA negativity. It is important to recognize, however, that persistent ANCA positivity does not provide reliable insight into when a relapse may occur (assuming it occurs at all). Disease relapse in a patient who is ANCA positive may not occur for months or even several years. Thus, decisions about whether to use remission maintenance treatment cannot be made on the basis of persistent ANCA positivity alone. Moreover, a patient's ANCA status can change. Third, in more than 3 decades since the identification of ANCA as a potential biomarker in AAV, no study has demonstrated convincingly that changes in ANCA titers are a reliable guide to the adjustment of treatment strategies in the short term; thus, treatment decisions should be based on the patient's overall clinical picture. Some of the data supporting these statements are provided below.

An analysis of the US Department of Defense database shows that almost all patients with GPA developed ANCA positivity in the 1.5 years prior to diagnosis, and the vast majority had a >20% per year increase in the titer prior to an established diagnosis (37). Persistent ANCA positivity 2 years after initiation of immunosuppression predicts a greater risk of relapse compared to ANCA negativity (36). Although a persistently positive ANCA assay indicates an increased risk of relapse in some patients, the association between ANCA titers and disease activity across multiple studies is in fact weak, which complicates inferences about individual patients from such data (38). Data about whether rising ANCA titers imply a greater risk of relapse are mixed (38–40).

Changes in ANCA titer have different implications according to specific scenarios. For example, multiple studies have found that an increase in PR3-ANCA was most associated with relapse in patients with renal involvement (HR 7.9) (38–40). Conversion of ANCA assay findings from negative to positive has been associated with an increased risk of relapse in multiple studies. Approximately two-thirds of patients who were ANCA negative at baseline became ANCA positive before relapse (29,30). However, one-sixth of patients who became ANCA positive did not relapse, underscoring the difficulty of applying trends in ANCA assay results across all patients (41,42). Two studies have confirmed that the risk of recurrent disease activity is extremely low in

patients who are both ANCA negative and have no detectable CD19+ B cells in their blood (3,42).

In summary, although there is a crude temporal correlation between increasing ANCA titer and risk of disease relapse, the relationship between ANCA kinetics and clinical disease activity makes clinical decision-making based on ANCA titers alone untenable. The 2021 ACR guidelines recommend against dosing immunosuppression based on ANCA titer alone (7).

Our patient. Despite achieving ANCA negativity, the patient experienced several disease relapses over a period of several years. During this time, his ANCA status correlated only loosely with disease activity. Changes in ANCA titers did not predict impending relapses or correlate closely with disease control. The relapses were treated with rituximab and glucocorticoids, but each relapse was associated with further loss of renal function. The patient eventually reached end-stage renal disease and underwent renal transplantation. Four months after receiving his renal allograft, he developed bilateral cytomegalovirus retinitis and suffered a major loss of vision.

What is the most effective approach to remission maintenance?

Rituximab is the preferred treatment for remission maintenance in most cases. A randomized trial of rituximab (dosed every 6 months) or azathioprine for maintenance therapy in AAV found that 29% of the azathioprine group experienced a major relapse by month 28 compared with only 5% of the rituximab group ($P = 0.002$) (43). The rates of serious adverse events and the immunoglobulin levels in the two groups were similar during follow-up.

The optimal dosing regimen of rituximab for remission maintenance in AAV remains uncertain. This is because no single regimen is appropriate for all patients. Some examples of the regimens employed are summarized in Table 3. The majority of patients with AAV require maintenance treatment. However, a significant minority of patients (e.g., some MPO-ANCA patients with mild disease) may not require ongoing remission maintenance treatment. AAV patients who are MPO-ANCA positive, who have nonsevere disease, who have never had a relapse, or who have little or no disease damage are good candidates for watchful waiting. All patients with AAV, regardless of their ANCA type—PR3-ANCA, MPO-ANCA, or ANCA negative—need to be followed up indefinitely. The need for ongoing treatment should be reassessed continually over time.

Remission maintenance therapy generally begins with rituximab initially at either 4 or 6 months after the remission induction infusions. Such a treatment interval can be repeated over time, but it is often possible (and wise) to lengthen the interval between rituximab administrations. This is particularly important in the era

of SARS-CoV-2. In our experience, some patients can eventually maintain remission with just 1 gm of rituximab every year.

Repeated rituximab use can be associated with hypogammaglobulinemia; estimates range from <10% to almost half of patients, though immunoglobulin replacement therapy is only required for symptomatic hypogammaglobulinemia with recurrent or severe infections in a minority of patients (18,44,45). Providers should check baseline immunoglobulin levels and monitor patients closely for infections if hypogammaglobulinemia ensues.

What other regimens can be considered for remission induction in the setting of contraindications or intolerance to the above options?

In the setting of intolerance or contraindications to rituximab, alternative options can be considered. Azathioprine, methotrexate, or mycophenolate are all reasonable options for remission maintenance in the proper clinical setting (46–50). Intravenous immunoglobulin can be considered when a particular scenario (e.g., sepsis or pregnancy) makes immunosuppression undesirable (7).

How are treatment considerations impacted by the specter of COVID-19?

Multiple studies have shown that after adjustment for comorbidities, autoimmune disease itself is not a risk factor for worse COVID-19 outcomes (51). However, those with iatrogenic B cell depletion from rituximab and other anti-CD20 monoclonal antibodies have both worse COVID-19–related outcomes and poor responses to vaccines (52). Rituximab use among patients with rheumatic disease is associated with 4-fold higher odds of severe COVID-19 outcomes and death compared with medications such as tumor necrosis factor inhibitors and methotrexate (53–55). Similar results have been seen in studies in multiple sclerosis, even after adjusting for disease severity and duration, comorbidities, glucocorticoid use, and other factors (56). Such data highlight the importance of careful contemplation of the timing of B cell depletion strategies in remission maintenance for AAV and illustrate an important shortcoming of treatment strategies that maintain B cell depletion indefinitely.

Glucocorticoids, particularly prednisone 10 mg daily or greater, are independent risk factors for worse COVID-19 outcomes including hospitalization or death (53,57). Furthermore, patients with moderate or high disease activity have increased mortality from COVID-19 compared to those in remission or with low disease activity, underscoring the importance of maintaining good disease control (53). This must be balanced carefully against the risks associated with different therapies.

Despite the special considerations required in the COVID-19 era, rituximab is still preferred as the first-line therapy for both remission induction and maintenance of remission. Cyclophosphamide

Table 3. Selected studies evaluating remission induction and remission maintenance treatment regimens in AAV*

Author, year (ref.)	Trial name	Therapy type	Treatment regimens	No. of subjects	Primary outcome measure	Primary results	Conclusion and comments
Jayne et al, 2003 (47)	CYCAZAREM	Maintenance	CYC (1.5 mg/kg/day) or AZA (2 mg/kg/day)	155	Relapse over 18 months	Relapse 15.5% with AZA vs. 13.7% with CYC ($P = 0.65$)	AZA similar to CYC for remission maintenance
de Groot et al, 2005 (26)	NORAM	Induction	Oral CYC (2 mg/kg/day) or oral MTX (20–25 mg weekly)	100	Remission at 6 months	Remission 89.8% with MTX vs. 93.5% with CYC ($P = 0.041$)	MTX less effective than CYC for remission induction in severe disease or pulmonary involvement
Harper, 2012 (11)	CYCLOPS	Induction	Pulse IV CYC (15 mg/kg every 2–3 weeks) or daily oral CYC (2 mg/kg/day) + prednisolone, then AZA (2 mg/kg/day) through month 18	149	Time to remission	Similar time to remission in each group (HR 1.098 [95% CI 0.78, 1.55]; $P = 0.59$)	IV CYC as effective as oral CYC and associated with less leukopenia
Hiemstra et al, 2010 (46)	IMPROVE	Maintenance	AZA (2 mg/kg/day) vs. MMF (2,000 mg/day) after induction with CYC and prednisone	156	Relapse-free survival through 48 months	Relapses more common with MMF than AZA (HR _{unadj} 1.69 [95% CI 1.06, 2.70]; $P = 0.03$)	MMF less effective than AZA for maintaining disease remission
Stone et al, 2010 (3)	RAVE	Induction	RTX (375 mg/m ² weekly for 4 weeks) vs. oral CYC (2 mg/kg/day)	197	GC-free remission at 6 months	Primary end point reached by 64% in RTX group vs. 53% in CYC group ($P < 0.001$)	RTX noninferior to CYC for induction
Guillevin et al, 2014 (43)	MAINRITSAN	Maintenance	RTX 500 mg IV days 0 and 14 and months 6, 12, and 18 or AZA daily for 22 months (starting dose 2 mg/kg/day)	115	Major relapse by month 28	Major relapse 29% with AZA vs. 5% with RTX ($P = 0.002$)	AZA less effective than RTX at maintaining remission
Charles et al, 2018 (62)	MAINRITSAN2	Maintenance	RTX infusions on a fixed schedule (days 0 and 14, then months 6, 12, 18) or individually tailored (500 mg at baseline, reinfusion when CD19+ B cells or ANCAs reappeared)	162	Relapse by month 28	Relapse 17.3% with tailored infusion vs. 9.9% with fixed dose ($P = 0.22$)	Relapse rates similar with tailored or fixed-dose RTX, with fewer infusions in the tailored RTX group
Jones et al, 2019 (22)	EUVAS	Induction	MMF 2–3 gm/day or pulsed CYC 15 mg/kg every 2–3 weeks, followed by AZA for maintenance	140	Remission by 6 months, compliance with GC taper	Remission 67% with MMF vs. 61% with CYC (risk difference 5.7% [90% CI –7.5%, 19%])	MMF noninferior to CYC for remission induction but higher relapse rate (19% with CYC vs. 33% with MMF)
Walsh et al, 2020 (6)	PEXIVAS	Induction	2 × 2 factorial: plasma exchange or no plasma exchange, standard-dose or reduced-dose GCs	352	Composite of death from any cause or end-stage renal disease	Composite end point reached by 28.4% with plasma exchange vs. 31% with no plasma exchange (HR 0.86 [95% CI 0.65, 1.13])	No reduction in death or end-stage renal disease with plasma exchange. Reduced-dose GCs noninferior to standard-dose GCs
Jayne et al, 2021 (20)	ADVOCATE	Induction	Oral avacopan 30 mg twice daily or oral prednisone + standard care, with either CYC or RTX	331	Remission at week 26 with no GCs in prior 4 weeks	Remission 72.3% with avacopan vs. 70.1% with prednisone ($P = 0.24$ for superiority, $P < 0.001$ for noninferiority)	Avacopan noninferior to prednisone taper for remission induction at week 26, superior to prednisone at week 52

* CYC = cyclophosphamide; AZA = azathioprine; MTX = methotrexate; IV = intravenous; HR = hazard ratio; 95% CI = 95% confidence interval; MMF = mycophenolate mofetil; HR_{unadj} = unadjusted hazard ratio; RTX = rituximab; GC = glucocorticoid; ANCAs = antineutrophil cytoplasmic antibodies (see Table 2 for other definitions).

is also associated with worse COVID-19 outcomes, and use of mycophenolate is limited by a lack of randomized trials showing benefit (58). For patients at lower risk of relapse, such as those with MPO-ANCA positivity and nonsevere disease, consideration should be given to limiting remission maintenance treatment or forgoing it altogether in favor of close follow-up. For those receiving scheduled rituximab, timing of the SARS-CoV-2 vaccine and booster doses must also be considered carefully. Conventional disease-modifying antirheumatic drugs may play a larger role in patients with nonsevere disease awaiting vaccination or booster dosing. For those with stable disease, vaccines should be completed 2–4 weeks prior to the subsequent rituximab dose (59). For those with stable disease taking methotrexate, azathioprine, or mycophenolate mofetil, it is reasonable to consider delaying treatment with these medications for 1–2 weeks following each vaccination dose (59,60). In addition to vaccination, tixagevimab/cilgavimab should be strongly considered as pre-exposure prophylaxis in those receiving heavy immunosuppression, particularly in patients with depleted B cells or known low or absent antibody response to the SARS-CoV-2 vaccine (61). If patients develop COVID-19 infection, they should be quickly referred for any available appropriate therapies, including monoclonal antibodies or antiviral treatments.

CONCLUSION

Remission induction treatment regimens are moving toward shorter courses and reduced doses of glucocorticoids, given the significant toxicities associated with these medications. Avacopan can now be considered a glucocorticoid-sparing agent to be used as part of the remission induction regimens in severe cases. Swift remission induction, thoughtful strategies for remission maintenance, and prudent stewardship of immunosuppressive therapies over the long-term are all essential to good outcomes in AAV. Prevention of infection, both COVID-19 and others, through vaccination and other prophylactic measures, is also a crucial component of care. In the GPA patient with severe disease described in this vignette, treatment was eventually successful in inducing remission, though his course was complicated by several relapses, underscoring the difficulty of predicting and managing disease recurrences in AAV. Future areas of research should focus on ongoing clinical challenges such as identifying novel biomarkers that reflect disease activity reliably and predict relapses; collecting long-term follow-up data to determine the optimal dose and duration of maintenance therapy in different subgroups of patients; and identifying additional novel treatment agents that reduce glucocorticoid toxicity.

AUTHOR CONTRIBUTIONS

Drs. Patel and Stone drafted the article, revised it critically for important intellectual content, and approved the final version to be published.

REFERENCES

1. Watts RA, Lane S, Scott DG. What is known about the epidemiology of the vasculitides? *Best Pract Res Clin Rheumatol* 2005;19:191–207.
2. Jennette JC. Overview of the 2012 revised International Chapel Hill Consensus Conference nomenclature of vasculitides. *Clin Exp Nephrol* 2013;17:603–6.
3. Stone JH, Merkel PA, Spiera R, Seo P, Langford CA, Hoffman GS, et al. Rituximab versus cyclophosphamide for ANCA-associated vasculitis. *N Engl J Med* 2010;363:221–32.
4. Jones RB, Tervaert JW, Hauser T, Luqmani R, Morgan MD, Peh CA, et al. Rituximab versus cyclophosphamide in ANCA-associated renal vasculitis. *N Engl J Med* 2010;363:211–20.
5. Unizony S, Villarreal M, Miloslavsky EM, Lu N, Merkel PA, Spiera R, et al. Clinical outcomes of treatment of anti-neutrophil cytoplasmic antibody (ANCA)-associated vasculitis based on ANCA type. *Ann Rheum Dis* 2016;75:1166–9.
6. Walsh M, Merkel PA, Peh CA, Szpirt WM, Puechal X, Fujimoto S, et al. Plasma exchange and glucocorticoids in severe ANCA-associated vasculitis. *N Engl J Med* 2020;382:622–31.
7. Chung SA, Langford CA, Maz M, Abril A, Gorelik M, Guyatt G, et al. 2021 American College of Rheumatology/Vasculitis Foundation guideline for the management of antineutrophil cytoplasmic antibody-associated vasculitis. *Arthritis Care Res (Hoboken)* 2021;73:1088–105.
8. Bénard V, Farhat C, Zarandi-Nowroozi M, Durand M, Charles P, Puechal X, et al. Comparison of two rituximab induction regimens for antineutrophil cytoplasm antibody-associated vasculitis: systematic review and meta-analysis. *ACR Open Rheumatol* 2021;3:484–94.
9. Hoffman GS, Kerr GS, Leavitt RY, Hallahan CW, Lebovics RS, Travis WD, et al. Wegener granulomatosis: an analysis of 158 patients. *Ann Intern Med* 1992;116:488–98.
10. Fauci AS, Wolff SM. Wegener's granulomatosis: studies in eighteen patients and a review of the literature. *Medicine (Baltimore)* 1973;63:535–61.
11. Harper L, Morgan M, Walsh M, Hoglund P, Westman K, Flossmann O, et al. Pulse versus daily oral cyclophosphamide for induction of remission in ANCA-associated vasculitis: long-term follow-up. *Ann Rheum Dis* 2012;71:955–60.
12. Wolff SM, Fauci AS, Horn RG, Dale DC. Wegener's granulomatosis. *Ann Intern Med* 1974;81:513–25.
13. Fauci AS, Haynes BF, Katz P, Wolff SM. Wegener's granulomatosis: prospective clinical and therapeutic experience with 85 patients for 21 years. *Ann Intern Med* 1983;98:76–85.
14. Houssiau FA, Vasconcelos C, D'Cruz D, Sebastiani GD, Garrido ED, Danieli MG, et al. Immunosuppressive therapy in lupus nephritis: the Euro-Lupus Nephritis Trial, a randomized trial of low-dose versus high-dose intravenous cyclophosphamide. *Arthritis Rheum* 2002;46:2121–31.
15. Ginzler EG, Dooley MA, Aranow C, Kim MY, Buyon J, Merrill JT, et al. Mycophenolate mofetil or intravenous cyclophosphamide for lupus nephritis. *N Engl J Med* 2005;353:2219–28.
16. Cortazar FB, Muhsin SA, Pendergraft WF III, Wallace ZS, Dunbar C, Laliberte K, et al. Combination therapy with rituximab and cyclophosphamide for remission induction in ANCA vasculitis. *Kidney Int Rep* 2018;3:394–402.
17. Pepper RJ, McAdoo SP, Moran SM, Kelly D, Scott J, Hamour S, et al. A novel glucocorticoid free maintenance regimen for ANCA associated vasculitis. *Rheumatology (Oxford)* 2019;58:260–8.
18. Tieu J, Smith RM, Gopaluni S, Kumaratne DS, McClure M, Manson A, et al. Rituximab associated hypogammaglobulinemia in autoimmune disease. *Front Immunol* 2021;12:671503.

19. Wegener's Granulomatosis Etanercept Trial (WGET) Research Group. Etanercept plus standard therapy for Wegener's granulomatosis. *N Engl J Med* 2005;352:351–61.
20. Jayne DR, Merkel PA, Schall TJ, Bekker P, Group AS. Avacopan for the treatment of ANCA-associated vasculitis. *N Engl J Med* 2021; 384:599–609.
21. Chanouzas D, McGregor JA, Nightingale P, Salama AD, Szpirt WM, Basu N, et al. Intravenous pulse methylprednisolone for induction of remission in severe ANCA associated vasculitis: a multi-center retrospective cohort study. *BMC Nephrol* 2019;20:58.
22. Jones RB, Hiemstra TF, Ballarin J, Blockmans DE, Brogan P, Bruchfeld A, et al. Mycophenolate mofetil versus cyclophosphamide for remission induction in ANCA-associated vasculitis: a randomised, non-inferiority trial. *Ann Rheum Dis* 2019;78:399–405.
23. Stone JH, McDowell PJ, Jayne DRW, et al. The glucocorticoid toxicity index: measuring change in glucocorticoid toxicity over time. *Semin Arthritis Rheum* 2022. doi: [10.1016/j.semarthrit.2022.152010](https://doi.org/10.1016/j.semarthrit.2022.152010). Epub ahead of print.
24. McDowell PJ, Stone JH, Zhang Y, Honeyford K, Dunn L, Logan RJ, et al. Quantification of glucocorticoid-associated morbidity in severe asthma using the glucocorticoid toxicity index. *J Allergy Clin Immunol Pract* 2021;9:365–72.
25. Jayne DR, Bruchfeld AN, Harper L, Schaiër M, Venning MC, Hamilton P, et al. Randomized trial of C5a receptor inhibitor avacopan in ANCA-associated vasculitis. *J Am Soc Nephrol* 2017;28:2756–67.
26. De Groot K, Rasmussen N, Bacon PA, Tervaert JW, Feighery C, Gregorini G, et al. Randomized trial of cyclophosphamide versus methotrexate for induction of remission in early systemic antineutrophil cytoplasmic antibody-associated vasculitis. *Arthritis Rheum* 2005;52:2461–9.
27. Hoffman GS, Leavitt RY, Kerr GS, Fauci AS. The treatment of Wegener's granulomatosis with glucocorticoids and methotrexate. *Arthritis Rheum* 1992;35:1322–9.
28. Buckley L, Guyatt G, Fink HA, Cannon M, Grossman J, Hansen KE, et al. 2017 American College of Rheumatology guideline for the prevention and treatment of glucocorticoid-induced osteoporosis. *Arthritis Rheumatol* 2017;69:1521–37.
29. Souza AW, Calich AL, Mariz HA, Ochtrop ML, Bacchiaga AB, Ferreira GA, et al. Recommendations of the Brazilian Society of Rheumatology for the induction therapy of ANCA-associated vasculitis. *Rev Bras Reumatol Engl Ed* 2017;57 Suppl:484–96.
30. Pneumococcal vaccination: summary of who and when to vaccinate. Centers for Disease Control and Prevention. 2020. URL: <https://www.cdc.gov/vaccines/vpd/pneumo/hcp/who-when-to-vaccinate.html>.
31. Walters G. Role of therapeutic plasmapheresis in ANCA-associated vasculitis. *Pediatr Nephrol* 2016;31:217–25.
32. Jayne DR, Gaskin G, Rasmussen N, Abramowicz D, Ferrario F, Guillevin L, et al. Randomized trial of plasma exchange or high-dosage methylprednisolone as adjunctive therapy for severe renal vasculitis. *J Am Soc Nephrol* 2007;18:2180–8.
33. Derebail VK, Falk RJ. ANCA-associated vasculitis—refining therapy with plasma exchange and glucocorticoids. *N Engl J Med* 2020;382: 671–2.
34. Specks U, Merkel PA, Seo P, Spiera R, Langford CA, Hoffman GS, et al. Efficacy of remission-induction regimens for ANCA-associated vasculitis. *N Engl J Med* 2013;369:417–27.
35. Walsh M, Flossmann O, Berden A, Westman K, Höglund P, Stegeman C, et al. Risk factors for relapse of antineutrophil cytoplasmic antibody-associated vasculitis. *Arthritis Rheum* 2012;64:542–8.
36. Karras A, Pagnoux C, Haubitz M, Groot K, Puechal X, Tervaert JW, et al. Randomised controlled trial of prolonged treatment in the remission phase of ANCA-associated vasculitis. *Ann Rheum Dis* 2017;76:1662–8.
37. Olson SW, Owshalimpur D, Yuan CM, Arbogast C, Baker TP, Oliver D, et al. Relation between asymptomatic proteinase 3 antibodies and future granulomatosis with polyangiitis. *Clin J Am Soc Nephrol* 2013;8:1312–8.
38. Finkelmann JD, Merkel PA, Schroeder DR, Hoffman GS, Spiera R, St. Clair EW, et al. Antiproteinase 3 antineutrophil cytoplasmic antibodies and disease activity in Wegener granulomatosis. *Ann Intern Med* 2007;147:611–9.
39. Kemna MJ, Damoiseaux J, Austen J, Winkens B, Peters J, van Paassen P, et al. ANCA as a predictor of relapse: useful in patients with renal involvement but not in patients with nonrenal disease. *J Am Soc Nephrol* 2015;26:537–42.
40. Fussner LA, Hummel AM, Schroeder DR, Silva F, Cartin-Ceba R, Snyder MR, et al. Factors determining the clinical utility of serial measurements of antineutrophil cytoplasmic antibodies targeting proteinase 3. *Arthritis Rheumatol* 2016;68:1700–10.
41. Watanabe H, Sada KE, Matsumoto Y, Harigai M, Amano K, Dobashi H, et al. Association between reappearance of myeloperoxidase-antineutrophil cytoplasmic antibody and relapse in antineutrophil cytoplasmic antibody-associated vasculitis: subgroup analysis of nationwide prospective cohort studies. *Arthritis Rheumatol* 2018;70:1626–33.
42. Charles P, Perrodeau E, Samson M, Bonnotte B, Neel A, Agard C, et al. Long-term rituximab use to maintain remission of antineutrophil cytoplasmic antibody-associated vasculitis: a randomized trial. *Ann Intern Med* 2020;173:179–87.
43. Guillevin L, Pagnoux C, Karras A, Khouatra C, Aumaitre O, Cohen P, et al. Rituximab versus azathioprine for maintenance in ANCA-associated vasculitis. *N Engl J Med* 2014;371:1771–80.
44. Barmettler S, Ong MS, Farmer JR, Choi H, Walter J. Association of immunoglobulin levels, infectious risk, and mortality with rituximab and hypogammaglobulinemia. *JAMA Netw Open* 2018;1:e184169.
45. Wade SD, Kyttaris VC. Rituximab-associated hypogammaglobulinemia in autoimmune rheumatic diseases: a single-center retrospective cohort study. *Rheumatol Int* 2021;41:1115–24.
46. Hiemstra TF, Walsh M, Mahr A, O'Savage C, de Groot K, Harper L, et al. Mycophenolate mofetil vs azathioprine for remission maintenance in antineutrophil cytoplasmic antibody-associated vasculitis: a randomized controlled trial. *JAMA* 2010;304:2381–8.
47. Jayne D, Rasmussen N, Andrassy KA, Bacon PA, Tervaert JW, Dadonienė J, et al. A randomized trial of maintenance therapy for vasculitis associated with antineutrophil cytoplasmic autoantibodies. *N Engl J Med* 2003;349:36–44.
48. Joy MS, Hogan SL, Jennette JC, Falk RJ, Nachman PH. A pilot study using mycophenolate mofetil in relapsing or resistant ANCA small vessel vasculitis. *Nephrol Dial Transplant* 2005;20:2725–32.
49. Koukoulaki M, Jayne D. Mycophenolate mofetil in anti-neutrophil cytoplasm antibodies-associated systemic vasculitis. *Nephron Clin Pract* 2006;102:100–7.
50. Silva F, Specks U, Kalra S, Hogan MC, Leung N, Sethi S, et al. Mycophenolate mofetil for induction and maintenance of remission in microscopic polyangiitis with mild to moderate renal involvement—a prospective, open-label pilot trial. *Clin J Am Soc Nephrol* 2010;5: 445–53.
51. Jones J, Faruqi A, Sullivan J, Calabrese C, Calabrese L. COVID-19 outcomes in patients undergoing B cell depletion therapy and those with humoral immunodeficiency states: a scoping review. *Pathog Immun* 2021;6:76–103.
52. Patel NJ, D'Silva KM, Hsu T, Dilorio M, Fu X, Cook C, et al. Coronavirus disease 2019 outcomes among recipients of anti-CD20 monoclonal antibodies for immune-mediated diseases: a comparative cohort study. *ACR Open Rheumatol* 2021;4:238–246.

53. Strangfeld A, Schäfer M, Gianfrancesco MA, Lawson-Tovey S, Liew JW, Ljung L, et al. Factors associated with COVID-19-related death in people with rheumatic diseases: results from the COVID-19 Global Rheumatology Alliance physician-reported registry. *Ann Rheum Dis* 2021;80:930–42.
54. Sparks JA, Wallace ZS, Seet AM, Gianfrancesco MA, Izadi Z, Hyrich KL, et al. Associations of baseline use of biologic or targeted synthetic DMARDs with COVID-19 severity in rheumatoid arthritis: results from the COVID-19 Global Rheumatology Alliance physician registry. *Ann Rheum Dis* 2021;80:1137–46.
55. Avouac J, Drumez E, Hachulla E, Seror R, Geogin-Lavialle S, El Mahou S, et al. COVID-19 outcomes in patients with inflammatory rheumatic and musculoskeletal diseases treated with rituximab: a cohort study. *Lancet Rheumatol* 2021;3:e419–26.
56. Sormani MP, De Rossi N, Schiavetti I, Carmisciano L, Cordioli C, Moiola L, et al. Disease-modifying therapies and coronavirus disease 2019 severity in multiple sclerosis. *Ann Neurol* 2021;89:780–9.
57. Gianfrancesco MA, Hyrich KL, Al-Adely S, Carmona L, Danila MI, Gossec L, et al. Characteristics associated with hospitalization for COVID-19 in people with rheumatic disease: data from the COVID-19 Global Rheumatology Alliance physician-reported registry. *Ann Rheum Dis* 2020;79:859–66.
58. Marques CD, Kakehasi AM, Pinheiro MM, Mota LM, Albuquerque CP, Silva CR, et al. High levels of immunosuppression are related to unfavourable outcomes in hospitalised patients with rheumatic diseases and COVID-19: first results of ReumaCoV Brasil registry. *RMD Open* 2021;7:e0014461.
59. Curtis JR, Johnson SR, Anthony DD, Arasaratnam RJ, Baden LR, Bass AR, et al. American College of Rheumatology Guidance for COVID-19 vaccination in patients with rheumatic and musculoskeletal diseases: version 1. *Arthritis Rheumatol* 2021;73:1093–07.
60. American College of Rheumatology. COVID-19 vaccine guidance summary for patients with rheumatic and musculoskeletal diseases. 2022. URL: <https://www.rheumatology.org/Portals/0/Files/COVID-19-Vaccine-Clinical-Guidance-Rheumatic-Diseases-Summary.pdf>.
61. US Food and Drug Administration. Coronavirus (COVID-19) update: FDA authorizes new long-acting monoclonal antibodies for pre-exposure prevention of COVID-19 in certain individuals. 2021. URL: <https://www.fda.gov/news-events/press-announcements/coronavirus-covid-19-update-fda-authorizes-new-long-acting-monoclonal-antibodies-pre-exposure>.
62. Charles P, Terrier B, Perrodeau E, Cohen P, Faguer S, Huart A, et al. Comparison of individually tailored versus fixed-schedule rituximab regimen to maintain ANCA-associated vasculitis remission: results of a multicentre, randomised controlled, phase III trial (MAINRITSAN2). *Ann Rheum Dis* 2018;77:1143–9.

EDITORIAL

Complement C4, the Major Histocompatibility Complex, and Autoimmunity

Timothy J. Vyse¹  and Betty P. Tsao²

For many autoimmune diseases, including systemic lupus erythematosus (SLE) and primary Sjögren's syndrome (SS), genome-wide association analyses (GWAS) reveal that the major histocompatibility complex (MHC) is the site of the strongest genetic association signals. These MHC associations have long been thought to arise from *HLA* alleles because of the role of these molecules in antigen presentation. One *HLA* allele showing a consistent association with autoimmune diseases is *HLA-DRB1*03:01* (*DR3*). The *DRB1*03:01* allele resides on an extended MHC haplotype, meaning that there is extensive correlation with co-inherited MHC alleles (1). The region of correlation (termed linkage disequilibrium [LD]) encompasses the entire classical MHC region from *HLA* class I through class III to *HLA* class II: specifically, from *HLA-B8* to *HLA-DQA1*05:01/DQB1*02:01*, which incorporates a common complement *C4A* null gene in class III. The complement *C4* locus is complex. There are 2 complement *C4* genes: *C4A* and *C4B*, which are coded adjacently in genomic regions and show marked DNA sequence similarity (homology). The 2 genes are subject to common structural variation with both gene deletions and gene duplications (2). These are outlined in Figure 1.

Such extensive LD and accompanying structural variation in the MHC have made identifying the causal genes very challenging. The *DRB1*03:01* allele (and by definition, all genetic variations that are correlated with it) has been associated with the following conditions: SLE, SS, myositis, type I diabetes mellitus, Addison's disease, Graves' disease, and myasthenia gravis. However, whether the causal genes on this extended region of the MHC are the same across these diseases or vary has been unclear. In SLE and SS, *HLA-DRB1*03:01* was associated with anti-SSA/Ro and anti-SSB/La production (3). These autoantibodies are not a feature of all diseases associated with this *HLA* allele. The same caveat applies to untangling this class of

HLA association from other potentially causal genetic factors in the MHC on the *DR3* haplotype.

Investigating the genetics of *C4* variation is technically difficult, because the changes in gene copy number cannot be determined using standard genotyping arrays that have been extensively used in GWAS. These arrays type single-nucleotide polymorphism (SNPs) but use the neighboring DNA sequence to accomplish this. In areas of extensive homology, the genotyping can therefore become inaccurate, and such regions are poorly represented on arrays and in GWAS. Thus, customized assays have been the tool to study the genetics of structurally complex areas of the genome. Traditionally, *C4* copy number was assayed using Southern blotting or complex quantitative polymerase chain reaction-based methods, but these are time-consuming and difficult to perform on a large scale.

Next-generation sequencing of the genome now provides new methods to investigate structural variation on a large scale. *C4A* and *C4B* can be distinguished by well characterized translated sequence differences. Combining metrics from sequencing that estimate the number of *C4* genes with 1 of the *C4A/C4B* ratio, the copy number of the 2 individual genes can be inferred. One such example is provided in the article by Lundtoft et al, in which the *C4* copy number is inferred by quantitative sequence representation after selection of the locus using hybridization (4). The authors describe an association of lower copy number of *C4A* with anti-SSA/SSB production in Swedish patients with SLE, primary SS, or myositis. They observe a dose-dependent association between *C4A* copy number and anti-SSA/SSB in all 3 diseases. Each decrease in copy number of *C4A* is associated with an increased risk of the production of both anti-SSA and anti-SSB (odds ratio [OR] 5.89 [95% confidence interval (95% CI) 4.83–7.23]), with the presence of either autoantibody (OR 2.37 [95% CI 2.02–2.77]), and with the absence of anti-SSA and anti-SSB (OR 1.53 [95% CI 1.36–1.73]) (4). However, the

¹Timothy J. Vyse, MA, FRCP, PhD, FMedSci: King's College London and Guy's Hospital, London, UK; ²Betty P. Tsao, PhD: Medical University of South Carolina, Charleston.

Author disclosures are available at <https://onlinelibrary.wiley.com/action/downloadSupplement?doi=10.1002%2Fart.42119&file=art42119-sup-0001-Disclosureform.pdf>.

Address correspondence to Timothy J. Vyse, MA, FRCP, PhD, FMedSci, King's College London, London SE1 9RT, UK. Email: timothy.vyse@kcl.ac.uk.

Submitted for publication March 1, 2022; accepted in revised form March 15, 2022.

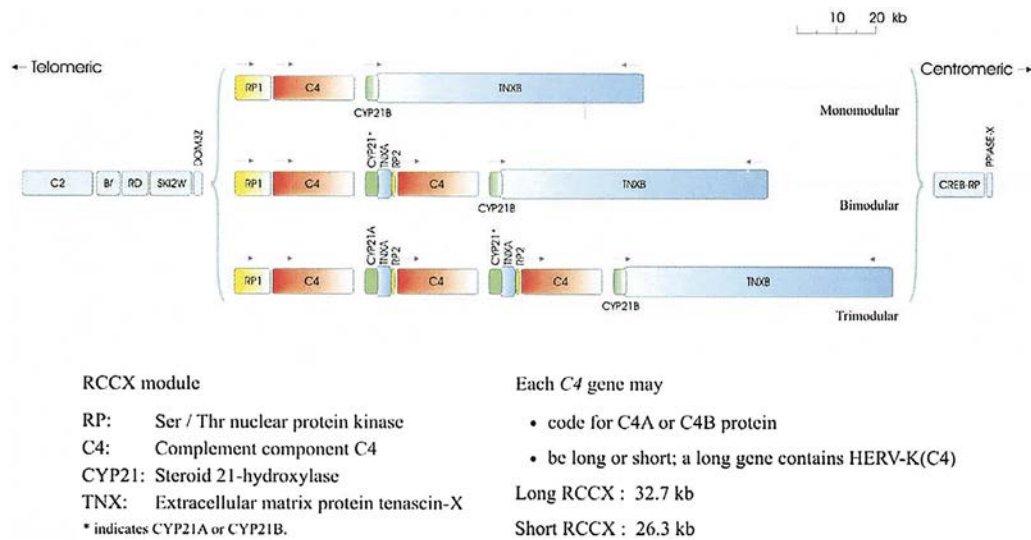


Figure 1. Variation at the C4 locus in the major histocompatibility complex class II region. The central arrangement with 2 C4 genes, C4A and C4B, was the most frequently observed pattern. Each homologous unit containing C4 is termed an RCCX module as an acronym of gene names; duplications and deletions of these RCCX modules are common. The functional gene within the duplicated segments is C4A or C4B.

question of whether this is driven by the complement gene remains unproven in this analysis based on these observations alone, due to the extensive LD described above.

An alternative strategy, using next-generation sequencing, can be used to study structural variation at the MHC. By analyzing whole-genome sequencing data, one can establish the relationship between the various forms of structural variation with genetic variants that flank the segmental C4 homologous regions. Such flanking regions will be represented on standard genotyping arrays. Essentially, sets of genetic variants that are genotyped on standard genotyping arrays can be used to infer the gene copy number of C4, because there is sufficient correlation between the structural variants and sets of variants in the adjacent MHC class III region (5). This approach has the great advantage that the imputed genetic variation of the C4 genes can be combined with genetic variation across the MHC. Although genotyping arrays do not directly genotype HLA alleles, the process of imputing HLA alleles from nearby SNP genotyping is well established (6).

Even if one can generate reliable C4 genetic data and combine this with genetic data from the MHC, the problem of LD remains. Importantly, the pattern of such correlation across the genome shows differences between ancestries. This observation was made recently in a study examining MHC associations in SLE with 1 cohort with European ancestry and another with African American ancestry (7). The LD was much less extensive in the African genome at the MHC compared to other common ancestries, and this greatly facilitated resolution of the genetic associations. Using imputation, all of the common haplotypes carrying the C4 variation could be imputed. That study confirmed the association of a lack of C4 with SLE (and primary SS), with C4A protecting more strongly than C4B in both illnesses. Comparing

European and African data, it was also shown that the association signals in SLE can best be explained by signals arising from copy number variation of C4 in the MHC locus and by a shared region in the class II region on HLA-DRB1*15:01 (in those with European ancestry) and HLA-DRB1*15:03 (in those with African ancestry) that likely operates to elevate HLA class II gene expression. These results corroborate a previous finding that HLA class II gene regulation contributes to MHC associations in SLE (8).

In schizophrenia, elevated C4 copy number is associated with an elevated disease risk, whereas in SLE and SS, lower copy numbers of C4 genes correlate with a higher disease risk (5). In all 3 illnesses, C4 alleles act more strongly in men than in women; common combinations of C4A and C4B generated 14-fold variation in the risk for lupus and 31-fold variation in the risk for SS in men (versus 6-fold and 15-fold among women, respectively), and it affected schizophrenia risk about twice as strongly in men as in women. At a protein level, both C4 and its effector (C3) were present at greater levels in men than women in cerebrospinal fluid ($P < 10^{-5}$ for both C4 and C3) and plasma among adults ages 20–50 years, corresponding to the ages of differential disease vulnerability. Sex differences in complement protein levels may help explain the larger effects of C4 alleles in men, women's greater risk of SLE and SS, and men's greater vulnerability to schizophrenia. These findings suggest that the complement system is a source of sexual dimorphism in vulnerability to diverse illnesses.

While C4A and C4B are 99% homologous, the genetic association of anti-SSA/SSB autoantibody production is stronger with a lower copy number of C4A than C4B. To understand their functional differences and the mechanism by which partial loss of C4 (C4A or C4B) promotes autoimmunity, Simoni et al used elegant

mouse experiments to show preferential effects of *C4A* on B cell tolerance (9). In the transgenic 564Igi autoreactive B cell mouse model (rearranged Ig heavy- and light-chain transgenes encoding IgG autoantibodies to nucleolar antigens) that has the murine *C4* locus modified to express either human *C4A* or *C4B*, human *C4A* expression reduces humoral autoimmunity more effectively than *C4B* due to greater efficiency of *C4A* in inducing self-antigen clearance associated with the follicular exclusion of autoreactive B cells.

Why anti-SSA and anti-SSB are preferentially associated with the MHC has been a fascinating question. SSA includes the following: SSA1 (Ro 52, also known as tripartite motif-containing 21), a cytosolic E3 ubiquitin ligase and antibody receptor with roles in multiple cellular processes, including antiviral functions (10,11); SSA2 (Ro 60), a ribonucleoprotein that resides in both cytoplasm and the nucleus with multiple functions, including binding to endogenous *Alu* retroelements which are induced by type I interferon and stimulate proinflammatory cytokine secretion (12); and SSB (small RNA binding exonuclease protection factor, La), a nuclear ribonucleoprotein with diverse functions including protection of nascent RNA polymerase III transcripts from exonuclease digestion (Gene ID: 6741). All 3 autoantigens showed subcellular redistribution to localize in apoptotic blebs (13). The development of autoantibodies to SSA/SSB occur before clinical onset of SLE (14,15) and SS (16,17), often among the first detectable wave of autoantibodies.

It is noteworthy that in SLE the 2 MHC genetic risk factors now identified (loss of *C4* and generic up-regulation of *HLA* class II) would not be expected to confer autoantigen specificity. Given the plethora of autoantibodies generated in SLE, this makes some intuitive sense. Why anti-SSA and anti-SSB are preferentially associated with the MHC remains unanswered. Is this seemingly specific association driven by other immunologic mechanisms relevant to SS, or does it have a mechanistic link with the MHC genetic findings? Perhaps there is some interaction between complement and the SSA/Ro antigen, which may be unique given its early appearance in pathology. Does inherited partial complement deficiency predispose one to any of the other autoimmune diseases that are associated with the *DR3* haplotype? As ever, new discoveries foster new and interesting questions.








AUTHOR CONTRIBUTIONS

Drs. Vyse and Tsao drafted the article, revised it critically for important intellectual content, and approved the final version to be published.

REFERENCES

- Dawkins RL, Leaver A, Cameron PU, Martin E, Kay PH, Christiansen FT. Some disease-associated ancestral haplotypes carry a polymorphism of TNF. *Hum Immunol* 1989;26:91–7.
- Chung EK, Yang Y, Rennebohm RM, Lokki ML, Higgins GC, Jones KN, et al. Genetic sophistication of human complement components *C4A* and *C4B* and RP-*C4*-CYP21-TNX (RCCX) modules in the major histocompatibility complex. *Am J Hum Genet* 2002;71:823–37.
- Morris DL, Fernando MM, Taylor KE, Chung SA, Nititham J, Alarcón-Riquelme ME, et al, on behalf of the Systemic Lupus Erythematosus Genetics Consortium. MHC associations with clinical and autoantibody manifestations in European SLE. *Genes Immun* 2014;15:210–7.
- Lundtoft C, Pucholt P, Martin M, Bianchi M, Lundström E, Eloranta ML, et al. Complement *C4* copy number variation is linked to SSA/Ro and SSB/La autoantibodies in systemic inflammatory autoimmune diseases. *Arthritis Rheumatol* 2022;74:1440–50.
- Sekar A, Bialas AR, de Rivera H, Davis A, Hammond TR, Kamitaki N, et al, on behalf of the Schizophrenia Working Group of the Psychiatric Genomics Consortium. Schizophrenia risk from complex variation of complement component 4. *Nature* 2016;530:177–83.
- Morris DL, Taylor KE, Fernando MM, Nititham J, Alarcón-Riquelme ME, Barcellos LF, et al, on behalf of the International MHC and Autoimmunity Genetics Network and the Systemic Lupus Erythematosus Genetics Consortium. Unraveling multiple MHC gene associations with systemic lupus erythematosus: model choice indicates a role for HLA alleles and non-HLA genes in Europeans. *Am J Hum Genet* 2012;91:778–93.
- Kamitaki N, Sekar A, Handsaker RE, de Rivera H, Tooley K, Morris DL, et al, on behalf of the Schizophrenia Working Group of the Psychiatric Genomics Consortium. Complement genes contribute sex-biased vulnerability in diverse disorders. *Nature* 2020;582:577–581.
- Raj P, Rai E, Song R, Khan S, Wakeland BE, Viswanathan K, et al. Regulatory polymorphisms modulate the expression of HLA class II molecules and promote autoimmunity. *Elife* 2016;5:e12089.
- Simoni L, Presumey J, van der Poel CE, Castrillon C, Chang SE, Utz PJ, et al. Complement *C4A* regulates autoreactive B cells in murine lupus. *Cell Rep* 2020;33:108330.
- Jones EL, Laidlaw SM, Dustin LB. TRIM21/Ro52 - roles in innate immunity and autoimmune disease. *Front Immunol* 2021;12:738473.
- Foss S, Bottermann M, Jonsson A, Sandlie I, James LC, Andersen JT. TRIM21—from intracellular immunity to therapy. *Front Immunol* 2019;10:2049.
- Hung T, Pratt GA, Sundararaman B, Townsend MJ, Chaivorapol C, Bhangale T, et al. The Ro60 autoantigen binds endogenous retroelements and regulates inflammatory gene expression. *Science* 2015;350:455–9.
- Ohlsson M, Jonsson R, Brokstad KA. Subcellular redistribution and surface exposure of the Ro52, Ro60 and La48 autoantigens during apoptosis in human ductal epithelial cells: a possible mechanism in the pathogenesis of Sjögren's syndrome. *Scand J Immunol* 2002;56:456–69.
- Arbuckle MR, McClain MT, Rubertone MV, Scofield RH, Dennis GJ, James JA, et al. Development of autoantibodies before the clinical onset of systemic lupus erythematosus. *N Engl J Med* 2003;349:1526–33.
- Eriksson C, Kokkonen H, Johansson M, Hallmans G, Wadell G, Rantapää-Dahlqvist S. Autoantibodies predate the onset of systemic lupus erythematosus in northern Sweden. *Arthritis Res Ther* 2011;13:R30.
- Theander E, Jonsson R, Sjöström B, Brokstad K, Olsson P, Henriksson G. Prediction of Sjögren's syndrome years before diagnosis and identification of patients with early onset and severe disease course by autoantibody profiling. *Arthritis Rheumatol* 2015;67:2427–36.
- Jonsson R, Theander E, Sjöström B, Brokstad K, Henriksson G. Autoantibodies present before symptom onset in primary Sjögren syndrome. *JAMA* 2013;310:1854–5.

Immunogenicity and Safety of Standard and Third-Dose SARS-CoV-2 Vaccination in Patients Receiving Immunosuppressive Therapy

Silje W. Syversen,¹  Ingrid Jyssum,² Anne T. Tveter,¹  Trung T. Tran,³ Joseph Sexton,¹ Sella A. Provan,¹ 
Siri Mjaaland,⁴ David J. Warren,³ Tore K. Kvien,²  Gunnveig Grødeland,⁵ Lise S. H. Nissen-Meyer,³ Petr Ríčanek,⁶
Adity Chopra,³ Ane M. Andersson,⁵  Grete B. Kro,³ Jørgen Jahnsen,⁷ Ludvig A. Munthe,⁵ Espen A. Haavardsholm,²
John T. Vaage,⁵ Fridtjof Lund-Johansen,⁵ Kristin K. Jørgensen,⁶  and Guro L. Goll¹ 

Objective. Immunogenicity and safety following receipt of the standard SARS-CoV-2 vaccination regimen in patients with immune-mediated inflammatory diseases (IMIDs) are poorly characterized, and data after receipt of the third vaccine dose are lacking. The aim of the study was to evaluate serologic responses and adverse events following the standard 2-dose regimen and a third dose of SARS-CoV-2 vaccine in IMID patients receiving immunosuppressive therapy.

Methods. Adult patients receiving immunosuppressive therapy for rheumatoid arthritis, spondyloarthritis, psoriatic arthritis, Crohn's disease, or ulcerative colitis, as well as healthy adult controls, who received the standard 2-dose SARS-CoV-2 vaccination regimen were included in this prospective observational study. Analyses of antibodies to the receptor-binding domain (RBD) of the SARS-CoV-2 spike protein were performed prior to and 2–4 weeks after vaccination. Patients with a weak serologic response, defined as an IgG antibody titer of ≤ 100 arbitrary units per milliliter (AU/ml) against the receptor-binding domain of the full-length SARS-Cov-2 spike protein, were allotted a third vaccine dose.

Results. A total of 1,505 patients (91%) and 1,096 healthy controls (98%) had a serologic response to the standard regimen ($P < 0.001$). Anti-RBD antibody levels were lower in patients (median 619 AU/ml interquartile range [IQR] 192–4,191) than in controls (median 3,355 AU/ml [IQR 896–7,849]) ($P < 0.001$). The proportion of responders was lowest among patients receiving tumor necrosis factor inhibitor combination therapy, JAK inhibitors, or abatacept. Younger age and receipt of messenger RNA-1273 vaccine were predictors of serologic response. Of 153 patients who had a weak response to the standard regimen and received a third dose, 129 (84%) became responders. The vaccine safety profile among patients and controls was comparable.

Conclusion. IMID patients had an attenuated response to the standard vaccination regimen as compared to healthy controls. A third vaccine dose was safe and resulted in serologic response in most patients. These data facilitate identification of patient groups at risk of an attenuated vaccine response, and they support administering a third vaccine dose to IMID patients with a weak serologic response to the standard regimen.

INTRODUCTION

The ongoing COVID-19 pandemic is a global health emergency. Vaccines are important in resolving this crisis, having been

proven to be efficacious and safe in the general population (1–4). Vaccines, however, rely on a functional immune system. Patients with immune-mediated inflammatory disease (IMID), including inflammatory joint and bowel diseases, have impaired immune

[ClinicalTrials.gov](https://clinicaltrials.gov) identifier: NCT04798625. EudraCT database no. 2021-003618-37.

The Norwegian Study of Vaccine Response to COVID-19 (Nor-vaC) was an investigator-initiated study with no initial funding. During its conduct, study grants were received from the Coalition for Epidemic Preparedness Innovations (CEPI), the K. G. Jebsen Foundation, Dr. Trygve Gythfeldt og frues Foundation, the Karin Fossum Foundation, Diakonhjemmet Hospital Research Foundation, Oslo University Hospital, the University of Oslo, and the South-eastern Norway Regional Health Authority.

¹Silje W. Syversen, MD, PhD, Anne T. Tveter, PhD, Joseph Sexton, PhD, Sella A. Provan, MD, PhD, Guro L. Goll, MD, PhD: Diakonhjemmet Hospital,

Oslo, Norway; ²Ingrid Jyssum, MD, Tore K. Kvien, MD, PhD, Espen A. Haavardsholm, MD, PhD: Diakonhjemmet Hospital and University of Oslo, Oslo, Norway; ³Trung T. Tran, PhD, David J. Warren, PhD, Lise S. H. Nissen-Meyer, MD, PhD, Adity Chopra, PhD, Grete B. Kro, MD, PhD: Oslo University Hospital, Oslo, Norway; ⁴Siri Mjaaland, PhD: Norwegian Institute of Public Health, Oslo, Norway; ⁵Gunnveig Grødeland, PhD, Ane M. Andersson, MD, Ludvig A. Munthe, MD, PhD, John T. Vaage, MD, PhD, Fridtjof Lund-Johansen, MD, PhD: Oslo University Hospital and University of Oslo, Oslo, Norway; ⁶Petr Ríčanek, MD, PhD, Kristin K. Jørgensen, MD, PhD: Akershus University Hospital, Lørenskog, Norway; ⁷Jørgen Jahnsen, MD, PhD: University of Oslo, Oslo, and Akershus University Hospital, Lørenskog, Norway.

systems due to treatment with immunosuppressive medications. There is a concern that immune responses to SARS-CoV-2 vaccines are attenuated in this large patient population, which is also at risk of severe COVID-19 (5,6). Patients with IMIDs were prioritized for vaccination to mitigate their COVID-19 risk, but because they were excluded from initial vaccine trials, there is a paucity of data on the efficacy and safety of SARS-CoV-2 vaccines in this population (1,2,7), as well as concerns regarding the risk of disease flares (5,8).

Rheumatoid arthritis (RA), spondyloarthritis (SpA), psoriatic arthritis (PsA), Crohn's disease (CD), and ulcerative colitis (UC) are different IMIDs, but they share several key features and are treated with many of the same immunosuppressive medications, such as tumor necrosis factor inhibitors (TNFi), non-TNFi biologics, metabolite inhibitors, and targeted small molecule drugs (9). It is important to identify which patients are at risk of a reduced vaccine response, due to either immunosuppression or underlying disease, yet it is still unclear whether the serologic response to vaccine among IMID patients should be monitored. In addition, no consensus currently exists on whether it would be beneficial to delay specific treatments in patients receiving vaccination (7). Observational studies of response to SARS-CoV-2 vaccine among IMID patients have been published recently, but they have generally involved few patients within each medication group (5,10–15).

The utility of 3 or more SARS-CoV-2 vaccine doses in immunosuppressed patients, as well as in the general population, is an urgent question in the global medical community and for policy makers (16,17). Findings of a recent study suggested that immunocompromised recipients of a solid organ transplant benefited from a third vaccine dose (18). Apart from a study of a third dose of vaccine in rituximab-treated RA patients, only a case report and small studies (involving 33 or 17 participants) have been published regarding the immunogenicity and safety of a third dose in IMID patients who were receiving other therapies and had no response to the 2-dose vaccination regimen (19–24). The prospective, observational Norwegian Study of Vaccine Response to COVID-19 (Nor-vaC) includes patients with any of 5 different IMIDs who are receiving any approved immunosuppressive medication. In this study, we evaluate the immunogenicity and safety of the standard 2-dose SARS-CoV-2 vaccination regimen in these groups and examine the response to a third vaccine dose in patients with a weak serologic response to the standard regimen.

PATIENTS AND METHODS

Participants, setting, and study design. Nor-vaC is an ongoing longitudinal observational study conducted at 2 Norwegian IMID referral centers: the Division of Rheumatology at Diakonhjemmet Hospital and the Department of Gastroenterology at Akershus University Hospital. Adult patients (age ≥ 18 years) with RA, SpA, PsA, UC, or CD who used any of the immunosuppressive medications of interest (Supplementary Materials, available on the *Arthritis & Rheumatology* website at <http://onlinelibrary.wiley.com/doi/10.1002/art.42153>) and intended to receive a SARS-CoV-2 vaccine were consecutively recruited into the study. All patients identified by hospital records as eligible for enrollment, based on a diagnosis of an IMID of interest, received an invitation to participate in the study prior to the initiation of the national vaccination program in February 2021. Healthy controls were either volunteer health care workers from Diakonhjemmet Hospital, Akershus University Hospital, and Oslo University Hospital or blood donors from Oslo University Hospital. In the present analyses, we included patients and healthy controls who provided blood specimens for serologic testing 2–4 weeks after receiving the second vaccine dose (Supplementary Figure 1, available on the *Arthritis & Rheumatology* website at <http://onlinelibrary.wiley.com/doi/10.1002/art.42153>). Patients with COVID-19 diagnosed before the second dose received only 1 dose of the standard vaccination regimen and were also included in the study.

Patients receiving CD20-depleting therapy were not included in the present analyses (Supplementary Figure 1). The study (ClinicalTrials.gov identifier: NCT04798625) was approved by an independent ethics committee (Regional Committees for Medical Research Ethics South East Norway, reference numbers 235424, 135924, and 204104) and by appropriate institutional review boards. All participants provided written informed consent.

During the Nor-vaC study, patients with a weak serologic response >3 weeks after completing the standard 2-dose regimen were recruited into a separate intervention study (EudraCT database no. 2021-003618-37) and allotted a third vaccine dose in July–August 2021. The cutoff for a weak serologic response (i.e., an IgG antibody level of ≤ 100 arbitrary units per milliliter [AU/ml] against the receptor-binding domain [RBD] of the full-length SARS-Cov-2 spike protein) when selecting patients qualifying for a third vaccine dose was based on discussions within the study group and with the Norwegian Institute of Public Health, with the aim of including not only patients with no response

Drs. Syversen and Jyssum contributed equally to this work. Drs. Vaage, Lund-Johansen, Jørgensen, and Goll contributed equally to this work.

A deidentified patient data set can be made available to researchers upon reasonable request. The data will only be made available after submission of a project plan outlining the reason for the request and any proposed analyses, and it will have to be approved by the Nor-vaC steering group. Project proposals can be submitted to the corresponding author. Data sharing will have to follow appropriate regulations.

Author disclosures are available at <https://onlinelibrary.wiley.com/action/downloadSupplement?doi=10.1002%2Fart.42153&file=art42153-sup-0001-Disclosureform.pdf>.

Address correspondence to Guro L. Goll, MD, PhD, Center for Treatment of Rheumatic and Musculoskeletal Diseases, Diakonhjemmet Hospital, PO Box 23 Vinderen, N-0319 Oslo, Norway. Email: GuroLovik.Goll@diakonshj.no.

Submitted for publication December 12, 2021; accepted in revised form April 28, 2022.

(i.e., an antibody level of <70 AU/ml) but also those with an impaired response (i.e., an antibody level of ≤100 AU). In the present observational study, the serologic response following receipt of a third dose is reported for 153 such patients. Those with inflammatory joint diseases (i.e., RA, SpA, and PsA), but not those with inflammatory bowel diseases (IBDs) (i.e., CD and UC), were asked to pause their medication from 1 week before through 2 weeks after receipt of the third vaccine dose.

Exposures. All patients and controls received SARS-CoV-2 vaccines according to the Norwegian national

vaccination program, administered by the Norwegian Institute of Public Health. Three SARS-CoV-2 vaccine types were available: ChAdOx1 and the messenger RNA (mRNA) vaccines BNT162b2 and mRNA-1273. The 2 mRNA vaccines were given with an interval of 3–6 weeks between the 2 doses. ChAdOx1 was withdrawn from the Norwegian national vaccination program in March 2021, and all persons who had received 1 dose of this vaccine received one of the mRNA vaccines as the second dose. According to the program, persons with COVID-19 diagnosed before the second dose received only 1 dose of the standard vaccination regimen.

Table 1. Baseline characteristics of IMID patients and healthy controls who received a standard 2-dose SARS-CoV-2 vaccination regimen and IMID patients who received a third dose*

Characteristic	Patients		Healthy controls (n = 1,114)
	Overall (n = 1,647)	Third-dose recipients (n = 153)	
Age, median years (IQR)	52 (40–63)	57 (46–67)	43 (32–55)
Sex			
Female	899 (55)	80 (52)	854 (77)
Male	748 (45)	73 (48)	260 (23)
CRP level, median mg/dl (IQR)	1 (1–3)	1 (1–4)	No data
BMI, median kg/m ² (IQR)	26 (23–29)	26 (24–29)	No data
IMID			
Joint			
Rheumatoid arthritis	566 (34)	52 (34)	NA
Psoriatic arthritis	295 (18)	21 (14)	NA
Spondyloarthritis	305 (19)	16 (10)	NA
Bowel			
Ulcerative colitis	195 (12)	17 (11)	NA
Crohn's disease	280 (17)	47 (31)	NA
Medication			
TNFi†			
Monotherapy	696 (42)	46 (30)	NA
Combination therapy	386 (23)	52 (34)	NA
Methotrexate	348 (21)	27 (18)	NA
Vedolizumab	55 (3)	7 (5)	NA
JAK inhibitor	50 (3)	11 (7)	NA
Ustekinumab	34 (2)	3 (2)	NA
Tocilizumab	32 (2)	2 (1)	NA
Abatacept	15 (1)	4 (3)	NA
Secukinumab	13 (1)	1 (1)	NA
Other‡	18 (1)	0	NA
Prednisolone comedication			
Overall	71 (4)	16 (10)	NA
Dose ≤7.5 mg	61/71 (86)	13/16 (81)	NA
Vaccine related§			
BNT162b2 regimen, 2 doses	1,152 (70)	131 (86)	625 (56)
mRNA-1273 regimen, 2 doses	401 (24)	14 (9)	246 (22)
Combination regimen, 2 doses	71 (4)	4 (3)	243 (22)
COVID-19 and 1 of any mRNA vaccine	23 (1)	4 (3)	0

* Except where indicated otherwise, values are no. (%) of patients or controls. IMID = immune-mediated inflammatory disease; IQR = interquartile range; CRP = C-reactive protein; BMI = body mass index; NA = not applicable.

† Monotherapy consisted of infliximab, etanercept, adalimumab, golimumab, or certolizumab pegol. Combination therapy consisted of methotrexate, sulfasalazine, leflunomide, or azathioprine, in addition to any tumor necrosis factor inhibitor (TNFi).

‡ Data are for sulfasalazine, leflunomide, azathioprine, risankizumab, and prednisolone monotherapy, each of which was received by <10 patients.

§ BNT162b2 and mRNA-1273 are messenger RNA (mRNA) vaccines. Combination regimen was defined as ChAdOx1 (first dose) + BNT162b2 or mRNA-1273 (second dose) or as BNT162b2 + mRNA-1273 in any sequence.

Assessments. Patients and controls were asked to provide serum samples prior to the first vaccine dose and 2–4 weeks after the second and third vaccine doses, respectively. Assessments of immunogenicity were performed at the Department of Immunology at Oslo University Hospital. The samples were first screened for antibodies to RBD at the full-length spike protein by using an in-house bead-based method, with seroconversion defined as an anti-RBD antibody level ≥ 5 AU (25,26). Measurement of the World Health Organization international standard for anti-RBD antibody showed that the screening assay has a lower detection limit of 1 binding antibody unit per milliliter (BAU/ml) and an upper dynamic range of ~ 100 BAU/ml. For quantification of antibody levels, most patient samples and a representative selection of control samples

(Supplementary Table 1) were thereafter analyzed using a second assay, with a dynamic range of 300–10,000 BAU (25). In this assay, effects of sera on binding of angiotensin-converting enzyme 2 to RBDs from SARS-CoV-2 variants were measured as a proxy for neutralizing antibody activity (25).

The cutoff for response was preset to an anti-RBD antibody level of 70 AU/ml, based on results obtained from healthy individuals, of whom 98% had levels >70 AU/ml after receipt of 2 vaccine doses (27). Moreover, calibration to the World Health Organization international standard showed that 70 AU/ml corresponds to ~ 40 BAU/ml. Using a SARS-CoV-2 (Wuhan) microneutralization assay, we have determined that 200 BAU/ml is the lower threshold for detection of neutralizing antibodies (28).

Table 2. Serologic response to the standard 2-dose SARS-CoV-2 vaccination regimen among healthy controls and among IMID patients overall and by clinical and demographic characteristic*

Population, characteristic	Response, proportion (%)	OR (95% CI)	P	Anti-RBD IgG level, median AU/ml (IQR)
Healthy controls	1,096/1,114 (98)	1	–	3,355 (896–7,849)
Patients, characteristic				
Overall	1,504/1,647 (91)	0.19 (0.11–0.32)	<0.001	619 (192–4,191)
IMID				
Joint				
Rheumatoid arthritis	503/566 (89)	0.16 (0.08–0.29)	<0.001	548 (194–4,311)
Psoriatic arthritis	286/295 (97)	0.19 (0.09–0.41)	<0.001	652 (215–4,501)
Spondyloarthritis	271/305 (89)	0.17 (0.08–0.36)	<0.001	689 (225–3,893)
Bowel				
Ulcerative colitis	184/195 (94)	0.13 (0.06–0.26)	<0.001	1,403 (219–5,940)
Crohn's disease	255/280 (91)	0.19 (0.08–0.45)	<0.001	409 (155–2,262)
Medication				
TNFi†				
Monotherapy	664/696 (95)	0.3 (0.15–0.57)	<0.001	726 (225–4,293)
Combination therapy	332/386 (86)	0.08 (0.04–0.15)	<0.001	312 (120–2,178)
Methotrexate	317/348 (91)	0.2 (0.09–0.42)	<0.001	709 (206–4,670)
Vedolizumab	52/55 (95)	0.31 (0.08–1.21)	0.091	2,415 (412–10,177)
JAK inhibitor	39/50 (78)	0.05 (0.02–0.12)	<0.001	361 (45–4,204)
Tocilizumab	32/32 (100)	–	–	956 (356–4,578)
Ustekinumab	32/34 (94)	0.19 (0.04–0.99)	0.049	3,286 (281–8,097)
Abatacept	8/15 (53)	0.01 (0–0.04)	<0.001	70 (38–138)
Secukinumab	11/13 (85)	0.2 (0.03–1.25)	0.086	1,165 (276–1,456)
Other‡	16/18 (89)	–	–	2,907 (391–8,981)
Vaccine related§				
BNT162b2 regimen, 2 doses	1,026/1,152 (89)	–	–	408 (170–2,205)
mRNA-1273 regimen, 2 doses	391/401 (98)	–	–	2,308 (377–8,812)
Combination regimen, 2 doses	65/71 (92)	–	–	699 (272–4,253)
COVID-19 and 1 of any mRNA vaccine	22/23 (96)	–	–	6,969 (878–10,768)
Other				
Age, years				
<30	169/176 (96)	–	–	2,247 (418–7,536)
30–65	1,070/1,155 (93)	–	–	667 (192–4,175)
>65	265/316 (84)	–	–	329 (155–1,838)
Female sex	826/899 (92)	–	–	682 (197–4,639)
Current smoker	143/157 (91)	–	–	446 (168–1,809)

* Response was defined as an IgG antibody level of ≥ 70 AU/ml against the receptor-binding domain (RBD) of SARS-CoV-2 spike protein, and it was evaluated using logistic regression analysis (adjusted for age, sex, and vaccine type), with healthy controls as the reference group. OR = odds ratio; 95% CI = 95% confidence interval; AU = arbitrary units (see Table 1 for other definitions).

† Monotherapy consisted of infliximab, etanercept, adalimumab, golimumab, or certolizumab pegol. Combination therapy consisted of methotrexate, sulfasalazine, leflunomide, or azathioprine, in addition to any TNFi.

‡ Data are for sulfasalazine, leflunomide, azathioprine, risankizumab, and prednisolone monotherapy, each of which was received by <10 patients.

§ BNT162b2 and mRNA-1273 are mRNA vaccines. Combination regimen was defined as ChAdOx1 (first dose) + BNT162b2 or mRNA-1273 (second dose) or as BNT162b2 + mRNA-1273 in any sequence.

The Norwegian Immunization Registry and Norwegian Surveillance System for Communicable Diseases provided information on the date of vaccination, the type of vaccine received, and, when applicable, the date of COVID-19 (29,30). Additionally, information regarding COVID-19 was also obtained from patient questionnaires.

Electronic data collection at Diakonhjemmet Hospital was conducted using the Services for Sensitive Data platform (University of Oslo), and by Viedoc, version 4 (Viedoc Technologies), at Akershus University Hospital. Demographic data were collected at baseline only, while data on medication use, patient-reported disease activity, and responses to COVID-19-related questions were also collected during follow-up. For healthy controls, age and sex were recorded. Disease activity scores (i.e., the Disease Activity Score in 28 joints [DAS28] for patients with RA and patients with PsA, the Ankylosing Spondylitis Disease Activity Score for patients with SpA, the Harvey-Bradshaw Index for CD, and the Partial Mayo Scoring Index for patients with UC) (31–34) were obtained at the baseline visit for patients with IBD and retrieved from the medical records for patients with inflammatory joint disease (i.e., from a clinic visit within 3 months before or after receipt of the first vaccine dose). Adverse events were reported ~14 days after receipt of the first, second, and third doses in all patients and in a subset ($n = 245$) of the healthy controls (i.e., health care workers from Diakonhjemmet Hospital and Akershus University Hospital).

Objectives and outcomes. The 2 main objectives of this study were 1) to assess humoral responses to standard SARS-CoV-2 vaccination in IMID patients receiving immunosuppressive therapy as compared to that in healthy controls, and 2) to assess changes in humoral responses after a third vaccine dose given to IMID patients with weak serologic responses to standard vaccination. Other objectives were to assess the safety of the standard regimen and the third dose and to identify predictors of serologic response in patients. The main end points were 1) the proportion of participants with a serologic response (i.e., an anti-RBD antibody level >70 AU/ml) and the anti-RBD antibody level following the standard regimen and third dose and 2) the change in levels of anti-RBD antibody after receipt of the third dose. Other end points included adverse events and predictors of the serologic response to the standard regimen and the third dose.

Statistical analysis. Demographic data, adverse events, and serologic response according to medication group were summarized using descriptive statistics. Comparisons of the serologic response between patients and controls were performed by logistic regression. Adjustments were made for sex, age, and vaccine type. Comparisons of anti-RBD antibody level between patients and healthy controls were performed using the Mann-Whitney U test. Pre-vaccination and post-vaccination samples collected from patients receiving a third dose were compared

by the Wilcoxon's signed rank test for paired samples. There were no missing data for the main variables. Predictors of response among patients were assessed by univariable and multivariable logistic regression. All tests were 2-sided, and P values of less than 0.05 were considered statistically significant. All analyses were performed using R, release 4.0.3.

RESULTS

Patient and control characteristics. Between February 2, 2021, and June 11, 2021, a total of 2,178 patients were included in the Nor-vaC study. A total of 1,647 eligible patients (566 with RA, 305 with SpA, 295 with PsA, 280 with CD, and 195 with UC; median age 52 years [interquartile range (IQR) 40–63]; female sex, 899 [55%]) and 1,114 healthy controls (median age 43 years [IQR 32–55]; female sex, 854 [77%]) underwent serologic testing after receipt of the standard 2-dose vaccination regimen and were included in the present analyses. Patient disposition is summarized in Supplementary Figure 1, available on the *Arthritis & Rheumatology* website at <http://onlinelibrary.wiley.com/doi/10.1002/art.42153>. Baseline characteristics of patients and controls are shown in Table 1 and Supplementary Tables 1 and 2, available at <http://onlinelibrary.wiley.com/doi/10.1002/art.42153>. The most common immunosuppressive medications were TNFi ($n = 1,082$ patients) and methotrexate monotherapy ($n = 348$). Seventy percent of patients and 56% of controls received BNT162b2 for doses 1 and 2. In total, 23 patients (1%) had COVID-19 before the second dose and received only the first of 2 doses in the standard vaccination regimen. Controls were included in this study only if they had received 2 vaccine doses and had no signs or symptoms consistent with clinical COVID-19.

Humoral response to the standard regimen. A total of 1,628 patients (98.8%) receiving immunosuppressive therapy and 1,110 healthy controls (99.6%) had detectable antibodies to SARS-CoV-2 (level, >5 AU/ml) after receiving the standard 2-dose vaccination regimen (Supplementary Figures 1A and B, available on the *Arthritis & Rheumatology* website at <http://onlinelibrary.wiley.com/doi/10.1002/art.42153>). In this population, 1,493 patients (91%) as compared to 1,096 healthy controls (98%) had anti-RBD antibody levels ≥ 70 AU/ml and were considered serologic responders ($P < 0.001$) (Table 2 and Supplementary Figures 1A and 1B, available at <http://onlinelibrary.wiley.com/doi/10.1002/art.42153>). Response was detected in $\geq 90\%$ of patients receiving methotrexate, TNFi monotherapy, ustekinumab, tocilizumab, or vedolizumab, in 80–90% of patients receiving TNFi combination therapy or secukinumab, and in $\leq 80\%$ receiving JAK inhibitors (78%) or abatacept (53%) (Table 2). To obtain more precise information about antibody levels, samples were reanalyzed using a quantitative assay (Supplementary Figures 1C and D, available at <http://onlinelibrary.wiley.com/doi/10.1002/art.42153>). Patients had

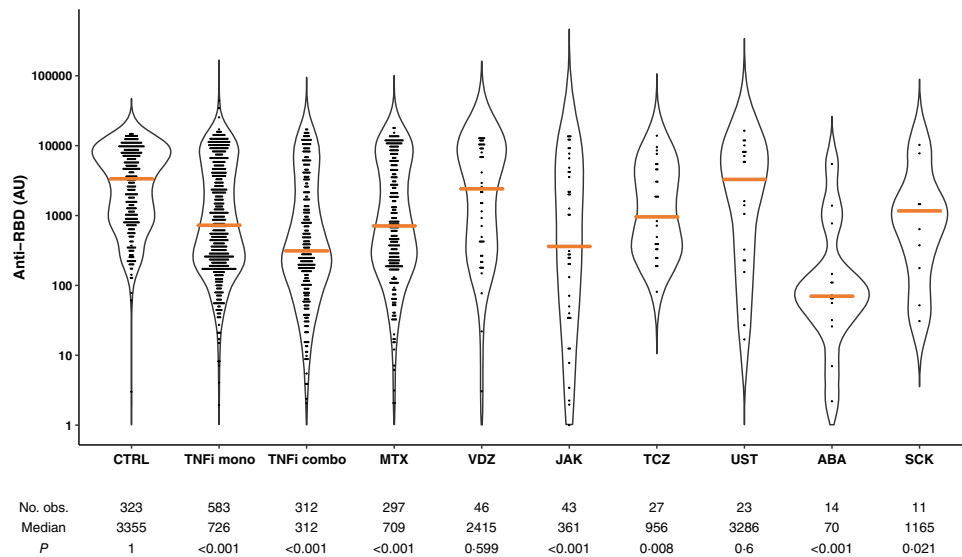


Figure 1. Violin plots of probability densities, smoothed by a kernel density estimator, of IgG antibody levels against the receptor-binding domain of SARS-CoV-2 spike protein (anti-RBD) after the standard 2-dose SARS-CoV-2 vaccination regimen among healthy controls (CTRL) and among patients with immune-mediated inflammatory disease (IMiD) stratified by immunosuppressive therapy. Points denote participants, and solid orange lines show group medians. *P* values show comparisons to CTRL and were calculated by Mann-Whitney U test. TNFi mono = tumor necrosis factor inhibitor monotherapy; TNFi combo = TNFi combination therapy; MTX = methotrexate; VDZ = vedolizumab; TCZ = tocilizumab; UST = ustekinumab; ABA = abatacept; SCK = secukinumab. Color figure can be viewed in the online issue, which is available at <http://onlinelibrary.wiley.com/doi/10.1002/art.42153/abstract>.

significantly lower levels of anti-RBD antibody as compared to healthy controls (median 619 AU/ml [IQR 192–4,191] and 3,355 AU/ml [IQR 896–7,849]) (Figure 1).

Predictors of response. Age (odds ratio [OR] 0.96, 95% confidence interval [95% CI] 0.94–0.98) and vaccination with mRNA-1273 as compared to BNT162b2 (OR 4.45, 95% CI 1.66–11.92) were identified as predictors of a serologic response following receipt of the standard 2-dose vaccination regimen (Table 3). A total of 98% of patients receiving mRNA-1273 as compared to 89% receiving BNT162b2 were responders, with median anti-RBD antibody levels of 2,308 AU/ml (IQR 377–8,812) and 408 AU/ml (IQR 170–2,205), respectively. Patients receiving TNFi combination therapy (OR 0.27, 95% CI 0.14–0.52), JAK inhibitors (OR 0.18, 95% CI 0.05–0.64), or abatacept (OR 0.01, 95% CI 0.01–0.13) were less likely to have a response following receipt of the standard regimen, compared to patients receiving TNFi monotherapy (Table 3). Pausing treatment did not improve vaccine response (Table 3). The same predictors (i.e., age, mRNA-1273 receipt, and comedication use) were identified in a subanalysis of patients receiving TNFi monotherapy or combination therapy (Supplementary Table 3, available on the *Arthritis & Rheumatology* website at <http://onlinelibrary.wiley.com/doi/10.1002/art.42153>).

Response to a third vaccine dose. A total of 153 patients (median age 57 years [IQR 46–67]; 80 female patients [52%]) with weak responses to the standard 2-dose regimen (anti-RBD

antibody levels ≤ 100 AU/ml) were allotted a third vaccine dose a median of 70 days (IQR 56–90) after the second vaccine dose. An increase in antibody levels was observed in 129 (94%) of 153 patients ($P < 0.001$), with a median change of 362 AU/ml (IQR 48–2,501) (Figure 2). Median antibody levels were 45 AU/ml (IQR 17–105) and 544 AU/ml (IQR 143–4,543) before and 2–4 weeks after receipt of the third vaccine dose, respectively (Figure 2). Percentages of responders, stratified by therapy, were as follows: 89% (41 of 46) among TNFi monotherapy recipients, 84% (44 of 52) among TNFi combination therapy recipients, 75% (21 of 28) among methotrexate recipients, 63% (7 of 11) among JAK inhibitor recipients, and 100% (4 of 4) among abatacept recipients. Except for age, no predictors of response to the third vaccine dose were identified (Supplementary Table 4, available on the *Arthritis & Rheumatology* website at <http://onlinelibrary.wiley.com/doi/10.1002/art.42153>).

Adverse events. Among recipients of the standard 2-dose vaccination regimen, adverse events were reported in 810 (50%) of 1,516 patients and 191 (78%) of 244 healthy controls, with a comparable safety profile (Figure 3 and Supplementary Table 5, available on the *Arthritis & Rheumatology* website at <http://onlinelibrary.wiley.com/doi/10.1002/art.42153>). Following receipt of the third dose, 70 patients (44%) reported adverse events; no new safety issues emerged, except for an increase in disease flares, which were reported by 26 patients (16%), all of whom had inflammatory joint disease. After receipt of the first and second doses, disease flare was reported by 78 patients (6%) and 88 patients (6%), respectively.

Table 3. Univariable and multivariable analyses to determine predictors of a serologic response among IMiD patients after receipt of the standard 2-dose SARS-CoV-2 vaccination regimen*

Potential predictor	Univariable analysis		Multivariable analysis	
	OR (95% CI)	P	OR (95% CI)	P
Demographic				
Age, years	0.96 (0.95–0.98)	<0.001	0.95 (0.93–0.97)	<0.001
Male sex	0.92 (0.62–1.37)	0.68	0.70 (0.41–1.22)	0.199
IMiD				
Joint				
Rheumatoid arthritis	1	–	1	–
Spondyloarthritis	1.53 (0.83–2.69)	0.16	0.39 (0.14–1.09)	0.066
Psoriatic arthritis	1.89 (0.99–3.63)	0.05	1.436 (0.47–3.91)	0.562
Bowel				
Crohn's disease	1.36 (0.81–2.28)	0.242	0.34 (0.13–0.89)	0.026
Ulcerative colitis	2.22 (1.11–4.45)	0.021	0.54 (0.18–1.58)	0.25
Medication				
TNFi†				
Monotherapy	1	–	1	–
Combination therapy	0.38 (0.23–0.64)	<0.001	0.27 (0.14–0.52)	<0.001
Methotrexate	0.61 (0.34–1.09)	0.089	0.36 (0.13–1.04)	0.286
Vedolizumab	1 (0.29–3.49)	0.998	1.17 (0.28–4.93)	0.824
JAK inhibitor	0.21 (0.09–0.49)	<0.001	0.18 (0.05–0.64)	0.007
Tocilizumab‡	Not done	0.978	Not done	0.983
Ustekinumab	0.92 (0.2–4.17)	0.917	0.36 (0.13–0.806)	0.528
Abatacept	0.02 (0.01–0.10)	<0.001	0.01 (0–0.013)	<0.001
Secukinumab	0.35 (0.04–3.11)	0.334	0.1 (0.01–1.21)	0.064
Prednisolone	0.27 (0.14–0.51)	<0.001	0.41 (0.13–1.24)	0.106
Vaccine related§				
BNT162b2 regimen, 2 doses	1	–	1	–
mRNA-1273 regimen, 2 doses	5.06 (2.29–11.18)	<0.001	4.45 (1.66–11.92)	0.002
Combination regimen, 2 doses	1.11 (0.46–2.69)	0.814	0.72 (0.24–2.12)	0.54
COVID-19 and 1 of any mRNA vaccine§	–	0.977	–	0.995
Other				
IBD or IJD duration	1 (0.98–1.02)	0.945	1.01 (0.99–1.04)	0.389
CRP level	0.97 (0.96–0.99)	0.01	0.97 (0.95–1.0)	0.018
BMI	1.01 (0.98–1.05)	0.474	1.03 (0.98–1.08)	0.292
Pause in medication¶	1.8 (0.81–4.03)	0.142	1.59 (0.5–5.07)	0.428

* Response was defined as an IgG antibody level of ≥70 AU/ml against the RBD of SARS-CoV-2 spike protein. IBD = inflammatory bowel disease; IJD = inflammatory joint disease (see Table 2 for other definitions).

† Monotherapy consisted of infliximab, etanercept, adalimumab, golimumab, or certolizumab pegol. Combination therapy consisted of methotrexate, sulfasalazine, leflunomide, or azathioprine.

‡ Because of the low number of tocilizumab recipients, analysis was not performed.

§ BNT162b2 and mRNA-1273 are mRNA vaccines. Combination regimen was defined as ChAdOx1 (first dose) + BNT162b2 or mRNA-1273 (second dose) or as BNT162b2 + mRNA-1273 in any sequence.

¶ Patient-reported pause in medication from 1 week before through 2 weeks after receipt of a vaccine dose.

DISCUSSION

This study, the largest to date on response to the standard 2-dose SARS-CoV-2 vaccination regimen in IMiD patients receiving immunosuppressive therapy, demonstrated that the percentage of responders and the anti-RBD antibody level were lower in 1,647 patients as compared to 1,114 healthy controls. Adverse reactions were comparable in the 2 groups. Among patients with a weak serologic response after the standard 2-dose regimen, the third dose was safe and resulted in a response in most recipients.

The study provides detailed information regarding the impact of commonly used immunosuppressive drugs for inflammatory joint diseases and IBDs on the serologic response to SARS-CoV-2 vaccines. A difference among the medications was shown, with the lowest proportion of responders observed among

recipients of abatacept (50%), JAK inhibitors (78%), TNFi used in combination with methotrexate or azathioprine (86%), and sekukinumab (88%), suggesting a rationale for postvaccination serologic monitoring in patients using these medications. Prior studies regarding the effect of abatacept and JAK inhibitors on the immunogenicity of SARS-CoV-2 vaccines differ in their conclusions, which may be due to the limited number of patients they evaluated (n = 8–16) (11,13,35). Data regarding the effect of TNFi on the immunogenicity of SARS-CoV-2 vaccines have also been conflicting (5,10–13,35). The Nor-vaC study included >1,000 TNFi recipients, roughly the same total number previously described across several smaller studies (35). In the present study, attenuated immunogenicity was mainly seen in TNFi recipients receiving combination therapy with azathioprine or methotrexate. These synthetic

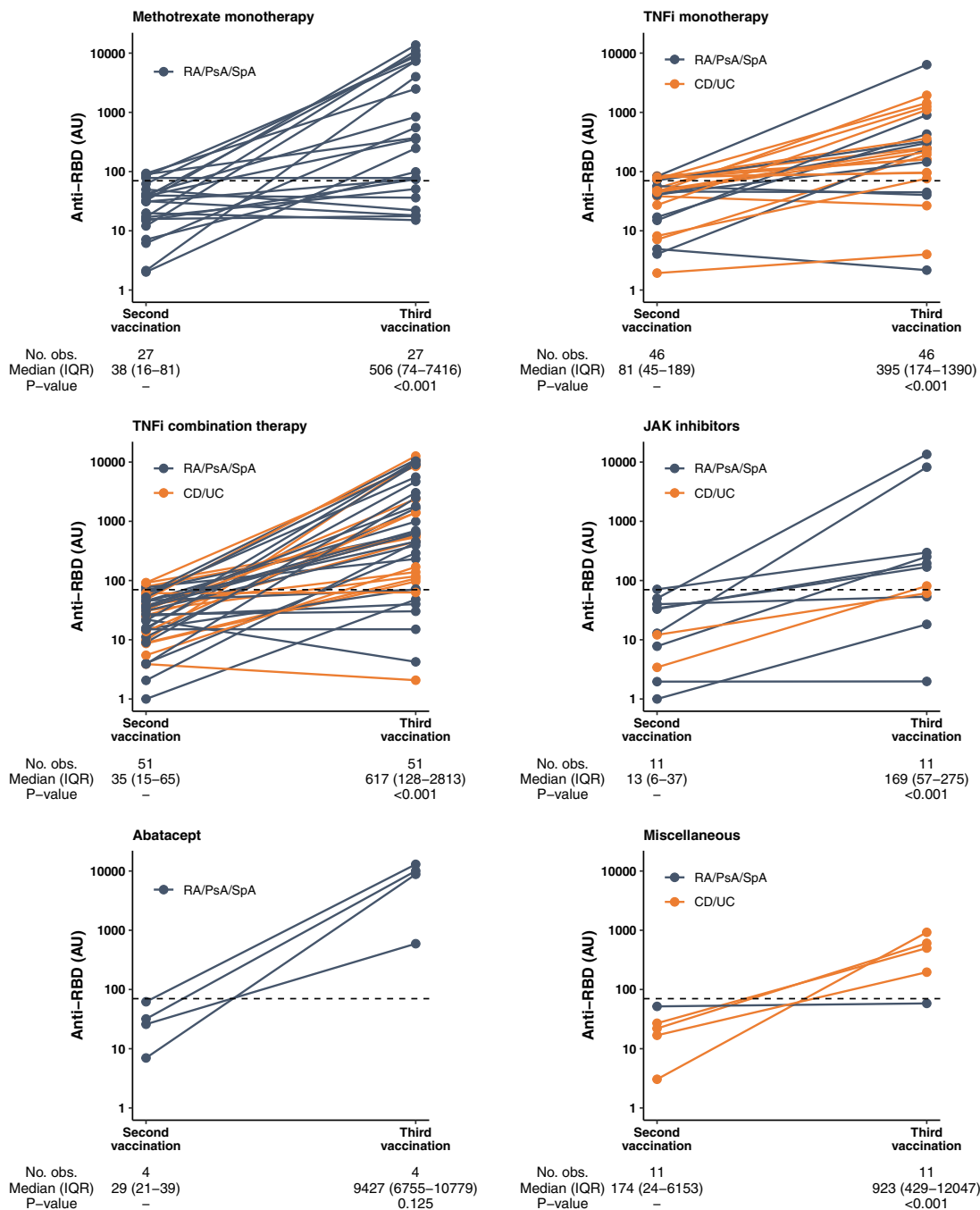


Figure 2. Anti-RBD levels after receipt of a third SARS-CoV-2 vaccine dose among IMiD patients with a weak response to the standard 2-dose vaccination regimen. Levels were measured 2–4 weeks after the second and third vaccine doses. Horizontal dotted lines indicate the serologic response cutoff (70 arbitrary units per milliliter [AU/ml]). Orange dots and lines indicate anti-RBD levels in individual patients with inflammatory bowel disease; blue dots and lines indicate levels in individual patients with inflammatory joint disease. *P* values were calculated by Wilcoxon paired test. RA = rheumatoid arthritis; PsA = psoriatic arthritis; SpA = spondyloarthritis; obs. = observations; IQR = interquartile range; CD = Crohn's disease; UC = ulcerative colitis; miscellaneous = vedolizumab, ustekinumab, tocilizumab, secukinumab, or azathioprine (see Figure 1 for other definitions).

drugs are known to reduce antidrug antibody responses to the TNF inhibitor itself, and it is reasonable to assume similar effects on vaccine immunogenicity (36).

Despite the relatively high response rates in most medication groups, the median anti-RBD antibody levels were significantly lower among patients, compared to healthy controls. There is

increasing evidence that antibody levels correlate to the degree of clinical protection against breakthrough COVID-19 (37) and that anti-RBD antibody levels correlate to SARS-CoV-2 neutralization levels, with higher levels needed for neutralizing novel virus strains (28,38). As antibody levels decay over time, it seems likely that patients who attain a weak antibody response after vaccination will

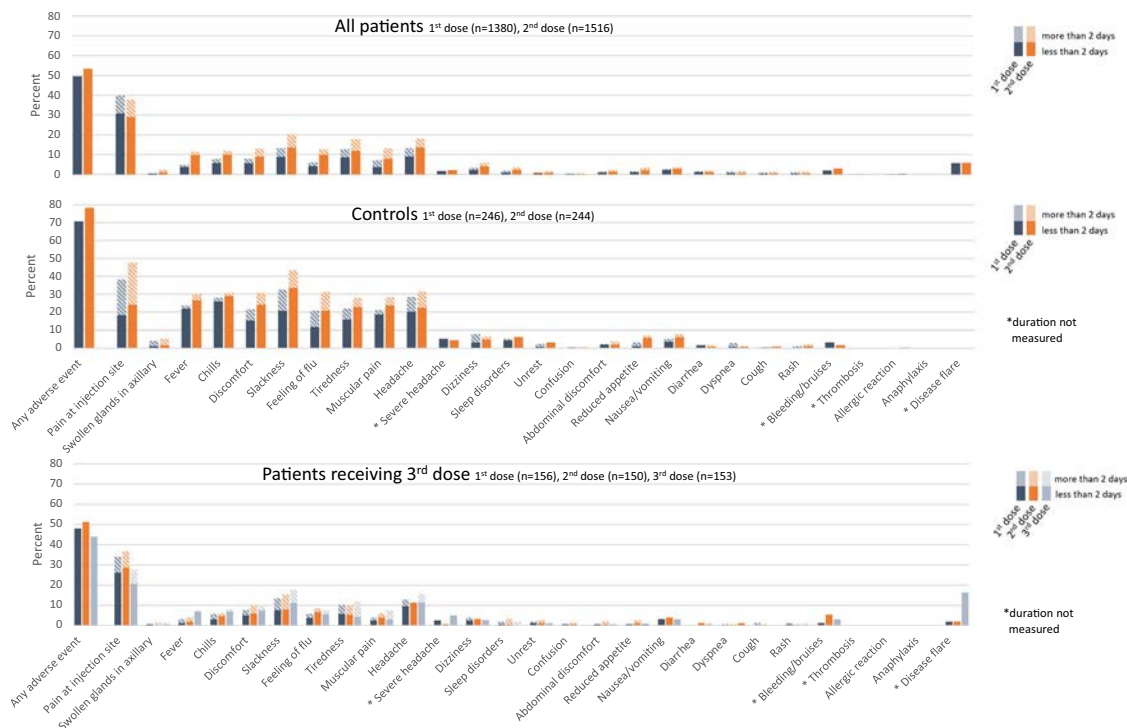


Figure 3. Type and duration of adverse events reported after doses 1 (blue bars) and 2 (orange bars) of SARS-CoV-2 vaccine among patients with immune-mediated inflammatory disease (IMID) and healthy controls and after dose 3 (gray bars) among IMID patients who had a weak serologic response (defined as <70 arbitrary units per milliliter) to doses 1 and 2. Adverse events were reported for all patients and a subset of 246 healthy controls described in Patients and Methods. Color figure can be viewed in the online issue, which is available at <http://onlinelibrary.wiley.com/doi/10.1002/art.42153/abstract>.

have a less durable response (39). Patients with a weak response may also have developed less robust immunologic memory responses (40). Further studies are needed to elucidate whether IMID patients receiving immunosuppressive therapy lose their protective immunity more quickly than the general population.

In addition to medication type, lower age and receipt of mRNA-1273 were predictors of a serologic response. Prior studies have suggested that mRNA-1273 may be more immunogenic than BNT162b2 in healthy subjects (41). To our knowledge, this is the first study presenting findings on the immunogenicity of different vaccine types in IMID patients. Subanalyses in TNFi recipients showed similar results.

In the 153 patients receiving a third vaccine dose, a response was induced in the majority of patients. The effectiveness of additional vaccine doses for immunocompromised patients, as well as the utility of booster shots for healthy people, is now being debated in the scientific community (16). Prior data on the immunogenicity of 3 SARS-CoV-2 vaccine doses in IMID patients who were receiving immunosuppressive drugs other than rituximab and had no response to the standard 2-dose vaccination regimen consist of case series and small studies ($n = 33$ and $n = 17$) and indicated a moderate additional humoral response following receipt of the third dose (19,23,24). The present data show a clear benefit in terms of serologic response, while the frequency and profile of reported adverse events were

comparable to those observed after receipt of the standard 2-dose regimen. We did not find that pausing medication benefited vaccine immunogenicity. The humoral response to the third dose was comparable in patients with inflammatory joint diseases, for whom a pause in medication was recommended, and in patients with IBDs, who did not receive this recommendation. Further, self-reported pausing of medication was not associated with a humoral response to the standard vaccination regimen. These results must be interpreted with caution, however.

There are limited data on the safety of SARS-CoV-2 vaccines in IMID patients (13,42). This study supports that these vaccines are safe in an immunosuppressed population, and it demonstrates that the frequency of reported adverse events was lower among IMID patients than among controls, with the same range of adverse events reported in both groups. This finding suggests that immunosuppressive medication might reduce the frequency of adverse events due to SARS-CoV-2 vaccines and might also reduce the vaccines' immunogenicity. A major concern has been whether the mRNA SARS-CoV-2 vaccines may cross-react with human proteins and aggravate autoimmunity (43). The Nor-vaC results are reassuring in this regard, as hardly any patients reported a disease flare after receiving the standard 2-dose vaccination regimen. However, we found a clear increase in disease flares among inflammatory joint disease

patients following receipt of the third dose. This was not seen in patients with IBDs. Among patients with inflammatory joint diseases, the increase may have been due to the recommended pause in medication from 1 week before through 2 weeks after receipt of the third dose.

Strengths of this study include the prospective study design, the broad inclusion criteria, the well-characterized population of patients, and the large sample sizes of patients and controls. A further strength is that the study population was drawn from both gastroenterology and rheumatology settings, enabling assessment of patients across a range of diseases who are being treated with the same medical compounds.

This study has some limitations. First, we did not measure cellular immune responses. The adaptive immune response to SARS-CoV-2 depends not only on virus-specific antibodies but also on T cell-mediated responses (44). Further studies are needed to determine if the serologic responses are predictive of protection against severe disease. Second, some medication groups included a low number of patients. Third, controls or patients with a normal antibody response to the standard 2-dose vaccination regimen were not given a third dose; hence, we could not evaluate the response to and safety of a third dose in these groups. Fourth, the patients were generally older than the controls, raising the possibility of biased results. However, we have corrected for age in all analyses comparing patients and controls. Fifth, full data on comorbidity were not available. Sixth, we cannot exclude the possibility that some of the participants may have had a subclinical SARS-CoV-2 infection. However, the rate of SARS-CoV-2 infection in Norway during the relevant period was very low.

The proportion of responders and the anti-RBD antibody levels were lower among IMID patients as compared to controls following receipt of the standard vaccination regimen. These data facilitate identification of patient groups who are at risk of an attenuated vaccine response and therefore should be considered for postvaccination serologic monitoring. Receipt of a third vaccine dose by patients with a weak response was safe and resulted in a response in most. These results will aid health care systems in the planning and implementation of SARS-CoV-2 vaccine programs aimed at IMID patients treated with immunosuppressive medication and will aid clinical decision-making regarding revaccinations and tailoring of medication to keep this vulnerable population protected against severe COVID-19.

ACKNOWLEDGMENTS

We thank the patient representatives in the study group—Kristin Isabella Kirkengen Espe, and Roger Thoresen—for their contributions. We also thank all study personnel, laboratory personnel, and other staff involved in the participating clinical departments and at Department of Immunology at Oslo University Hospital, particularly Synnøve Aure (Akershus University Hospital) and May Britt Solem and Kjetil Bergsmark (Diakonhjemmet Hospital).

AUTHOR CONTRIBUTIONS

All authors were involved in drafting the article or revised in critically for important intellectual content, and all authors approved the final version to be published. Dr. Goll had full access to all of the data in the study and takes responsibility for the integrity of the data and the accuracy of the data analysis.

Study conception and design. Syversen, Jyssum, Warren, Kvien, Munthe, Haavardsholm, Vaage, Lund-Johansen, Jørgensen, Goll.

Acquisition of data. Syversen, Jyssum, Tveter, Tran, Grødeland, Nissen-Meyer, Ricanek, Chopra, Andersson, Jahnsen, Munthe, Vaage, Lund-Johansen, Jørgensen, Goll.

Analysis and interpretation of data. Syversen, Jyssum, Tveter, Sexton, Provan, Mjaaland, Grødeland, Kro, Jahnsen, Munthe, Vaage, Lund-Johansen, Jørgensen, Goll.

REFERENCES

1. Baden LR, El Sahly HM, Essink B, Kotloff K, Frey S, Novak R, et al. Efficacy and safety of the mRNA-1273 SARS-CoV-2 vaccine. *N Engl J Med* 2021;384:403–16.
2. Polack FP, Thomas SJ, Kitchin N, Absalon J, Gurtman A, Lockhart S, et al. Safety and efficacy of the BNT162b2 mRNA Covid-19 vaccine. *N Engl J Med* 2020;383:2603–15.
3. Haas EJ, Angulo FJ, McLaughlin JM, Anis E, Singer SR, Khan F, et al. Impact and effectiveness of mRNA BNT162b2 vaccine against SARS-CoV-2 infections and COVID-19 cases, hospitalisations, and deaths following a nationwide vaccination campaign in Israel: an observational study using national surveillance data. *Lancet* 2021;397:1819–29.
4. Vasileiou E, Simpson CR, Shi T, Kerr S, Agrawal U, Akbari A, et al. Interim findings from first-dose mass COVID-19 vaccination roll-out and COVID-19 hospital admissions in Scotland: a national prospective cohort study. *Lancet* 2021;397:1646–57.
5. Friedman MA, Curtis JR, Winthrop KL. Impact of disease-modifying antirheumatic drugs on vaccine immunogenicity in patients with inflammatory rheumatic and musculoskeletal diseases. *Ann Rheum Dis* 2021;80:1255–65.
6. Ungaro RC, Brenner EJ, Geary RB, Kaplan GG, Kissous-Hunt M, Lewis JD, et al. Effect of IBD medications on COVID-19 outcomes: results from an international registry. *Gut* 2021;70:725–32.
7. Curtis JR, Johnson SR, Anthony DD, Arasaratnam RJ, Baden LR, Bass AR, et al. American College of Rheumatology guidance for COVID-19 vaccination in patients with rheumatic and musculoskeletal diseases: version 3. *Arthritis Rheumatol* 2021;73:e60–75.
8. D'Amico F, Rabaud C, Peyrin-Biroulet L, Danese S. SARS-CoV-2 vaccination in IBD: more pros than cons. *Nat Rev Gastroenterol Hepatol* 2021;18:211–3.
9. Schett G, McInnes IB, Neurath MF. Reframing immune-mediated inflammatory diseases through signature cytokine hubs. *N Engl J Med* 2021;385:628–39.
10. Kennedy NA, Goodhand JR, Bewshea C, Nice R, Chee D, Lin S, et al. Anti-SARS-CoV-2 antibody responses are attenuated in patients with IBD treated with infliximab. *Gut* 2021;70:865–75.
11. Deepak P, Kim W, Paley MA, Yang M, Carvidi AB, Demissie EG, et al. Effect of immunosuppression on the immunogenicity of mRNA vaccines to SARS-CoV-2: a prospective cohort study. *Ann Intern Med* 2021;174:1572–85.
12. Boekel L, Steenhuis M, Hooijberg F, Besten YR, van Kempen ZL, Kummer LY, et al. Antibody development after COVID-19 vaccination in patients with autoimmune diseases in the Netherlands: a substudy of data from two prospective cohort studies. *Lancet Rheumatol* 2021;3:e778.

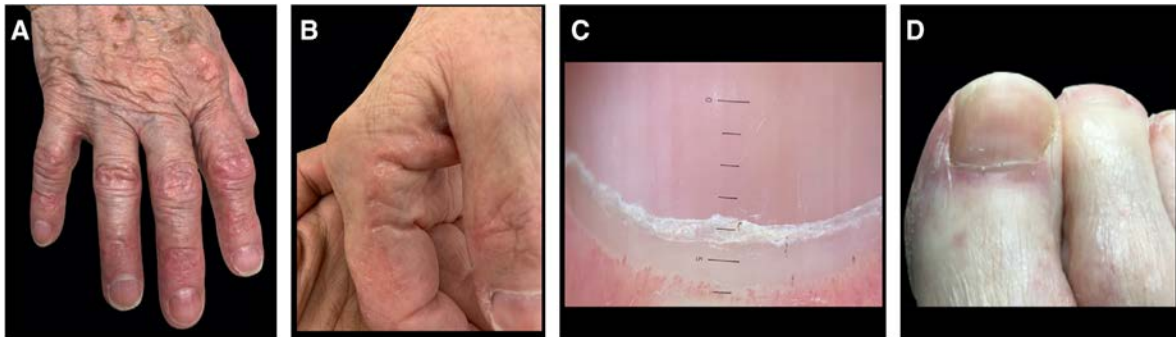
13. Furer V, Eviatar T, Zisman D, Peleg H, Paran D, Levartovsky D, et al. Immunogenicity and safety of the BNT162b2 mRNA COVID-19 vaccine in adult patients with autoimmune inflammatory rheumatic diseases and in the general population: a multicentre study. *Ann Rheum Dis* 2021;80:1330–8.
14. Kappelman MD, Weaver KN, Boccieri M, Firestine A, Zhang X, Long MD. Humoral immune response to messenger RNA COVID-19 vaccines among patients with inflammatory bowel disease. *Gastroenterology* 2021;161:1340–3.
15. Melmed GY, Botwin GJ, Sobhani K, Li D, Prostko J, Figueiredo J, et al. Antibody responses after SARS-CoV-2 mRNA vaccination in adults with inflammatory bowel disease. *Ann Intern Med* 2021;174:1768–70.
16. Bar-On YM, Goldberg Y, Mandel M, Bodenheimer O, Freedman L, Kalkstein N, et al. Protection of BNT162b2 vaccine booster against Covid-19 in Israel. *N Engl J Med* 2021;385:1393–400.
17. Patalon T, Gazit S, Pitzer VE, Prunas O, Warren JL, Weinberger DM. Odds of testing positive for SARS-CoV-2 following receipt of 3 vs 2 doses of the BNT162b2 mRNA vaccine. *JAMA Intern Med* 2021;182:179–84.
18. Del Bello A, Abravanel F, Marion O, Couat C, Esposito L, Lavayssière L, et al. Efficiency of a boost with a third dose of anti-SARS-CoV-2 messenger RNA-based vaccines in solid organ transplant recipients. *Am J Transplant* 2021;22:322–3.
19. Connolly CM, Teles M, Frey S, Boyarsky BJ, Alejo JL, Werbel WA, et al. Booster-dose SARS-CoV-2 vaccination in patients with autoimmune disease: a case series. *Ann Rheum Dis* 2021;81:291–3.
20. Felten R, Gallais F, Schleiss C, Chatelus E, Javier RM, Pijnenburg L, et al. Cellular and humoral immunity after the third dose of SARS-CoV-2 vaccine in patients treated with rituximab. *Lancet Rheumatol* 2021;4:e13–6.
21. Baker MC, Mallajosyula V, Davis MM, Boyd SD, Nadeau KC, Robinson WH. Effective viral vector SARS-CoV-2 booster vaccination in a patient with rheumatoid arthritis after initial ineffective messenger RNA vaccine response. *Arthritis Rheumatol* 2021;74:541–8.
22. Jyssum I, Kared H, Tran TT, Tveter AT, Provan SA, Sexton J, et al. Humoral and cellular immune responses to two and three doses of SARS-CoV-2 vaccines in rituximab-treated patients with rheumatoid arthritis: a prospective, cohort study. *Lancet Rheumatol* 2021;4:e177–87.
23. Schmiedeberg K, Vuilleumier N, Pagano S, Albrich WC, Ludewig B, Kempis JV, et al. Efficacy and tolerability of a third dose of an mRNA anti-SARS-CoV-2 vaccine in patients with rheumatoid arthritis with absent or minimal serological response to two previous doses. *Lancet Rheumatol* 2022;4:e11–3.
24. Simon D, Tascilar K, Fagni F, Schmidt K, Krönke G, Kleyer A, et al. Efficacy and safety of SARS-CoV-2 revaccination in non-responders with immune-mediated inflammatory disease. *Ann Rheum Dis* 2022;81:1023–7.
25. Tran TT, Vaage EB, Mehta A, Chopra A, Kolderup A, Anthi AK, et al. Multiplexed measurement of binding- and neutralizing antibodies to SARS-CoV-2 variants in 12,000 post-vaccine sera [preprint]. *BioRxiv* 2022. doi: [10.1101/2022.03.26.484261](https://doi.org/10.1101/2022.03.26.484261);2022.03.26.484261. E-pub ahead of print.
26. Holter JC, Pischke SE, de Boer E, Lind A, Jennum S, Holten AR, et al. Systemic complement activation is associated with respiratory failure in COVID-19 hospitalized patients. *Proc Natl Acad Sci U S A* 2020;117:25018–25.
27. König M, Lorentzen ÅR, Torgauten HM, Tran TT, Schikora-Rustad S, Vaage EB, et al. Humoral immunity to SARS-CoV-2 mRNA vaccination in multiple sclerosis: the relevance of time since last rituximab infusion and first experience from sporadic revaccinations. *J Neurol Neurosurg Psychiatry* 2021. doi: [10.1136/jnnp-2021-327612](https://doi.org/10.1136/jnnp-2021-327612). E-pub ahead of print.
28. Nguyen D, Simmonds P, Steenhuis M, Wouters E, Desmecht D, Garigliany M, et al. SARS-CoV-2 neutralising antibody testing in Europe: towards harmonisation of neutralising antibody titres for better use of convalescent plasma and comparability of trial data. *Euro Surveill* 2021;26:2100568.
29. Norwegian Institute of Public Health. Norwegian Immunisation Registry (SYSVAK), 2021. URL: <https://www.fhi.no/en/hn/health-registries/norwegian-immunisation-registry-sysvak/>.
30. Norwegian Institute of Public Health. Norwegian Surveillance System for Communicable Diseases (MSIS), 2019. URL: <https://www.fhi.no/en/hn/health-registries/msis/>.
31. Prevoo ML, van't Hof MA, Kuper HH, van Leeuwen MA, van de Putte LB, van Riel PL. Modified disease activity scores that include twenty-eight-joint counts: development and validation in a prospective longitudinal study of patients with rheumatoid arthritis. *Arthritis Rheum* 1995;38:44–8.
32. Lukas C, Landewé R, Sieper J, Dougados M, Davis J, Braun J, et al, for the Assessment of Spondyloarthritis International Society. Development of an ASAS-endorsed disease activity score (ASDAS) in patients with ankylosing spondylitis. *Ann Rheum Dis* 2009;68:18–24.
33. Harvey RF, Bradshaw JM. A simple index of Crohn's-disease activity. *Lancet* 1980;315:514.
34. Lewis JD, Chuai S, Nessel L, Lichtenstein GR, Aberra FN, Ellenberg JH. Use of the noninvasive components of the Mayo score to assess clinical response in ulcerative colitis. *Inflamm Bowel Dis* 2008;14:1660–6.
35. Jena A, Mishra S, Deepak P, Kumar MP, Sharma A, Patel YI, et al. Response to SARS-CoV-2 vaccination in immune mediated inflammatory diseases: systematic review and meta-analysis. *Autoimmun Rev* 2021;21:102927.
36. Atiqi S, Hooijberg F, Loeff FC, Rispens T, Wolbink GJ. Immunogenicity of TNF-inhibitors [review]. *Front Immunol* 2020;11:312.
37. Gilbert PB, Montefiori DC, McDermott AB, Fong Y, Benkeser D, Deng W, et al. Immune correlates analysis of the mRNA-1273 COVID-19 vaccine efficacy clinical trial. *Science* 2022;375:43–50.
38. Cromer D, Steain M, Reynaldi A, Schlub TE, Wheatley AK, Juno JA, et al. Neutralising antibody titres as predictors of protection against SARS-CoV-2 variants and the impact of boosting: a meta-analysis. *Lancet Microbe* 2022;3:e52–61.
39. Okamoto M, Kawada S, Fujii N, Matsukawa K, Shimagami H, Ishikawa N, et al. Rapid attenuation of anti-SARS-CoV-2 antibody in patients with musculoskeletal diseases who reinitiated intensive immunosuppressive therapies after COVID-19. *Arthritis Rheumatol* 2022;74:726–8.
40. Dan JM, Mateus J, Kato Y, Hastie KM, Yu ED, Faliti CE, et al. Immunological memory to SARS-CoV-2 assessed for up to 8 months after infection. *Science* 2021;371:eabf4063.
41. Steensels D, Pierlet N, Penders J, Mesotten D, Heylen L. Comparison of SARS-CoV-2 antibody response following vaccination with BNT162b2 and mRNA-1273. *JAMA* 2021;326:1533–5.
42. Botwin GJ, Li D, Figueiredo J, Cheng S, Braun J, McGovern DPB, et al. Adverse events after SARS-CoV-2 mRNA vaccination among patients with inflammatory bowel disease. *Am J Gastroenterol* 2021;116:1746–51.

43. Vojdani A, Kharrazian D. Potential antigenic cross-reactivity between SARS-CoV-2 and human tissue with a possible link to an increase in autoimmune diseases. *Clin Immunol* 2020;217:108480.

44. Ni L, Ye F, Cheng ML, Feng Y, Deng YQ, Zhao H, et al. Detection of SARS-CoV-2-specific humoral and cellular immunity in COVID-19 convalescent individuals. *Immunity* 2020;52:971–7.

DOI 10.1002/art.42110


Clinical Images: Hydroxyurea-induced dermatomyositis-like rash



The patient, a 78-year-old woman, presented to the dermatology clinic with self-reported “irritated hands,” which she attributed to frequent handwashing. She had no relief after use of skin care products and potent topical steroids for 3 months. Her clinical history was notable for polycythemia vera, for which she had been taking hydroxyurea for at least 10 years. Examination revealed significant erythema and scaling of the nail folds, interphalangeal joints (A and D), and both palms, with hyperkeratosis and a desquamating eruption on the medial thumb and lateral index finger of the right hand (“mechanic’s hands”) (B). Polarized light dermoscopy (Heine Delta 20T; Heine Optotechnik) of the proximal nail folds showed dilated capillary loops and capillary dropout (C; original magnification $\times 16$). There was no muscle weakness or other cutaneous signs of dermatomyositis. The antinuclear antibody titer was 1:80, and the creatine kinase level (34 IU/liter) was within normal limits. Hydroxyurea treatment was discontinued because it is known to be the most common cause of drug-induced dermatomyositis, which can present even after many years of use (1,2). Although the patient’s dermatomyositis can be associated with polycythemia vera itself, which can further progress to myelofibrosis, this was less likely in our patient because she experienced significant improvement in erythema and pruritus 1 month after hydroxyurea discontinuation. In summary, hydroxyurea-induced dermatomyositis is an amyopathic dermatomyositis with cutaneous lesions identical to those associated with classic dermatomyositis. Recognition that drugs such as hydroxyurea can cause dermatomyositis is paramount because lesions can improve by stopping treatment with these agents, rather than by initiating immunosuppressive therapy.

Supported by HCA Healthcare and/or an HCA Healthcare-affiliated entity. The views expressed in this publication represent those of the author(s) and do not necessarily represent the official views of HCA Healthcare or any of its affiliated entities. We thank Dr. Philip Barton (Ocala Dermatology and Skin Cancer Center) for his clinical input in this case. Author disclosures are available at <https://onlinelibrary.wiley.com/action/downloadSupplement?doi=10.1002%2Fart.42110&file=art42110-sup-0001-Disclosureform.pdf>.

1. Nofal A, El-Din ES. Hydroxyurea-induced dermatomyositis: true amyopathic dermatomyositis or dermatomyositis-like eruption? *Int J Dermatol* 2012;51:535–41.
2. Zappala TM, Rodins K, Muir J. Hydroxyurea induced dermatomyositis-like eruption [review]. *Australas J Dermatol* 2012;53:e58–60.

Sweta Subhadarshani, MBBS, MD, MRCP(SCE)
 minse@mail.uc.edu
 University of Central Florida
 Orlando, FL
 Susie Min, BS 
 University of Cincinnati College of Medicine
 Cincinnati, OH
 Kathryn Holloway, MD
 Matthew Steadmon, MD
 Ocala Dermatology and Skin Cancer Center
 Ocala, FL

Five-Year Structural Changes in the Knee Among Patients With Meniscal Tear and Osteoarthritis: Data From a Randomized Controlled Trial of Arthroscopic Partial Meniscectomy Versus Physical Therapy

Jamie E. Collins,¹ Swastina Shrestha,² Elena Losina,³ Robert G. Marx,⁴ Ali Guermazi,⁵ Mohamed Jarraya,⁶ Morgan H. Jones,² Bruce A. Levy,⁷ Lisa A. Mandl,⁴ Emma E. Williams,² Rick W. Wright,⁸ Kurt P. Spindler,⁹ and Jeffrey N. Katz,¹ on behalf of the METEOR Investigator Group

Objective. To estimate the risk of magnetic resonance imaging (MRI)–based structural changes in knee osteoarthritis (OA) among individuals with meniscal tear and knee OA, using MRIs obtained at baseline and 18 and 60 months after randomization in a randomized controlled trial of arthroscopic partial meniscectomy (APM) versus physical therapy (PT).

Methods. We used data from the Meniscal Tear in Osteoarthritis Research (METEOR) trial. MRIs were read using the MRI OA Knee Score (MOAKS). We used linear mixed-effects models to examine the association between treatment group and continuous MOAKS summary scores, and Poisson regression to assess categorical changes in knee joint structure. Analyses assessed changes in OA between baseline and month 18 and between months 18 and 60. We performed both intention-to-treat and as-treated analyses.

Results. The analytic sample included 302 participants. For both treatment groups, more OA changes were seen during the early interval than during the later interval. ITT analysis revealed that, between baseline and month 18, APM was significantly associated with an increased risk of having a worsening cartilage surface area score, involving both any worsening across all knee joint subregions (risk ratio [RR] 1.35 [95% confidence interval (95% CI) 1.14, 1.61]) and the number of subregions damaged (RR 1.44 [95% CI 1.13, 1.85]) having a worsening effusion-synovitis score (RR 2.62 [95% CI 1.32, 5.21]), and having ≥ 1 additional subregion with osteophytes (RR 1.24 [95% CI 1.02, 1.50]). Significant associations were detected between months 18 and 60 only for having any subregion with a worsening osteophyte score (RR 1.28 [95% CI 1.04, 1.58]).

Conclusion. These findings suggest that the association between APM and MRI-based structural changes in knee OA is most apparent during the initial 18 months after surgery. The reason for attenuation of this association over longer follow-up merits further investigation.

INTRODUCTION

Knee osteoarthritis (OA) is a prevalent and disabling chronic condition that affects >14 million US adults (1). Among patients

with knee OA, meniscal tear is prevalent. Over 90% of patients with symptomatic knee OA have concomitant meniscal tear on magnetic resonance imaging (MRI) (2). For patients with degenerative meniscal tear and OA who experience pain and functional

ClinicalTrials.gov identifier: NCT00597012.

Supported by the National Institute of Arthritis and Musculoskeletal and Skin Diseases, NIH (grant P30-AR-072577). Dr. Collins' work was supported by an RRF Investigator Award. Dr. Losina's work was supported by the National Institute of Arthritis and Musculoskeletal and Skin Diseases, NIH (grants R01-AR-055557 and K24-AR-057827).

¹Jamie E. Collins, PhD, Jeffrey N. Katz, MD, MSc: Brigham and Women's Hospital and Harvard Medical School, Boston, Massachusetts; ²Swastina Shrestha, MS, Morgan H. Jones, MD, MPH, Emma E. Williams, BA: Brigham and Women's Hospital, Boston, Massachusetts; ³Elena Losina, PhD: Brigham and Women's Hospital, Harvard Medical School, and Boston University School of Public Health, Boston, Massachusetts; ⁴Robert G. Marx, MD, MSc, Lisa A. Mandl, MD, MPH: Hospital for Special Surgery and Weill Cornell Medicine, New York, New York; ⁵Ali Guermazi,

MD, PhD: Boston University School of Medicine, Boston, Massachusetts; ⁶Mohamed Jarraya, MD: Massachusetts General Hospital, Boston, Massachusetts; ⁷Bruce A. Levy, MD: Mayo Clinic, Rochester, Minnesota; ⁸Rick W. Wright, MD: Vanderbilt University Medical Center, Nashville, Tennessee; ⁹Kurt P. Spindler, MD: Cleveland Clinic, Cleveland, Ohio.

Author disclosures are available at <https://onlinelibrary.wiley.com/action/downloadSupplement?doi=10.1002%2Fart.42105&file=art42105-sup-0001-Disclosureform.pdf>.

Address correspondence to Jamie E. Collins, PhD, Orthopedics and Arthritis Center for Outcomes Research, Department of Orthopedic Surgery, Brigham and Women's Hospital, 75 Francis Street, BTM 5-016, Boston, MA, 02115. Email: jcollins13@bwh.harvard.edu.

Submitted for publication April 23, 2021; accepted in revised form February 28, 2022.

limitations, treatment options include a nonsurgical approach, consisting of physical therapy (PT) and pharmacologic pain management (including injection-administered drugs), and a surgical approach, comprising arthroscopic partial meniscectomy (APM).

Several studies have examined associations between meniscal tear and its treatment modalities and structural changes in the joint. Meniscal damage has been associated with future cartilage loss (3), and APM has been associated with the development and radiographic progression of OA (4,5). Observational data from the Osteoarthritis Initiative suggested that patients undergoing APM had an increased risk of undergoing total knee replacement (6), while in a randomized controlled trial (RCT), Katz et al observed that 10% of participants with symptomatic meniscal tear treated with APM underwent total knee replacement within 5 years, compared to 2% of those who underwent PT (7). The mechanism behind this phenomenon remains unclear. One possibility is that surgery is associated with greater structural worsening of the knee joint. In 3 recent studies, investigators reported 5-year outcomes of RCTs of APM versus nonoperative treatment or sham surgical procedure and pointed to the potential for a modestly increased risk of radiographic worsening in the APM group (5,8,9). However, these trials included participants largely free from radiographic OA at baseline, did not use MRI (which is more sensitive in assessing structural worsening than plain radiography), and did not include serial imaging.

In an earlier analysis of the Meniscal Tear in Osteoarthritis Research (METEOR) trial cohort, we showed that participants treated with APM had a higher odds of worsening for several MRI-based markers of knee OA, including cartilage surface area damage, osteophyte size, and effusion-synovitis, 18 months after randomization as compared to patients treated with PT (10). Whether this short-term association between APM and MRI-based structural worsening persists over a longer follow-up period is not yet known.

Our present study aimed to address this gap in the literature and further our understanding of the link between APM and OA progression. To these ends, we used MRIs from 5-year follow-up of METEOR trial participants to assess the effects of surgical and nonsurgical treatments on structural changes in OA.

MATERIALS AND METHODS

Study sample. We used data from the METEOR trial, a multicenter RCT of APM with PT versus PT alone in patients with degenerative meniscal tear, symptoms consistent with meniscus tear, and evidence of mild-to-moderate knee OA, defined as evidence of osteophytes or full-thickness cartilage defect on MRI or evidence of OA on plain radiography (i.e., a Kellgren/Lawrence [K/L] grade of 2 or 3) (11,12). Participants eligible for the trial were ≥ 45 years old at baseline, had knee pain for ≥ 4 weeks, had evidence on knee MRI of a meniscal tear that extended to the surface of the meniscus, and had evidence of OA on

either MRI or radiography. The detailed inclusion and exclusion criteria are published elsewhere (13). The original trial protocol and statistical analysis plan are available with the main publication associated with the trial (12).

In the trial, surgeons used standard arthroscopic portals and trimmed the damaged portion of the meniscus to a stable rim in participants who underwent APM (13). They did not penetrate the subchondral bone but trimmed loose fragments of bone and cartilage. Treatment for the PT group consisted of a standardized strengthening-based PT protocol that included weekly sessions with a physical therapist and home-based exercises (13). The trial allowed participants in both groups to follow up with their surgeon throughout the study if symptoms persisted despite the assigned treatment. Consequently, participants assigned to the PT group were permitted to cross over to the APM group.

Outcomes. At baseline, participants underwent MRI as part of their routine clinical care and to confirm meniscal tear. All MRIs were obtained using the following clinical sequence library: sagittal intermediate- or proton density-weighted fat-suppressed, axial intermediate- or proton density-weighted fat-suppressed, coronal intermediate- or proton density-weighted fat-suppressed, and coronal non-fat-suppressed T1-weighted sequences. These sequences are appropriate for semiquantitative assessment of cartilage damage, bone marrow lesions (BMLs), meniscal and ligament lesions, and synovitis and joint effusion. Participants were invited back at months 18 and 60 after randomization to undergo repeat MRIs using the same library of clinical sequences as that for baseline images. MRIs were read by an experienced radiologist (AG or MJ), using the MRI OA Knee Score (MOAKS) (14). The radiologist was unblinded with regard to time point but blinded with regard to treatment and demographic characteristics. The MOAKS system describes key pathoanatomic features, including BMLs, cartilage surface area damage, cartilage thickness damage, osteophytes, effusion-synovitis, and Hoffa-synovitis. In the MOAKS system, the knee joint is divided into subregions, and each subregion is scored on an ordinal scale of 0–3 for a given feature.

For BMLs, cartilage surface area and thickness, and osteophytes, we assessed structure by summing the subregion scores for each feature. BML size, cartilage surface area damage, and cartilage thickness damage are assessed in 14 subregions, allowing a total summary score of 0–42. Osteophyte size is assessed in 12 locations, allowing a total summary score of 0–36. We also created 2 categorical indicators of structural change between the first and last MRIs during each study interval (i.e., between baseline and 18 months and between 18 and 60 months): 1) an increase in score in any subregion and 2) an increase in score for ≥ 1 additional subregion (10,15,16). BML size, cartilage damage, and osteophyte size were evaluated across all subregions in the primary analysis. In sensitivity analyses, we investigated the medial and lateral compartments separately. In the MOAKS system, effusion-synovitis and Hoffa-synovitis are each rated on an

ordinal scale of 0–3. Changes in effusion-synovitis and Hoffa-synovitis were categorized as improvement or no change versus worsening on MRI. In sensitivity analyses, we evaluated the following 3-level outcome: improvement versus no change versus worsening on MRI.

Covariates. Variables obtained by participant questionnaire and used in the analysis included demographic features (age, sex, race and ethnicity, and body mass index [BMI]) and baseline Knee Injury and Osteoarthritis Outcome Score (KOOS) for the pain and activities in daily living (ADL) subscales (range 0–100, with 100 being most severe) (17). K/L grade was obtained by reading the baseline radiograph. We categorized meniscal damage at baseline into 5 groups, based on the MOAKS system: 1) root tear (posterior root), 2) maceration (partial or complete, in any compartment), 3) long complex or horizontal tears (spanning 2 or 3 regions), 4) short complex or horizontal tears (visualized in only 1 region), and 5) simple tears, comprising vertical and radial tears (18).

Analytic sample. We included participants with ≥ 1 MRI at baseline, 18 months, and/or 60 months after randomization. Participants crossing over from the PT group to the APM group > 6 months after randomization were excluded from all analyses, to ensure that participants analyzed in the surgical group in as-treated analyses were exposed to surgery for ≥ 12 months before assessment by MRI, permitting a clinically sensible time for any effects of surgery on structural change to occur.

As recommended for trials with nontrivial loss to follow-up or crossover, we performed both intention-to-treat (ITT) and as-treated analyses (19). The approaches have slightly different interpretations and distinct advantages and disadvantages. In the ITT analysis, participants were analyzed according to randomization group, irrespective of treatment received. This pragmatic approach reflects the range of events that might occur following a treatment decision in clinical practice, and it maintains the balance of potential confounders among study groups that is achieved by randomization (20). However, results of ITT analysis are affected by the trial-specific pattern of adherence to the treatment regimen and thus show the effect of treatment assignment on outcome (19). In the as-treated analysis, participants crossing over from the PT group to the APM group ≤ 6 months after randomization were analyzed in the APM group. This approach aims to estimate the effectiveness of the treatment received. However, the decision to comply with the treatment protocol may not be random and may disrupt the balance of potential confounders that is gained through randomization (21,22).

Statistical analysis. We compared baseline characteristics of participants included in the analytic cohort to those of participants excluded from analysis. We evaluated the association

between baseline characteristics and treatment group to determine whether the characteristics were balanced between the groups for both the ITT and as-treated analyses.

Continuous outcomes. We used linear mixed-effects models to assess the association between treatment group and MOAKS summary score within each imaging domain (i.e., BMLs, cartilage surface area, cartilage thickness, and osteophytes) (23). We used a time \times treatment interaction term to estimate the effect of structural change during the 2 intervals: baseline to 18 months and 18 to 60 months.

Categorical outcomes. We used Poisson regression with robust error variance to assess the association between treatment group and categorical change in joint structure, estimating the ratio of the risk of MRI-based worsening in the APM group to the risk in the PT group for each outcome (i.e., BML size, cartilage surface area damage, cartilage thickness damage, osteophyte size, effusion-synovitis, and Hoffa-synovitis). This approach allows for the computation of risk ratios (RRs). Our primary analysis used data imputed under the missing-at-random assumption, which is described below.

Table 1. Baseline clinical and demographic characteristics among 302 Meniscal Tear in Osteoarthritis Research (METEOR) trial participants*

Sex	
Male	128 (42.4)
Female	174 (57.6)
Race	
Non-White	48 (15.9)
White	254 (84.1)
Age, years	58.1 \pm 7.4
BMI, kg/m ²	30 \pm 6
KOOS pain subscale score [†]	46.7 \pm 16
WOMAC pain subscale score [†]	40.6 \pm 17.3
KOOS ADL subscale score [†]	37 \pm 18.2
Kellgren/Lawrence grade	
0	28 (9.3)
1	61 (20.2)
2	116 (38.4)
3	97 (32.1)
Meniscal tear [‡]	
None or signal abnormality	4 (1.4)
Nondegenerative, simple	37 (12.8)
Short, degenerative, complex	102 (35.3)
Long, degenerative, complex	89 (30.8)
Root	57 (19.7)
Location [§]	
Medial	200 (70.2)
Lateral	44 (15.4)
Both	41 (14.4)

* Values are the number (%) of participants or mean \pm SD. BMI = body mass index; KOOS = Knee Injury and Osteoarthritis Outcome Score; WOMAC = Western Ontario and McMaster Universities Osteoarthritis Index; ADL = Activities in Daily Living.

[†] Values are from baseline and on a scale of 0–100, with 100 being most severe.

[‡] Values exclude 13 participants without baseline magnetic resonance imaging.

[§] Values exclude 4 participants without tear or with signal abnormality only.

Missing data. Our primary analyses were conducted under the missing-at-random assumption, which asserts that missing data may depend on observed outcomes or covariates but not on unobserved outcomes. Continuous data were analyzed with linear mixed-effects models, which can handle imbalanced data that are missing at random. There is no requirement that each participant be measured at the same time points or that participants have the same number of measurements, and participants with only 1 observation contribute to the estimation of the fixed effects (23). Categorical change cannot be created if data are missing; therefore, we imputed missing data for categorical outcomes, using multiple imputation for participants with missing data at any of the 3 imaging time points. Details of the multiple imputation procedure are provided in the Supplementary Materials, available on the *Arthritis & Rheumatology* website at <http://onlinelibrary.wiley.com/doi/10.1002/art.42105>. In our primary analysis, we imputed values for the following variables under the

missing-at-random assumption, assuming that missing data were associated with observed data: baseline K/L grade, sex, race, BMI, baseline pain, function, mental health index, and musculoskeletal pain index, and observed longitudinal MOAKS score (24,25).

Previous work has suggested that structural progression of OA in participants undergoing total knee replacement may occur at a faster rate than that in participants not undergoing this procedure (7). Thus, data for participants who withdrew from the study to undergo total knee replacement may be deemed missing not at random (MNAR); structural progression for such individuals may be worse than expected on the basis of observed covariates alone. We performed sensitivity analyses using multiple imputation to investigate data that were potentially MNAR because of total knee replacement (25). Details are provided in the Supplementary Materials, available on the *Arthritis & Rheumatology* website at <http://onlinelibrary.wiley.com/doi/10.1002/art.42105>. As a

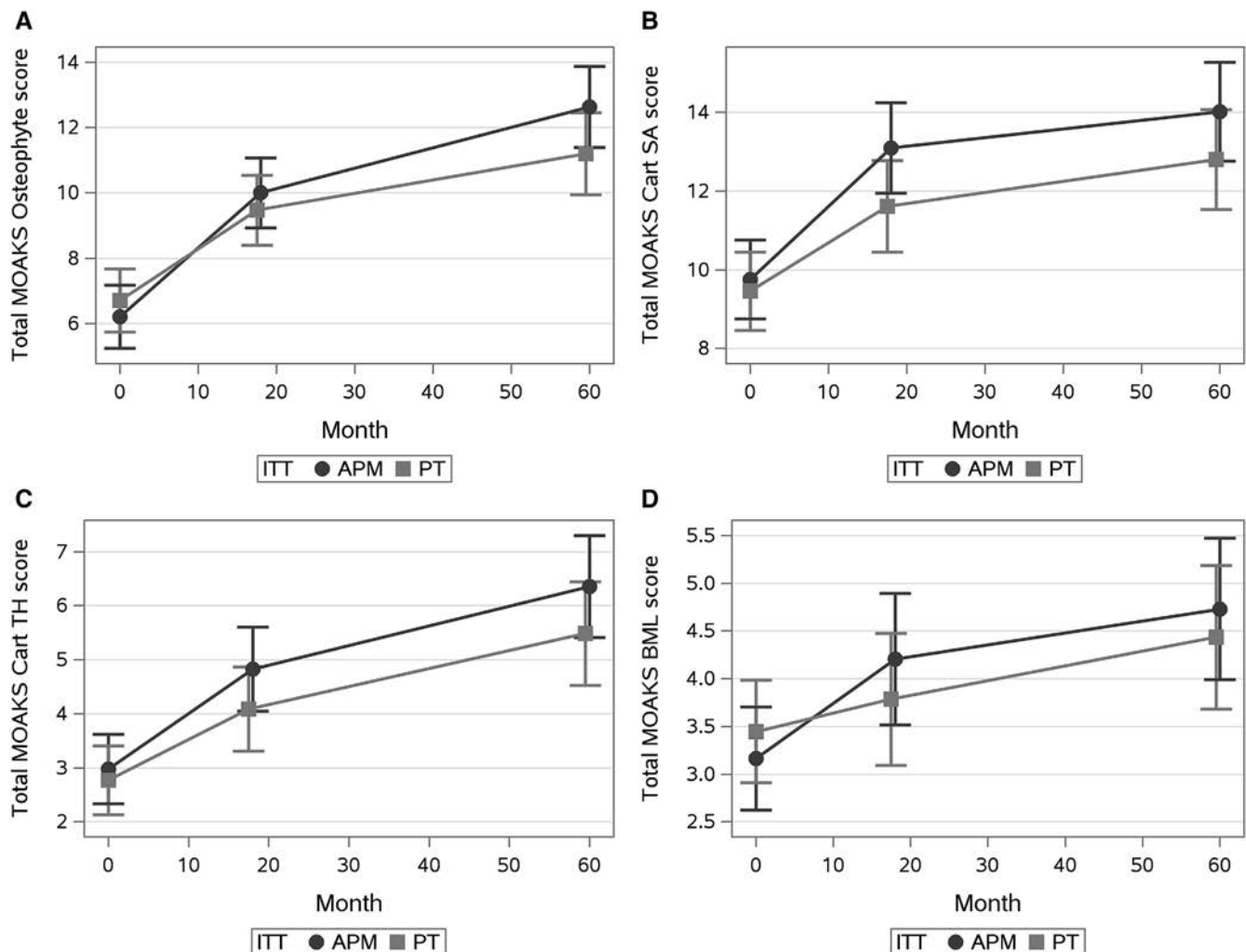


Figure 1. Linear mixed-effects models of the total Magnetic Resonance Imaging Osteoarthritis Knee Score (MOAKS) in the arthroscopic partial meniscectomy (APM) and physical therapy (PT) groups, by outcome and time point, for the intention-to-treat (ITT) population. Values are the adjusted means (95% confidence intervals). BML = bone marrow lesion; Cart SA = cartilage surface area; Cart TH = cartilage thickness.

final sensitivity analysis, we conducted complete case analysis, including only those participants with complete data at all 3 time points.

P values less than 0.05 were considered statistically significant. All analyses were conducted using SAS 9.4 (SAS Institute).

RESULTS

Sample. Of the 351 randomized participants, 316 (90%) had ≥ 1 baseline, 18-, or 60-month MRI available for central reading. Fourteen participants crossed over from the PT group to the APM group >6 months after randomization, leaving 302 participants (86% of the original sample) in the ITT and as-treated analyses. In the ITT analysis, we compared the 154 participants randomized to the APM group to the 148 randomized to undergo PT. Eight participants randomized to the APM group crossed over to the PT group (i.e., did not undergo surgery), and 47 participants randomized to the PT group crossed over to the APM group ≤ 6 months after randomization, leaving 193 and 109 participants in the APM and PT groups, respectively, for as-treated analyses. The baseline characteristics of participants excluded from the analysis did not differ from those of

participants included in the analysis (Supplementary Table 1, available on the *Arthritis & Rheumatology* website at <http://onlinelibrary.wiley.com/doi/10.1002/art.42105>).

Fifty-eight percent of participants included in the analytic sample were female, and 84% were White (Table 1). The mean \pm SD values at baseline for select characteristics were as follows: age, 58 \pm 7 years; BMI, 30 \pm 6 kg/m²; KOOS pain subscale score, 47 \pm 16; and KOOS ADL subscale score, 37 \pm 18. A total of 70% of participants had meniscal tear in the medial compartment only, 15% had tear in the lateral compartment only, and 14% had tear in both compartments. Baseline MRI data were available for 96% of participants, month 18 MRI data were available for 75%, and month 60 data were available for 56% (Supplementary Tables 2 and 3, available on the *Arthritis & Rheumatology* website at <http://onlinelibrary.wiley.com/doi/10.1002/art.42105>). Among those crossing over from the PT group to the APM group and included in this analysis, the median time to crossover was 76 days. For both the ITT and as-treated analyses, study groups were balanced with regard to baseline characteristics (Supplementary Tables 2 and 3). Descriptive statistics for MOAKS scores, stratified by treatment group, are provided in Supplementary Table 4, available on the *Arthritis & Rheumatology* website at <http://onlinelibrary.wiley.com/doi/10.1002/art.42105>.

Table 2. Changes in MOAKS score in the APM and PT groups, by imaging domain and study period, for the ITT and as-treated populations*

Population, domain, period	Total change in score			Change in score per 12 months			<i>P</i>
	Mean (95% CI)		Absolute difference in mean (95% CI)	Mean (95% CI)		Absolute difference in mean (95% CI)	
	APM (n = 154)	PT (n = 148)		APM (n = 154)	PT (n = 148)		
ITT							
Osteophytes							
BL to 18 months	3.8 (3.2, 4.4)	2.8 (2.2, 3.4)	1.0 (0.2, 1.9)	2.5 (2.1, 2.9)	1.9 (1.4, 2.3)	0.7 (0.1, 1.3)	0.0189
18–60 months	2.6 (2.0, 3.2)	1.7 (1.1, 2.3)	0.9 (0.0, 1.8)	0.8 (0.6, 0.9)	0.5 (0.3, 0.7)	0.3 (0.0, 0.5)	0.0403
Cartilage surface area							
BL to 18 months	3.3 (2.8, 3.9)	2.2 (1.6, 2.7)	1.2 (0.4, 2.0)	2.2 (1.8, 2.6)	1.4 (1.1, 1.8)	0.8 (0.2, 1.3)	0.0048
18–60 months	0.9 (0.3, 1.6)	1.2 (0.5, 1.9)	−0.3 (−1.2, 0.7)	0.3 (0.1, 0.4)	0.3 (0.1, 0.5)	−0.1 (−0.3, 0.2)	0.5702
Cartilage thickness							
BL to 18 months	1.8 (1.4, 2.3)	1.3 (0.9, 1.7)	0.5 (−0.1, 1.1)	1.2 (1.0, 1.5)	0.9 (0.6, 1.2)	0.4 (0.0, 0.7)	0.0744
18–60 months	1.5 (1.0, 2.0)	1.4 (0.9, 1.9)	0.1 (−0.6, 0.8)	0.4 (0.3, 0.6)	0.4 (0.3, 0.5)	0.0 (−0.2, 0.2)	0.7054
Bone marrow lesions							
BL to 18 months	1.0 (0.5, 1.6)	0.3 (−0.2, 0.9)	0.7 (−0.1, 1.5)	0.7 (0.3, 1.1)	0.2 (−0.1, 0.6)	0.5 (−0.1, 1.0)	0.0791
18–60 months	0.5 (0.0, 1.1)	0.6 (0.1, 1.2)	−0.1 (−0.9, 0.7)	0.2 (0.0, 0.3)	0.2 (0.0, 0.3)	0.0 (−0.3, 0.2)	0.7570
As-treated							
(n = 193) (n = 109)							
Osteophytes							
BL to 18 months	3.6 (3.1, 4.1)	2.6 (1.9, 3.4)	1.0 (0.1, 1.9)	2.4 (2.1, 2.8)	1.8 (1.3, 2.3)	0.6 (0.0, 1.3)	0.0375
18–60 months	2.4 (1.9, 3.0)	1.8 (1.0, 2.5)	0.7 (−0.2, 1.6)	0.7 (0.5, 0.9)	0.5 (0.3, 0.7)	0.2 (−0.1, 0.5)	0.1343
Cartilage surface area							
BL to 18 months	3.0 (2.5, 3.6)	2.2 (1.5, 2.9)	0.9 (0.0, 1.7)	2.0 (1.7, 2.4)	1.5 (1.0, 1.9)	0.6 (0.0, 1.2)	0.0550
18–60 months	1.2 (0.6, 1.8)	0.8 (0.1, 1.6)	0.4 (−0.6, 1.3)	0.3 (0.2, 0.5)	0.2 (0.0, 0.4)	0.1 (−0.2, 0.4)	0.4495
Cartilage thickness							
BL to 18 months	1.8 (1.4, 2.2)	1.2 (0.7, 1.7)	0.6 (0.0, 1.2)	1.2 (1.0, 1.4)	0.8 (0.5, 1.1)	0.4 (0.0, 0.8)	0.0562
18–60 months	1.3 (0.9, 1.8)	1.6 (1.1, 2.2)	−0.3 (−1.0, 0.4)	0.4 (0.3, 0.5)	0.5 (0.3, 0.6)	−0.1 (−0.3, 0.1)	0.4208
Bone marrow lesions							
BL to 18 months	0.9 (0.4, 1.4)	0.3 (−0.4, 1.0)	0.6 (−0.2, 1.5)	0.6 (0.3, 0.9)	0.2 (−0.3, 0.6)	0.4 (−0.1, 1.0)	0.1361
18–60 months	0.6 (0.1, 1.1)	0.6 (−0.1, 1.2)	0.0 (−0.8, 0.8)	0.2 (0.0, 0.3)	0.2 (0.0, 0.3)	0.0 (−0.2, 0.2)	0.9555

* Analysis was performed using linear mixed-effects modeling. MOAKS = Magnetic Resonance Imaging Knee Osteoarthritis Score; APM = arthroscopic partial meniscectomy; PT = physical therapy; ITT = intention-to-treat; 95% CI = 95% confidence interval; BL = baseline.

Table 3. Risk of a worsening MOAKS score in the APM group relative to that in the PT group, by imaging domain and study period, for the ITT and as-treated populations*

Domain, category, period	ITT, RR (95% CI)	<i>P</i>	As-treated, RR (95% CI)	<i>P</i>
Osteophytes				
≥1 additional SR with worsening score				
BL to 18 months	1.24 (1.02, 1.50)	0.0309	1.24 (1.01, 1.53)	0.0446
18–60 months	1.21 (0.81, 1.82)	0.3535	1.19 (0.75, 1.87)	0.4548
Any SR with worsening score				
BL to 18 months	1.14 (1.00, 1.32)	0.0572	1.13 (0.96, 1.32)	0.1354
18–60 months	1.28 (1.04, 1.58)	0.0196	1.16 (0.91, 1.48)	0.2352
Cartilage surface area				
≥1 additional SR with worsening score				
BL to 18 months	1.44 (1.13, 1.85)	0.0037	1.44 (1.05, 1.96)	0.0240
18–60 months	1.19 (0.69, 2.05)	0.5195	1.23 (0.73, 2.09)	0.4345
Any SR with worsening score				
BL to 18 months	1.35 (1.14, 1.61)	0.0007	1.28 (1.04, 1.56)	0.0188
18–60 months	1.02 (0.74, 1.40)	0.9016	0.95 (0.68, 1.33)	0.7704
Cartilage thickness				
≥1 additional SR with worsening score				
BL to 18 months	1.14 (0.88, 1.49)	0.3251	1.10 (0.81, 1.49)	0.5442
18–60 months	1.26 (0.86, 1.84)	0.2341	0.95 (0.66, 1.35)	0.7599
Any SR with worsening score				
BL to 18 months	1.16 (0.93, 1.44)	0.2006	1.13 (0.91, 1.41)	0.2794
18–60 months	1.15 (0.85, 1.57)	0.3657	0.97 (0.74, 1.28)	0.8495
Bone marrow lesions				
≥1 additional SR with worsening score				
BL to 18 months	1.32 (0.96, 1.82)	0.0851	1.09 (0.76, 1.58)	0.6293
18–60 months	1.43 (0.97, 2.10)	0.0722	1.33 (0.88, 2.02)	0.1741
Any SR with worsening score				
BL to 18 months	1.24 (1.01, 1.53)	0.0374	1.09 (0.87, 1.36)	0.4661
18–60 months	1.11 (0.92, 1.35)	0.2804	1.07 (0.87, 1.32)	0.5041
Hoffa-synovitis				
Worsening score				
BL to 18 months	0.85 (0.47, 1.53)	0.5897	1.56 (0.78, 3.10)	0.2045
18–60 months	1.45 (0.63, 3.34)	0.3726	1.17 (0.51, 2.71)	0.7038
Effusion-synovitis				
Worsening score				
BL to 18 months	2.62 (1.32, 5.21)	0.0060	2.09 (0.97, 4.51)	0.0594
18–60 months	0.92 (0.50, 1.71)	0.7974	0.88 (0.43, 1.80)	0.7280

* Analyses were performed after imputing missing data; see Materials and Methods for more information. RR = risk ratio; SR = subregion (see Table 2 for other definitions).

Change in osteophyte score. Figure 1A and Table 2 show findings of ITT analysis of the estimated total osteophyte score, by time point and interval. Compared to the score in the PT group, the score in the APM group worsened (i.e., increased) by ~0.7 more points (95% confidence interval [95% CI] 0.1, 1.3) per 12 months between baseline and 18 months and by ~0.3 additional points (95% CI 0.0, 0.5) per 12 months between 18 and 60 months. The risks of having ≥1 additional subregion with a worsening score and having any subregion with a worsening score were higher in the APM group during both periods (Table 3).

Results were similar in the as-treated analyses. The osteophyte score in the APM group worsened by a greater margin as compared to the PT group during both periods (Table 2), and the risks of having ≥1 additional subregion with a worsening score and having any subregion with a worsening score were also greater for both periods, although these associations did

not reach statistical significance in the 18–60-month period (Table 3).

Change in cartilage surface area damage scores. The estimated total cartilage surface area scores, stratified by time point, are presented in Figures 1B (ITT analysis) and 2B (as-treated analysis). In both sets of analyses, participants in the APM group appeared to be at elevated risk of MRI-based worsening from baseline to 18 months but not from 18 to 60 months, compared to the PT group. In the ITT analysis, the risk of worsening in any subregion was 1.35 times higher (95% CI 1.14, 1.61) in the APM group, compared to the PT group, from baseline to month 18, while the risk of worsening from months 18 to 60 was similar between the groups (RR 1.02 [95% CI 0.74, 1.40]) (Table 3). Similar associations were seen in the as-treated analyses.

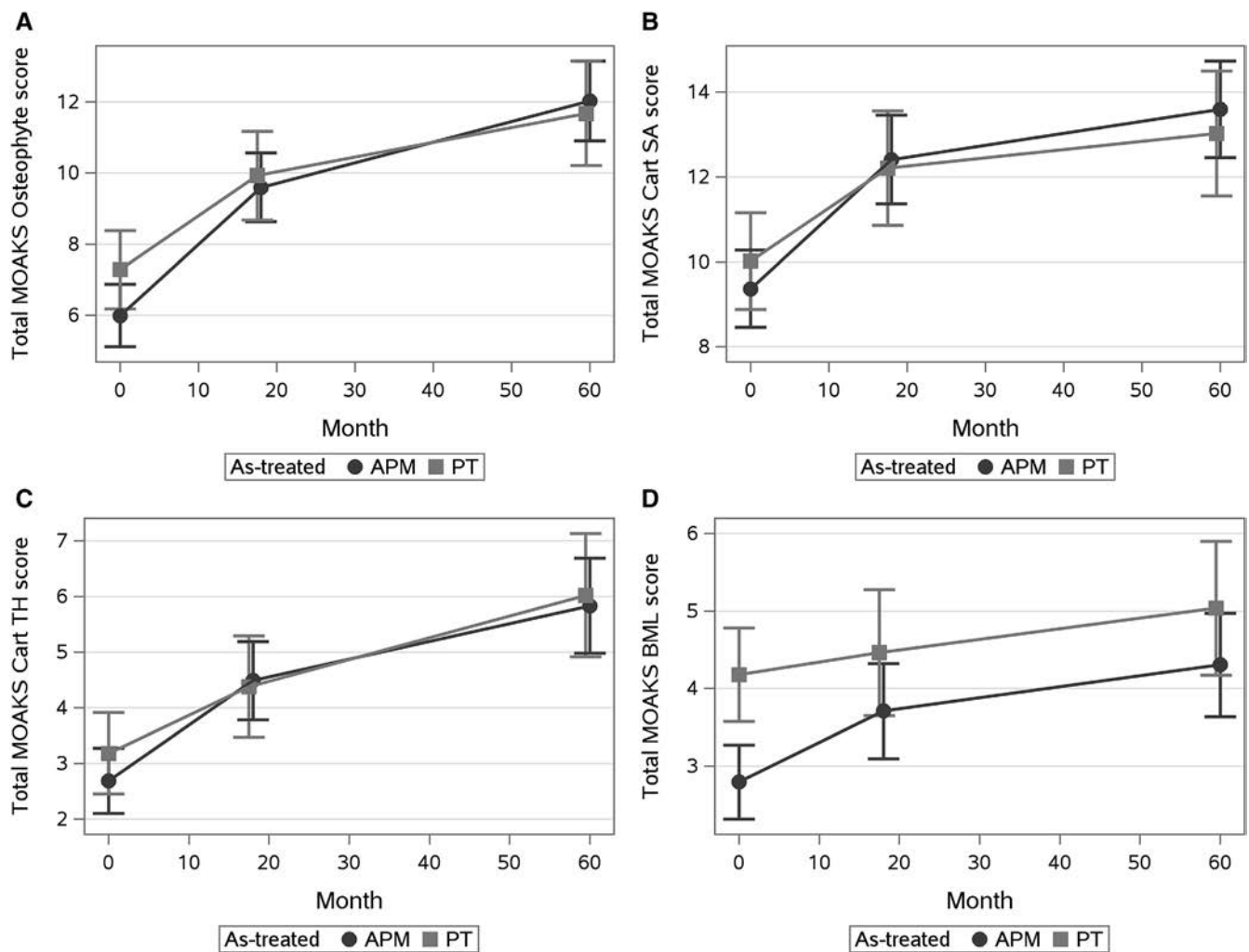


Figure 2. Linear mixed-effects models of the total MOAKS score in the APM and PT groups, by outcome and time point, for the as-treated population. Values are the adjusted means (95% confidence intervals). See Figure 1 for definitions.

Change in cartilage thickness damage scores. For both the ITT and as-treated analyses, participants in the APM group had slightly elevated although nonsignificant worsening in cartilage thickness scores from baseline to 18 months as compared to the PT group (Table 2). Associations between treatment group and having any subregion with a worsening score and having ≥ 1 additional subregion with a worsening score were attenuated for the 18–60-month period, with RRs close to 1 and nonsignificant in the as-treated and ITT analyses (Table 3).

Change in BML scores. The APM group had a greater worsening in the total BML score from baseline to 18 months for both as-treated and ITT analyses, although these associations were nonsignificant; differences from months 18 to 60 were close to 0 (Table 2). There were slightly increased risks in the APM group of having any subregion with a worsening score and having ≥ 1 additional subregion with a worsening score over both periods, although, again, these associations were largely nonsignificant (Table 3).

Change in effusion-synovitis and Hoffa-synovitis scores. In both the as-treated and ITT analyses, participants in the APM group had a higher risk of a worsening effusion-synovitis score from baseline to 18 months as compared to those in the PT group, with RRs of 2.09 (95% CI 0.97, 4.51) and 2.62 (95% CI 1.32, 5.21), respectively (Table 3). We did not observe an association between treatment group and changes in the effusion-synovitis score over the 18–60-month interval, with RRs close to 1 for both as-treated and ITT analyses. We did not observe any significant associations between changes in Hoffa-synovitis score and treatment group for either period in ITT or as-treated analyses (Table 3).

Sensitivity analyses. *Missing data.* The results were generally robust to the sensitivity analyses for missing data, with a few minor differences. The association between continuous osteophyte score over months 18–60 and treatment group was statistically significant in the primary analysis for the ITT population. In the MNAR sensitivity analyses, this association was significant in both the ITT

and as-treated analyses under all MNAR scenarios (Supplementary Table 7, available on the *Arthritis & Rheumatology* website at <http://onlinelibrary.wiley.com/doi/10.1002/art.42105>). In terms of change per 12 months, the magnitude of the difference in score between the APM and PT groups was greater from baseline to 18 months than from months 18 to 60 under all conditions. The association between the change in continuous cartilage surface area damage score and treatment group over months 18–60 became statistically significant under the most extreme MNAR scenario, from a difference of 0.3 points in favor of APM (i.e., a greater change in score for the PT group) in the primary analysis (Table 2) to a difference of 1.3 points in favor of PT (Supplementary Table 7) in the sensitivity analysis, but only for the as-treated analysis, not the ITT analysis. Again, the magnitude of the difference in score between the APM and PT groups was greater from baseline to 18 months than from months 18 to 60 under all conditions. Results of the MNAR sensitivity analyses for categorical outcomes were similar to those of the primary analysis (Supplementary Table 9, available on the *Arthritis & Rheumatology* website at <http://onlinelibrary.wiley.com/doi/10.1002/art.42105>).

A total of 147 participants (49% of the analytic sample) had MRI data from all 3 time points. Results of sensitivity analysis using this complete case sample were similar to those of the primary analyses (Supplementary Tables 8, 10, and 11, available on the *Arthritis & Rheumatology* website at <http://onlinelibrary.wiley.com/doi/10.1002/art.42105>).

Effusion-synovitis and Hoffa-synovitis outcomes. Sensitivity analyses included a 3-level change variable (i.e., improvement versus no change versus worsening on MRI), and results aligned with those of the main analysis, showing a significant association with treatment group only for the change in effusion-synovitis score from baseline to 18 months (Supplementary Table 6, available on the *Arthritis & Rheumatology* website at <http://onlinelibrary.wiley.com/doi/10.1002/art.42105>). In both ITT and as-treated analyses, a greater percentage of participants in the PT group experienced improved effusion-synovitis outcomes from baseline to 18 months, compared to the percentage in the APM group.

Compartment-specific worsening. Results of sensitivity analyses evaluating changes in the medial and lateral compartments separately were similar in magnitude and direction to results of the respective primary analyses (Supplementary Tables 12–17, available on the *Arthritis & Rheumatology* website at <http://onlinelibrary.wiley.com/doi/10.1002/art.42105>).

DISCUSSION

We used MRIs obtained at baseline and months 18 and 60 of follow-up in the METEOR trial to assess the association between surgical and nonsurgical treatment of meniscal tear and MRI-based structural worsening of OA. These changes were measured as worsening MOAKS scores for cartilage (thickness and surface area damage), BML size, osteophyte size, effusion-

synovitis, and Hoffa-synovitis. Both groups exhibited worsening across all imaging domains and time points, although progression was more pronounced from baseline to 18 months after randomization than from 18 to 60 months after randomization. Compared to the PT group, the APM group had significantly greater MRI-based worsening in cartilage surface area, effusion-synovitis, and osteophytes from baseline to 18 months after randomization. Progression of osteophyte size (i.e., having any subregion with a worsening score, worsening total score) was significantly greater in the APM group from 18 to 60 months after randomization; however, we did not observe differences between the 2 treatment groups in progression of the other MRI-based outcomes from 18 to 60 months. Results were generally robust across various definitions of change and between ITT and as-treated analyses.

Our findings add to a growing body of literature in which investigators assess imaging-based changes in knee joint structure after meniscal tear and treatment by means of an RCT, a study design that allows researchers to disentangle the effect of meniscal tear from the effect of APM. In an as-treated analysis of adults with suspected meniscal injury who were randomized to undergo surgery (APM, in the majority of cases) or exercise therapy, Sonesson et al demonstrated that the K/L grade based on the 5-year follow-up MRI was more severe than that based on the baseline MRI for 60% of participants in the surgery group, compared to 37% in the exercise group (5). While the finding was striking, this difference was not statistically significant ($P = 0.06$), and the sample size was modest, including ~50% of the original cohort (55 participants in the surgery group and 27 in the nonsurgery group) (5).

In the primary ITT analysis of 5-year follow-up data from an RCT comparing exercise therapy to APM in patients with MRI-verified medial degenerative meniscal tear, Berg et al did not observe statistically significant or clinically meaningful differences in Osteoarthritis Research Society International (OARSI) joint space narrowing grade, OARSI osteophyte grade, or incidence of radiographic knee OA (defined as a K/L grade of 2 or higher) between the exercise therapy and APM groups (8). The medial fixed quantitative joint space width (JSW) decreased 0.20 mm (95% CI –0.09, 0.48) more from baseline to 5 years among participants in the APM group, compared to participants in the exercise group. However, the per-protocol and as-treated analyses both showed a significantly greater decrease in fixed quantitative JSW in the APM group than in the exercise group, with as-treated analysis revealing a between-group difference of 0.53 mm (95% CI 0.34, 0.73) (8).

Finally, in the 5-year follow-up analysis of the Finnish Degenerative Meniscus Lesion Study (FIDELITY), in which APM was compared to a sham surgical procedure among participants with MRI-confirmed meniscal tear and without knee OA at baseline, Sihvonen et al reported that 72% in the APM group, compared to 60% in the sham surgery group, experienced progression in radiographic tibiofemoral knee OA by ≥ 1 grade, for an adjusted

risk difference of 13% (95% CI -2% , 28%) (9). In addition, the authors reported that the APM group had greater progression in the OARSI summary score (calculated as the sum of the joint space narrowing and osteophyte grades and ranging from 0 to 18), with an adjusted between-group difference of 0.7 (95% CI 0.1, 1.3). In the aggregate, these 3 studies are consistent in providing evidence of slightly more radiographic structural progression following APM as compared to exercise therapy among persons treated for meniscal tear.

The results from the METEOR trial add to this growing body of literature assessing the effect of treatment on structural changes in persons with meniscal tear. The METEOR trial is unique in that it included participants with baseline knee OA (71% had a K/L grade of 2 or higher), utilized MRIs rather than radiographs to assess structural progression, and included MRIs from the interim time point of 18 months after randomization, which allowed assessment of early progression (from 0 to 18 months after randomization) versus late progression (from 18 to 60 months after randomization). In the METEOR trial, the extent of structural progression in both groups and the associations between treatment and structural progression were most notable in the first 18 months following treatment.

Results presented here align with our earlier analysis of this cohort, which examined categorical MRI-based changes over the first 18 months of follow-up (10). Between 18 and 60 months, participants in both groups experienced slower MRI-based worsening. With the exception of osteophyte score, the greater progression in the APM group as compared to the PT group during the first 18 months was not apparent between 18 and 60 months. This interim time point is another key difference between this work and the 3 radiographic analyses summarized above. Whereas the prior analyses provided a single estimate of the 5-year change in radiographic parameters, our interim (month 18) time point permitted us to show that the differences in progression between surgically and conservatively treated subjects were observed primarily from baseline to 18 months. The reason that the effect of APM on progression is more apparent in the 18 months after surgery than over a longer follow-up period merits further investigation.

While these MRI- and radiography-based studies suggest that APM may be associated with greater MRI-based worsening than PT over the short term, the clinical meaning of these findings is uncertain. In a recent analysis of the METEOR trial cohort, investigators evaluated whether greater worsening in cartilage surface area, cartilage thickness, and osteophyte scores between 0 and 18 months is clinically important by analyzing the association between these early MRI-based structural changes and changes in pain and function over 18 to 60 months (26). The study found no clinically important associations between early structural changes and subsequent changes in pain. Further research is needed to ascertain whether these differences in structural progression observed in the years following APM, compared to PT,

are associated with differences in symptom progression over the longer term. We previously reported on patient-reported outcomes, including KOOS pain and WOMAC function, over 5 years in the METEOR trial (7). We found considerable improvements in both treatment groups that were maintained over the 5-year follow-up period, suggesting that the structural progression we have documented here may not have had clinical consequences over the first 5 years of follow-up. However, individuals who received APM in the METEOR trial were 5-fold more likely than those in the PT group (10% versus 2% of participants) to undergo total knee replacement during the 5-year follow-up period (7).

We acknowledge several limitations to our investigation. Nearly one-third (30%) of the METEOR trial cohort crossed over from the PT group to the APM group in the first 6 months of follow-up. Crossover, along with substantial dropout prior to 5 years, may have disturbed the balance of baseline characteristics achieved through randomization. To address this, we performed both ITT and as-treated analyses. During APM, surgeons were able to trim loose fragments of bone and cartilage that appeared to be causing mechanical symptoms. We cannot exclude the possibility that these surgical interventions, rather than progression of underlying joint damage, gave rise to the early changes in MOAKS cartilage surface area scores. We did not collect data on synovial or serum biomarkers. The METEOR trial enrolled participants with imaging evidence of mild-to-moderate knee OA on either radiography or MRI. Thus, while all subjects had evidence of cartilage damage on MRI, we acknowledge that not all participants met the radiographic definition of OA (i.e., a K/L grade of 2 or higher). Finally, while the radiologist was blinded to treatment and all demographic characteristics, he was unblinded to time point. While this could lead to scoring more change over time as compared to a blinded reading, it should not affect between-group comparisons.

In summary, METEOR trial participants treated with APM showed heightened progression in osteophyte, cartilage surface area, and effusion-synovitis scores from baseline to 18 months, but only osteophyte scores remained significantly different between treatment groups over the subsequent 18–60-month period. The clinical meaning of these findings remains uncertain. Further research is required to determine the relationship of these structural changes to symptoms and other patient-centered outcomes.

AUTHOR CONTRIBUTIONS

All authors were involved in drafting the article or revising it critically for important intellectual content, and all authors approved the final version to be published. Dr. Collins had full access to all of the data in the study and takes responsibility for the integrity of the data and the accuracy of the data analysis.

Study conception and design. Losina, Marx, Guermazi, Jones, Levy, Mandl, Wright, Spindler, Katz.





Acquisition of data. Losina, Guermazi, Jarraya, Katz.

Analysis and interpretation of data. Collins, Shrestha, Losina, Williams, Katz.

REFERENCES

1. Deshpande BR, Katz JN, Solomon DH, Yelin EH, Hunter DJ, Messier SP, et al. Number of persons with symptomatic knee osteoarthritis in the US: impact of race and ethnicity, age, sex, and obesity. *Arthritis Care Res (Hoboken)* 2016;68:1743–50.
2. Bhattacharyya T, Gale D, Dewire P, Totterman S, Gale ME, McLaughlin S, et al. The clinical importance of meniscal tears demonstrated by magnetic resonance imaging in osteoarthritis of the knee. *J Bone Joint Surg Am* 2003;85:4–9.
3. Hunter DJ, Zhang YQ, Niu JB, Tu X, Amin S, Clancy M, et al. The association of meniscal pathologic changes with cartilage loss in symptomatic knee osteoarthritis. *Arthritis Rheum* 2006;54:795–801.
4. Petty CA, Lubowitz JH. Does arthroscopic partial meniscectomy result in knee osteoarthritis? A systematic review with a minimum of 8 years' follow-up. *Arthroscopy* 2011;27:419–24.
5. Sonesson S, Kvist J, Yakob J, Hedevidik H, Gauffin H. Knee arthroscopic surgery in middle-aged patients with meniscal symptoms: a 5-year follow-up of a prospective, randomized study. *Orthop J Sports Med* 2020;8:2325967119893920.
6. Rongen JJ, Rovers MM, van Tienen TG, Buma P, Hannink G. Increased risk for knee replacement surgery after arthroscopic surgery for degenerative meniscal tears: a multi-center longitudinal observational study using data from the osteoarthritis initiative. *Osteoarthritis Cartilage* 2017;25:23–9.
7. Katz JN, Shrestha S, Losina E, Jones MH, Marx RG, Mandl LA, et al. Five-year outcome of operative and nonoperative management of meniscal tear in persons older than forty-five years. *Arthritis Rheumatol* 2020;72:273–81.
8. Berg B, Roos EM, Englund M, Kise NJ, Tiulpin A, Saarakkala S, et al. Development of osteoarthritis in patients with degenerative meniscal tears treated with exercise therapy or surgery: a randomized controlled trial. *Osteoarthritis Cartilage* 2020;28:897–906.
9. Sihvonen R, Paavola M, Malmivaara A, Itälä A, Joukainen A, Kalske J, et al. Arthroscopic partial meniscectomy for a degenerative meniscus tear: a 5 year follow-up of the placebo-surgery controlled FIDELITY (Finnish Degenerative Meniscus Lesion Study) trial. *Br J Sports Med* 2020;54:1332–9.
10. Collins JE, Losina E, Marx RG, Guermazi A, Jarraya M, Jones MH, et al. Early MRI-based changes in patients with meniscal tear and osteoarthritis: eighteen-month data from a randomized controlled trial of arthroscopic partial meniscectomy versus physical therapy. *Arthritis Care Res (Hoboken)* 2019;72:630–40.
11. Kellgren JH, Lawrence JS. Radiological assessment of osteoarthrosis. *Ann Rheum Dis* 1957;16:494–502.
12. Katz JN, Brophy RH, Chaisson CE, de Chaves L, Cole BJ, Dahm DL, et al. Surgery versus physical therapy for a meniscal tear and osteoarthritis. *N Engl J Med* 2013;368:1675–84.
13. Katz JN, Chaisson CE, Cole B, Guermazi A, Hunter DJ, Jones M, et al. The MeTeOR trial (Meniscal Tear in Osteoarthritis Research): rationale and design features. *Contemp Clin Trials* 2012;33:1189–96.
14. Hunter DJ, Guermazi A, Lo GH, Grainger AJ, Conaghan PG, Boudreau RM, et al. Evolution of semi-quantitative whole joint assessment of knee OA: MOAKS (MRI Osteoarthritis Knee Score). *Osteoarthritis Cartilage* 2011;19:990–1002.
15. Collins JE, Losina E, Nevitt MC, Roemer FW, Guermazi A, Lynch JA, et al. Semiquantitative imaging biomarkers of knee osteoarthritis progression: data from the Foundation for the National Institutes of Health Osteoarthritis Biomarkers Consortium. *Arthritis Rheumatol* 2016;68:2422–31.
16. Roemer FW, Guermazi A, Collins JE, Losina E, Nevitt MC, Lynch JA, et al. Semi-quantitative MRI biomarkers of knee osteoarthritis progression in the FNIH biomarkers consortium cohort: methodologic aspects and definition of change. *BMC Musculoskelet Disord* 2016;17:466.
17. Roos EM, Lohmander LS. The Knee Injury and Osteoarthritis Outcome Score (KOOS): from joint injury to osteoarthritis. *Health Qual Life Outcomes* 2003;1:64.
18. MacFarlane LA, Yang H, Collins JE, Guermazi A, Jones MH, Teeple E, et al. Associations among meniscal damage, meniscal symptoms and knee pain severity. *Osteoarthritis Cartilage* 2017;25:850–7.
19. Hernan MA, Hernandez-Diaz S. Beyond the intention-to-treat in comparative effectiveness research. *Clin Trials* 2012;9:48–55.
20. Gupta SK. Intention-to-treat concept: a review. *Perspect Clin Res* 2011;2:109–12.
21. Sainani KL. Making sense of intention-to-treat. *PM R* 2010;2:209–13.
22. Shrier I, Steele RJ, Verhagen E, Herbert R, Riddell CA, Kaufman JS. Beyond intention to treat: what is the right question? *Clin Trials* 2014;11:28–37.
23. Cnaan A, Laird NM, Slasor P. Using the general linear mixed model to analyse unbalanced repeated measures and longitudinal data. *Stat Med* 1997;16:2349–80.
24. Rubin D. Multiple imputation for nonresponse in surveys. New York: Wiley; 1989.
25. Bell ML, Fairclough DL. Practical and statistical issues in missing data for longitudinal patient-reported outcomes. *Stat Methods Med Res* 2014;23:440–59.
26. Katz JN, Collins JE, Jones M, Spindler KP, Marx RG, Mandl LA, et al. Association between structural change over 18 months and subsequent symptom change in middle-aged persons treated for meniscal tear. *Arthritis Care Res (Hoboken)* 2021. doi: <http://onlinelibrary.wiley.com/doi/10.1002/acr.24796>. E-pub ahead of print.

Do Glucocorticoid Injections Increase the Risk of Knee Osteoarthritis Progression Over 5 Years?

Augustin Latourte,¹  Anne-Christine Rat,²  Abdou Omorou,³ Willy Ngueyon-Sime,⁴ Florent Eymard,⁵ Jérémie Sellam,⁶ Christian Roux,⁷ Hang-Korng Ea,¹  Martine Cohen-Solal,¹ Thomas Bardin,¹  Johann Beaudreuil,⁸ Francis Guillemin,³ and Pascal Richette¹

Objective. Recent findings have demonstrated that intraarticular (IA) glucocorticoid injections can be deleterious for knees with osteoarthritis (OA). This study was undertaken to assess, in a real-life setting, the risk of knee OA progression in patients who received IA glucocorticoid injections over a 5-year follow-up period.

Methods. We used marginal structural modeling with inverse probability of treatment weighting to determine the causal association between IA glucocorticoid injections and the 5-year risk of disease progression in patients with symptomatic knee OA from the Knee and Hip Osteoarthritis Long-term Assessment cohort. OA progression was defined as an incident total knee replacement (TKR) and/or radiographic worsening (Kellgren/Lawrence [K/L] grade or joint space narrowing [JSN]). We also examined these outcomes in knees that received IA hyaluronan (IAHA) injections.

Results. Among the 564 patients with knee OA included in the study sample, 51 (9.0%) and 99 (17.5%) received IA glucocorticoid or IAHA injections, respectively, and 414 (63.1%) did not receive any injection during follow-up. Compared to untreated knees, those treated with IA glucocorticoid injections had a similar risk of incident TKR (hazard ratio [HR] 0.92 [95% confidence interval (95% CI) 0.20, 4.14]; $P = 0.91$) or K/L grade worsening (HR 1.33 [95% CI 0.64, 2.79]; $P = 0.44$). IAHA injections had no effect on the risk of TKR (HR 0.81 [95% CI 0.14, 4.63]; $P = 0.81$) or K/L grade worsening (HR 1.36 [95% CI 0.85, 2.17]; $P = 0.20$). Similar results were obtained for JSN, and when TKR and radiographic outcomes were combined.

Conclusion. In this study, IA glucocorticoid injections for symptomatic knee OA did not significantly increase the 5-year risk of incident TKR or radiographic worsening. These findings should be interpreted cautiously and replicated in other cohorts.

INTRODUCTION

Osteoarthritis (OA) of the knee is a highly prevalent disease among adults and a major source of disability. Current treatments aim to alleviate both pain and functional disability by a combination of pharmacologic and nonpharmacologic approaches (1).

Among intraarticular (IA) treatment options (2), IA glucocorticoid injections for knee OA are recommended by international societies to

treat knee OA symptoms (3,4). Meta-analyses found IA glucocorticoid injections to be efficacious for pain in the short term (i.e., 2–4 weeks), with an overall good safety profile (5). However, the effect of repeated IA glucocorticoid injections on cartilage or other joint tissues is unclear. Preclinical studies suggested a time- and dose-dependent effect of steroids on cartilage, high doses and long duration being associated with detrimental effects (6). A large randomized controlled trial of patients with knee OA receiving IA glucocorticoid

Supported by the French Society of Rheumatology and ART-Viggo Association.

¹Augustin Latourte, MD, PhD, Hang-Korng Ea, MD, PhD, Martine Cohen-Solal, MD, PhD, Thomas Bardin, MD, PhD, Pascal Richette, MD, PhD: Université de Paris, INSERM, UMR-S 1132 BIOSCAR, and Rheumatology Department, AP-HP, Lariboisière Hospital, Paris, France; ²Anne-Christine Rat, MD, PhD: Caen Normandie University, UMR-S 1075–Mobilités: Vieillessement, Pathologie, Santé COMETE, Caen, France, Rheumatology Department, CHU Caen, Caen, France, and Université de Lorraine, EA 4360, APEMAC, Nancy, France; ³Abdou Omorou, MD, PhD, Francis Guillemin, MD, PhD: Université de Lorraine, EA 4360, APEMAC, and Inserm CIC 1433 Epidémiologie Clinique, CHRU Nancy, Université de Lorraine Vandoeuvre-lès-Nancy, Nancy, France; ⁴Willy Ngueyon-Sime, PhD: CHU Caen, Caen, France; ⁵Florent Eymard, MD, PhD: Rheumatology Department, Henri Mondor Hospital, AP-HP, Créteil, France; ⁶Jérémie Sellam, MD, PhD: Rheumatology Department,

Sorbonne Université, AP-HP, Saint-Antoine Hospital, Inserm UMRS_938, FHU PaCeMM, Paris, France; ⁷Christian Roux, MD, PhD: Rheumatology Department, CHU Pasteur 2, LAMHES EA6309, UMR7277 iBV CNRS, Nice Sophia Antipolis University, France; ⁸Johann Beaudreuil, MD, PhD: Université de Paris, INSERM, UMR-S 1132 BIOSCAR, and Physical Medicine and Rehabilitation department, Lariboisière–Fernand Widal hospital, Paris, France.

Author disclosures are available at <https://onlinelibrary.wiley.com/action/downloadSupplement?doi=10.1002%2Fart.42118&file=art42118-sup-0001-Discloureform.pdf>.

Address correspondence to Pascal Richette, MD, PhD, Service de Rhumatologie, Hôpital Lariboisière, 2 rue Ambroise Paré, 75010 Paris, France. Email: pascal.richette@aphp.fr.

Submitted for publication July 8, 2021; accepted in revised form March 9, 2022.

injections every 3 months over 2 years found that IA glucocorticoid injections significantly decreased the cartilage volume as measured by magnetic resonance imaging (MRI) (7). Recently, Zeng et al found that patients from the Osteoarthritis Initiative (OAI) cohort who received IA glucocorticoids experienced worsening of both Kellgren/Lawrence (K/L) grade (8) and joint space width during a follow-up period of up to 48 months (9).

These aforementioned studies raised some debate (10), notably because of their relatively short duration (2 years) and the high number of IA glucocorticoid injections performed in the clinical trial regardless of OA symptoms (7). Given the increasing incidence of OA, the paucity of robust treatment for knee OA pain, and the large number of IA glucocorticoid injections performed worldwide (10,11), there is a need to clarify the impact of IA glucocorticoid injections on joint structure in a standard care setting.

To address this issue, we used data from a population-based cohort of patients with symptomatic knee OA during a 5-year follow-up period. A marginal structural model (MSM) with inverse probability of treatment weighting (IPTW) was used to determine the causal association between IA glucocorticoid injections and risk of incident total knee replacement (TKR) as a primary outcome. Because the severity of joint damage is not the sole factor associated with the decision to perform TKR (12), we also examined the impact of IA glucocorticoid injections on K/L grade worsening to address structural progression. For comparison, we assessed the effect of intraarticular hyaluronan (IAHA) injections on these outcomes, because some studies reported that IAHA injections might delay TKR (13–15).

PATIENTS AND METHODS

Study design and patients. The Knee and Hip Osteoarthritis Long-term Assessment (KHOALA) cohort is a French multicenter, population-based cohort of 878 patients ages 40–75 years with symptomatic knee and/or hip OA according to the American College of Rheumatology criteria (16) and with a K/L grade of ≥ 2 on radiographic images. Details of this cohort have been described elsewhere (17). For the purpose of this work, we included patients with symptomatic knee OA at baseline who had completed the 5-year follow-up, representing our study population.

Data collection. Patients were followed up annually using self-report questionnaires. Data collected included sociodemographic features, clinical data, and treatments received. Participants were asked whether they received IA glucocorticoid or IAHA injections during the past 12 months. Patient-reported outcomes included knee-related pain score on a visual analog scale (VAS; 0–100 mm) and function and pain scores on the normalized Western Ontario and McMaster Universities Osteoarthritis Index (WOMAC, 0–100 mm) (18).

Patients had knee radiographs at baseline (year 0) and years 3 and 5. Weight-bearing anteroposterior, posteroanterior

semiflexed, and axial/sky radiographs of both knees were obtained and were transferred to a centralized radiology center for reading and storage. All radiographs were read by 2 independent and trained readers who were blinded with regard to clinical data and were scored according to K/L grade. Interobserver agreement was $\kappa = 0.58$, and intraobserver reliability for each reader was $\kappa = 0.78$ and 0.73 , respectively. Other severe joint-related adverse events (such as osteonecrosis) were also reported by the readers. TKR procedures were self-reported by participants. In case of discrepancies in these self-reported data during follow-up (e.g., change of date and/or side of TKR, or TKR inconsistently reported from one year to the next), data were cross-checked with radiographs or hospitalization data when feasible. Accordingly, unverifiable data were not kept in the database.

Statistical analysis. To assess the effects of IA glucocorticoid injections on knee OA progression, we first examined the risk of joint replacement: TKR was considered the primary outcome and IA glucocorticoid injections the exposure. Next, we assessed the impact of IA glucocorticoid injections on radiographic worsening defined as an increase in K/L grade of ≥ 1 at 5 years of follow-up versus baseline. A similar approach was used for IAHA injections. To ensure that the observed effect of one treatment would not be confounded by the other, we excluded patients who received both treatments in the same knee (IA glucocorticoid and IAHA injections) from the analyzed sample of our primary analysis. All analyses were performed at the joint level (i.e., by independently considering the right and left knee joint of each participant [each participant contributing to 2 statistical units]) to determine the association between IA glucocorticoid injections and risk of incident TKR within the treated knee, estimating hazard ratios (HRs) and 95% confidence intervals (95% CIs). We used a generalized estimating equations model to account for within-patient correlation.

The association between IA glucocorticoid injections and 5-year risk of TKR was analyzed using an MSM, an adapted methodology for analyzing causal association when using observational longitudinal data (19). Associations estimated in observational studies cannot usually be interpreted as causal effects, because the exposed and unexposed subjects are not identical, which results in confounding effects (fixed and time-varying confounders) (Supplementary Figure 1, available on the *Arthritis & Rheumatology* website at <https://onlinelibrary.wiley.com/doi/10.1002/art.42118>). MSM generates a pseudo-population in which exposed and unexposed subjects are similar by eliminating fixed and time-varying confounding. For this purpose, each subject is assigned a weight proportional to the inverse of the probability that each subject had received a treatment at a given time, given a chosen set of covariates (IPTW) (20).

Fixed covariates at inclusion were sex, age, education level, body mass index (BMI), and K/L grade. Time-varying covariates

were comorbidities (Groll comorbidity index [21]) and standardized WOMAC pain and function scores (0–100 mm). At each follow-up (year k), IPTW was calculated with data for fixed covariates (year k = 0) and time-varying covariates at year k – 1 (lagged value) and k.

First, we calculated a propensity score for the exposure (IA glucocorticoid injections) by using logistic regression models. Second, we used the IPTW of being exposed at each follow-up visit (i.e., from year 0 to year 5) to create a pseudo-population (weighted sample), in which the exposure was unconfounded by fixed and time-varying covariates. Third, we tested the balance diagnosis of the weight by analyzing the range and distribution (mean of the weight might be close to 1). Finally, we fitted a general linear model using the calculated weight to estimate the causal effect of receiving IA glucocorticoid injections on the

5-year risk of TKR and survival rate and survival rate difference at each follow-up visit.

In a second step, we investigated the effect of IA glucocorticoid injections on K/L grade worsening by using the same MSM. For this analysis, we excluded individuals who underwent TKR during the 5-year follow-up period as well as those who had a K/L grade of 4 at baseline. We used data collected from the 0-year (baseline), 3-year, and 5-year visits, when radiography was performed. A similar statistical approach was used for IAHA injections. Data on participants undergoing TKR or those lost to follow-up were censored.

We also conducted several sensitivity analyses. First, considering that patients who underwent TKR might have experienced significant progression before a scheduled radiographic

Table 1. Baseline characteristics of the participants with knee OA who received IA glucocorticoid injections*

	No injections (n = 414)	IA glucocorticoid injections (n = 51)	P
Age, mean ± SD years	61.8 ± 8.6	65.3 ± 8.4	0.006
Female	270 (65.2)	37 (72.5)	0.30
BMI, mean ± SD kg/m ²	30 ± 6.2	31.2 ± 6.4	0.18
Associated hip OA	32 (7.7)	3 (5.9)	0.64
Size of municipality of residence			0.78
<2,000 people	148 (35.7)	14 (27.5)	
2,000-49,999 people	184 (44.4)	23 (45.1)	
≥50,000 people	82 (19.8)	14 (27.5)	
Education level			0.35
Primary/middle school	97 (23.5)	16 (32.7)	
High school	219 (53.2)	24 (49.0)	
More than high school	96 (23.3)	9 (18.4)	
K/L grade			0.005
2	203 (49.0)	17 (33.3)	
3	124 (30.2)	13 (25.5)	
4	87 (21.0)	21 (41.2)	
VAS pain score (range 0–100 mm), mean ± SD	35.5 ± 25.5	49.1 ± 26.2	0.0005
WOMAC score, mean ± SD			
Function score (range 0–100 mm)	31.1 ± 22.3	41.6 ± 23.4	0.002
Pain score (range 0–100 mm)	30.4 ± 19.1	38.3 ± 19.6	0.006
No. of painful joints			0.42
0	29 (7.0)	1 (2.0)	
1	101 (24.6)	14 (27.5)	
≥2	184 (68.6)	36 (70.6)	
SF-36 score, mean ± SD			
PCS score	42.6 ± 9.0	38.1 ± 7.1	0.0006
MCS score	46.5 ± 11.2	43.7 ± 11.5	0.10
OAKHQOL score, mean ± SD			
Physical activity score	68.4 ± 22.4	60.2 ± 21.2	0.014
Mental health score	76.4 ± 21.0	71.3 ± 22.5	0.10
Pain score	63.0 ± 25.0	53.3 ± 24.0	0.01
Groll functional comorbidity index, mean ± SD	3 ± 1.5	3.5 ± 1.5	0.01
Previous joint replacement surgery	14 (3.4)	2 (3.9)	0.69
Time from inclusion in KHOALA to first symptoms, mean ± SD years	13.5 ± 8.5	14.3 ± 8.2	0.34
Time from inclusion in KHOALA to OA diagnosis, mean ± SD years	7.7 ± 5.9	9.3 ± 5.2	0.43

* Except where indicated otherwise, data are the number (%). OA = osteoarthritis; IA = intraarticular; BMI = body mass index; K/L = Kellgren/Lawrence; VAS = visual analog scale; WOMAC = Western Ontario and McMaster Universities Osteoarthritis Index; SF-36 = Short Form 36; PCS = physical component summary; MCS = mental component summary; OAKHQOL = Osteoarthritis Knee and Hip Quality of Life questionnaire; KHOALA = Knee and Hip Osteoarthritis Long-term Assessment cohort.

assessment (22), we combined K/L grade worsening and TKR as the outcome. Second, we included the knees that received both types of injections during the follow-up in the analyzed sample, censoring them when the type of injection changed. For this analysis, since the change in treatment could occur before the first radiographic assessment, we used the combined outcome (K/L grade worsening and TKR) to address progression. Third, because the concerns regarding long-term safety of IA glucocorticoid injections are related to cartilage loss rather than other components of the K/L grading system (like osteophytes), we specifically investigated tibiofemoral JSN using a semiquantitative score (0 = none; 1 = mild; 2 = moderate; 3 = severe; 4 = complete JSN), and defined progression as an increase of ≥ 1 during follow-up.

Statistical analyses involved an SAS macro available at <https://www.hsph.harvard.edu/causal/software/> and SAS, version 9.4. *P* values less than 0.05 were considered significant.

RESULTS

Characteristics of the study sample. Tables 1 and 2 show the baseline characteristics of participants who received IA glucocorticoid or IAHA injections and factors associated with the probability of exposure. The mean \pm SD age of the whole knee OA cohort ($n = 656$) was 62.2 years \pm 8.5, 70.3% were female, and 74.5% had a K/L grade of 2 or 3. The mean \pm SD VAS pain score was 38.8 mm \pm 25.4, and the mean \pm SD WOMAC function and pain scores were 34.2 mm \pm 22.4 and 33.2 mm \pm 19.4, respectively. During the study period, IA glucocorticoid and IAHA injections were reported by 51 patients (7.8%) and 99 patients (15.1%), respectively, and 92 patients (14.0%) received both treatments. The mean \pm SD number of reported IA glucocorticoid and IAHA injections during the 5-year follow-up period was 1.9 \pm 1.4 and 2.2 \pm 1.6, respectively. Patients who received IA glucocorticoid or IAHA injections did not differ in age, sex, BMI,

Table 2. Baseline characteristics of the participants who received IAHA injections*

	No injections ($n = 414$)	IAHA injections ($n = 99$)	<i>P</i>
Age, mean \pm SD years	61.8 \pm 8.6	62.1 \pm 7.7	0.75
Female	270 (65.2)	77 (77.8)	0.016
BMI, mean \pm SD kg/m ²	30 \pm 6.2	30.0 \pm 6.1	0.98
Associated hip OA	32 (7.7)	7 (7.1)	0.82
Size of municipality of residence			0.55
<2,000 people	148 (35.7)	30 (30.3)	
2,000-49,999 people	184 (44.4)	46 (46.5)	
$\geq 50,000$ people	82 (19.8)	23 (23.2)	
Education level			0.17
Primary/middle school	97 (23.5)	16 (16.2)	
High school	219 (53.2)	53 (53.5)	
More than high school	96 (23.3)	30 (30.3)	
K/L grade			0.17
2	203 (49.0)	33 (33.3)	
3	124 (30.2)	25 (25.3)	
4	87 (21.0)	41 (41.4)	
VAS pain score (range 0–100 mm), mean \pm SD	35.5 \pm 25.5	43.0 \pm 23.0	0.0001
WOMAC score, mean \pm SD			
Function score (range 0–100 mm)	31.1 \pm 22.3	41.0 \pm 20.0	0.01
Pain score (range 0–100 mm)	30.4 \pm 19.1	38.3 \pm 17.3	0.0003
No. of painful joints			0.32
0	29 (7.0)	11 (11.1)	
1	101 (24.6)	26 (26.3)	
≥ 2	184 (68.6)	62 (62.6)	
SF-36 score, mean \pm SD			
PCS score	42.6 \pm 9.0	37.8 \pm 8.8	<0.0001
MCS score	46.5 \pm 11.2	46.5 \pm 10.8	0.97
OAKHQOL score, mean \pm SD			
Physical activity score	68.4 \pm 22.4	59.7 \pm 21.1	0.0008
Mental health score	76.4 \pm 21.0	69.9 \pm 22.1	0.008
Pain score	63.0 \pm 25.0	57.6 \pm 22.6	0.06
Groll functional comorbidity index, mean \pm SD	3 \pm 1.5	3.1 \pm 1.9	0.38
Previous joint replacement surgery	14 (3.4)	5 (2.6)	0.76
Time from inclusion in KHOALA to first symptoms, mean \pm SD years	13.5 \pm 8.5	12.8 \pm 7.2	0.75
Time from inclusion in KHOALA to OA diagnosis, mean \pm SD years	7.7 \pm 5.9	10.3 \pm 6.3	0.0002

* Except where indicated otherwise, data are the number (%). IAHA = intraarticular hyaluronan (see Table 1 for other definitions).

or comorbidities and had similar pain levels/function scores and K/L grades at baseline.

Effect of intraarticular injections on incident TKR.

Over 5 years of follow-up and among the 564 patients included in the sample, 59 patients (10.5%) underwent knee replacement surgery. After adjustment for potential confounders, IA glucocorticoid injections did not increase the risk of TKR compared to no injections (HR 0.92 [95% CI 0.20, 4.14; $P = 0.91$]) (Figure 1). Similarly, IAHA injections did not increase the risk of TKR compared to no injections (HR 0.81 [95% CI 0.14, 4.63; $P = 0.81$]) (Figure 2).

Effect of intraarticular injections on radiographic worsening.

Next, we used K/L grade worsening as an alternative end point for knee OA progression. We excluded from this analysis patients who underwent TKR during the 5-year follow-up period and those who had a baseline K/L grade of 4, leaving 327 patients (49.8%) in the analyzed sample. The risk of K/L grade worsening for IA glucocorticoid and IAHA injections versus no injections was 1.33 (95% CI 0.64, 2.79; $P = 0.44$) and 1.36 (95% CI 0.85, 2.17; $P = 0.20$), respectively, indicating no

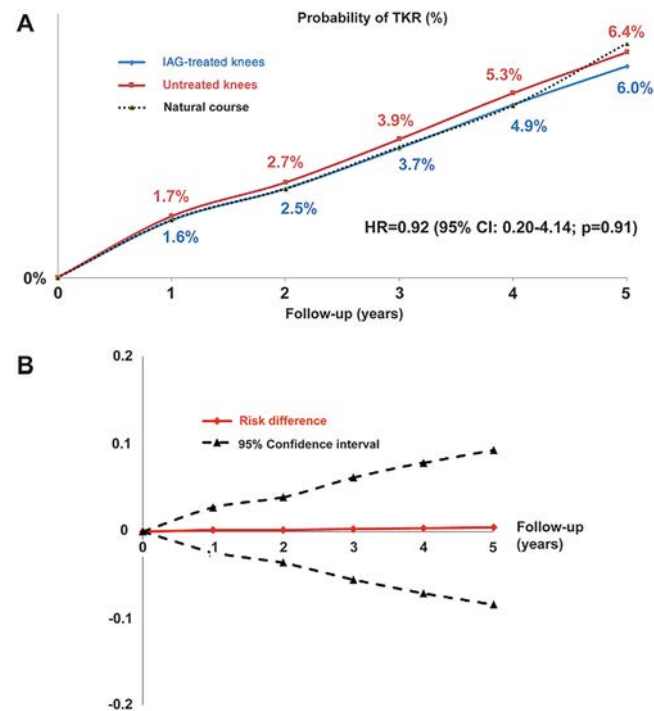


Figure 1. Cumulative incidence (A) and risk difference (B) of total knee replacement (TKR) in knees left untreated or treated with intraarticular glucocorticoid (IAG) injections over 5 years of follow-up. In A, the curves represent the 5-year cumulative incidence using the hypothesis that all patients received IA glucocorticoid injections or that no patient received any injection during follow-up. The dashed black line represents the cumulative incidence observed in the sample (without any hypothesis). HR = hazard ratio; 95% CI = 95% confidence interval.

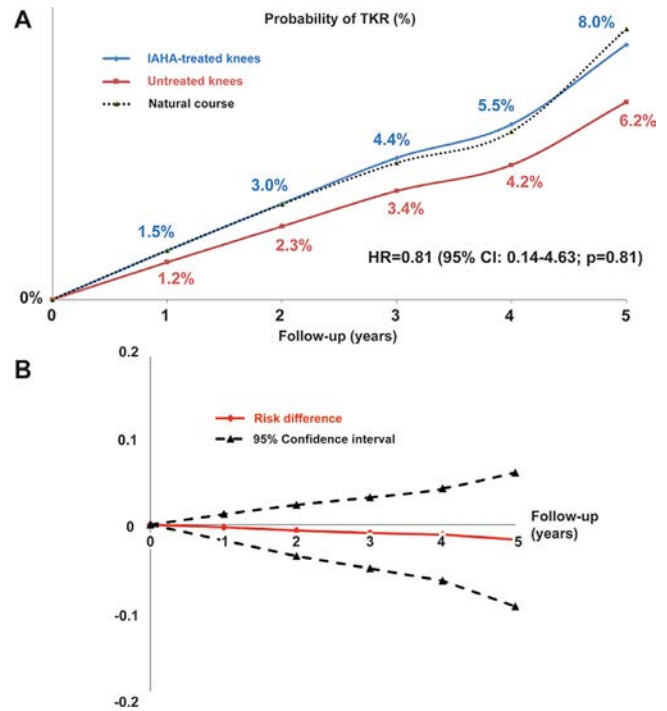


Figure 2. Cumulative incidence (A) and risk difference (B) of TKR in knees treated or not with intraarticular hyaluronan (IAHA) injections over 5 years of follow-up. In A, the curves represent the 5-year cumulative incidence using the hypothesis that all patients received IAHA injections or that no patient received any injection during follow-up. The dashed black line represents the cumulative incidence observed in the sample (without any hypothesis). See Figure 1 for other definitions.

significant impact of IA injections on K/L grade worsening. Only 1 case of incident osteonecrosis occurred during the follow-up, in a knee that did not previously receive intraarticular injections.

Sensitivity analyses.

The results did not change when K/L grade worsening and TKR were combined in a single outcome for knee OA progression, with an HR of 1.32 (95% CI 0.47, 3.72; $P = 0.60$) and an HR of 1.13 (95% CI 0.56, 2.29; $P = 0.73$) for IA glucocorticoid and IAHA injections, respectively. We also did not observe any impact of IA glucocorticoid and IAHA injections on OA progression when we used a semiquantitative score for JSN instead of the K/L grade (HR 0.90 [95% CI 0.37, 2.22; $P = 0.82$] for IA glucocorticoid injections and HR 1.16 [95% CI 0.68, 1.96; $P = 0.59$] for IAHA injections).

When we included the knees that received both IA glucocorticoid and IAHA injections during follow-up (Supplementary Table 1, available on the *Arthritis & Rheumatology* website at <https://onlinelibrary.wiley.com/doi/10.1002/art.42118>), censoring them when the type of injection changed, it did not significantly change our results with IA glucocorticoid injections (HR 0.97 [95% CI 0.53, 1.76; $P = 0.91$] for K/L grade worsening/TKR and HR 0.70 [95% CI 0.41, 1.18; $P = 0.18$] for JSN worsening/TKR) or with IAHA injections (HR 0.98 [95% CI 0.55, 1.75; $P = 0.96$])

for K/L grade worsening/TKR and HR 1.14 [95% CI 0.76, 1.69; $P = 0.53$] for JSN worsening/TKR).

DISCUSSION

Recent studies have raised concerns with regard to putative, deleterious effects of IA glucocorticoid injections in patients with knee OA (7,9,23). IA glucocorticoid injections are widely used in clinical practice, so we aimed to clarify their long-term tolerance on joint structure in a “real-life” setting.

Here, we used an MSM to investigate the causality between IA glucocorticoid injections and a “hard” outcome (i.e., TKR), along with radiographic progression to assess joint degradation. An MSM was used here to account for time-varying confounders, particularly pain, function, and comorbidities, which are known factors affecting the decision for both IA glucocorticoid injections and TKR. Our data, which reflect real-life routine practice in a population-based cohort of 564 knee OA patients, are reassuring. Indeed, we could not find any statistically significant impact of IA glucocorticoid injections on incident TKR or K/L grade worsening. Similarly, IAHA injections did not influence these outcomes.

The efficacy of IA glucocorticoid injections to alleviate pain in patients with knee OA has been demonstrated in several clinical studies and meta-analyses (24–26). Their efficacy is short term: IA glucocorticoid injections provided greater benefit versus a placebo within 1–4 weeks (standardized mean difference -0.48 [95% CI -0.70 , -0.27]) (27), after which there was no significant difference between groups. A dose–response effect is suggested by some studies, showing that high-dose administration of glucocorticoids might provide greater benefit (28).

Severe known adverse events of IA glucocorticoid injections include an increase in blood glucose levels in people with diabetes mellitus (29) and local sepsis after injections, which is overall very rare, estimated at 1 in 162,000 with the use of a steroid packaged in a sterile syringe (30). Another concern is an increased risk of periprosthetic joint infection after preoperative injections, which should be avoided ≥ 3 months before knee replacement (31,32).

Beyond these relatively short-term adverse events, the long-term effects of glucocorticoids on joint tissues are a matter of debate. By their antiinflammatory properties, glucocorticoids target synovitis, a key driver of pain and subsequent structural damage in knee OA (33,34). In a rat model of OA, glucocorticoids reduced synovial inflammation and joint damage score (35). In humans, targeting synovitis with IA glucocorticoid injections was associated with clinical improvement (36). Therefore, beyond their analgesic properties, IA glucocorticoid injections could hypothetically prevent inflammation-related joint degradation in knee OA.

Some open-label studies and randomized controlled trials found no impact of long-term IA glucocorticoid injections on joint structure assessed on radiographs, with a follow-up that did not exceed 2 years (37–39). However, small changes in cartilage volume or thickness are more accurately detected by MRI

quantitative measurements (40). Data from a large randomized controlled trial in patients with knee OA showed that IA injection of 40 mg of triamcinolone acetonide every 3 months over 2 years, regardless of symptoms, did not have any long-term benefit on pain and resulted in significantly greater cartilage volume loss than saline: the mean change in cartilage thickness as assessed by MRI was -0.21 and -0.10 mm in the IA glucocorticoid and placebo groups, respectively (between-group difference -0.11 mm [95% CI -0.20 , -0.03 mm]) (7). Given the very small between-group difference and the study design, which does not reflect routine care, the clinical significance of this finding is unclear (3). Indeed, although cartilage loss is associated with increased risk of knee replacement (22,41), whether this between-group difference might translate into an increased rate of knee replacement is uncertain. In contrast, other open-label studies and randomized controlled trials demonstrated no impact of long-term IA glucocorticoid injections on joint structure (37–39).

Real-life data are useful to inform the risks associated with IA glucocorticoid injections as performed in routine care. Retrospective case series from a single department demonstrated the occurrence of accelerated OA progression after IA glucocorticoid injections (23), but no firm conclusion can be drawn because of the retrospective design. This case series also raised concerns about a possible risk of osteonecrosis following IA glucocorticoids, but we did not observe such adverse events in our cohort. An observational study, conducted in the OAI, using a methodology similar to ours, showed that repeated IA glucocorticoid injections were associated with an increased risk of knee OA progression as assessed by imaging (JSN or K/L grade worsening) and/or incident TKR over 48 months (8). The reasons for this discrepancy with our data are unclear but may be due to differences in outcome criteria, number and type of injectable glucocorticoids, medical practices, and participant characteristics.

The mechanisms by which IA glucocorticoid injections might have detrimental effects on cartilage are unclear. A systematic review of in vitro and animal studies showed that high-dose steroids were associated with gross cartilage damage and chondrocyte toxicity (6), but low-dose steroids were associated with cell growth and recovery from damage in some experiments (6,42). Therefore, steroids seem to have a time- and dose-dependent effect on cartilage. Given our reassuring findings, and considering the results of the randomized controlled trial by McAlindon et al (7), we believe that IA glucocorticoid injections should not be repeatedly performed over the long term in patients with paucisymptomatic knee OA but rather should be used to treat flares, as is usually done in routine care, without fearing subsequent joint degradation.

For comparison, we assessed the impact of IAHA injections on knee OA progression. Previous studies found that IAHA injections could increase the cartilage volume and modulate the levels of joint biomarkers (43,44). In addition, observational studies reported that IAHA injections might delay TKR (13–15,45).

However, the design of the latter studies precludes ascertaining any causality, and therefore, they did not provide a good level of evidence to support the chondroprotective property of HA. Consistent with a recent nested case–control study (46), we found no impact of IAHA injections on incident TKR. These findings suggest that the delay in TKR reported in the previous studies was not causal but rather due to other factors.

Our study had strengths that deserve comment. KHOALA is a well-phenotyped cohort of knee and hip OA patients that aimed to identify prognostic factors of OA course, providing data in a real-life setting (16) with a long follow-up. This cohort provides a representative sample of individuals with knee OA along with their treatment in our country. We used an MSM allowing for inference of causal relations in estimating the treatment effects by adjusting for time-varying confounders, which may also be intermediate variables, and by controlling for bias from potential informative dropout.

However, our study also had some limitations that need to be discussed. First, we used K/L grade worsening to define knee OA progression, a commonly used tool that is not without pitfalls. K/L grades 2 and 3 encompass various degrees of JSN. Replacing K/L grade with a semiquantitative score for JSN did not change our results, but it should be noted that JSN itself may reflect other pathologies than cartilage loss, such as meniscal extrusion (40). Future studies should use MRI to assess cartilage loss and joint tissues damage with more precision (47). Second, our results are based on a relatively small number of patients, and one might speculate that, given our relatively wide confidence bounds of estimates, our study was underpowered to detect an effect of IA glucocorticoids or IAHA on knee OA progression. To address this issue, we performed several sensitivity analyses, the results of which were similar to those of the primary analysis.

Third, our population is representative of a French population with symptomatic knee OA who were treated in a primary care setting, and thus, our findings cannot be generalized to other populations. Beyond differences in demographic data, treatment rates and the use of TKR can vary substantially from country to country, depending on local guidelines and the healthcare system. However, Bucci et al recently reported very similar results in the OAI and the Multicenter Osteoarthritis Study; for example, IA glucocorticoid injections were not associated with an increased risk of knee OA progression when compared to IAHA injections, and these findings strengthen the validity of our data (48). Additionally, we do not have data on the type of glucocorticoids used or hyaluronan type and dosage. Finally, queries on IA glucocorticoid or IAHA injections were recorded annually within the 12 months before the study visit, and therefore, we cannot exclude a recall bias in our study.

In conclusion, in a cohort of patients with symptomatic knee OA in a real-life setting, we found that patients treated with IA

glucocorticoid injections were at a similar risk of TKR or radiologic progression over 5 years compared to untreated patients. Similar findings were obtained for IAHA injections. These data are reassuring and need to be replicated in other cohorts.

ACKNOWLEDGMENTS

We thank all patients included in the KHOALA cohort. We thank the ART-Viggo Association and the French Osteoarthritis Study Group for their financial support.

AUTHOR CONTRIBUTIONS

All authors were involved in drafting the article or revising it critically for important intellectual content, and all authors approved the final version to be published. Dr. Latourte had full access to all of the data in the study and takes responsibility for the integrity of the data and the accuracy of the data analysis.

Study conception and design. Latourte, Rat, Omorou, Ngueyon-Sime, Guillemin, Richette.

Acquisition of data. Rat, Roux, Guillemin.

Analysis and interpretation of data. Latourte, Rat, Omorou, Ngueyon-Sime, Eymard, Sellam, Roux, Ea, Cohen-Solal, Bardin, Beaudreuil, Guillemin, Richette.

REFERENCES

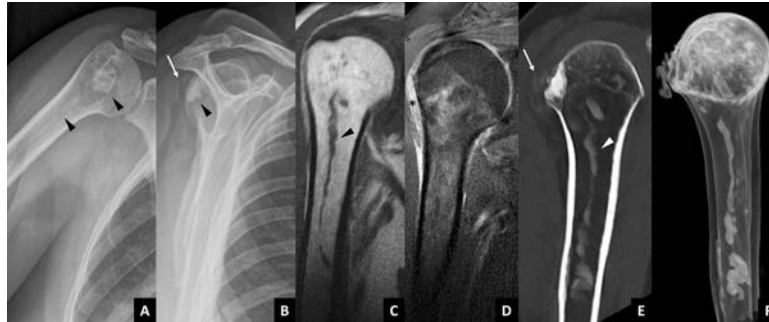
- Hunter DJ, Bierma-Zeinstra S. Osteoarthritis. *Lancet* 2019;393:1745–59.
- Jones IA, Togashi R, Wilson ML, Heckmann N, Vangsness CT Jr. Intra-articular treatment options for knee osteoarthritis [review]. *Nat Rev Rheumatol* 2019;15:77–90.
- Kolasinski SL, Neogi T, Hochberg MC, Oatis C, Guyatt G, Block J, et al. 2019 American College of Rheumatology/Arthritis Foundation guideline for the management of osteoarthritis of the hand, hip, and knee. *Arthritis Rheumatol* 2020;72:220–33.
- Bannuru RR, Osani MC, Vaysbrot EE, Arden NK, Bennell K, Bierma-Zeinstra SM, et al. OARSJ guidelines for the non-surgical management of knee, hip, and polyarticular osteoarthritis. *Osteoarthritis Cartilage* 2019;27:1578–89.
- Bannuru RR, Natov NS, Obadan IE, Price LL, Schmid CH, McAlindon TE. Therapeutic trajectory of hyaluronic acid versus glucocorticoid in the treatment of knee osteoarthritis: a systematic review and meta-analysis. *Arthritis Rheum* 2009;61:1704–11.
- Wernecke C, Braun HJ, Dragoo JL. The effect of intra-articular glucocorticoid on articular cartilage: a systematic review. *Orthop J Sports Med* 2015;3:2325967115581163.
- McAlindon TE, LaValley MP, Harvey WF, Price LL, Driban JB, Zhang M, et al. Effect of intra-articular triamcinolone vs saline on knee cartilage volume and pain in patients with knee osteoarthritis: a randomized clinical trial. *JAMA* 2017;317:1967–75.
- Kellgren JH, Lawrence JS. Radiological assessment of osteoarthrosis. *Ann Rheum Dis* 1957;16:494–502.
- Zeng C, Lane NE, Hunter DJ, Wei J, Choi HK, McAlindon TE, et al. Intra-articular glucocorticoid and the risk of knee osteoarthritis progression: results from the Osteoarthritis Initiative. *Osteoarthritis Cartilage* 2019;27:855–62.
- Conaghan PG. Glucocorticoid and osteoarthritis progression: a confounded issue. *Osteoarthritis Cartilage* 2019;27:e5–6.

11. Singh JA, Yu S, Chen L, Cleveland JD. Rates of total joint replacement in the United States: future projections to 2020-2040 using the national inpatient sample. *J Rheumatol* 2019;46:1134-40.
12. Huynh C, Puyraimond-Zemmour D, Maillefert JF, Conaghan PG, Davis AM, Gunther KP, et al. Factors associated with the orthopaedic surgeon's decision to recommend total joint replacement in hip and knee osteoarthritis: an international cross-sectional study of 1905 patients. *Osteoarthritis Cartilage* 2018;26:1311-8.
13. Altman R, Lim S, Steen RG, Dasa V. Hyaluronic acid injections are associated with delay of total knee replacement surgery in patients with knee osteoarthritis: evidence from a large U.S. health claims database. *PLoS One* 2015;10:e0145776.
14. Ong KL, Anderson AF, Niazi F, Fierlinger AL, Kurtz SM, Altman RD. Hyaluronic acid injections in medicare knee osteoarthritis patients are associated with longer time to knee arthroplasty. *J Arthroplasty* 2016;31:1667-73.
15. Delbarre A, Amor B, Bardoulat I, Tetafort A, Pelletier-Fleury N. Do intra-articular hyaluronic acid injections delay total knee replacement in patients with osteoarthritis—a Cox model analysis. *PLoS One* 2017;12:e0187227.
16. Altman R, Asch E, Bloch D, Bole G, Borenstein D, Brandt K, et al. Development of criteria for the classification and reporting of osteoarthritis: classification of osteoarthritis of the knee. *Arthritis Rheum* 1986;29:1039-49.
17. Guillemin F, Rat AC, Roux CH, Fautrel B, Mazieres B, Chevalier X, et al. The KHOALA cohort of knee and hip osteoarthritis in France. *Joint Bone Spine* 2012;79:597-603.
18. Bellamy N, Buchanan WW, Goldsmith CH, Campbell J, Stitt LW. Validation study of WOMAC: a health status instrument for measuring clinically important patient relevant outcomes to antirheumatic drug therapy in patients with osteoarthritis of the hip or knee. *J Rheumatol* 1988;15:1833-40.
19. Robins JM, Hernan MA, Brumback B. Marginal structural models and causal inference in epidemiology. *Epidemiology* 2000;11:550-60.
20. Moodie EE, Stephens DA. Marginal structural models: unbiased estimation for longitudinal studies. *Int J Public Health* 2011;56:117-9.
21. Groll DL, To T, Bombardier C, Wright JG. The development of a comorbidity index with physical function as the outcome. *J Clin Epidemiol* 2005;58:595-602.
22. Eckstein F, Boudreau RM, Wang Z, Hannon MJ, Wirth W, Cotofana S, et al. Trajectory of cartilage loss within 4 years of knee replacement—a nested case-control study from the osteoarthritis initiative. *Osteoarthritis Cartilage* 2014;22:1542-9.
23. Kompel AJ, Roemer FW, Murakami AM, Diaz LE, Crema MD, Guermazi A. Intra-articular corticosteroid injections in the hip and knee: perhaps not as safe as we thought? *Radiology* 2019;293:656-63.
24. Arroll B, Goodyear-Smith F. Corticosteroid injections for osteoarthritis of the knee: meta-analysis. *BMJ* 2004;328:869.
25. Bannuru RR, Schmid CH, Kent DM, Vaysbrot EE, Wong JB, McAlindon TE. Comparative effectiveness of pharmacologic interventions for knee osteoarthritis: a systematic review and network meta-analysis. *Ann Intern Med* 2015;162:46-54.
26. Juni P, Hari R, Rutjes AW, Fischer R, Silleto MG, Reichenbach S, et al. Intra-articular corticosteroid for knee osteoarthritis. *Cochrane Database Syst Rev* 2015:CD005328.
27. Da Costa BR, Hari R, Juni P. Intra-articular glucocorticoid for osteoarthritis of the knee. *JAMA* 2016;316:2671-2.
28. Felson DT. Intra-articular glucocorticoid and knee osteoarthritis: interpreting different meta-analyses. *JAMA* 2016;316:2607-8.
29. Russell SJ, Sala R, Conaghan PG, Habib G, Vo Q, Manning R, et al. Triamcinolone acetonide extended-release in patients with osteoarthritis and type 2 diabetes: a randomized, phase 2 study. *Rheumatology (Oxford)* 2018;57:2235-41.
30. Seror P, Pluvinage P, d'Andre FL, Benamou P, Attuil G. Frequency of sepsis after local corticosteroid injection (an inquiry on 1160000 injections in rheumatological private practice in France). *Rheumatology (Oxford)* 1999;38:1272-4.
31. Richardson SS, Schairer WW, Sculco TP, Sculco PK. Comparison of infection risk with corticosteroid or hyaluronic acid injection prior to total knee arthroplasty. *J Bone Joint Surg Am* 2019;101:112-8.
32. Uson J, Rodriguez-Garcia SC, Castellanos-Moreira R, O'Neill TW, Doherty M, Boesen M, et al. EULAR recommendations for intra-articular therapies. *Ann Rheum Dis* 2021;80:1299-305.
33. Mathiessen A, Conaghan PG. Synovitis in osteoarthritis: current understanding with therapeutic implications. *Arthritis Res Ther* 2017;19:18.
34. MacFarlane LA, Yang H, Collins JE, Jarraya M, Guermazi A, Mandl LA, et al. Association of Changes in effusion-synovitis with progression of cartilage damage over eighteen months in patients with osteoarthritis and meniscal tear. *Arthritis Rheumatol* 2019;71:73-81.
35. Ashraf S, Mapp PI, Walsh DA. Contributions of angiogenesis to inflammation, joint damage, and pain in a rat model of osteoarthritis. *Arthritis Rheum* 2011;63:2700-10.
36. O'Neill TW, Parkes MJ, Maricar N, Marjanovic EJ, Hodgson R, Gait AD, et al. Synovial tissue volume: a treatment target in knee osteoarthritis (OA). *Ann Rheum Dis* 2016;75:84-90.
37. Conaghan PG, Hunter DJ, Cohen SB, Kraus VB, Berenbaum F, Lieberman JR, et al. Effects of a single intra-articular injection of a microsphere formulation of triamcinolone acetonide on knee osteoarthritis pain: a double-blinded, randomized, placebo-controlled, multinational study. *J Bone Joint Surg Am* 2018;100:666-77.
38. Raynaud JP, Buckland-Wright C, Ward R, Choquette D, Haraoui B, Martel-Pelletier J, et al. Safety and efficacy of long-term intraarticular steroid injections in osteoarthritis of the knee: a randomized, double-blind, placebo-controlled trial. *Arthritis Rheum* 2003;48:370-7.
39. Spitzer AI, Richmond JC, Kraus VB, Gomoll A, Jones DG, Huffman KM, et al. Safety and efficacy of repeat administration of triamcinolone acetonide extended-release in osteoarthritis of the knee: a phase 3b, open-label study. *Rheumatol Ther* 2019;6:109-24.
40. Eckstein F, Guermazi A, Gold G, Duryea J, Le Graverand MP, Wirth W, et al. Imaging of cartilage and bone: promises and pitfalls in clinical trials of osteoarthritis. *Osteoarthritis Cartilage* 2014;22:1516-32.
41. Hitzl W, Wirth W, Maschek S, Cotofana S, Nevitt M, John MR, et al. Greater lateral femorotibial cartilage loss in osteoarthritis initiative participants with incident total knee arthroplasty: a prospective cohort study. *Arthritis Care Res (Hoboken)* 2015;67:1481-6.
42. Klocke R, Lévassieur K, Kitas GD, Smith JP, Hirsch G. Cartilage turnover and intra-articular corticosteroid injections in knee osteoarthritis. *Rheumatol Int* 2018;38:455-9.
43. Henrotin Y, Bannuru R, Malaise M, Ea HK, Confavreux C, Bentin J, et al. Hyaluronan derivative HYMOVIS(R) increases cartilage volume and type II collagen turnover in osteoarthritic knee: data from MOKHA study. *BMC Musculoskelet Disord* 2019;20:293.
44. Henrotin Y, Berenbaum F, Chevalier X, Marty M, Richette P, Rannou F. Reduction of the serum levels of a specific biomarker of cartilage degradation (Coll2-1) by hyaluronic acid (KARTILAGE(R) CROSS) compared to placebo in painful knee osteoarthritis patients: the EPI-KART study, a pilot prospective comparative randomized double blind trial. *BMC Musculoskelet Disord* 2017;18:222.

45. Dasa V, Lim S, Heeckt P. Real-world evidence for safety and effectiveness of repeated courses of hyaluronic acid injections on the time to knee replacement surgery. *Am J Orthop (Belle Mead NJ)* 2018;47.
46. Shewale AR, Barnes CL, Fischbach LA, Ounpraseuth ST, Painter JT, Martin BC. Comparative effectiveness of intra-articular hyaluronic acid and corticosteroid injections on the time to surgical knee procedures. *J Arthroplasty* 2017;32:3591–7.
47. Hunter DJ, Altman RD, Cicuttini F, Crema MD, Duryea J, Eckstein F, et al. OARSI clinical trials recommendations: Knee imaging in clinical trials in osteoarthritis. *Osteoarthritis Cartilage* 2015;23:698–715.
48. Bucci J, Chen X, LaValley M, Nevitt M, Torner J, Lewis CE, et al. Progression of knee osteoarthritis with use of intraarticular glucocorticoids versus hyaluronic acid. *Arthritis Rheumatol* 2022;74:223–6.

DOI 10.1002/art.42117

Clinical Images: Intraosseous calcification migration: journey to the center of the bone



The patient, a 62-year-old woman without a notable history of medical complications, presented to the emergency department with acute right shoulder pain. On physical examination, she had no fever, but right shoulder mobilization was impossible because of the pain. Findings from laboratory investigations, including C-reactive protein level, were normal. The patient received complete imaging evaluation to better understand the cause of pain. Initial radiographs of the humerus showed an intraosseous opacity of the humeral head at the insertion of the infraspinatus tendon, which extended to the medullary cavity of the humerus (**arrowheads in A and B**) with soft tissue calcifications (**arrow in B**). Coronal T1-weighted magnetic resonance imaging (MRI) revealed an intramedullary linear area of low signal intensity (**C**), which was associated with bone marrow edema. The edema was shown on T2-weighted MRI as diffuse intraosseous, high signal intensity (**D**). Significant subacromial bursitis was also identified (**asterisk in D**). A sagittal computed tomography scan showed low attenuating calcifications at the insertion of the infraspinatus tendon (**arrow in E**), which were associated with cortical erosion and condensation of the adjacent bone. We could clearly identify the path of migration of soft calcification into the medullary cavity (**arrowheads in C and E**) as linear low signal intensity on T1-weighted MRI. Volume rendering reconstruction from CT (**F**) demonstrated deep migration of the calcification into the bone. No mass resembling an abscess or a tumor was shown. The patient's imaging features and clinical presentation were consistent with hydroxyapatite deposition disease of the infraspinatus tendon with intraosseous calcification migration. No biopsy was needed to confirm diagnosis. The patient's pain was relieved with intrabursal glucocorticoid injection and calcification trituration. The migration of calcification resulting from hydroxyapatite deposition disease may show deep and remote extension into the bone (1–3). Calcification migration can also occur in the subacromial bursa or in muscles. A thorough investigation with multimodality imaging is required to rule out infection or tumors.

Author disclosures are available at <https://onlinelibrary.wiley.com/action/downloadSupplement?doi=10.1002%2Fart.42117&file=art42117-sup-0001-Disclosureform.pdf>.

1. Flemming DJ, Murphey MD, Shekitka KM, Temple HT, Jelinek JJ, Kransdorf MJ. Osseous involvement in calcific tendinitis: A retrospective review of 50 cases. *AJR Am J Roentgenol* 2003;181:965–72.
2. Malghem J, Omoumi P, Lecouvet F, Vande Berg B. Intraosseous migration of tendinous calcifications: cortical erosions, subcortical migration and extensive intramedullary diffusion, a SIMS series. *Skeletal Radiol* 2015;44:1403–12.
3. Cholet C, Guerini H, Pessis E, Drapé JL, Campagna R. Ultrasound features of painful intraosseous migration of pectoralis major tendinous calcifications with follow-up. *J Ultrasound* 2020;23:411–7.

Clément Cholet, MD 
 Hôpital Saint-Antoine
 and Sorbonne Médecine Université
 Justine Mugnier, MD
 Anne Miquel, MD
 Hôpital Saint-Antoine
 Juliette Petit, MD
 Jérémie Sellam, MD, PhD
 Lionel Arrivé, MD
 Hôpital Saint-Antoine
 and Sorbonne Médecine Université
 Paris, France

Vertebral Bone Mineral Density, Vertebral Strength, and Syndesmophyte Growth in Ankylosing Spondylitis: The Importance of Bridging

Sovira Tan,¹ Hadi Bagheri,² David Lee,³ Ahmad Shafiei,² Tony M. Keaveny,⁴ Lawrence Yao,² and Michael M. Ward¹

Objective. To examine the relationship between vertebral trabecular bone mineral density (tBMD), vertebral strength, and syndesmophytes in patients with ankylosing spondylitis (AS) using quantitative computed tomography (QCT).

Methods. We performed QCT of the spine to measure syndesmophytes and tBMD in 5 vertebrae (T11–L3) in 61 patients with AS. Finite element analysis was performed to measure vertebral strength in compressive overload, including in trabecular and cortical compartments. In cross-sectional analyses, we examined associations of syndesmophyte height with tBMD and vertebral strength in each vertebra. In 33 patients followed up for 2 years, we investigated whether baseline tBMD and vertebral strength predicted syndesmophyte growth in the same vertebra, and vice versa.

Results. In the cross-sectional analyses, 126 vertebrae had bridging, 77 vertebrae had nonbridging syndesmophytes, and 83 vertebrae had no syndesmophytes. There were strong inverse associations between syndesmophyte height and tBMD, total strength, and trabecular strength only among bridged vertebrae. In the longitudinal analysis, nonbridged vertebrae with low tBMD (adjusted $\beta = -0.01$ [95% confidence interval (95% CI) $-0.019, -0.0012$]) and low strength (adjusted $\beta = -0.0003$ [95% CI $-0.0004, -0.0002$]) had more syndesmophyte growth over time. Similar associations were absent among bridged vertebrae. Conversely, vertebrae with bridging at baseline had a significant loss in percent tBMD over time (adjusted $\beta = -0.001$ [95% CI $-0.0017, -0.0004$]).

Conclusion. Associations between syndesmophytes and vertebral density and strength in AS differ between bridged and nonbridged vertebrae. Among nonbridged vertebrae, low tBMD and strength are associated with syndesmophyte growth. Bridging is associated with large subsequent losses in tBMD, possibly due to mechanical offloading.

INTRODUCTION

Syndesmophyte formation is a hallmark of ankylosing spondylitis (AS), but AS is also often accompanied by vertebral osteopenia (1). The opposing pathologic processes of bone formation and bone loss can occur simultaneously and in close proximity in the spine, in a manner possibly unique to AS. Both processes may lead to structural damage and functional consequences. Syndesmophytes may lead to bridging and loss of flexibility, whereas trabecular bone loss can predispose to vertebral fractures (2,3). Syndesmophyte formation and trabecular bone loss

also share the risk factors of smoking and inflammation, and although data on the effects of nonsteroidal antiinflammatory drug (NSAID) treatment on bone in the setting of AS are limited, treatment with tumor necrosis factor inhibitors (TNFi) can improve bone mineral density (BMD) and may slow syndesmophyte development (4–9).

Despite these commonalities, whether, and how, these processes are related is not well understood. It has been hypothesized that bridging syndesmophytes may promote bone loss by reducing vertebral mobility (10). However, 2 longitudinal studies have suggested the inverse, that low bone mineral density

The views presented herein are those of the authors and do not necessarily represent those of the National Institutes of Health or the United States Government.

Supported by the Intramural Research Program of the National Institute of Arthritis and Musculoskeletal and Skin Diseases, NIH (grant ZIA-AR-041153) and the NIH Clinical Center.

¹Sovira Tan, PhD, Michael M. Ward, MD, MPH: National Institute of Arthritis and Musculoskeletal and Skin Diseases, NIH, Bethesda, Maryland; ²Hadi Bagheri, MD, Ahmad Shafiei, MD, Lawrence Yao, MD: NIH Clinical Center, Bethesda, Maryland; ³David Lee, PhD: O. N. Diagnostics,

Berkeley, California; ⁴Tony M. Keaveny, PhD: University of California, Berkeley.

Author disclosures are available at <https://onlinelibrary.wiley.com/action/downloadSupplement?doi=10.1002%2Fart.42120&file=art42120-sup-0001-Disclosureform.pdf>.

Address correspondence to Sovira Tan, PhD, National Institute of Arthritis and Musculoskeletal and Skin Diseases, NIH, 10 Center Drive, Building 10CRC, Room 4-1339, Bethesda, MD 20892-1468. Email: tanso@mail.nih.gov.

Submitted for publication October 28, 2021; accepted in revised form March 15, 2022.

(BMD) predicts syndesmophyte formation (11,12). It has also been proposed that bone loss results in vertebral instability, which is hypothesized to then promote syndesmophyte development as a compensatory mechanism (13). Understanding this association is important because it could indicate whether treatments aimed at maintaining or improving BMD will also affect the progression of spinal fusion.

Investigations of the relationship between syndesmophyte growth and bone loss in AS have been limited by the methods used to measure both syndesmophytes and BMD. Dual x-ray absorptiometry (DXA), a 2-dimensional modality, is not valid in many patients with AS because the anteroposterior projection can include syndesmophytes and posterior vertebral elements, often leading to the counterintuitive result that vertebral BMD increases with time (14). Studies using lateral DXA have also reported increases in BMD over time (15,16). In contrast, quantitative computed tomography (QCT), a 3-dimensional modality, can selectively measure trabecular BMD (tBMD), and its measurements correlate with bone histomorphometry (17). Similarly, the assessment of syndesmophytes has relied on plain radiography, which, like DXA, is a 2-dimensional projection with problems of superimposition. Additionally, the accepted reading method, the modified Stoke AS Spine Score (18), only examines syndesmophytes at anterior vertebral corners (19). QCT is an alternative modality with better accuracy in syndesmophyte detection along the entire vertebral rim and better sensitivity to change (20,21).

To date, no study has utilized CT to measure both vertebral BMD and syndesmophytes. Previous studies in which BMD was measured using QCT relied on radiography for the detection of syndesmophytes (10,17,22–27). In the majority of studies, DXA has been used for BMD and radiography has been used for syndesmophytes (11,12,15,16,28–30). Most studies have also globally examined the lumbar spine, although an analysis of associations within individual vertebrae may provide more mechanistic insights. In addition, study of the mechanical strength of vertebrae may provide further understanding of syndesmophyte development, beyond that provided by BMD. Vertebral strength is a measure of the breaking force of the vertebra under the action of a compressive overload, and is determined not only by BMD, but also by 3-dimensional geometry, local variations of cortical and trabecular bone, and the spatial distribution of bone density (31). Mechanistically, vertebral strength may be more closely related than BMD to syndesmophyte development. It is possible, for example, that bone strength can be maintained in the face of reduced tBMD if there are geometric or other morphologic adaptations that provide alternative mechanisms of strength to the overall vertebral body. No prior studies have used finite element analysis to examine the relationship of vertebral strength with syndesmophytes in AS.

Our goal was to investigate the relationship between vertebral BMD, strength, and syndesmophytes using QCT (32). In cross-sectional analyses, we examined the specific associations

of volumetric tBMD and trabecular and cortical bone strength with syndesmophyte involvement in the same vertebra. In longitudinal analyses, we examined whether baseline tBMD and vertebral strength predicted syndesmophyte growth, or if baseline syndesmophyte involvement predicted subsequent loss in vertebral tBMD. We hypothesized that bridging has a mechanical offloading effect on vertebral trabecular bone, and therefore sought to determine whether associations differed between bridged and nonbridged vertebrae.

PATIENTS AND METHODS

Patients. Patients were enrolled in a prospective study of the use of spine CT to quantitate syndesmophytes in AS (20,21). Inclusion criteria were as follows: age ≥ 18 years, presence of AS according to the modified New York criteria (33), and absence of extensive lumbar spine fusion as determined by radiography (Bath AS Radiology Index [BASRI] score < 4) (34). The study protocol was approved by the Institutional Review Board of the National Institute of Arthritis and Musculoskeletal and Skin Diseases (protocol no. 04-AR-0205), and all patients provided written informed consent.

The main study was a prospective longitudinal study with spine CT scans performed at baseline, 1 year, and 2 years, and clinical assessments performed every 4 months. We enrolled at least 5 subjects in BASRI categories 0, 1, 2, and 3 to include patients with a range of syndesmophyte involvement. Other patients were enrolled in substudies that required a single visit with a spine CT scan. In all cases, clinical assessments included physical examination, medication histories, and history of patient-reported measures. We computed the alternative AS Disease Activity Score (ASDAS) (35) based on the Bath AS Disease Activity Index (BASDAI) (36) and C-reactive protein levels.

CT scanning. Patients enrolled early in the study (62%) were scanned using a Philips Brilliance 64 CT scanner (slice thickness 1.5 mm) or GE Lightspeed Ultra (slice thickness 1.25 mm). More recently enrolled patients (38%) were scanned using a Siemens Somatom Flash or Somatom Force scanner (slice thickness 1.0 mm). Estimated average absorbed radiation dose was 8.01 mSv.

We computed syndesmophyte height around the vertebral rim using a validated semiautomated method with high reliability and sensitivity to change (32). In each disc space, the 360° of the vertebral rim was divided into 72 angular sectors of 5° each. In each angular sector, height was computed for ascending and descending syndesmophytes and normalized to the local intervertebral disc space height so that bridging had a value of 1, values between 0 and 1 represented the proportion of the disc space spanned by syndesmophytes, and 0 indicated the absence of syndesmophytes. In the present study, we were interested in all syndesmophytes originating from a vertebral body,

rather than in each disc space. Therefore, for each vertebral body, we added all ascending syndesmophytes from the upper end plate, descending syndesmophytes from the lower end plate, and all bridging syndesmophytes from either end plate. The sum is a score termed syndesmophyte height, which has a possible range of 0–144, with 144 indicating total fusion with both neighboring vertebrae. The extent of bridging was the number of angular sectors with a score of 1 on either the upper or lower end plate.

Initial scans were performed from T10 to L4, while later scans also included the thoracic spine. To standardize the levels examined, we limited the analysis to 5 vertebrae (T11, T12, L1, L2, and L3) for which data were available from all patients. Data from T10 and L4 were needed to compute syndesmophyte heights for T11 and L3, respectively.

We used disc height loss, as seen on the lateral view, by the semiquantitative Videman scale to identify degenerative disc disease (37). Discs with a score of 2 (disc narrower than the adjacent superior disc) or 3 (endplates almost touching) were classified as having degeneration.

Volumetric tBMD. Trabecular BMD was calculated for each vertebral body (in mg/cm^3) by relating measured voxel intensity to a calibration phantom scanned with each patient. The calculation was performed using Mindways version 6.1 QCT Pro software. This US Food and Drug Administration-cleared software allows the user to select a region of interest in trabecular bone for which BMD is then computed (see Supplementary Figure 1, available on the *Arthritis & Rheumatology* website at <http://onlinelibrary.wiley.com/doi/10.1002/art.42120>). Measurement of tBMD was performed by investigators who were blinded with regard to syndesmophyte results. Intrarater reliability for tBMD measurements, tested on 20 randomly selected vertebrae, was 0.974.

Finite element analysis by biomechanical CT (BCT).

Finite element analysis was performed on scans of 25 patients in the longitudinal study who were selected to include a range of syndesmophyte involvement. BCT allows for a finite element analysis to compute a measurement of bone strength, which is the force (in newtons) required to virtually break the patient's bone in a standardized loading configuration. This type of virtual stress test combines image processing, bone biomechanics, and the well-established engineering structural analysis technique of non-linear finite element analysis to simulate a typical fracturing event: a compressive overload on the vertebra (Supplementary Figure 2, <http://onlinelibrary.wiley.com/doi/10.1002/art.42120>). BCT testing was performed with O. N. Diagnostics VirtuOst version 1.2 software, which is FDA-cleared both to assess fracture risk and to monitor bone loss and treatment. Details of these assessments have been reported elsewhere (31). Briefly, the target vertebra was segmented from the CT image, registered to a standardized orientation for loading, and the voxels were

calibrated to standardized density units. To construct the finite element model, the bone was converted to 1-mm cube-shaped elements, and each element was assigned element-specific elastic and failure properties. Vertebral total strength was then defined as the simulated force when applying a uniform compression to the vertebral body to a strain of 2%.

A separate finite element analysis was then performed to compute the trabecular strength of each vertebral body. This was done by first virtually removing the cortex and subjecting the remaining bone to the same compressive overload. The contribution from the cortical compartment was then computed as the difference between whole-bone total strength and trabecular strength.

Statistical analysis. We performed 2 main analyses: a cross-sectional analysis using baseline data from all patients, and an analysis of changes over time using data from patients in the longitudinal protocol. In both cases, the unit of analysis was the individual vertebra.

In the cross-sectional analysis, we first examined the association between tBMD (the independent variable) and syndesmophyte height (the dependent variable) using regression analysis. This analysis tested whether vertebrae with lower tBMD were more likely to have extensive syndesmophytes than vertebrae with higher tBMD. We implemented the regression models as generalized estimating equations to account for the non-independence of vertebrae from the same patient, and adjusted for patient age, sex, smoking status (former/current versus never), vertebral level, current NSAID use, current TNFi use, and C-reactive protein (CRP) level. We performed stratified analyses to investigate whether the association between tBMD and syndesmophytes was modified by the presence of bridging. Models with alternative functional forms of tBMD (e.g., linear or quadratic terms) were compared for goodness-of-fit using the quasi-likelihood under the independence model criterion.

These analyses were repeated using data from the finite element analysis. We examined vertebral total strength, trabecular strength, cortical strength, and proportion of cortical strength contribution to total strength (cortical strength/total strength) as separate independent variables and syndesmophyte height as the dependent variable. We used generalized estimating equation models adjusted for patient age, sex, smoking status, vertebral level, current NSAID use, current TNFi use, and CRP level, and stratified the analyses by the presence or absence of bridging.

In the longitudinal analyses, we first examined the association of both tBMD and vertebral strength at baseline with change in syndesmophyte height in the same vertebra over the subsequent 2 years, using a multiple regression model. Next, we examined the association of syndesmophyte height at baseline with percent change in tBMD in the same vertebra over the subsequent 2 years. Comparison of these results would indicate if

tBMD was more likely to predict or follow syndesmophyte growth. These models were again implemented as generalized estimating equations, with adjustment for patient age, sex, smoking status, vertebral level, NSAID use, TNFi use, and mean ASDAS on 7 visits over the 2 years. Data from the CT scans at 1 year were not included. We adjusted for ASDAS rather than CRP level in the longitudinal analyses to incorporate aspects of patient-reported assessment. These analyses were repeated after excluding vertebrae with adjacent degenerated discs. Associations were considered to be statistically significant if the 95% confidence interval (95% CI) of regression coefficients excluded 0. SAS version 9.4 was used for data analysis.

RESULTS

Study cohort. We studied 61 patients in the cross-sectional analysis, 25 of whom were included in the finite element analysis. Thirty-three patients participated in the longitudinal study. Most patients were young-adult or middle-aged men, and the mean duration of AS was 18.2 years (Table 1).

Mean disease activity was low according to the BASDAI and moderate according to the ASDAS. Twenty-one patients (34.4%) had been treated with TNFi for a median of 25 months (interquartile range 13–62). In the longitudinal cohort, 6 patients (18.2%) were treated with TNFi. No patients had been treated with bisphosphonates, other antiresorptive or anabolic medications, or biologics other than TNFi.

Cross-sectional associations with tBMD. Data on syndesmophyte height were available for 286 of 305 vertebrae in the cross-sectional analysis. Syndesmophyte height could not be calculated for 12 vertebrae (in 6 patients) because of extensive discitis, and data on T11 were missing for 7 patients because T10 was not completely in the field of view. Mean \pm standard deviation syndesmophyte height among all vertebrae was 17.2 ± 28.1 units (Table 1). Eighty-three vertebrae (29%) had no syndesmophytes, 77 vertebrae (26.9%) had only nonbridged syndesmophytes, and 126 vertebrae (44%) had a bridging syndesmophyte in at least 1 sector. Syndesmophyte heights and the frequency of

Table 1. Baseline characteristics of the patients with AS at study enrollment*

Characteristic	All patients (n = 61)	Finite element analysis (n = 25)	Longitudinal sample (n = 33)
Age, years	45.1 \pm 11.3	46.3 \pm 11.2	45.8 \pm 11.9
Men, no. (%)	52 (85.3)	23 (92.0)	28 (84.8)
Race, no. (%)			
White	52 (85.3)	21 (84.0)	28 (84.8)
Black	3 (4.9)	1 (4.0)	2 (6.1)
Asian	6 (9.8)	3 (12.0)	3 (9.1)
Smoking history, no. (%)			
Nonsmoker	40 (65.6)	17 (68.0)	21 (63.7)
Former smoker	19 (31.1)	7 (28.0)	11 (33.3)
Current smoker	2 (3.3)	1 (4.0)	1 (3.0)
Duration of AS, years	18.2 \pm 11.2	19.9 \pm 11.1	20.6 \pm 12.3
BASDAI	2.9 \pm 1.9	2.9 \pm 2.1	2.9 \pm 1.9
BASFI	26.2 \pm 22.7	26.4 \pm 23.1	25.3 \pm 21.2
ASDAS	1.9 \pm 0.8	1.9 \pm 1.0	2.1 \pm 0.8
Lumbar mSASSS, median (IQR)	4 (0–8.5)	4 (0–10)	4 (0–9)
CRP, median (IQR) mg/liter	3.0 (1.7–4.4)	0.4 (0.4–11.2)	5.4 (1.4–9.0)
Current treatment, no. (%)			
NSAIDs	44 (72.1)	17 (68.0)	25 (75.8)
Sulfasalazine	3 (4.9)	1 (4.0)	2 (6.1)
TNFi	22 (36.1)	5 (20.0)	6 (18.2)
Prednisone	3 (4.9)	1 (4.0)	1 (3.0)
Syndesmophyte height, units (range 0–144)	17.2 \pm 28.1	23.1 \pm 35.0	18.4 \pm 31.4
Any bridging, no. (%)	45 (73.7)	21 (84.0)	23 (69.7)
Trabecular BMD, mg/cm ³	131.9 \pm 31.8	126.7 \pm 31.2	132.5 \pm 32.1
Total strength, N	–	8,611 \pm 2,205	–
Trabecular strength, N	–	4,753 \pm 1,423	–
Cortical strength, N	–	3,812 \pm 867	–
Proportion cortical strength, %	–	45.0 \pm 5.4	–

*Except where indicated otherwise, values are the mean \pm SD. Syndesmophyte height, trabecular bone mineral density (BMD), total strength, trabecular strength, cortical strength, and cortical strength proportion are shown for all vertebral levels. AS = ankylosing spondylitis; BASDAI = Bath Ankylosing Spondylitis Disease Activity Index (score range 0–10); BASFI = Bath Ankylosing Spondylitis Functional Index (score range 0–100); ASDAS = Ankylosing Spondylitis Disease Activity Score; mSASSS = modified Stoke Ankylosing Spondylitis Spine Score (score range 0–36); IQR = interquartile range; CRP = C-reactive protein; NSAIDs = nonsteroidal anti-inflammatory drugs; TNFi = tumor necrosis factor inhibitor.

bridging were greater at T11 and T12 than in the lumbar vertebrae. Mean tBMD was 131.9 mg/cm³ among all vertebrae.

There was an inverse association between tBMD and syndesmophyte height at each vertebral level, with Spearman's correlation coefficients of -0.59 , -0.53 , -0.45 , -0.32 , and -0.49 at T11, T12, L1, L2, and L3, respectively. This inverse association was also present in pooled data (Figure 1), including after adjustment for patient age, sex, smoking status, vertebral level, NSAID use, TNFi use, and CRP level (Supplementary Table 1, <http://onlinelibrary.wiley.com/doi/10.1002/art.42120>). The association was best fit as a curvilinear relationship, with little association between tBMD and syndesmophyte height at high tBMD, but a much stronger association at tBMD <120 mg/cm³. However, several vertebrae with low tBMD had no or only small syndesmophytes. TNFi use did not correlate with syndesmophyte height. Results were similar when adjusted for duration of AS instead of age (Supplementary Table 1).

When patients were stratified by the presence or absence of bridging, no significant association was found between tBMD and syndesmophyte height among vertebrae that were not bridged ($n = 160$) (Figure 1 and Supplementary Table 1), although an inverse association was evident when adjusted for duration of AS instead of age. In contrast, there was a strong inverse curvilinear relationship among vertebrae with bridging ($n = 126$). Mean duration of AS was somewhat higher among patients in the bridging group compared to the nonbridging group (19.4 years versus 16.7 years), as was mean age (48.4 years versus 42.7 years) and the proportion of men (90.5% versus 81.2%).

There was a similar inverse curvilinear relationship between tBMD and the extent of bridging among vertebrae with any

bridging (Figure 1 and Supplementary Table 1). Trabecular BMD >120 mg/cm³ was not associated with extensive bridging, while vertebrae with tBMD <120 mg/cm³ were more likely to have more extensive bridging. Among bridged vertebrae, there was no association between tBMD and the number of vertebral levels that were bridged, suggesting that tBMD was not influenced by bridging in neighboring vertebrae (Supplementary Table 2, <http://onlinelibrary.wiley.com/doi/10.1002/art.42120>).

Cross-sectional associations with vertebral strength.

Data on vertebral strength were available for 119 of 125 vertebrae (58 without bridging and 61 with bridging). Among all vertebrae, the total strength was a mean \pm SD 8,611 \pm 2,205 newtons (Table 1). Vertebral strength was directly correlated with tBMD, with a slightly stronger correlation among bridged vertebrae than nonbridged vertebrae (Supplementary Figure 3, <https://onlinelibrary.wiley.com/doi/10.1002/art.42120>).

In unadjusted analyses, syndesmophyte height was inversely correlated with total vertebral strength (Spearman's rank correlation = -0.33), trabecular strength ($r = -0.41$), and cortical strength ($r = -0.19$) (Supplementary Table 3, <https://onlinelibrary.wiley.com/doi/10.1002/art.42120>). These associations were stronger among bridged vertebrae than nonbridged vertebrae. Syndesmophyte height was directly correlated with proportion cortical strength among all vertebrae ($r = 0.37$), both in bridged and nonbridged subsets.

In the pooled adjusted analyses of nonbridged vertebrae, there was no association between syndesmophyte height and total strength (Figure 2 and Supplementary Table 4, <http://onlinelibrary.wiley.com/doi/10.1002/art.42120>). There

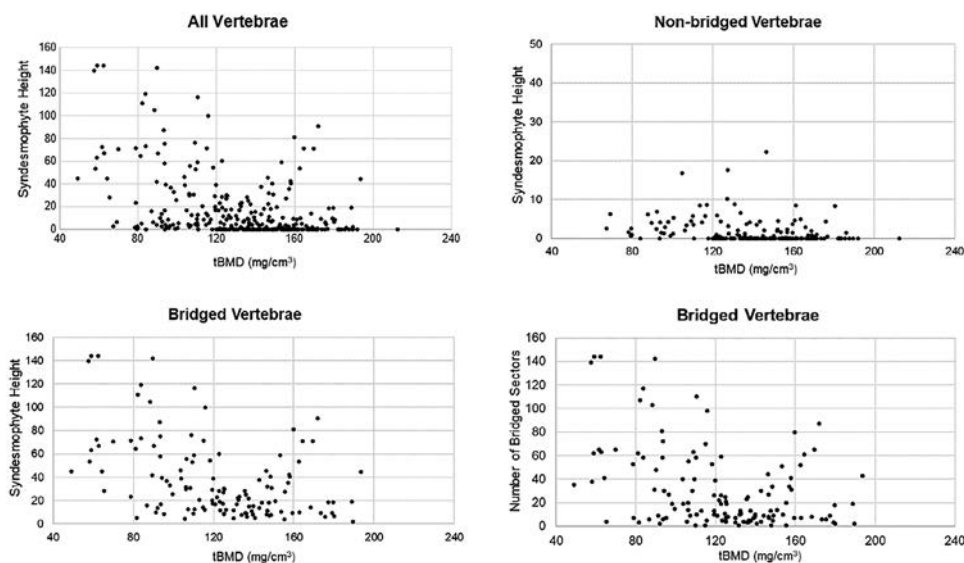


Figure 1. Association between trabecular bone mineral density (tBMD) and syndesmophyte height at baseline in 61 patients with ankylosing spondylitis, and the relationship between tBMD and the extent of vertebral bridging. Scatterplots show results for all vertebrae ($n = 286$), non-bridged vertebrae ($n = 160$), bridged vertebrae ($n = 126$), and the number of bridged sectors among bridged vertebrae. Possible syndesmophyte height range was 1–144 units.

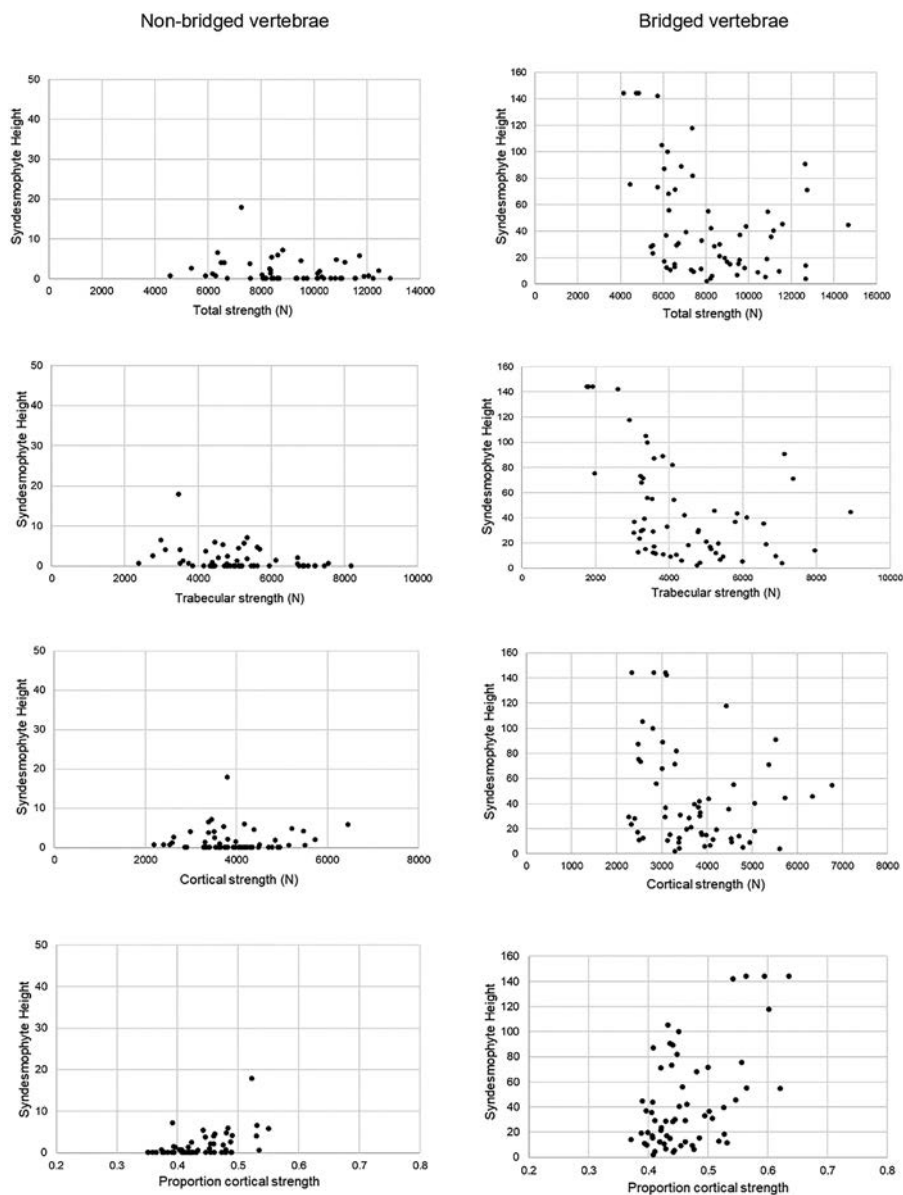


Figure 2. Association between syndesmophyte height and total strength, trabecular strength, cortical strength, and cortical strength proportion (cortical strength/total strength) among nonbridged vertebrae ($n = 58$) and bridged vertebrae ($n = 61$) in the finite element analysis ($n = 119$ vertebrae).

was a significant inverse association between syndesmophyte height and trabecular strength, and a significant direct association with the proportion cortical strength. There was no association between syndesmophyte height and cortical strength.

Among bridged vertebrae, there were strong inverse associations between syndesmophyte height and total strength, trabecular strength, and cortical strength, and there was a direct association between syndesmophyte height and proportion cortical strength (Figure 2 and Supplementary Table 4). Results of the cross-sectional analysis of trabecular strength were therefore consistent with those of the analysis of tBMD, indicating that more syndesmophytes were present in vertebrae with lower trabecular density and strength. The finite element analysis

revealed the unique finding that syndesmophytes were more common among vertebrae with higher cortical strength relative to total strength.

Longitudinal associations. Of 165 vertebrae potentially evaluable from the 33 patients in the longitudinal study, we included data on 149 vertebrae. Data were missing for 11 vertebrae because of limited field of view on either the baseline or year 2 scan, and the year 2 scan of 1 patient could not be processed for tBMD. Over the 2-year follow-up period, tBMD decreased by a mean \pm SD of $4.6 \pm 9.2\%$ in all vertebrae, $3.6 \pm 7.6\%$ in nonbridged vertebrae, and $5.9 \pm 10.8\%$ in bridged vertebrae. Syndesmophyte height increased by a mean \pm SD of 2.7 ± 4.8

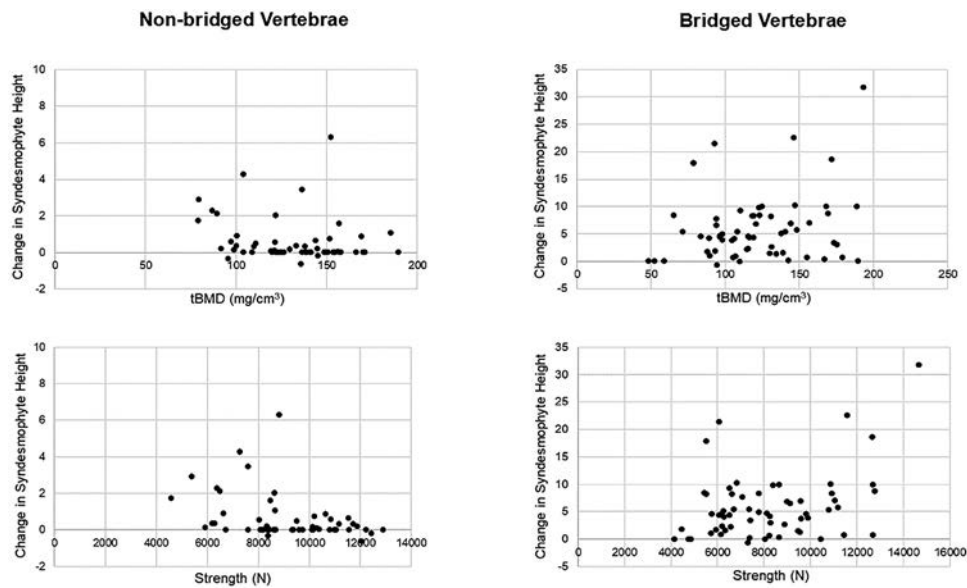


Figure 3. Association between trabecular bone mineral density (tBMD) and vertebral strength at baseline and change in syndesmophyte height over 2 years among nonbridged vertebrae ($n = 83$) and bridged vertebrae ($n = 66$). Y-axis scales of each scatterplot have been adjusted to accommodate the larger changes in syndesmophyte height among bridged vertebrae.

units. Based on determination of the mean ASDAS score among all patients, 18%, 30%, 46%, and 6% of patients had inactive disease, moderate disease activity, high disease activity, and very high disease activity, respectively.

We then tested whether baseline tBMD was associated with changes in syndesmophyte height over 2 years (Figure 3 and Supplementary Table 5, <http://onlinelibrary.wiley.com/doi/10.1002/art.42120>). Among the 83 nonbridged vertebrae, we found that vertebrae with lower baseline tBMD had more syndesmophyte growth over the subsequent 2 years (adjusted $\beta = -0.01$ [95% CI $-0.019, -0.0012$]). Because 50 vertebrae had no syndesmophytes at baseline, and because new syndesmophytes rarely develop in 2 years, we repeated the analysis among the 33 vertebrae with syndesmophytes at baseline. Results were similar in this subgroup, with a slightly larger effect estimate (adjusted $\beta = -0.0133$ [95% CI $-0.024, -0.0024$]). In contrast, there was no relationship between tBMD at baseline and subsequent

syndesmophyte growth among bridged vertebrae (Supplementary Table 5). Mean ASDAS was not associated with change in syndesmophytes in these models.

We next tested whether baseline vertebral strength was associated with changes in syndesmophyte height over 2 years. Among nonbridged vertebrae, lower vertebral total strength at baseline was correlated with more syndesmophyte growth over the subsequent 2 years (adjusted $\beta = -0.0003$ [95% CI $-0.0004, -0.0002$]) (Figure 3 and Supplementary Table 5). This association was also present for trabecular strength and cortical strength separately. In contrast, there was no association between vertebral strength and syndesmophyte growth among bridged vertebrae (Supplementary Table 5).

The analyses described above were then repeated after excluding 11 vertebrae from the longitudinal cohort, and 9 vertebrae from the finite element analysis cohort with adjacent degenerated discs. Results were very similar to those obtained in the

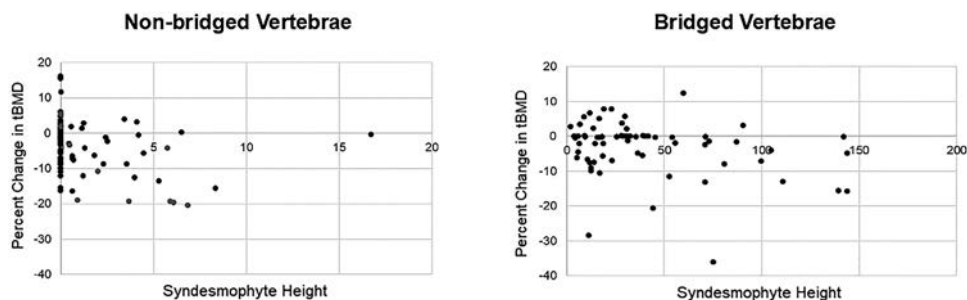


Figure 4. Association between syndesmophyte height at baseline and percent change in trabecular bone mineral density (tBMD) at 2 years among nonbridged vertebrae ($n = 83$) and bridged vertebrae ($n = 66$). X-axis scales of each scatterplot have been adjusted to accommodate the range of syndesmophyte heights present among bridged vertebrae. Dots represent individual vertebrae.

overall cohorts, with low tBMD and low vertebral strength predictive of more syndesmophyte growth only in nonbridged vertebrae (Supplementary Table 6, <http://onlinelibrary.wiley.com/doi/10.1002/art.42120>).

Finally, we tested whether baseline syndesmophyte height was associated with the percent change in tBMD over the subsequent 2 years (Figure 4 and Supplementary Table 7, <https://onlinelibrary.wiley.com/doi/10.1002/art.42120>). No association was found among nonbridged vertebrae, but bridged vertebrae with higher syndesmophyte height at baseline had greater losses of tBMD over 2 years (adjusted $\beta = -0.001$ [95% CI $-0.0017, -0.0004$]). Results were similar after exclusion of vertebrae with adjacent degenerated discs (Supplementary Table 8, <https://onlinelibrary.wiley.com/doi/10.1002/art.42120>).

DISCUSSION

The presence of vertebral bone loss and syndesmophyte formation in close proximity in AS represents a major paradox, and the relationship between these processes has not been clearly defined (26). By examining tBMD, bone strength, and syndesmophytes in the same vertebra using CT, we demonstrated that this association differs depending on the presence of bridging. Among nonbridged vertebrae, those with lower tBMD and lower bone strength tended to have more syndesmophytes at baseline and had more syndesmophyte growth over time. However, among bridged vertebrae, there was a strong inverse association between tBMD and syndesmophytes in the cross-sectional analysis, particularly in vertebrae with more extensive bridging. In the longitudinal analysis, more extensively bridged vertebrae underwent greater loss of tBMD over time, while loss of tBMD did not consistently occur among vertebrae without bridging. Therefore, bridging plays a critical role in modifying the process of vertebral bone loss in AS.

Previous cross-sectional studies that used QCT demonstrated that lower lumbar tBMD was associated with the presence of syndesmophytes (25,26), more extensive spinal changes (24), or bridging (10,23), but the proliferative changes in these studies were not restricted to the lumbar spine. Only

Karberg et al (25) limited the examination of syndesmophytes to the lumbar spine, and only 2 studies adjusted for patient age (24,26). In a 10-year longitudinal study of 15 patients, mean lumbar QCT-measured BMD was lower at baseline and decreased more over time in patients with any bridged vertebrae than in patients without bridging (22). These results suggested that bridging may have a more specific association with vertebral bone loss than with syndesmophytes in general.

Our longitudinal results indicated that, in the absence of bridging and presumably earlier in the course of AS, lower vertebral tBMD and lower bone strength were associated with greater subsequent syndesmophyte growth. In early AS, vertebral osteopenia has been attributed to the effects of both local and systemic inflammation (38–41). This hypothesis is supported by reports of improvement in vertebral BMD with TNFi treatment (42–44). We did not find consistent associations between mean ASDAS and changes in tBMD or syndesmophytes over time, possibly because tBMD mediated the association between inflammation and syndesmophyte growth. Alternatively, the lack of consistent associations may be because the ASDAS was not assessed frequently enough, because of limitations in this measure, or because systemic inflammation may be less important than local inflammation in mediating these changes (40,41). However, higher ASDAS as well as lower vertebral strength were associated with more syndesmophyte growth over time among nonbridged vertebrae. Current TNFi use was not associated with tBMD in our analysis, but it is important to note that this does not reflect changes that might follow the initiation of TNFi treatment.

Consistent with Wolff's Law and concepts of bone adaptation, vertebral tBMD and strength are normally maintained by functional forces acting on the spine, explaining why vertebral bone is rapidly lost during space flight or prolonged bedrest (45–48). In healthy individuals, age-related decreases in vertebral BMD affect trabecular bone primarily, particularly in men, such that cortical bone provides a larger proportion of the resistance to compressive forces in older persons (49–52). Consistent with this pattern, results of the finite element analysis indicated that lower trabecular strength in AS was associated with a larger relative contribution of cortical strength to total vertebral strength. Our

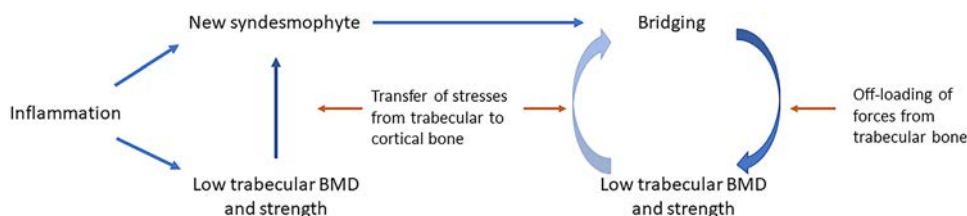


Figure 5. Proposed model of the associations between vertebral bone loss and syndesmophyte development. In the absence of bridging, inflammation at entheses directly leads to new syndesmophyte development while local and/or systemic inflammation leads to loss of vertebral trabecular bone mineral density (tBMD). Low tBMD contributes to syndesmophyte development as a result of the transfer of stresses from trabecular bone to cortical bone. Over time, in vertebrae that develop bridging, the additional structural support provided by this column of bone serves to offload functional forces from trabecular bone and results in further loss of tBMD. In turn, the loss of tBMD may promote more extensive bridging as more functional stress is shifted from trabecular to cortical bone.

results suggest a model in which, in the absence of bridging (perhaps more common in early AS), low tBMD, lower vertebral strength, and a higher proportional contribution of cortical strength to total bone strength promote syndesmophyte development (Figure 5). In this model, inflammation may lead to syndesmophyte development directly through enthesitis, but also indirectly through low tBMD and lower vertebral strength (13). Loss of tBMD may also explain the historical observation of rapid spine fusion in patients with AS who were treated with body casts (53,54). The finding that vertebral strength was more strongly associated with syndesmophyte growth than was tBMD may indicate the importance of changes in bone microarchitecture, as has previously been reported in peripheral bones in AS (55).

Among bridged vertebrae, our data indicate that the converse association holds: more extensive bridging is associated with lower tBMD and trabecular strength, and leads to greater loss of tBMD over time. Although this association may reflect the effects of vertebral inflammation, the strong association with the extent of bridging is more consistent with a mechanical effect. Specifically, trabecular bone loss in the setting of extensive bridging may be a consequence of vertebral offloading. Extensive bridging may act as a scaffold (or column, in engineering terms) that relieves compressive forces from trabecular bone, and transfers these forces to the cortical shells of the adjoined vertebrae (Figure 5). Experiencing less compressive force, trabecular bone is lost more rapidly. This may also establish a positive feedback loop between low vertebral tBMD and bridging. Additional longitudinal studies with longer follow-up are needed to confirm this hypothesis.

A major strength of this study was the use of CT to quantitate syndesmophytes and volumetric tBMD precisely, thereby avoiding the confounding that has occurred in many prior studies. Additionally, we examined associations within individual vertebrae and stratified by bridging. Finite element analysis provided biomechanical evidence of links between tBMD, vertebral strength, and syndesmophyte formation. This study is limited in that we followed up relatively few patients longitudinally and for only 2 years. We do not know if similar associations are present in other regions of the spine. More patients and larger vertebral segments are needed to investigate whether bridging across several vertebrae differentially affects bone loss. The associations we found were not related to disc degeneration, but further study of the potential role of disc degeneration in syndesmophyte development is needed.

Our findings indicate that the association between vertebral bone loss and syndesmophytes in AS is complex, likely stage-specific, and bidirectional. Clear evidence of the unique role of bridging in mediating low tBMD has been lacking, although the relationship has been suspected previously. Low tBMD in AS should therefore be considered in the context of whether bridging syndesmophytes are present or not, as the primary mechanisms underlying low bone density are likely different. Treatments

targeting inflammation may be more effective in improving tBMD in nonbridged vertebrae. Conversely, among bridged vertebrae, where mechanical offloading may primarily be responsible, antiresorptive or anabolic medications may be more effective treatments for improving tBMD.

AUTHOR CONTRIBUTIONS

All authors were involved in drafting the article or revising it critically for important intellectual content, and all authors approved the final version to be published. Dr. Ward had full access to all of the data in the study and takes responsibility for the integrity of the data and the accuracy of the data analysis.

Study conception and design. Tan, Keaveny, Yao, Ward.

Acquisition of data. Tan, Bagheri, Lee, Shafiei, Ward.

Analysis and interpretation of data. Tan, Bagheri, Lee, Shafiei, Keaveny, Yao, Ward.

REFERENCES

1. Magrey M, Khan MA. Osteoporosis in ankylosing spondylitis [review]. *Curr Rheumatol Rep* 2010;12:332–36.
2. Ralston SH, Urquhart GD, Brzeski M, Sturrock RD. Prevalence of vertebral compression fractures due to osteoporosis in ankylosing spondylitis. *BMJ* 1990;300:563–5.
3. Van der Weijden MA, van der Horst-Bruinsma IE, van Denderen JC, Dijkmans BA, Heymans MW, Lems WF. High frequency of vertebral fractures in early spondylarthropathies. *Osteoporosis Int* 2012;23:1683–90.
4. Ward MM, Hendrey MR, Malley JD, Learch TJ, Davis JC Jr, Reveille JD, et al. Clinical and immunogenetic prognostic factors for radiographic severity in ankylosing spondylitis. *Arthritis Rheum* 2009; 61:859–66.
5. Poddubnyy D, Haibel H, Listing J, Märker-Hermann E, Zeidler H, Braun J, et al. Baseline radiographic damage, elevated acute-phase reactant levels, and cigarette smoking status predict spinal radiographic progression in early axial spondylarthritis. *Arthritis Rheum* 2012;64:1388–98.
6. Wang R, Bathon JM, Ward MM. Nonsteroidal antiinflammatory drugs as potential disease-modifying medications in axial spondyloarthritis [review]. *Arthritis Rheumatol* 2020;72:518–28.
7. Pray C, Feroz NI, Haroon NN. Bone mineral density and fracture risk in ankylosing spondylitis: a meta-analysis. *Calcif Tissue Int* 2017;101: 182–92.
8. Park JW, Kim MJ, Lee JS, Ha YJ, Park JK, Kang EH, et al. Impact of tumor necrosis factor inhibitor versus nonsteroidal antiinflammatory drug treatment on radiographic progression in early ankylosing spondylitis: its relationship to inflammation control during treatment. *Arthritis Rheumatol* 2019;71:82–90.
9. Haroon N, Inman RD, Learch TJ, Weisman MH, Lee M, Rahbar MH, et al. The impact of tumor necrosis factor α inhibitors on radiographic progression in ankylosing spondylitis. *Arthritis Rheum* 2013;65: 2645–54.
10. Fauny M, Morizot C, Allado E, Verhoeven F, Abluisson E, Semaan M, et al. Consequences of spinal ankylosis on bone trabecular fragility assessed on CT scans in patients with ankylosing spondylitis: a retrospective study. *Joint Bone Spine* 2020;87:625–31.
11. Kim HR, Hong YS, Park SH, Ju JH, Kang KY. Low bone mineral density predicts the formation of new syndesmophytes in patients with axial spondyloarthritis. *Arthritis Res Ther* 2018;20:231.
12. Kim JW, Chung MK, Lee J, Kwok SK, Kim WU, Park SH, et al. Low bone mineral density of vertebral lateral projections can predict spinal

- radiographic damage in patients with ankylosing spondylitis. *Clin Rheumatol* 2019;38:3567–74.
13. Van Mechelen M, Lories RJ. Microtrauma: no longer to be ignored in spondyloarthritis? [review]. *Curr Opin Rheumatol* 2016; 28:176–80.
 14. Kaya A, Ozgocmen S, Kamanli A, Ardicoglu O. Bone loss in ankylosing spondylitis: does syndesmophyte formation have an influence on bone density changes? *Med Princ Pract* 2009;18:470–6.
 15. Klingberg E, Lorentzon M, Mellstrom D, Geiger M, Göthlin J, Hilme E, et al. Osteoporosis in ankylosing spondylitis—prevalence, risk factors and methods of assessment. *Arthritis Res Ther* 2012;14:R108.
 16. Deminger A, Klingberg E, Lorentzon M, Geiger M, Göthlin J, Hedberg M, et al. Which measuring site in ankylosing spondylitis is best to detect bone loss and what predicts the decline: results from a 5-year prospective study. *Arthritis Res Ther* 2017;19:273.
 17. Lee YS, Schlotzhauer T, Ott SM, van Vollenhoven R, Hunter J, Shapiro J, et al. Skeletal status of men with early and late ankylosing spondylitis. *Am J Med* 1997;103:233–41.
 18. Creemers MC, Franssen MJ, van 't Hof MA, Gribnau FW, van de Putte LB, van Riel PL. Assessment of outcome in ankylosing spondylitis: an extended radiographic scoring system. *Ann Rheum Dis* 2005; 64:127–9.
 19. Wanders AJ, Landewé RB, Spoorenberg A, Dougados M, van der Linden S, Mielants H, et al. What is the most appropriate radiologic scoring method for ankylosing spondylitis? A comparison of the available methods based on the Outcome Measures in Rheumatology Clinical Trials filter. *Arthritis Rheum* 2004;50:2622–32.
 20. Tan S, Yao J, Flynn JA, Yao L, Ward MM. Quantitative measurement of syndesmophyte volume and height in ankylosing spondylitis using CT. *Ann Rheum Dis* 2014;73:544–50.
 21. Tan S, Yao J, Flynn JA, Yao L, Ward MM. Quantitative syndesmophyte measurement in ankylosing spondylitis using CT: longitudinal validity and sensitivity to change over 2 years. *Ann Rheum Dis* 2015; 74:437–43.
 22. Korkosz M, Gasowski J, Grzanka P, Gorczowski J, Pluskiewicz W, Jeka S, et al. Baseline new bone formation does not predict bone loss in ankylosing spondylitis as assessed by quantitative computed tomography (QCT)—10-year follow-up. *BMC Musculoskeletal Dis* 2011;12:121.
 23. Devogelaer JP, Maldague B, Malghem J, Deuxchaisnes CN. Appendicular and vertebral bone mass in ankylosing spondylitis: a comparison of plain radiographs with single- and dual-photon absorptiometry and with quantitative computed tomography. *Arthritis Rheum* 1992; 35:1062–7.
 24. Lange U, Kluge A, Strunk J, Teichmann J, Bachmann G. Ankylosing spondylitis and bone mineral density—what is the ideal tool for measurement? *Rheumatol Int* 2005;26:115–20.
 25. Karberg K, Zochling J, Sieper J, Felsenberg D, Braun J. Bone loss is detected more frequently in patients with ankylosing spondylitis with syndesmophytes. *J Rheumatol* 2005;32:1290–8.
 26. Klingberg E, Lorentzon M, Göthlin J, Mellström D, Geiger M, Ohlsson C, et al. Bone microarchitecture in ankylosing spondylitis and the association with bone mineral density, fractures, and syndesmophytes. *Arthritis Res Ther* 2013;15:R179.
 27. El Maghraoui A, Tellal S, Chaouir S, Lebbar K, Bezza A, Nouijai A, et al. Bone turnover markers, anterior pituitary and gonadal hormones, and bone mass evaluation using quantitative computed tomography in ankylosing spondylitis. *Clin Rheumatol* 2005;24:346–51.
 28. Ghazlani I, Ghazi M, Nouijai A, Mounach A, Rezqi A, Achemlal L, et al. Prevalence and risk factors of osteoporosis and vertebral fractures in patients with ankylosing spondylitis. *Bone* 2009;44:772–6.
 29. Wildberger L, Boyadzhieva V, Hans D, Stoilov N, Rashkov R, Aubry-Rozier B. Impact of lumbar syndesmophyte on bone health as assessed by bone density (BMD) and bone texture (TBS) in men with axial spondyloarthritis. *Joint Bone Spine* 2017;84:463–6.
 30. Marques ML, Ramiro S, Machado PM, van der Heijde D, van Gaalen FA. No relationship between bone mineral density and syndesmophyte formation at the same level in the lumbar spine of patients with radiographic axial spondyloarthritis. *RMD Open* 2020; 6:e001391.
 31. Keaveny TM, Clarke BL, Cosman F, Orwoll ES, Siris ES, Khosla S, et al. Biomechanical Computed Tomography analysis (BCT) for clinical assessment of osteoporosis. *Osteoporos Int* 2020;31:1025–48.
 32. Tan S, Yao J, Flynn JA, Yao L, Ward MM. Quantitation of circumferential syndesmophyte height along the vertebral rim in ankylosing spondylitis using computed tomography. *J Rheumatol* 2015;42:472–8.
 33. Van der Linden S, Valkenburg HA, Cats A. Evaluation of diagnostic criteria for ankylosing spondylitis: a proposal for modification of the New York criteria. *Arthritis Rheum* 1984;27:361–8.
 34. Mackay K, Mack C, Brophy S, Calin A. The Bath Ankylosing Spondylitis Radiology Index (BASRI): a new, validated approach to disease assessment. *Arthritis Rheum* 1998;41:2263–70.
 35. Ortolan A, Ramiro S, van Gaalen F, Kvien TK, Landewe RB, Machado PM, et al. Development and validation of an alternative Ankylosing Spondylitis Disease Activity Score when patient global assessment is unavailable. *Rheumatology (Oxford)* 2021;60:638–48.
 36. Garrett S, Jenkinson T, Kennedy LG, Whitelock H, Gaisford P, Calin A. A new approach to defining disease status in ankylosing spondylitis: the Bath Ankylosing Spondylitis Disease Activity Index. *J Rheumatol* 1994;21:2286–91.
 37. Jarraya M, Guermazi A, Lorbergs AL, Brochin E, Kiel DP, Bouxsein ML, et al. A longitudinal study of disc height narrowing and facet joint osteoarthritis at the thoracic and lumbar spine, evaluated by computed tomography: the Framingham Study. *Spine J* 2018;18: 2065–73.
 38. Gratacós J, Collado A, Pons F, Osaba M, Sanmartí R, Roqué M, et al. Significant loss of bone mass in patients with early, active ankylosing spondylitis: a followup study. *Arthritis Rheum* 1999;42:2319–24.
 39. Maillefert JF, Aho LS, El Maghraoui A, Dougados M, Roux C. Changes in bone density in patients with ankylosing spondylitis: a two-year follow-up study. *Osteoporosis Int* 2001;12:605–9.
 40. Briot K, Durnez A, Paternotte S, Miceli-Richard C, Dougados M, Roux C. Bone oedema on MRI is highly associated with low bone mineral density in patients with early inflammatory back pain: results from the DESIR cohort. *Ann Rheum Dis* 2013;72:1914–9.
 41. Wang D, Hou Z, Gong Y, Chen S, Lin L, Xiao Z. Bone edema on magnetic resonance imaging is highly associated with low bone mineral density in patients with ankylosing spondylitis. *PLoS One* 2017;12: e0189569.
 42. Haroon NN, Sriganthan J, Al Ghanim N, Inman RD, Cheung AM. Effect of TNF- α inhibitor treatment on bone mineral density in patients with ankylosing spondylitis: a systematic review and meta-analysis. *Semin Arthritis Rheum* 2014;44:155–61.
 43. Ashany D, Stein EM, Goto R, Goodman SM. The effect of TNF inhibition on bone density and fracture risk and of IL17 inhibition on radiographic progression and bone density in patients with axial spondyloarthritis: a systematic literature review. *Curr Rheumatol Rep* 2019;21:20.
 44. Beek JK, Rusman T, van der Weijden MA, Lems WF, van Denderen JC, Konsta M, et al. Long-term treatment with TNF- α inhibitors improves bone mineral density but not vertebral fracture progression in ankylosing spondylitis. *J Bone Miner Res* 2019;34:1041–8.
 45. Stavnychuk M, Mikolajewicz N, Corlett T, Morris M, Komarova SV. A systematic review and meta-analysis of bone loss in space travelers. *NPJ Microgravity* 2020;6:13.




46. Kroiner B, Toft B. Vertebral bone loss: an unheeded side effect of therapeutic bed rest. *Clin Sci (Lond)* 1983;64:537–40.
47. Leblanc AD, Schneider VS, Evans HJ, Engelbretson DA, Krebs JM. Bone mineral loss and recovery after 17 weeks of bed rest. *J Bone Miner Res* 1990;5:843–50.
48. Burkhart K, Allaire B, Anderson DE, Lee D, Keaveny TM, Bouxsein ML. Effects of long-duration spaceflight on vertebral strength and risk of spine fracture. *J Bone Miner Res* 2020;35:269–76.
49. Christiansen BA, Kopperdahl DL, Kiel DP, Keaveny TM, Bouxsein ML. Mechanical contributions of the cortical and trabecular compartments contribute to differences in age-related changes in vertebral body strength in men and women assessed by QCT-based finite element analysis. *J Bone Miner Res* 2011;26:974–83.
50. Faulkner KG, Cann CE, Hasegawa BH. Effect of bone distribution on vertebral strength: assessment with patient-specific nonlinear finite element analysis. *Radiology* 1991;179:669–74.
51. Homminga J, Weinans H, Gowin W, Felsenberg D, Huiskes R. Osteoporosis changes the amount of vertebral trabecular bone at risk of fracture but not the vertebral load distribution. *Spine* 2001;26:1555–60.
52. Crawford P, Camp JJ, Khosla S, Keaveny TM. Structure-function relationships and determinants of vertebral strength in elderly women [abstract]. Orthopaedic Research Society: Abstracts from the 51st Annual Meeting, Washington, DC, 2005. URL: <https://www.ors.org/Transactions/51/0032.pdf>.
53. Turney HF. Ankylosing spondylitis. *Proc Royal Soc Med* 1952;45:57–62.
54. Godfrey RG. Treatment of ankylosing spondylitis [review]. *Brit Med J* 1978;2:720.
55. Nigil Haroon N, Szabo E, Raboud JM, McDonald-Blumer H, Fung L, Josse RG, et al. Alterations of bone mineral density, bone micro-architecture and strength in patients with ankylosing spondylitis: a cross-sectional study using high-resolution peripheral quantitative computerized tomography and finite element analysis. *Arthritis Res Ther* 2015;17:377.

Erratum

DOI 10.1002/art.42274

In the letter by Wang et al in the June 2022 issue of *Arthritis & Rheumatology* (Airway Obstruction as a Pulmonary Manifestation of Rheumatoid Arthritis: Comment on the Article by Prisco et al [pages 1095–1096]), the email address for the corresponding author, James Cheng-Chung Wei, MD, PhD, was missing and the authors requested that it be added. Correspondence can be addressed to Dr. Wei's email at jccwei@gmail.com.

Small Molecule Inhibitors of Nuclear Export and the Amelioration of Lupus by Modulation of Plasma Cell Generation and Survival

Javier Rangel-Moreno,¹  Maria de la Luz Garcia-Hernandez,¹  Teresa Owen,¹ Jennifer Barnard,¹ Enrique Becerril-Villanueva,² Trinayan Kashyap,³ Christian Argueta,³ Armando Gamboa-Dominguez,⁴ Sharon Tamir,³ Yosef Landesman,³ Bruce I. Goldman,¹ Christopher T. Ritchlin,¹  and Jennifer H. Anolik¹

Objective. To investigate the hypothesis that selective inhibitors of nuclear export (SINE compounds), recently approved for treatment of refractory plasma cell (PC) malignancy, may have potential in the treatment of lupus.

Methods. Female NZB/NZW mice were treated with the SINE compound KPT-350 or vehicle control. Tissue specimens were harvested and analyzed by flow cytometry, using standard markers. Nephritis was monitored by determining the proteinuria score and by histologic analysis of kidney specimens. Serum anti-double-stranded DNA (anti-dsDNA) levels were measured by enzyme-linked immunosorbent assay, and total numbers of IgG-secreting and dsDNA-specific antibody-secreting cells were assessed by enzyme-linked immunospot assay.

Results. KPT-350 abrogated murine lupus nephritis at both early and late stages of the disease and rapidly impaired generation of autoreactive PCs in germinal centers (GCs). SINE compounds inhibited the production of NF- κ B-driven homeostatic chemokines by stromal cells, altering splenic B and T cell strategic positioning and significantly reducing follicular helper T cell, GC B cell, and autoreactive PC counts. KPT-350 also decreased levels of cytokines and chemokines involved in PC survival and recruitment in the kidney of lupus-prone mice. Exportin 1, the target of SINE compounds, was detected in GCs of human tonsils, splenic B cells of lupus patients, and multiple B cell subsets in the kidneys of patients with lupus nephritis.

Conclusion. Collectively, our results provide support for the therapeutic potential of SINE compounds, via their targeting of several molecular and cellular pathways critical in lupus pathogenesis, including autoantibody production by plasma cells.

INTRODUCTION

Lupus is a prototypical, chronic autoimmune disease that preferentially affects minority women and can involve multiple organs (1). Its heterogeneous clinical presentation and progression challenge diagnosis and treatment. Although advances in

lupus management have improved patient survival, morbidity related to cardiovascular disease, infections, and other complications, combined with high mortality in a subset of lupus patients, create a persistent, unmet need for new treatments. A thorough understanding of lupus pathogenesis is key to developing novel and alternative therapies for patients in whom the disease is

Supported by the National Institute of Allergy and Infectious Diseases, NIH, Small Business Innovation Research program (award 2R44-AI-124949-02). Dr. Rangel-Moreno's work was supported by the Department of Medicine, University of Rochester Medical Center, and the NIH (award RO1-AI-111914). Dr. Ritchlin's work was supported by the NIH (award RO1-AR-0169000). Dr. Anolik's work was supported by the National Institute of Arthritis and Musculoskeletal and Skin Diseases, NIH, Accelerating Medicines Partnership (awards 1UH2-AR-067690 and R21-AR-071670), and the Bertha and Louis Weinstein research fund.

¹Javier Rangel-Moreno, PhD, Maria de la Luz Garcia-Hernandez, PhD, Teresa Owen, BS, Jennifer Barnard, BS, Bruce I. Goldman, MD, Christopher T. Ritchlin, MD, MPH, Jennifer H. Anolik, MD, PhD: University of Rochester Medical Center, Rochester, New York; ²Enrique Becerril-Villanueva, PhD: Instituto Nacional de Psiquiatría Ramón de la

Fuente, Mexico City, Mexico; ³Trinayan Kashyap, MS, Christian Argueta, PhD, Sharon Tamir, BA, Yosef Landesman, PhD: Karyopharm Therapeutics, Newton, Massachusetts; ⁴Armando Gamboa-Dominguez, MD, PhD, MS: Instituto Nacional de Ciencias Médicas y Nutrición "Salvador Zubirán," Mexico City, Mexico.

Author disclosures are available at <https://onlinelibrary.wiley.com/action/downloadSupplement?doi=10.1002%2Fart.42128&file=art42128-sup-0001-Disclosureform.pdf>.

Address correspondence to Jennifer H. Anolik, MD, PhD, or Javier Rangel-Moreno, PhD, Department of Medicine, Division of Allergy, Immunology, and Rheumatology, University of Rochester, 601 Elmwood Avenue, Box 695, Rochester, NY 14642. Email: jennifer_anolik@urmc.rochester.edu or javier_rangel-moreno@urmc.rochester.edu.

Submitted for publication October 8, 2021; accepted in revised form March 22, 2022.

refractory to treatment with current drugs and biologics (2). In lupus, B cells are central in generating autoreactive germinal center (GC) B cells and plasma cells (PCs), the latter being the source of pathogenic autoantibodies (3). B cells also influence lupus through antibody-independent mechanisms such as autoantigen presentation (4), provision of costimulatory signals to T cells, and production of T cell-activating cytokines (5). Thus, B cells were considered attractive targets for improving the treatment of lupus patients. Surprisingly, B cell depletion generated inconsistent and controversial results in lupus clinical trials. While some studies showed the benefit of B cell depletion (6), others failed to demonstrate improvement in lupus or lupus nephritis (7,8). Despite efficient B cell depletion, PCs remain elusive targets because they lack CD20. PCs are critical in the amplification of pathologic inflammation (9,10). Thus, modulation of PC differentiation and survival might ameliorate inflammation and provide alternative therapies for patients with lupus refractory to B cell depletion and other available therapeutics.

Selective inhibitors of nuclear export (SINE compounds) are oral agents that inhibit the export of cargo molecules (i.e., protein and messenger RNA [mRNA]) from the nucleus to the cytoplasm, a process orchestrated by chromosome region maintenance 1, also known as exportin 1 (11). SINEs sequester tumor suppressor proteins in the nucleus and have been successfully used in the treatment of hematologic malignancies, solid tumors, and nonmalignant autoimmune diseases (11–14). SINE compounds also have antiinflammatory and antiproliferative effects, including inhibition of NF- κ B signaling. Interestingly, because of their efficient elimination of multiple myeloma cells (15), SINEs were recently approved for the treatment of refractory myeloma (16). These results led us to hypothesize that SINE compounds might deplete autoreactive PCs in lupus.

MATERIALS AND METHODS

Mice. Groups of 5 female NZB/NZW mice per cage were housed according to the guidelines of the animal facility at the University of Rochester. All experiments were approved by the University of Rochester Committee on Animal Resources. Because of the heterogeneity in disease progression, cohorts of 8 female NZB/NZW mice with similar double-stranded DNA (dsDNA) antibody titers were randomly enrolled in experimental groups. Female NZB/NZW mice received 3 doses weekly of vehicle or the SINE compound KPT-350 by oral gavage for 8 consecutive weeks; doses were 5 mg/kg or 7.5 mg/kg for induction therapy, based on the animal's weight on the day of administration. At the end of treatment, mice were euthanized by suffocation with carbon dioxide, followed by cervical dislocation. Kidney damage was monitored weekly by measuring the protein level in urine specimens, using commercial dipsticks (Uristix; Bayer). Serum, spleens, kidneys, and bone marrow specimens were collected

to evaluate the immunologic course of experimental lupus and the efficacy of SINE therapy.

Study approval. Collection of specimens from lupus autopsy subjects was conducted with written and signed consent from their family members, in accordance with the Declaration of Helsinki and after approval from the Ethical Committee of the National Institute of Medical Sciences and Nutrition “Salvador Zubirán.” Analysis of deidentified tissue specimens was performed according to protocols approved by the University of Rochester Institutional Review Board. Patients met the American College of Rheumatology 1997 revised criteria for systemic lupus erythematosus (SLE) (17) or received a clinical diagnosis of SLE from an experienced rheumatologist.

All animal care and experimental procedures were conducted according to the Guide for the Care and Use of Laboratory Animals and approved by the Institutional Animal Care and Use Committee of the University of Rochester Medical Center. Demographic and clinical data from autopsied SLE subjects are shown in Supplementary Table 1, available on the *Arthritis & Rheumatology* website at <https://onlinelibrary.wiley.com/doi/10.1002/art.42128>. Detailed materials and methods are also included in the Supplementary Materials, available at <https://onlinelibrary.wiley.com/doi/10.1002/art.42128>. Single-cell RNA sequencing data on immune cells from kidneys of patients with lupus nephritis were obtained from the Accelerating Medicines Partnership—Rheumatoid Arthritis, System Lupus Erythematosus public immunogenomics portal for analysis (18).

Statistical analysis. Results are expressed as the mean \pm SEM. Statistically significant differences were determined by the Mann-Whitney test or by one-way analysis of variance with the Kruskal-Wallis test, using GraphPad Prism software. Correlation was determined by calculating Pearson r values. P values less than or equal to 0.05 were considered statistically significant.

RESULTS

Amelioration of lupus nephritis by KPT-350 in lupus-prone mice. Female, 27-week-old NZB/NZW mice with active autoimmune disease (based on positivity for dsDNA-specific autoantibodies) were orally treated (3 times per week for 8 weeks) with KPT-350 (5 mg/kg or 7.5 mg/kg) to assess the effect of the SINE compound on lupus nephritis (Figure 1). KPT-350 doses were chosen on the basis of the amounts used in other models of inflammatory disease (19,20). Protein levels were measured weekly to monitor the impact of therapy on nephritis. Protein levels steadily increased in the control group, with 50% of mice having a proteinuria score of 3+ (i.e., ≥ 150 mg/dl) at the time of euthanasia (Figure 1A). In contrast, all mice treated with

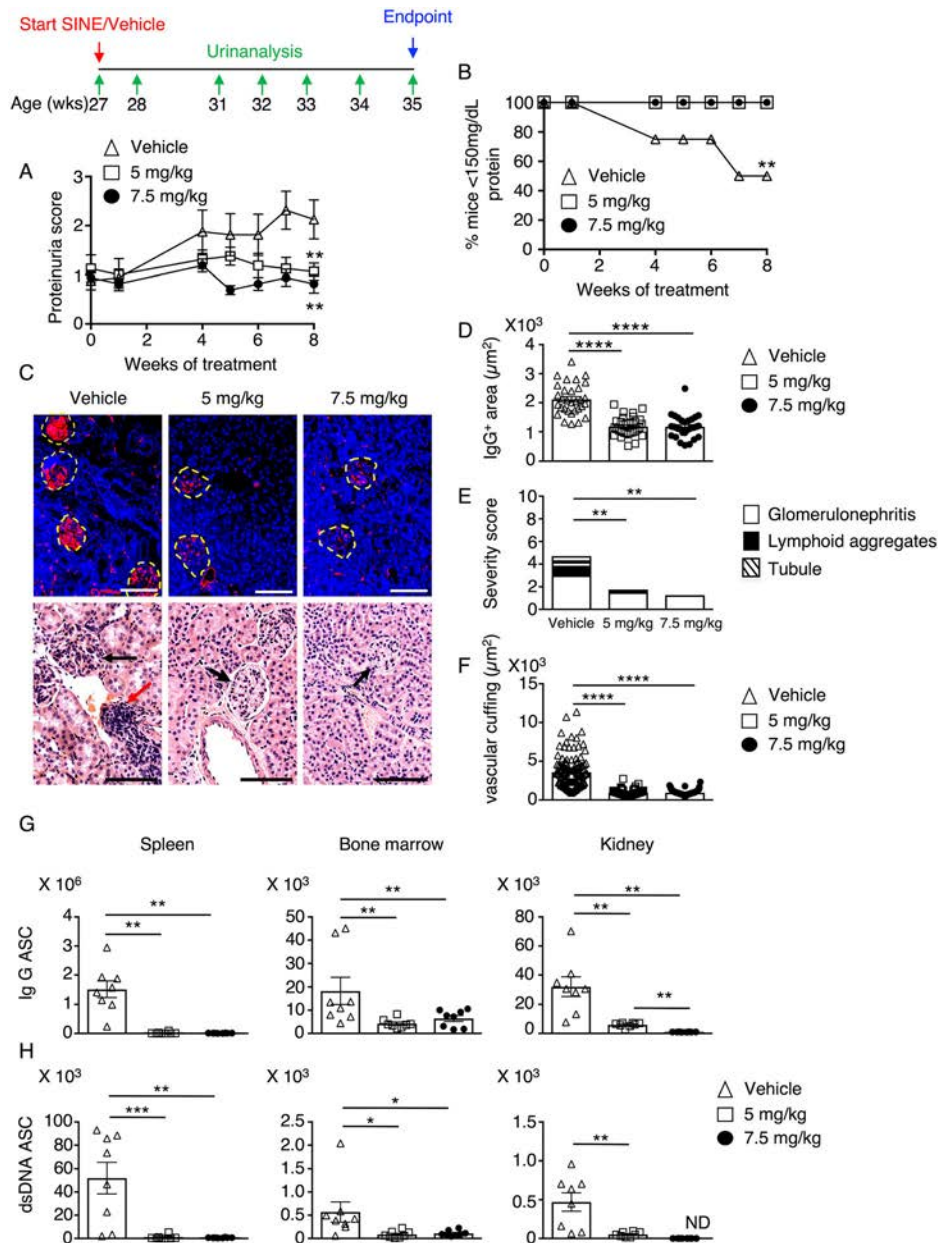


Figure 1. Effect of the selective inhibitor of nuclear export (SINE) KPT-350 on lupus nephritis and the generation of antibody-secreting cells (ASCs) in 27-week-old female NZB/NZW mice treated with vehicle or KPT-350 (5 mg/kg or 7.5 mg/kg) by oral gavage 3 times per week for 8 weeks. **A**, Changes in proteinuria scores. **B**, Percentage of mice with low proteinuria scores (i.e., <3+ [<150 mg/dl]). **C**, Representative stains of kidney specimens, showing IgG deposition (red) in glomeruli (yellow dashed lines) (original magnification $\times 100$; top) and hypercellular glomeruli in control mice (**black arrows**) versus normal glomeruli in treated animals, and perivascular lymphoid aggregates (**red arrows**) (original magnification $\times 400$; bottom). Bars = 100 μ m. **D–F**, IgG deposition revealed by morphometric analysis (**D**), severity scores for glomerulonephritis, lymphoid aggregates, and tubular damage (**E**), and vascular cuffing (**F**). **G** and **H**, Numbers of IgG-secreting ASCs (**G**) and autoreactive, double-stranded DNA (dsDNA)-specific ASCs (**H**). Unless indicated otherwise, representative results from 3 independent experiments are shown ($n = 7–8$ mice/group). Symbols represent individual mice; bars show the mean \pm SEM. * = $P \leq 0.05$; ** = $P \leq 0.005$; *** = $P \leq 0.0005$; **** = $P \leq 0.0001$, by one-way analysis of variance or Mann-Whitney test.

KPT-350 maintained a proteinuria score of $\sim 1+$ (i.e., ~ 50 mg/dl) (Figures 1A and B).

Immune complexes activate the complement cascade and stimulate the production of chemokines, which attract inflammatory cells to kidneys of lupus-prone mice (21,22). In control mice, we

observed extensive IgG deposition (Figures 1C and D), a massive accumulation of inflammatory cells in the glomeruli, dilation and degeneration of renal tubules, and engrossment of the basement membrane, which, together, are indicative of fibrosis and the deposition of immune complexes and collagen (Figure 1C). Conversely,

less IgG deposition, fewer inflammatory cells in glomeruli, and almost normal kidney architecture were observed in mice receiving KPT-350 at doses of 5 mg/kg or 7.5 mg/kg (Figure 1C). Mean severity scores for glomerulonephritis (Figure 1E) and the average area occupied by perivascular lymphocytes were significantly lower in kidneys of treated mice (Figure 1F).

Collectively, these data indicate that KPT-350 ameliorated immune complex deposition, local inflammation, and nephritis in lupus-prone mice.

Elimination of autoreactive antibody-secreting cells (ASCs) by KPT-350 in lupus-prone mice. We next enumerated isotype-switched and dsDNA-specific ASCs, using an enzyme-linked immunospot assay. Consistent with impaired IgG deposition in the kidneys of KPT-350-treated mice, we found a statistically significant reduction in the number of IgG-secreting and dsDNA-specific ASCs in the spleens of mice treated with KPT-350 (Figures 1G and H). Numbers of IgG-secreting ASCs were also decreased in the bone marrow and kidneys (Figure 1G). Dramatic reductions in the number of dsDNA-specific ASCs were also seen in bone marrow and kidneys after KPT-350 treatment (Figure 1H). Of note, we did not detect dsDNA-specific ASCs in the kidneys of mice treated with KPT-350 at a dose of 7.5 mg/kg. In agreement with the reduction in the number of dsDNA-specific ASCs, the serum concentration of dsDNA-specific antibodies was considerably lower after KPT-350 treatment (Supplementary Figures 1A and B, available on the *Arthritis & Rheumatology* website at <https://onlinelibrary.wiley.com/doi/10.1002/art.42128>). Importantly, serum IgG levels were comparable in control and treated mice (Supplementary Figure 1C).

Impairment of PC generation by KPT-350 in splenic GCs of NZB/NZW mice. In murine lupus, splenomegaly is associated with lymphoid follicle hyperplasia, accumulation of macrophages and PCs around arterioles in the red pulp (23), and spontaneous formation of GCs that play an active role in the production of autoreactive, short-lived plasmablasts and mature, long-lived PCs (24). Spleens of mice treated with KPT-350 for 8 weeks (Supplementary Figure 2, available on the *Arthritis & Rheumatology* website at <https://onlinelibrary.wiley.com/doi/10.1002/art.42128>) were hypocellular (Supplementary Figures 2A and B) and had a smaller white pulp (Supplementary Figures 2C and D).

We found densely populated GCs containing large, proliferating peanut agglutinin-positive B220^{low} B blasts in the spleens of control mice (Figure 2A). In sharp contrast, GCs were small in the spleen of KPT-350-treated mice (Figure 2A). The average size of GCs and the percentage of the spleen section area occupied by GCs were significantly lower in mice treated with KPT-350 (Figures 2B and C). Next, we stained spleen sections with antibodies against proliferating cell nuclear antigen (PCNA) and IgG to enumerate isotype-switched PCs. In addition, a considerable

number of proliferating and nonproliferating IgG-secreting cells were located close to GCs (visible as PCNA-positive clusters) in control mice. Also, numerous nonproliferating IgG-secreting cells were detected in the splenic red pulp (Figure 2A). Fewer proliferating and nonproliferating ASCs were detected both inside GCs and in the red pulp of mice treated with KPT-350 (Figures 2A and D). These results indicate that KPT-350 impacts the production of splenic IgG-secreting PCs via potent modulation of GC formation/organization.

We next enumerated follicular helper T (T_{fh}) cells, GC B cells, plasmablasts, and mature PCs by flow cytometry (the gating strategy is shown in Supplementary Figure 3, available on the *Arthritis & Rheumatology* website at <https://onlinelibrary.wiley.com/doi/10.1002/art.42128>). Consistent with the splenic hypocellularity and smaller white pulp we described earlier, numbers of CD19⁺ B cells, CD3⁺ T cells (data not shown), GC B cells (Figure 2E), and T_{fh} cells (Figure 2F) were significantly diminished in mice treated with KPT-350. We found a similar reduction in the number of plasmablasts (i.e., IgG-secreting CD19⁺ cells expressing both κ light chain and major histocompatibility complex [MHC] class II) and mature PCs (i.e., IgG-secreting CD19⁺ cells expressing κ light chain but not MHC class II) in the spleen (Figures 2G and H) and bone marrow (data not shown) after therapy. These results suggest that KPT-350 impairs the production and maintenance of splenic T_{fh} cells and GC B cells, affecting plasmablast and PC generation.

Potent modulation of autoreactive GC responses by short-term KPT-350 treatment. The low concentration of dsDNA-specific antibodies, even after 4 weeks of treatment with KPT-350 (Supplementary Figures 1A and B, available at <https://onlinelibrary.wiley.com/doi/10.1002/art.42128>), suggested that KPT-350 rapidly modulated experimental lupus. To further examine the kinetics of the response to the SINE compound, we treated 27-week-old lupus-prone mice with a 7.5 mg/kg dose of KPT-350 for 1 week (Supplementary Figure 4, available on the *Arthritis & Rheumatology* website at <https://onlinelibrary.wiley.com/doi/10.1002/art.42128>). There was a reduction in the numbers of T_{fh} cells and GC B cells even after this short treatment period (Supplementary Figures 4A and B), accompanied by a drastic decrease in the size and number of GCs (Supplementary Figures 4C–E) and lower numbers of IgG-secreting PCs (Supplementary Figure 4F). Short-term KPT-350 therapy reduced the numbers of isotype-switched ASCs (Supplementary Figure 4G) and dsDNA-specific ASCs (Supplementary Figure 4H). Collectively, these results confirmed the rapid and potent effect of SINE drugs on splenic GC responses and the production of autoreactive plasma cells. The more potent impact on splenic PCs as compared to bone marrow and kidney PCs suggests a dominant effect on PC generation in GCs, rather than on PC survival in peripheral organs.

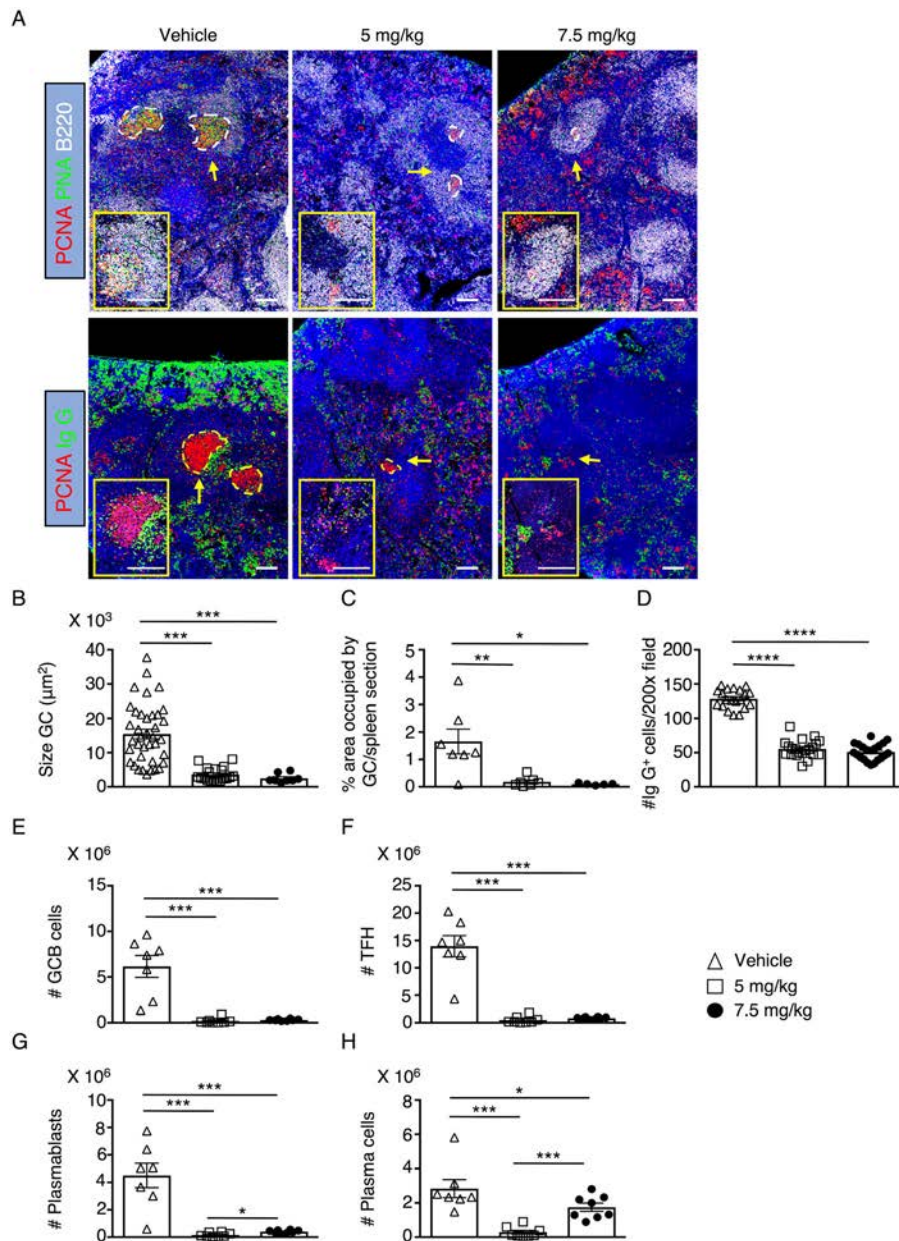


Figure 2. Effect of KPT-350 on germinal center (GC) responses and generation of splenic, isotype-switched plasma cells (PCs) in 27-week-old female NZB/NZW mice treated with vehicle or KPT-350 (5 mg/kg or 7.5 mg/kg) by oral gavage 3 times per week for 8 weeks. **A**, Four-by-four mosaics of representative spleen sections stained with antibodies against proliferating cell nuclear antigen (PCNA; red), peanut agglutinin (PNA; green), and CD45R (B220; white) to visualize GCs (top), and detection of GCs (visible as PCNA-positive clusters) and IgG-secreting PCs in spleens by anti-PCNA staining and anti-mouse IgG staining, respectively (bottom). **Insets**, Higher magnification views of GCs indicated by **yellow arrows**. Bars = 100 µm; original magnification × 200. **B–D**, GC size (**B**), percentage of spleen section area occupied by GCs (**C**), and number of IgG-secreting cells per field (original magnification × 200) (**D**). **E–H**, CD19+PNA+CD95+ GC B cells (**E**), CD3+CD4+CXCR5+PD-1+ICOS+ follicular helper T (TFH) cells (**F**), CD19+CD138+kappalight+MHCII^{high} plasmablasts (**G**), and CD19+CD138+kappalight+MHCII^{low} mature PCs (**H**) enumerated in spleens by flow cytometry. Unless indicated otherwise, representative results from 3 independent experiments are shown (n = 7–8 mice/group). Symbols represent individual mice; bars show the mean ± SEM. * = P ≤ 0.05; ** = P ≤ 0.005; *** = P ≤ 0.0005; **** = P ≤ 0.0001, by Mann-Whitney test. PD-1 = programmed death 1; ICOS = inducible costimulator; kappalight = κ light chain; MHCII = major histocompatibility complex class II.

Impact of KPT-350 on GCs and memory B cell responses. Based on classical GC responses against hapten-protein conjugates (25), we vaccinated C57BL/6 mice with 4-hydroxy-3-nitrophenylacetyl-ovalbumin (NP-Ova) conjugates

at different times relative to KPT-350 administration, to better define the impact of KPT-350 on GC formation and stability and memory B cell responses. First, to test the effect of the SINE on GC formation and generation of nonautoreactive PCs, we

vaccinated female C57BL/6 mice with NP₁₆-Ova in alum and treated the mice with KPT-350 for 2 weeks during the initial immune response (Supplementary Figure 5A, available on the *Arthritis & Rheumatology* website at <https://onlinelibrary.wiley.com/doi/10.1002/art.42128>). To evaluate the effects of the SINE on GC stability, we started KPT-350 treatment on day 28 (Supplementary Figure 5A). Finally, to determine the impact of KPT-350

on memory B cell responses, C57BL/6 mice were vaccinated with 100 µg of NP₁₆-Ova in alum on day 0 and, after resting for 2 months, were vaccinated with a 200-µg NP₁₆-Ova booster and then treated with KPT-350 for 2 weeks (Supplementary Figure 5A) (26). As expected, splenic Tfh cell and GC B cell counts decreased starting on day 0 in NP₁₆-Ova-vaccinated mice treated with KPT-350. Perhaps more surprisingly, Tfh cell and

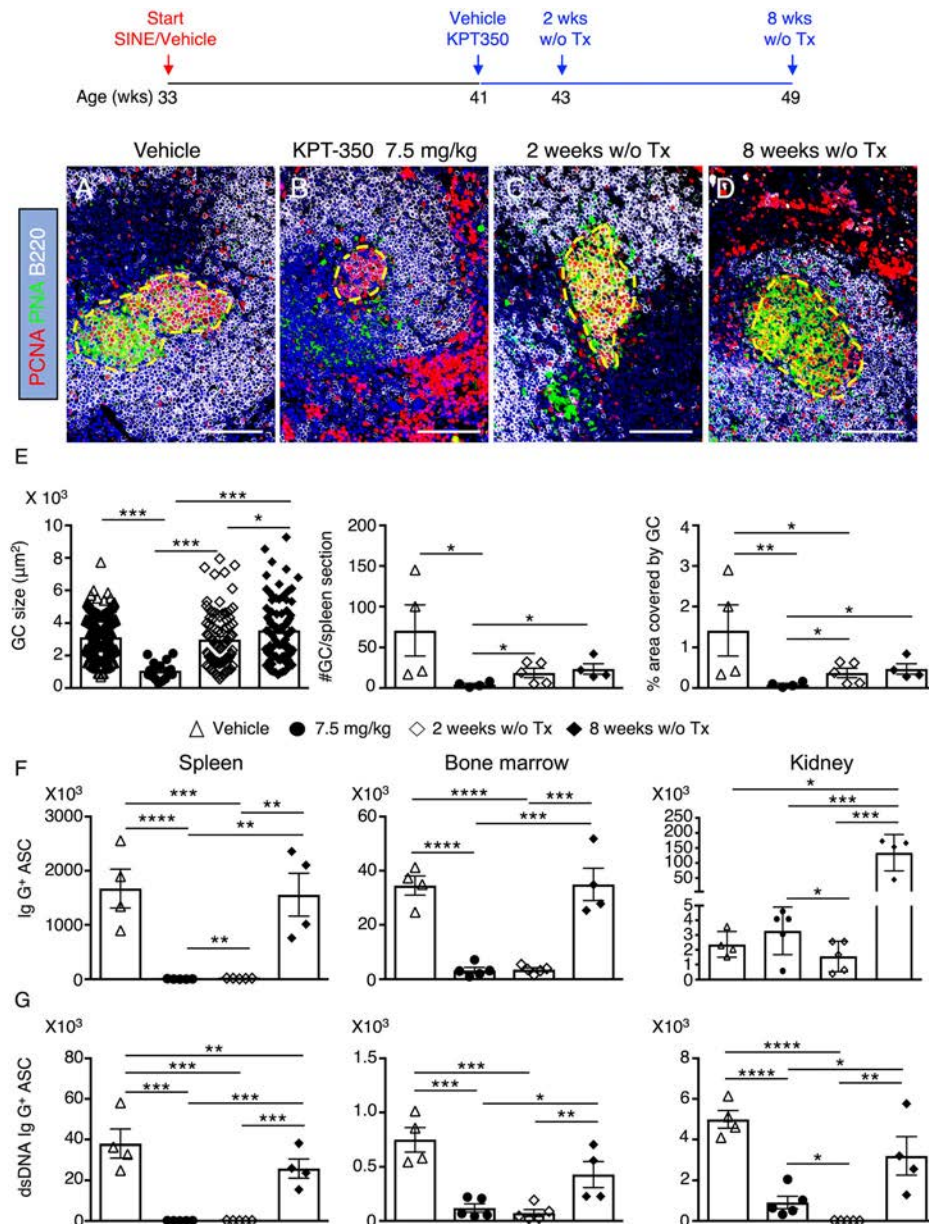


Figure 3. Effect of the SINE KPT-350 on germinal centers (GCs) 2 and 8 weeks after withdrawal of KPT-350 therapy in 27-week-old female NZB/NZW mice treated with vehicle or KPT-350 (5 mg/kg or 7.5 mg/kg) by oral gavage 3 times per week for 8 weeks. **A–D**, Representative stains of spleen tissue for detection of GCs immediately after vehicle (**A**) or KPT-350 (**B**) cessation and 2 weeks (**C**) and 8 weeks (**D**) after KPT-350 cessation. Bars = 100 µm. **E**, GC size (left), GC count per spleen section (middle), and percentage of spleen section area occupied by GCs (right). **F** and **G**, Isotype-switched (**F**) and autoreactive dsDNA-specific (**G**) ASCs enumerated by enzyme-linked immunospot in the spleen (left), bone marrow (middle), and kidney (right) immediately after vehicle or KPT-350 cessation and 2 weeks and 8 weeks after KPT-350 cessation. Unless indicated otherwise, representative results from 3 independent experiments are shown (n = 8 mice/group). Symbols represent individual mice; bars show the mean ± SEM. * = P ≤ 0.05; ** = P ≤ 0.005; *** = P ≤ 0.0005; **** = P ≤ 0.0001, by Mann-Whitney test. See Figure 1 for other definitions.

GC B cell counts were also drastically reduced during GC formation/maintenance and memory B cell responses (Supplementary Figures 5B–D).

GCs support the generation and selection of high-affinity ASCs. Consistent with this, we found a significant reduction in the number of NP⁴-specific ASCs in the spleen and bone marrow of mice treated with KPT-350 during the phase of GC formation (treatment 1) (Supplementary Figures 6A and B, available on the *Arthritis & Rheumatology* website at <https://onlinelibrary.wiley.com/doi/10.1002/art.42128>). Although numbers of high-affinity NP⁴-specific ASCs were significantly decreased in the spleen of mice treated with KPT-350 after GC formation (treatment 2) and during memory B cell responses (Supplementary Figures 6C and E), they were not affected in the bone marrow (Supplementary Figures 6D and F). Collectively, these results show that the spleen is the main target of KPT-350, which modulates multiple stages of the GC response by impairing Tfh cells, GC B cells, and the production of ASCs.

Duration of KPT-350 therapeutic effects after treatment withdrawal. To further define the duration of the

effects of KPT-350, we treated 33-week-old mice with 7.5 mg/kg of KPT-350 for 8 weeks and then withdrew therapy (Figure 3). We found a significant histologic impairment in GCs (Figures 3A–E). In turn, numbers of IgG-secreting and dsDNA-specific ASCs were dramatically reduced after 8 weeks of treatment with the SINE compound. Interestingly, GC structures began to recover as early as 2 weeks after KPT-350 therapy was stopped (Figures 3C and E), but the production of isotype-switched and dsDNA-specific splenic ASCs was still significantly abrogated at this time (Figures 3F and G). Also, autoreactive splenic ASCs did not reach numbers found in the control group, even 8 weeks after suspension of therapy (Figure 3G). In contrast, levels of both IgG-secreting and autoreactive ASCs had recovered in the bone marrow (Figures 3F and G). However, the numbers of autoreactive ASCs in the kidney remained low 8 weeks after therapy withdrawal (Figure 3G). Kidney perivascular inflammatory cells slowly reaccumulated (Supplementary Figures 7A–E, available on the *Arthritis & Rheumatology* website at <https://onlinelibrary.wiley.com/doi/10.1002/art.42128>). The proteinuria score remained low 2 weeks after therapy withdrawal but rebounded by 8 weeks, suggesting the need for a maintenance dosing schedule

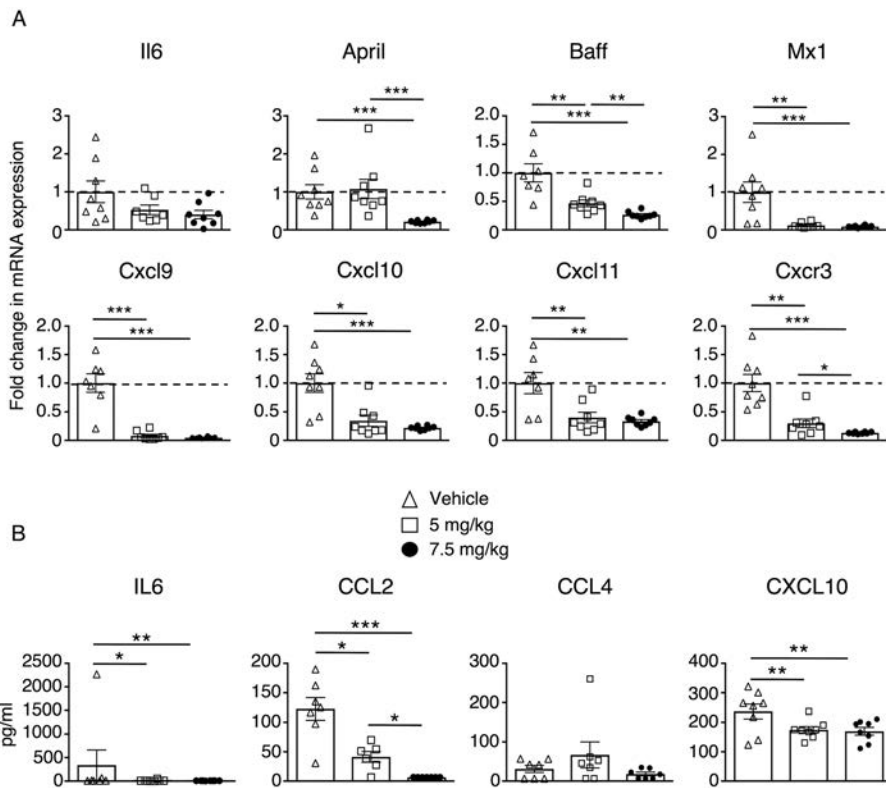


Figure 4. Effect of KPT-350 on expression of chemokines and survival factors for autoreactive plasma cells (PCs) in inflamed kidneys of 27-week-old female NZB/NZW mice treated with vehicle or KPT-350 (5 mg/kg or 7.5 mg/kg) by oral gavage 3 times per week for 8 weeks. **A**, Fold differences in mRNA expression relative to GAPDH between treated and untreated mice for genes involved in PC survival (top) or chemokines orchestrating migration of antibody-secreting cells to survival niches (bottom). Expression was analyzed by quantitative polymerase chain reaction, and fold differences were calculated using the $\Delta\Delta C_t$ method. **B**, Serum concentration of key molecules in lupus pathogenesis. Unless indicated otherwise, representative results from 3 independent experiments are shown ($n = 7-8$ mice/group). Symbols represent individual mice; bars show the mean \pm SEM. * = $P \leq 0.05$; ** = $P \leq 0.005$; *** = $P \leq 0.0005$, by Mann-Whitney test.

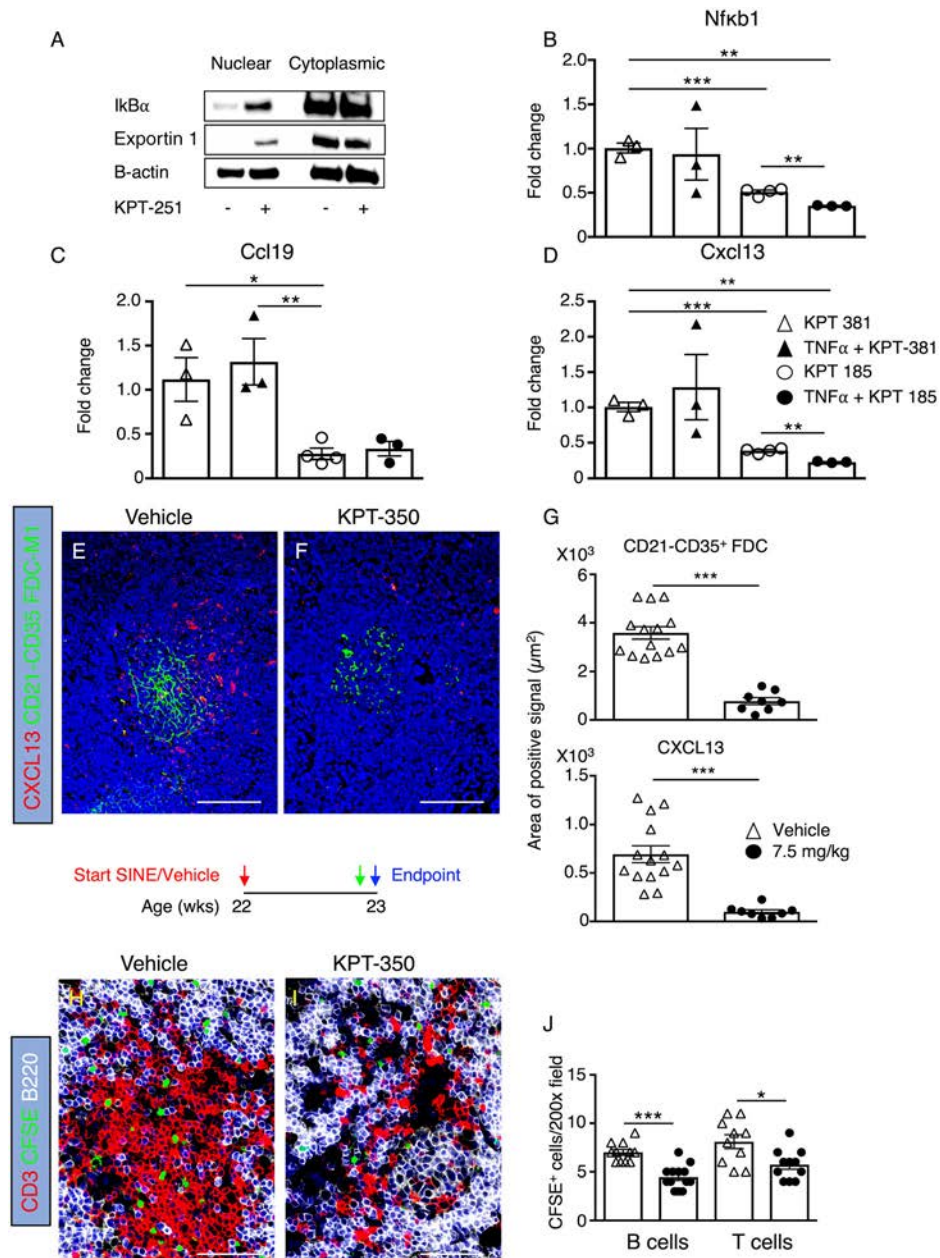


Figure 5. Effect of selective inhibitors of nuclear export (SINE compounds) on NF- κ B-dependent production of stromal cell-derived chemokines that attract immune cells to the spleen, in 27-week-old female NZB/NZW mice. **A**, Representative Western blots for I κ B α and exportin 1 in cytoplasmic and nuclear fractions of splenic stromal cells stimulated with tumor necrosis factor (TNF α ; 20 ng/ml) and incubated with or without the SINE KPT-251. **B–D**, Fold change in mRNA expression for *Nfkb1* (**B**), *Ccl19* (**C**), and *Cxcl13* (**D**) in TNF-stimulated cells relative to cells incubated with KPT-185 or inactive stereoisomer (KPT-381). **E** and **F**, Representative immunofluorescence stains for CXCL13+ cells (red) and CD21-CD35+FDCM1+ follicular dendritic cells (FDCs; green) in the spleen after receiving vehicle (**E**) or KPT-350 (**F**) for 8 weeks. Bars = 100 μ m; original magnification \times 200. **G**, Dimensions of FDC networks (top) and areas covered by CXCL13 (bottom). **H** and **I**, Representative stains for carboxy-fluorescein succinimidyl ester (CFSE)-positive T and B cells (green), CD3+ T cells (red), and B220+ B cells (white) in spleens of mice that received vehicle (**H**) or KPT-350 (**I**). Original magnification \times 200. **J**, Quantitation of strategic positioning of CFSE-labeled CD3+ T cells and B220+ B cells in spleens of NZB/NZW mice ($n = 5$ –8 mice/group). Symbols represent individual mice; bars show the mean \pm SEM. * = $P \leq 0.05$; ** = $P \leq 0.005$; *** = $P \leq 0.0005$, by Mann-Whitney test.

for sustained suppression of autoimmunity (Supplementary Figure 7F). These data support the rapid reversibility of the effects of KPT-350 on GCs but a more prolonged and favorable effect on autoreactive ASC numbers and overall renal inflammation.

Modulation of PC-attracting chemokines and survival factors by KPT-350 in kidneys of lupus-prone mice. Splenic ASCs are attracted to bone marrow and sites of inflammation by CXCL12, CCL2, and interferon- γ (IFN γ)-induced

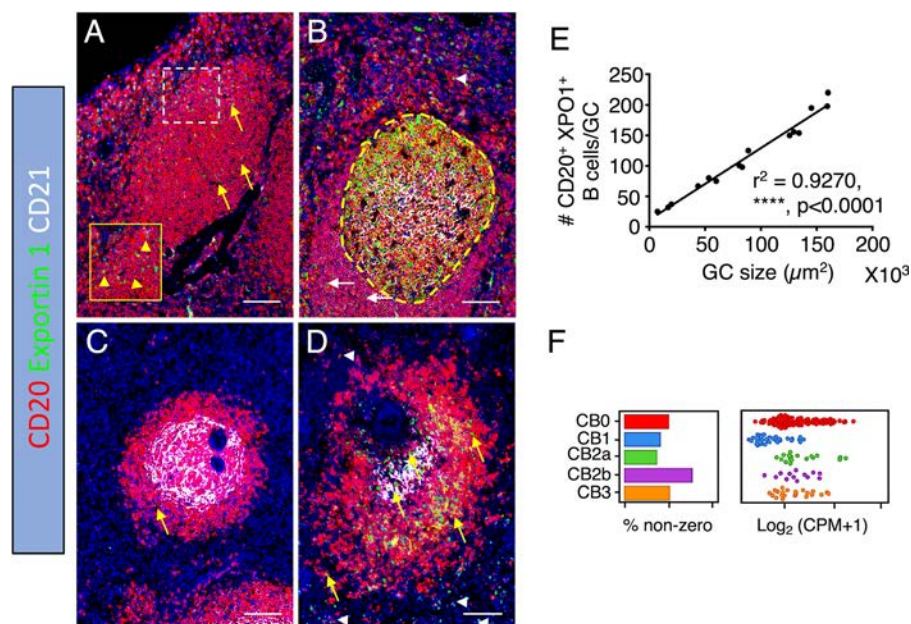


Figure 6. Detection of exportin 1 in tonsillar germinal centers (GCs) and secondary lymphoid organs of lupus patients. **A–D**, Four-by-four representative mosaic stains for exportin 1 (green), CD20 (red), and CD21 (white) in tonsillar primary follicles (**A**) and a tonsillar active GC (yellow dashed line) (**B**) from a healthy individual, and in splenic secondary lymphoid follicles from a healthy individual (**C**) and a lupus patient (**D**). Exportin 1–positive B cells were observed in primary and secondary lymphoid follicles (**yellow arrows**), the tonsillar mantle zone (**white arrows**), and extrafollicular areas (**white arrowheads**), with greater nuclear localization in lupus patients (**yellow arrowheads**). Inset in **A** shows the region of interest defined by the white dashed square. Bars = 1,000 μm; original magnification × 200. **E**, Correlation between GC size and number of exportin 1–positive CD20+ B cells per tonsillar GC. **F**, Single-cell RNA sequencing data obtained from the public immunogenomics portal of the Accelerating Medicines Partnership Program—Rheumatoid Arthritis, System Lupus Erythematosus phase I, showing high expression of exportin 1 by B cells in kidneys of lupus patients. CB0 = activated B cells; CB1 = plasma cells/plasmablasts; CB2a = naive B cells, CB2b = plasmacytoid dendritic cells; CB3 = interferon gene–stimulated B^{high} cells.

chemokines (27). For example, autoreactive PCs are enriched in the kidneys of lupus-prone mice, and B cell depletion modulates PC accumulation in the kidneys by decreasing the expression of mRNA encoding survival factors (i.e., BAFF, APRIL, and interleukin-6 [IL-6]) and chemotactic factors in this anatomic location (28). Additionally, type I IFN induces the production of survival factors for ASCs (29). Importantly, KPT-350 therapy significantly reduced expression of mRNA coding for molecules critical for ASC survival in inflamed kidneys (i.e., IL-6, APRIL, and BAFF). In addition, the significant reduction in the expression of mRNA encoding Mx-1 suggests that KPT-350 affected local production of type I IFN, which in turn may decrease the production of survival factors for PCs in the kidney (Figure 4A). We also found a significant reduction in the expression of mRNA encoding IFN-induced chemokines (i.e., CXCL9, CXCL10, and CXCL11) and their primary chemokine receptor, CXCR3 (Figure 4A). Consistent with the reduction in expression of mRNA encoding IL-6 in lupus-prone mice, we detected a decrease in the amount of IL-6 protein in sera. Serum concentrations of CCL2, CCL4, and CXCL10 proteins were also significantly reduced in KPT-350–treated mice (Figure 4B). Thus, our results indicate that KPT-350 strongly modulates both the attraction and production of survival factors for ASCs in the kidneys of lupus-prone mice.

Disruption of stromal cells and NF-κB-mediated compartmentalization of immune cells in spleens of lupus-prone mice due to inhibition of nuclear export.

Stromal cells produce homeostatic chemokines, which orchestrate B and T cell recruitment to secondary lymphoid organs, maximizing their interactions and facilitating the induction of highly regulated immune responses (30). In agreement with the smaller size of splenic white pulp in KPT-350–treated mice, splenic B and T cell areas were significantly affected by long-term treatment with the SINE (Supplementary Figures 8A–D, available on the *Arthritis & Rheumatology* website at <https://onlinelibrary.wiley.com/doi/10.1002/art.42128>). The total number of B cells was reduced considerably after short-term and long-term treatment, whereas the T cell count decreased only after long-term treatment (Supplementary Figures 8E and F). Thus, we hypothesized that SINE compounds might target stromal cell–driven attraction of immune cells to the spleen, explaining the profound impact of KPT-350 on GCs and autoreactive PC generation.

To mechanistically define the effect of KPT-350 on stromal cells, we stimulated adherent stromal cells with tumor necrosis factor (TNF) in the presence or absence of the SINE compound KPT-251 *in vitro*. As we expected, and consistent with previous

studies involving other cell types (31), inhibition of nuclear export caused sequestration of exportin 1 and I κ B α in the nuclei of TNF-stimulated stromal cells treated with KPT-251, without affecting their levels in the cytoplasm (Figure 5A). Nuclear I κ B α retention disrupts NF- κ B signaling in stromal cells (12). Noncanonical NF- κ B signaling in stromal cells is critical in the production of homeostatic chemokines, which maintain the organization of T and B cell zones in secondary lymphoid organs (32), and binding of NF- κ B complexes to the I κ B α DNA promoter is required to activate transcription of the gene encoding I κ B α (33).

As an indication of the inhibition of NF- κ B signaling by SINE compounds, we observed that expression of *Nfkb1* mRNA was reduced in TNF-stimulated stromal cells incubated with the SINE compound (Figure 5B). In agreement with the critical role of NF- κ B signaling in homeostatic chemokine production, we also found decreased expression of *Ccl19* and *Cxcl13* mRNA after inhibition of nuclear export in splenic stromal cells (Figures 5C and D). To confirm the impact of SINEs on CXCL13 production, we next stained sections of spleen specimens from lupus-prone mice treated in vivo with KPT-350, with antibodies specific for CXCL13 and markers for follicular dendritic cells (FDCs; i.e., CD21/CD35 and FDC-M1). CXCL13-producing stromal cells and FDCs were abundant in spleens of mice receiving vehicle (Figures 5E and G). In contrast, the area covered by splenic CXCL13 and FDCs was significantly decreased in lupus-prone mice treated with KPT-350 (Figures 5F and G).

To further demonstrate that impaired production of homeostatic chemokines affects strategic positioning of T and B cells in the spleens of lupus-prone mice, we transferred 10 million cells labeled with carboxyfluorescein succinimidyl ester (CFSE) to mice that received vehicle or KPT-350 3 times for 1 week (Supplementary Figure 8, available on the *Arthritis & Rheumatology* website at <https://onlinelibrary.wiley.com/doi/10.1002/art.42128>). Although the SINE compound did not affect the accumulation of CFSE-labeled T and B cells in the spleen (Supplementary Figures 8G and H, available at <https://onlinelibrary.wiley.com/doi/10.1002/art.42128>), there was a significant reduction in the numbers of CFSE-labeled T and B cells in the T and B cell zones, respectively, of lupus-prone mice (Figures 5H–J). These findings suggest that inhibition of nuclear export in stromal cells compromises the strategic positioning of T and B cells. In turn, this impairs B cell–driven differentiation of stromal cells into FDCs and production of CXCL13, a homeostatic chemokine critical in the attraction of CXCR5+ antigen-specific B cells and Tfh cells, which are essential components of GCs.

Expression of exportin 1 in GCs of human tonsils, secondary lymphoid organs, and kidney-infiltrating B cells of lupus patients. Given the impact of inhibition of nuclear export on autoreactive splenic GCs in lupus-prone mice, we examined the expression of exportin 1—the target of SINE compounds—in inflamed human tonsils. Exportin 1 expression

was observed in B cells from primary follicles (Figure 6A), the mantle zone (Figure 6B), and extrafollicular locations (Figure 6B). Of note, exportin 1–expressing CD20+ B cells were most numerous in active GCs (Figure 6B), and the number increased proportionally with the size of tonsillar GCs (Figure 6E). Exportin 1–expressing CD20+ B cells were rare in the splenic B cell follicles of healthy individuals (Figure 6C) and more numerous in the secondary lymphoid follicles in the spleen of lupus patients (Figure 6D). Finally, analysis of phase I data from the Accelerating Medicines Partnership (18) confirmed the expression of exportin 1 by multiple B cell populations (i.e., plasma cells and IFN-stimulated B^{high}, naive B, and activated B cells) isolated from the kidneys of lupus patients (Figure 6F). Thus, these results show the relevance of SINE compounds in targeting exportin 1 in pathogenic B cell subsets of lupus patients.

DISCUSSION

Here, we demonstrated that the SINE compound KPT-350 effectively abrogated lupus nephritis and caused profound reductions in the number of autoreactive ASCs in the spleen, bone marrow, and inflamed kidney. This effect is mediated by strong modulation of splenic GCs via inhibition of homeostatic chemokine production by stromal cells and altered T and B cell positioning. Additionally, concentrations of factors implicated in the migration and survival of autoreactive ASCs (i.e., BAFF, APRIL, IL6, and IFN γ -induced chemokines) were dramatically reduced in the kidney by KPT-350. Moreover, reduced Mx-1 expression in the kidneys of treated mice provides evidence for modulation of type I IFN signaling, which in turn may alter PC survival (Supplementary Figure 9, available on the *Arthritis & Rheumatology* website at <https://onlinelibrary.wiley.com/doi/10.1002/art.42128>). Collectively, our results demonstrate that SINEs have potent and multipronged effects on pathways that are key for PC generation, survival, and maintenance.

Profound inhibition of GC reactions was particularly evident with prolonged in vivo KPT-350 treatment. In addition to histologic findings, Tfh cells and GC B cells were significantly reduced with SINE treatment. The effect of KPT-350 might be directly mediated via its effects on T cells, B cells, stromal cells, or multiple cell populations. Indeed, Tfh cells are crucial in GC formation and differentiation of B cells into memory B lymphocytes and PCs. In turn, GC B cells influence the commitment and maintenance of Tfh cells (34,35). SINE compounds inhibit NF- κ B signaling through nuclear retention of I κ B α (31). Nuclear export of I κ B α is required to maintain NF- κ B activation in mature B cells, supporting proliferation and survival responses, including survival of GC centroblasts. Thus, SINEs may have direct effects on B cells in our model.

Interestingly, we did not find any differences in the mRNA expression for proapoptotic genes (e.g., *Bax* and *Casp3*) and antiapoptotic genes (e.g., *Bcl2*) or increased caspase 3 staining

in the spleen of treated mice (data not shown). This led us to explore other potential mechanisms modulating GCs. Indeed, our data support a direct effect on stromal cells, which would be expected to have indirect effects on GC B cells and Tfh cells. NF- κ B-dependent production of homeostatic chemokines (i.e., CXCL13, CCL19, CCL21, and BAFF) by stromal cells is critical for proper B cell compartmentalization and secondary lymphoid organ formation (30,36). Further, homeostatic chemokines maintain GC integrity and support PC survival (34). In this regard, we found a markedly reduced expression of splenic CXCL13 with KPT-350 treatment. In addition, NF- κ B-dependent production of CXCL13 by stromal cells was drastically reduced as a consequence of disrupting NF- κ B signaling by targeting exportin 1-mediated nuclear export. This likely explains the impaired B cell positioning in the splenic white pulp in our transfer experiments and the inhibition of GC responses.

In terms of other mechanisms, it is notable that SINE treatment significantly reduced IL-6 expression, a cytokine instrumental in Tfh cell differentiation (37–39). Recently it was shown that IL-6 inhibits IL-2 responsiveness in T cells, facilitating the generation of Tfh cells in GCs. Thus, inhibition of nuclear export may impair the production of Tfh cells by reducing IL-6 production (40). Regardless of whether the dominant effect is on Tfh cells, GC B cells, or both, SINEs potently modulate GC formation, maintenance, and expansion of memory Tfh cells and GC B cells. While we have not excluded the possibility that SINE compounds directly affect ASC survival, we believe the reduction in the number of autoreactive ASCs is more likely derived from the modulation of splenic GCs and the disruption of ASC migration to the bone marrow and inflamed kidneys. Although myeloma PCs are sensitive to the direct effects of SINE compounds owing to enhanced cell cycle arrest and apoptosis (15), our results suggest that normal PCs might be more resistant to SINE therapy in NZB/NZW mice.

Another critical finding was reduced IFN signaling in the kidney with KPT-350 treatment, including lower expression of mRNA encoding Mx-1, IFN-regulated chemokines, IL-6, APRIL, and BAFF. It was reported that the nuclear export of mRNA coding for IFN α was blocked by leptomycin B (41). In preliminary studies, we demonstrated that KPT-350 inhibited IFN α production by plasmacytoid DCs (data not shown). IFN α stimulates B cell proliferation and PC production through an IL-6-dependent mechanism (42) and promotes differentiation of naive T cells into Tfh cells (43). Interestingly, IL-6 is produced by myeloid dendritic cells stimulated by CD40L in the presence of IFN α and plasmacytoid DCs stimulated by Toll-like receptor ligands (43,44). Type I IFN also stimulates the production of ASC survival factors (45). These results indicate that modulation of type I IFN signaling by SINE compounds in the kidney likely influences development and maintenance of autoreactive ASCs.

ASCs generated in the spleen respond to chemotactic cues produced in distal anatomic niches that contain various cells

(i.e., neutrophils, eosinophils, and stromal cells), which secrete ASC survival factors such as BAFF, APRIL, and IL-6 (29,46,47). Additionally, plasmablasts and PCs express unique chemokine receptors (i.e., CCR2, CXCR3, and CXCR4) that guide ASCs to sites of inflammation and bone marrow (27,48). Although we observed a SINE-mediated reduction of several factors involved in migration and survival of autoreactive PCs in the kidney (IFN γ -induced chemokines, BAFF, APRIL, and IL-6), we did not detect any differences in the bone marrow. Thus, a decrease in the numbers of autoreactive PCs in the bone marrow with prolonged treatment may reflect the impaired production of splenic autoreactive ASCs.

Our experimental results suggest that inhibition of nuclear export represents a novel approach for treating lupus, via multipronged effects on autoreactive PCs and other inflammatory cells in multiple organs that abrogate nephritis. The expression of exportin 1 by tonsillar GC B cells and B cells in the spleen and kidney of lupus patients further supports the translational potential of this approach. Indeed, the recent approval of SINE compounds for the treatment of refractory multiple myeloma and their tolerability in clinical trials involving healthy individuals (49–51) make them an attractive treatment approach for lupus and other inflammatory disorders. Though the significant inhibition of GC responses is a critical mechanism for the beneficial effects of SINEs in lupus, we acknowledge the potential for immune suppression. Importantly, we have demonstrated that GC inhibition by KPT-350 is rapidly reversible upon treatment cessation, but with a slower reaccumulation of autoreactive PCs and a slower increase in proteinuria score, raising the possibility of intermittent treatment for the optimal balance of risks and benefits.

AUTHOR CONTRIBUTIONS

All authors were involved in drafting the article or revising it critically for important intellectual content, and all authors approved the final version to be published. Drs. Rangel-Moreno and Anolik had full access to all of the data in the study and take responsibility for the integrity of the data and the accuracy of the data analysis.

Study conception and design. Rangel-Moreno, Anolik.

Acquisition of data. Rangel-Moreno, Garcia-Hernandez, Owen, Barnard, Becerril-Villanueva, Kashyap, Argueta, Gamboa-Dominguez, Tamir, Landesman, Goldman, Ritchlin, Anolik.

Analysis and interpretation of data. Rangel-Moreno, Garcia-Hernandez, Ritchlin, Anolik.

ADDITIONAL DISCLOSURES

Authors Kashyap, Argueta, Tamir, and Landesman are employees of Karyopharm.



REFERENCES

1. Ahmed S, Anolik JH. B-cell biology and related therapies in systemic lupus erythematosus. *Rheum Dis Clin North Am* 2010;36:109–30.
2. Bongu A, Chang E, Ramsey-Goldman R. Can morbidity and mortality of SLE be improved? *Best Pract Res Clin Rheumatol* 2002;16:313–32.

3. Chan OT, Madaio MP, Shlomchik MJ. The central and multiple roles of B cells in lupus pathogenesis. *Immunol Rev* 1999;169:107–21.
4. Mamula MJ, Fatenejad S, Craft J. B cells process and present lupus autoantigens that initiate autoimmune T cell responses. *J Immunol* 1994;152:1453–61.
5. Lund FE, Randall TD. Effector and regulatory B cells: modulators of CD4+ T cell immunity [review]. *Nat Rev Immunol* 2010;10:236–47.
6. Looney RJ, Anolik JH, Campbell D, Felgar RE, Young F, Arend LJ, et al. B cell depletion as a novel treatment for systemic lupus erythematosus: a phase I/II dose-escalation trial of rituximab. *Arthritis Rheum* 2004;50:2580–9.
7. Merrill JT, Neuwelt CM, Wallace DJ, Shanahan JC, Latinis KM, Oates JC, et al. Efficacy and safety of rituximab in moderately-to-severely active systemic lupus erythematosus: the randomized, double-blind, phase II/III systemic lupus erythematosus evaluation of rituximab trial. *Arthritis Rheum* 2010;62:222–33.
8. Rovin BH, Furie R, Latinis K, Looney RJ, Fervenza FC, Sanchez-Guerrero J, et al. Efficacy and safety of rituximab in patients with active proliferative lupus nephritis: the Lupus Nephritis Assessment with Rituximab study. *Arthritis Rheum* 2012;64:1215–26.
9. Hiepe F, Dörner T, Hauser AE, Hoyer BF, Mei H, Radbruch A. Long-lived autoreactive plasma cells drive persistent autoimmune inflammation. *Nat Rev Rheumatol* 2011;7:170–8.
10. Hoyer BF, Moser K, Hauser AE, Peddinghaus A, Voigt C, Eilat D, et al. Short-lived plasmablasts and long-lived plasma cells contribute to chronic humoral autoimmunity in NZB/W mice. *J Exp Med* 2004;199:1577–84.
11. Nguyen KT, Holloway MP, Altura RA. The CRM1 nuclear export protein in normal development and disease. *Int J Biochem Mol Biol* 2012;3:137–51.
12. Etchin J, Sun Q, Kentsis A, Farmer A, Zhang ZC, Sanda T, et al. Anti-leukemic activity of nuclear export inhibitors that spare normal hematopoietic cells. *Leukemia* 2013;27:66–74.
13. Kau TR, Way JC, Silver PA. Nuclear transport and cancer: from mechanism to intervention. *Nat Rev Cancer* 2004;4:106–17.
14. Zhang KJ, Wang M. Potential effects of CRM1 inhibition in mantle cell lymphoma. *Chin J Cancer Res* 2012;24:374–87.
15. Tai YT, Landesman Y, Acharya C, Calle Y, Zhong MY, Cea M, et al. CRM1 inhibition induces tumor cell cytotoxicity and impairs osteoclastogenesis in multiple myeloma: molecular mechanisms and therapeutic implications. *Leukemia* 2014;28:155–65.
16. Chari A, Vogl DT, Gavriatopoulou M, Nooka AK, Yee AJ, Huff CA, et al. Oral selinexor-dexamethasone for triple-class refractory multiple myeloma. *N Engl J Med* 2019;381:727–38.
17. Hochberg MC, for the Diagnostic and Therapeutic Criteria Committee of the American College of Rheumatology. Updating the American College of Rheumatology revised criteria for the classification of systemic lupus erythematosus [letter]. *Arthritis Rheum* 1997;40:1725.
18. Arazi A, Rao DA, Berthier CC, Davidson A, Liu Y, Hoover PJ, et al. The immune cell landscape in kidneys of patients with lupus nephritis. *Nat Immunol* 2019;20:902–14.
19. Wakamatsu K, Nanki T, Miyasaka N, Umezawa K, Kubota T. Effect of a small molecule inhibitor of nuclear factor- κ B nuclear translocation in a murine model of arthritis and cultured human synovial cells. *Arthritis Res Ther* 2005;7:R1348–59.
20. Perwitasari O, Johnson S, Yan X, Register E, Crabtree J, Gabbard J, et al. Antiviral efficacy of verdinexor in vivo in two animal models of influenza A virus infection. *PLoS One* 2016;11:e0167221.
21. Crispin JC, Liossis SN, Kis-Toth K, Lieberman LA, Kyttaris VC, Juang YT, et al. Pathogenesis of human systemic lupus erythematosus: recent advances. *Trends Mol Med* 2010;16:47–57.
22. Kwok SK, Tsokos GC. New insights into the role of renal resident cells in the pathogenesis of lupus nephritis. *Korean J Intern Med* 2018;33:284–9.
23. Harris AA, Kamishima T, Horita T, Atsumi T, Fujita N, Omatsu T, et al. Splenic volume in systemic lupus erythematosus. *Lupus* 2019;18:1119–20.
24. Luzina IG, Atamas SP, Storrer CE, daSilva LC, Kelsoe G, Papadimitriou JC, et al. Spontaneous formation of germinal centers in autoimmune mice. *J Leukoc Biol* 2001;70:578–84.
25. Jacob J, Kassir R, Kelsoe G. In situ studies of the primary immune response to (4-hydroxy-3-nitrophenyl)acetyl. I. The architecture and dynamics of responding cell populations. *J Exp Med* 1991;173:1165–75.
26. Rangel-Moreno J, Moyron-Quiroz JE, Carragher DM, Kusser K, Hartson L, Moquin A, et al. Omental milky spots develop in the absence of lymphoid tissue-inducer cells and support B and T cell responses to peritoneal antigens. *Immunity* 2009;30:731–43.
27. Lugar PL, Love C, Grammer AC, Dave SS, Lipsky PE. Molecular characterization of circulating plasma cells in patients with active systemic lupus erythematosus. *PLoS One* 2012;7:e44362.
28. Wang W, Rangel-Moreno J, Owen T, Barnard J, Nevarez S, Ichikawa HT, et al. Long-term B cell depletion in murine lupus eliminates autoantibody-secreting cells and is associated with alterations in the kidney plasma cell niche. *J Immunol* 2014;192:3011–20.
29. Palanichamy A, Bauer JW, Yalavarthi S, Meednu N, Barnard J, Owen T, et al. Neutrophil-mediated IFN activation in the bone marrow alters B cell development in human and murine systemic lupus erythematosus. *J Immunol* 2014;192:906–18.
30. Randall TD, Carragher DM, Rangel-Moreno J. Development of secondary lymphoid organs. *Annu Rev Immunol* 2008;26:627–50.
31. Kashyap T, Argueta C, Aboukameel A, Unger TJ, Klebanov B, Mohammad RM, et al. Selinexor, a selective inhibitor of nuclear export (SINE) compound, acts through NF- κ B deactivation and combines with proteasome inhibitors to synergistically induce tumor cell death. *Oncotarget* 2016;7:78883–95.
32. Carragher DM, Rangel-Moreno J, Randall TD. Ectopic lymphoid tissues and local immunity. *Semin Immunol* 2008;20:26–42.
33. Ito CY, Kazantsev AG, Baldwin AS Jr. Three NF- κ B sites in the I κ B- α promoter are required for induction of gene expression by TNF α . *Nucleic Acids Res* 1994;22:3787–92.
34. Heise N, De Silva NS, Silva K, Carette A, Simonetti G, Pasparakis M, et al. Germinal center B cell maintenance and differentiation are controlled by distinct NF- κ B transcription factor subunits. *J Exp Med* 2014;211:2103–18.
35. De Silva NS, Anderson MM, Carette A, Silva K, Heise N, Bhagat G, et al. Transcription factors of the alternative NF- κ B pathway are required for germinal center B-cell development. *Proc Natl Acad Sci U S A* 2016;113:9063–8.
36. Wuerzberger-Davis SM, Chen Y, Yang DT, Kearns JD, Bates PW, Lynch C, et al. Nuclear export of the NF- κ B inhibitor I κ B α is required for proper B cell and secondary lymphoid tissue formation. *Immunity* 2011;34:188–200.
37. Korn T, Mitsdoerffer M, Croxford AL, Awasthi A, Dardalhon VA, Galileos G, et al. IL-6 controls Th17 immunity in vivo by inhibiting the conversion of conventional T cells into Foxp3+ regulatory T cells. *Proc Natl Acad Sci U S A* 2008;105:18460–5.
38. Eto D, Lao C, DiToro D, Barnett B, Escobar TC, Kageyama R, et al. IL-21 and IL-6 are critical for different aspects of B cell immunity and redundantly induce optimal follicular helper CD4 T cell (Tfh) differentiation. *PLoS One* 2011;6:e17739.
39. Vinuesa CG, Cyster JG. How T cells earn the follicular rite of passage. *Immunity* 2011;35:671–80.

40. Papillion A, Powell MD, Chisolm DA, Bachus H, Fuller MJ, Weinmann AS, et al. Inhibition of IL-2 responsiveness by IL-6 is required for the generation of GC-TFH cells. *Sci Immunol* 2019;4.
41. Kimura T, Hashimoto I, Nagase T, Fujisawa J. CRM1-dependent, but not ARE-mediated, nuclear export of IFN- α 1 mRNA. *J Cell Sci* 2004; 117:2259–70.
42. Jego G, Palucka AK, Blanck JP, Chalouni C, Pascual V, Banchereau J. Plasmacytoid dendritic cells induce plasma cell differentiation through type I interferon and interleukin 6. *Immunity* 2003; 19:225–34.
43. Cucak H, Yrlid U, Reizis B, Kalinke U, Johansson-Lindbom B. Type I interferon signaling in dendritic cells stimulates the development of lymph-node-resident T follicular helper cells. *Immunity* 2009;31: 491–501.
44. Bonnefoy F, Couturier M, Clauzon A, Remy-Martin JP, Gaugler B, Tiberghien P, et al. TGF-beta-exposed plasmacytoid dendritic cells participate in Th17 commitment. *J Immunol* 2011;186:6157–64.
45. Mathian A, Gallegos M, Pascual V, Banchereau J, Koutouzov S. Interferon- α induces unabated production of short-lived plasma cells in pre-autoimmune lupus-prone (NZBxNZW)F1 mice but not in BALB/c mice. *Eur J Immunol* 2011;41:863–72.
46. Chu VT, Frohlich A, Steinhauser G, Scheel T, Roch T, Fillatreu S, et al. Eosinophils are required for the maintenance of plasma cells in the bone marrow. *Nat Immunol* 2011;12:151–9.
47. Belnoue E, Pihlgren M, McGaha TL, Tougne C, Rochat AF, Bossen C, et al. APRIL is critical for plasmablast survival in the bone marrow and poorly expressed by early-life bone marrow stromal cells. *Blood* 2008; 111:2755–64.
48. Tarte K, Zhan F, De Vos J, Klein B, Shaughnessy J Jr. Gene expression profiling of plasma cells and plasmablasts: toward a better understanding of the late stages of B-cell differentiation. *Blood* 2003;102: 592–600.
49. Azizian NG, Li Y [review]. XPO1-dependent nuclear export as a target for cancer therapy. *J Hematol Oncol* 2020;13:61.
50. Nishihori T, Baz R. Selective inhibitors of nuclear export (SINEs) in myeloma: breakthrough or bust? *Expert Opin Drug Saf* 2020;19: 113–5.
51. Widman DG, Gornisiewicz S, Shacham S, Tamir S. In vitro toxicity and efficacy of verdinexor, an exportin 1 inhibitor, on opportunistic viruses affecting immunocompromised individuals. *PLoS One* 2018;13: e0200043.

Global Transcriptomic Profiling Identifies Differential Gene Expression Signatures Between Inflammatory and Noninflammatory Aortic Aneurysms

Benjamin Hur, Matthew J. Koster,  Jin Sung Jang, Cornelia M. Weyand, Kenneth J. Warrington, and Jaeyun Sung 

Objective. To identify hallmark genes and biomolecular processes in aortitis using high-throughput gene expression profiling, and to provide a range of potentially new drug targets (genes) and therapeutics from a pharmacogenomic network analysis.

Methods. Bulk RNA sequencing was performed on surgically resected ascending aortic tissues from inflammatory aneurysms (giant cell arteritis [GCA] with or without polymyalgia rheumatica, $n = 8$; clinically isolated aortitis [CIA], $n = 17$) and noninflammatory aneurysms ($n = 25$) undergoing surgical aortic repair. Differentially expressed genes (DEGs) between the 2 patient groups were identified while controlling for clinical covariates. A protein–protein interaction model, drug–gene target information, and the DEGs were used to construct a pharmacogenomic network for identifying promising drug targets and potentially new treatment strategies in aortitis.

Results. Overall, tissue gene expression patterns were the most associated with disease state than with any other clinical characteristic. We identified 159 and 93 genes that were significantly up-regulated and down-regulated, respectively, in inflammatory aortic aneurysms compared to noninflammatory aortic aneurysms. We found that the up-regulated genes were enriched in immune-related functions, whereas the down-regulated genes were enriched in neuronal processes. Notably, gene expression profiles of inflammatory aortic aneurysms from patients with GCA were no different than those from patients with CIA. Finally, our pharmacogenomic network analysis identified genes that could potentially be targeted by immunosuppressive drugs currently approved for other inflammatory diseases.

Conclusion. We performed the first global transcriptomics analysis in inflammatory aortic aneurysms from surgically resected aortic tissues. We identified signature genes and biomolecular processes, while finding that CIA may be a limited presentation of GCA. Moreover, our computational network analysis revealed potential novel strategies for pharmacologic interventions and suggests future biomarker discovery directions for the precise diagnosis and treatment of aortitis.

INTRODUCTION

The etiology and pathogenic mechanisms leading to noninfectious inflammation of the aortic wall (aortitis) remain largely unknown. In clinical practice, distinguishing patients with inflammatory aortic aneurysms from those with noninflammatory aortic aneurysms may be difficult, since aortitis may be asymptomatic or associated with nonspecific symptoms (1,2). Moreover, there

are currently no laboratory diagnostic markers specifically for aortitis or for 2 of its most common underlying conditions, i.e., giant cell arteritis (GCA) and clinically isolated aortitis (CIA) (1,3,4). Therefore, the unmet need for patients with aortitis include the discovery of novel biomolecular features that stratify inflammatory and noninflammatory aortic aneurysms and thereby complement current diagnostic approaches and improve long-term treatment outcomes.

Supported in part by Mayo Clinic Benefactors. Drs. Hur and Sung's work was supported in part by the Mayo Clinic Center for Individualized Medicine. Drs. Koster, Weyand, and Warrington's work was supported in part by the Mayo Clinic Division of Rheumatology.

Benjamin Hur, PhD, Matthew J. Koster, MD, Jin Sung Jang, PhD, Cornelia M. Weyand, MD, PhD, Kenneth J. Warrington, MD, Jaeyun Sung, PhD: Mayo Clinic, Rochester, Minnesota.

Drs. Warrington and Sung contributed equally to this work as co-senior authors.

Author disclosures are available at <https://onlinelibrary.wiley.com/action/downloadSupplement?doi=10.1002%2Fart.42138&file=art42138-sup-0001-Disclosureform.pdf>.

Address correspondence to Jaeyun Sung, PhD, 200 1st Street SW, Rochester, MN 55905. Email: Sung.Jaeyun@mayo.edu.

Submitted for publication January 5, 2022; accepted in revised form March 8, 2022.

Previously, Quimson et al investigated the histopathologic and radiologic differences between inflammatory and noninflammatory aortic aneurysms in patients who underwent open aortic aneurysm repair (2). Their study uncovered 5 factors (i.e., age at the time of surgery, sex, absence of coronary artery disease, diameter of the aneurysms, arterial wall thickening) that were associated with aortitis. Moreover, the investigators found that, among patients who underwent open surgical repair of aortic aneurysms (inflammatory or noninflammatory), elderly women with no history of coronary artery disease and aortic wall thickening were more likely to have histologic evidence of aortitis.

Despite the significance of previous observations by others, our understanding of aortitis can be advanced further by identifying disease-associated biomolecular processes using high-throughput technologies. To this point, genome-wide expression analyses with RNA sequencing (RNA-seq)—which have yet to be performed in aortitis—provide a promising avenue for subsequent studies (5).

In this study, we performed, for the first time, global transcriptomic profiling using RNA-seq on surgically resected inflammatory and noninflammatory aortic aneurysms in order to reveal differences in their tissue gene expression. Our approach demonstrates the utility of bulk transcriptomic sequencing for the discovery of not only signature genes and cellular functions of aortitis, but also potentially novel therapeutic targets.

PATIENTS AND METHODS

Subject and aortic specimen identification. Subjects in whom thoracic aortic replacement was performed between January 1, 2012 and December 31, 2019 were identified retrospectively through the use of current procedural terminology (CPT) coding. All aortic specimens had been previously reviewed by a vascular histopathologist. Inclusion criteria for aortitis samples was a description of “active giant cell aortitis” in the resected ascending aortic tissue. Charts were manually reviewed, and patients with features suggestive of localized or systemic infection were excluded. Age- and sex-matched comparators were identified among patients with noninflammatory aortic aneurysm resection during the same study period. Clinical parameters, including erythrocyte sedimentation rate, C-reactive protein, historical use of glucocorticoids, glucocorticoid dose at time of surgery, presence of systemic symptoms, history of other rheumatic diseases, smoking history, and use of aspirin, statin and angiotensin-converting enzyme (ACE)/angiotensin II receptor blocker (ARB) medications, were abstracted for both inflammatory aortic aneurysm (aortitis) and noninflammatory aortic aneurysm comparators. The clinical and demographic characteristics of the study participants are summarized in Table 1.

This study was approved by the Mayo Clinic Institutional Review Board (no. 17-010612MJJK) in accordance with the Declaration of Helsinki. All methods and procedures were performed

Table 1. Clinical and demographic characteristics of the study participants*

	Inflammatory aortic aneurysms (n = 25)	Noninflammatory aortic aneurysms (n = 25)
Female sex	15 (60)	17 (68)
Age, years		
Median (IQR)	75.9 (70.5–78.0)	72.1 (69.4–76.1)
Range	61.1–84.3	54.5–83.5
ESR, mm/hour		
Median (IQR)	6.0 (4.3–16.5)	12.5 (7.8–25.3)
Range	0–25	2–43
N/A (no.)	11	15
CRP, mg/liter		
Median (IQR)	4.25 (3.0–5.7)	2.9 (2.8–3.7)
Range	2.90–14.1	2.0–64.1
N/A (no.)	11	17
Treatment		
Prednisone	1 (4)	0 (0)
Aspirin	15 (60)	12 (48)
Statin	9 (36)	15 (60)
ACE/ARB	11 (44)	18 (72)
Smoking history		
Current	6 (24)	3 (12)
Former	9 (36)	8 (32)
Never	10 (40)	14 (56)
History of other rheumatic diseases		
PMR	5 (20)	0 (0)
GCA	2 (8)	0 (0)
GCA with PMR	1 (4)	0 (0)
Other (iritis, psoriasis, gout)	0 (0)	3 (12)
None	17 (68)	22 (88)

* Except where indicated otherwise, values are the number (%) of subjects. IQR = interquartile range; ESR = erythrocyte sedimentation rate; N/A = not assessed; CRP = C-reactive protein; ACE = angiotensin-converting enzyme; ARB = angiotensin II receptor blocker; PMR = polymyalgia rheumatica; GCA = giant cell arteritis.

in accordance with the Mayo Clinic Institutional Review Board guidelines and regulations.

Formalin-fixed paraffin-embedded (FFPE) block sectioning and aortic tissue preparation.

FFPE blocks containing ascending aortic aneurysm tissues were cut into 10- μ m thick sections. Prior to cutting, the microtomes and workstations were cleaned to prevent DNase and RNase contamination. New blades were used between blocks. The flotation bath contained Milli-Q water (DNase- and RNase-free) and was cleaned between blocks. CitriSolv was used to remove paraffin. Tissues were then washed with absolute ethanol and dried with a heat block at 37°C.

RNA purification, library preparation, and sequencing.

Once dry, the tissues were added with buffer PKD and proteinase K, and placed in a QIAcube for the RNA purification (extraction). On the instrument, the wash buffers used were red blood cell, RPE, and ethanol. RNA was then eluted in

RNAse-free water. The quality control of the total RNA was performed by the Qubit and Agilent 2100 Bioanalyzer. DV200 values (the percentage of RNA fragments >200 nucleotides) were determined by 2100 expert software. Samples with DV200 values above 30% were used for library preparation. Libraries were prepared using a TruSeq RNA Exome Capture kit (Illumina) following the manufacturer's protocol with minor modifications. Briefly, 500 ng of FFPE RNA was used for synthesizing the first-strand complementary DNA (cDNA) at 42°C, and the second-strand cDNA was generated at 16°C for 1 hour with a second-strand marking buffer. Double-stranded cDNA was A-tailed, ligated with index adapters, and amplified over 15 cycles. The cDNA library was quantified using Qbit (ThermoFisher Scientific) and Agilent TapeStation D1000, and 200 ng of each library was pooled for exome enrichment and capture. The pooled library was amplified over 10 cycles after finishing the second enrichment. The final libraries were quantified using an Agilent TapeStation D1000 and Qubit double-stranded DNA broad range assay kit. Finally, the 101-bp, paired-end reads were sequenced on an Illumina HiSeq4000 platform. Importantly, samples of inflammatory and noninflammatory aortic aneurysms were not sequenced separately, thus negating the need for batch correction protocols.

Pre-processing and aligning RNA-seq data. FASTQC was used to estimate the quality of the generated paired-end reads (.fastq files). No files were reported to have a flag of poor sequence quality. Paired-end raw reads were trimmed by trimomatic (version 0.38) (6) with the following parameter: ILLUMINA-CLIP:TruSeq3-PE:2:30:10. Next, STAR (version 2.5.4b) (7) was used to align the trimmed paired-end reads on the human reference genome (hg38). RSEM (version 1.3.1; -star-sjdboverhang 100) (8) was used to calculate transcripts per million (TPM) from the .bam files generated by STAR. Gene annotations for hg38 were retrieved from the UCSC Genome Browser.

Investigation of global transcriptome variance. Transcriptomes composed of \log_2 -transformed TPM (with a pseudocount addition of 0.001) values of 26,475 genes from 50 samples (25 with inflammatory aortic aneurysms and 25 with noninflammatory aortic aneurysms) were projected onto a principal component analysis (PCA) ordination plot. Agglomerative hierarchical clustering (Euclidean distance, complete-linkage) was performed on the gene expression profiles ($n = 50$) to observe clusters associated with clinical and demographic characteristics (i.e., inflammatory status of aortitis, ACE/ARB use, aspirin use, sex, history of other rheumatic diseases, smoking history, and statin use).

Identification of clinical covariates. A logistic linear regression model was used to identify clinical covariates associated with inflammatory and noninflammatory aortic aneurysms. The inflammatory status (inflammatory or noninflammatory) was

used as the response variable, while the predictors (i.e., sex, smoking history, age, aspirin use, statin use, ACE/ARB use, history of other rheumatic diseases) were individually assessed. P values were retrieved for the corresponding regression coefficient of the predictor variables. Predictors with P values less than 0.1 were considered as potential confounders and were adjusted for during the identification of differentially expressed genes (DEGs).

Identification of DEGs. DESeq2 (version 1.26.0) (9) was used to identify DEGs between patient groups with inflammatory aortic aneurysms ($n = 25$) and noninflammatory aortic aneurysms ($n = 25$), those with aortitis with GCA/polymyalgia rheumatica (PMR) (documented diagnosis or clinical features compatible with GCA and/or PMR, $n = 8$), and those with CIA (inflammatory aortitis without diagnosis of, or clinical features compatible with, either GCA or PMR, $n = 17$). Of note, statin use, ACE/ARB use, and history of other rheumatic diseases were considered as potential confounders ($P < 0.1$, coefficient of the logistic regression model) and were adjusted for during the identification of up-regulated DEGs ($\log_2[\text{fold change}] > 2$; Benjamini-Hochberg-adjusted $P < 0.01$) and down-regulated DEGs ($\log_2[\text{fold change}] < -2$; Benjamini-Hochberg-adjusted $P < 0.01$). All DEG analysis results are summarized in Supplementary Table 1, available on the *Arthritis & Rheumatology* website at <https://onlinelibrary.wiley.com/doi/10.1002/art.42138>.

Functional annotation and gene set enrichment analysis. The up-regulated and down-regulated DEGs were analyzed using PANTHER (version 16.0) (10) for functional annotations and DAVID (version 6.8) (11) for gene set enrichment analysis. PANTHER was used to obtain the gene protein class and biological pathway annotation, and DAVID was used to obtain statistically enriched Gene Ontology (GO) terms (12) from the following categories: Biological Process (GOTERM_BP_FAT), Cellular Component (GOTERM_CC_FAT), and Molecular Function (GOTERM_MF_FAT). GO terms with Expression Analysis Systematic Explorer scores (i.e., a P value from a modified Fisher's exact test [11]) less than 0.05 were considered to be statistically enriched.

Construction of the pharmacogenomic network. A pharmacogenomic network was constructed with human protein-protein interaction (PPI) information from the STRING database (version 11) (13) and drug-gene interaction information from the Drug Gene Interaction Database (version 4.0) (14). First, a DEG-specific interactome was constructed by mapping the aforementioned up-regulated and down-regulated DEGs to the "high-confidence" (combined score >0.7 in STRING) PPI network. From this high-confidence PPI network, the following nodes and edges were discarded during network construction: nodes (genes and proteins were considered as equals) that were

not mapped by DEGs, and edges (interaction between 2 different nodes) that do not connect 2 different DEGs. As a result, an interactome comprising 71 nodes (DEGs) and 122 edges was constructed (Supplementary Figure 1, available on the *Arthritis & Rheumatology* website at <https://onlinelibrary.wiley.com/doi/10.1002/art.42138>). From this, the largest connected component (LCC) of the interactome was identified, leaving 36 nodes and 92 edges. Finally, the Drug Gene Interaction Database was used to create a pharmacogenomic network by linking US Food and Drug Administration (FDA)-approved drugs that are known to target (directly or indirectly) any of the corresponding nodes of the LCC.

Data availability. Source codes and data sets that were used in this study are available at: https://github.com/jaeyunsung/Aortitis_2022.

RESULTS

Genome-wide expression profiles of inflammatory and noninflammatory aortic aneurysms. Figure 1A illustrates our analysis strategy to identify differential gene expression

signatures between inflammatory and noninflammatory aortic aneurysms from 50 surgically resected aortic tissue samples. We first investigated whether the clinical characteristics (i.e., disease condition, ACE/ARB use, aspirin use, statin use, sex, history of other rheumatic diseases, smoking history) cluster according to the gene expression profiles acquired from the FFPE tissues. Using PCA (Figure 1B) and hierarchical clustering (Figure 1C), we observed that gene expression profiles of 26,475 genes were the most distinguishable based upon disease condition (inflammatory or noninflammatory aortic aneurysm) compared to other clinical characteristics.

Next, we examined whether there were any statistical associations between disease condition and other clinical characteristics to identify potential confounders in our study. Using logistic regression, we identified ACE/ARB use ($P = 0.048$), statin use ($P = 0.093$), and the history of other rheumatic diseases ($P = 0.099$) as being associated with disease condition. Henceforth, these clinical characteristics were considered as confounding variables while investigating the relationship between inflammatory/noninflammatory aortic aneurysm and global gene expression. In contrast, aspirin use ($P = 0.396$), sex ($P = 0.556$), and smoking history ($P = 0.260$) were considered not to be associated with disease condition.

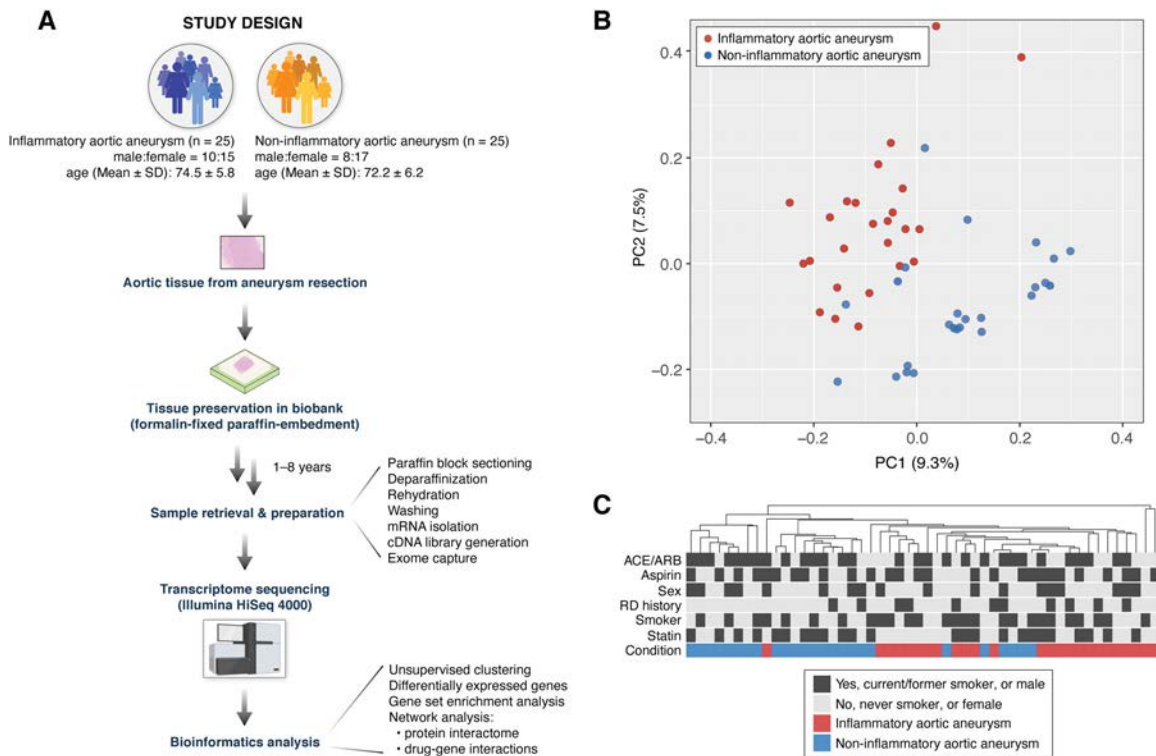


Figure 1. Data analysis pipeline and unsupervised clustering results on genome-wide expression (transcriptome) profiles of inflammatory and noninflammatory aortic aneurysms. **A**, Study design to investigate transcriptomic differences between inflammatory and noninflammatory aortic aneurysms. **B**, Principal components analysis (PCA) of gene expression profiles (26,475 total genes) from 50 surgically resected ascending aortic tissue samples across 2 patient groups (inflammatory aortic aneurysm, n = 25; noninflammatory aneurysm, n = 25). **C**, Hierarchical clustering on all 50 gene expression profiles, showing samples clustering together by disease condition (inflammatory/noninflammatory aortic aneurysms) more than by any other clinical characteristic (i.e., angiotensin-converting enzyme [ACE]/angiotensin II receptor blocker [ARB] use, aspirin use, sex, history of rheumatic disease [RD], smoking history, and statin use). Heatmap of gene expression profiles is not shown due to space constraints.

Identification of DEGs between inflammatory and noninflammatory aortic aneurysms.

We found transcriptomic differences between inflammatory and noninflammatory aortic aneurysms while adjusting for the aforementioned clinical covariates. From 26,475 total genes, we identified 159 up-regulated genes in inflammatory aortic aneurysms, including *CXCL9*, *TEX28*, *CLEC5A*, and *OR8B2*, and 93 down-regulated genes, including *PLD5*, *SFRP1*, *CARTPT*, and *FAR2P1* (Figure 2A). Among the 159 up-regulated genes, 99 mapped onto PANTHER protein classes, including “metabolite interconversion enzyme” (24 of 99 [24.2%]), “defense/immunity protein” (13 of 99 [13.1%]), and “intercellular signal molecule” (12 of 99 [12.1%]) (Figure 2B). Additionally, 29 up-regulated genes mapped onto PANTHER biological pathways, of which “inflammation mediated by chemokine and cytokine signaling pathway” (6 of 29 [20.7%]) was the most abundant annotation (Figure 2C). Alternatively, among the 93 down-regulated genes, 50 genes mapped onto PANTHER protein classes, including “transporter” (13 of 50 [26%]), “transmembrane signal receptor” (7 of 50 [14%]), and “cell adhesion molecule” (5 of 50 [10%]) (Figure 2D). Finally, 56 of the down-regulated genes mapped onto PANTHER biological pathways, of which “Wnt signaling pathway” (6 of 56 [10.7%]) was the most abundant (Figure 2E). *P* values and fold change for all genes are listed in Supplementary Table 1. Full details of our functional classification results are summarized in Supplementary Tables 2–5, available on the *Arthritis & Rheumatology* website at <https://onlinelibrary.wiley.com/doi/10.1002/art.42138>.

No significant differences in tissue gene expression displayed between GCA/PMR and CIA.

GCA is typically associated with various clinical presentations, such as headache, temporal artery abnormalities, elevated markers of inflammation, and PMR (4,15). Meanwhile, patients with CIA are generally asymptomatic, and aortitis is often incidentally identified within histopathology (16). Interestingly, however, inflammatory aortic aneurysms of GCA and CIA are radiographically and histopathologically indistinguishable. Moreover, it remains unclear whether CIA is truly isolated to the aorta or represents a subclinical systemic vasculitis. As there has not been any investigation into the gene expression differences between GCA and CIA, we sought to compare transcriptomes of aortic tissue resections between these 2 clinical phenotypes. Strikingly, there were no significant differences in gene expression profiles between GCA/PMR and CIA (Benjamini-Hochberg-adjusted $P < 0.1$) (Supplementary Table 6, available on the *Arthritis & Rheumatology* website at <https://onlinelibrary.wiley.com/doi/10.1002/art.42138>), indicating that CIA may be pathophysiologically closely related to GCA.

Functional enrichment of DEGs between inflammatory and noninflammatory aortic aneurysms.

Having identified DEGs and their protein class and biological pathway annotations, we next investigated whether the up- and down-regulated genes display statistically significant enrichment in GO terms. Among the 159 up-regulated genes, we identified 228 enriched GO terms (Supplementary Table 7, available on the *Arthritis & Rheumatology* website at <https://onlinelibrary.wiley.com/doi/10.1002/art.42138>).

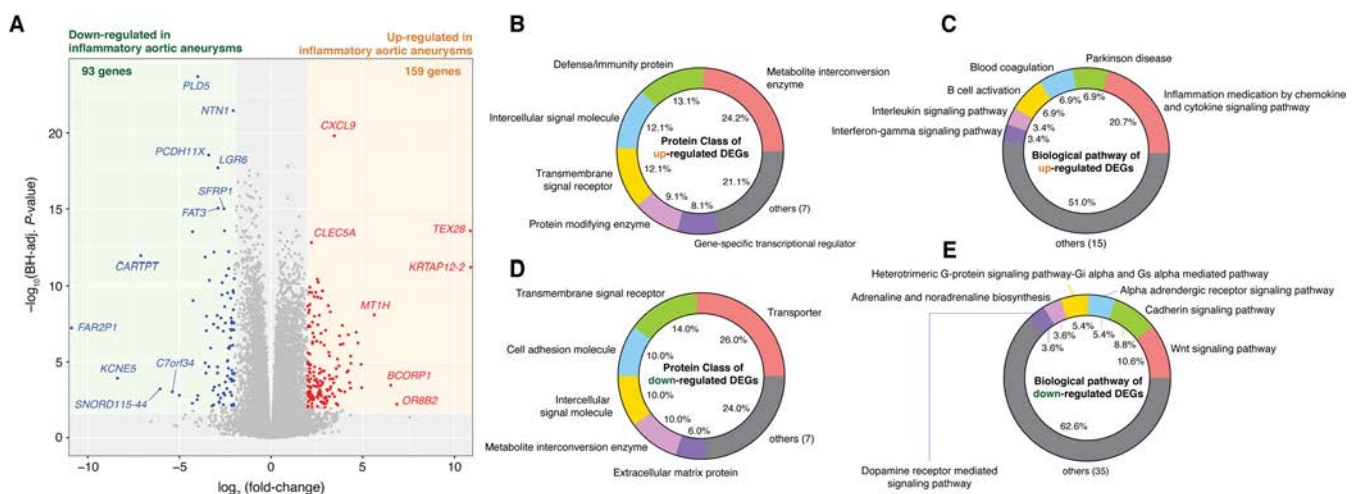


Figure 2. Differentially expressed genes (DEGs) and their functional categories revealed transcriptomic signatures of inflammatory aortic aneurysms. **A**, Identification of 159 and 93 genes significantly up-regulated and down-regulated, respectively, in inflammatory aortic aneurysms (Benjamini-Hochberg (BH)-adjusted $P < 0.01$, and \log_2 [fold change in mean expression values] > 2). **B** and **C**, Protein classes (**B**) and biological pathways (**C**) of the up-regulated DEGs. **D** and **E**, Protein classes (**D**) and biological pathways (**E**) of the down-regulated DEGs. DEGs and fold changes in gene expression were calculated using DESeq2 (version 1.30.0), while controlling for angiotensin-converting enzyme/angiotensin II receptor blocker use, statin use, and history of other rheumatic disease. Functional classification of protein class and biological pathways was performed using the PANTHER database (version 16.0).

wiley.com/doi/10.1002/art.42138), the top 10 of which were all associated with immune response (Figure 3A), as can be expected given the nature of the disease being studied. Interestingly, several GO terms were of the response to microbial agents (e.g., “cellular response to interferon-gamma,” “response to molecule of bacterial origin,” and “defense response to bacterium”) (Supplementary Table 7).

The top 10 GO terms shared a considerable number of genes which could be driving the robust immune signature (Figure 3B). In particular, we identified 19 genes common to the top 3 GO terms (i.e., “immune response,” “defense response,” “inflammatory response”) enriched in the up-regulated DEGs (Supplementary Figures 2A–C, available on the *Arthritis & Rheumatology* website at <https://onlinelibrary.wiley.com/doi/10.1002/art.42138>). Several of these genes were previously reported to be associated with autoimmune or inflammatory diseases. One example is *IL23R*, which encodes for the receptor of a key proinflammatory cytokine (interleukin-23 [IL-23]) that stimulates the proliferation of Th17 cells in inflammatory diseases (17). *IL23R* is located upstream of the JAK/STAT signaling pathway, which has been implicated in the pathogenesis of several inflammatory and autoimmune diseases, such as rheumatoid arthritis, inflammatory bowel disease, and psoriasis (15).

Similarly, we identified an up-regulation of *IL1A*, which encodes for a proinflammatory cytokine (IL-1 α) that can cause severe acute or chronic inflammation when dysregulated (18). The role of *IL1A* in human inflammatory aortic aneurysms is not fully understood; however, it has been shown in a mouse model that *Il1a* deficiency can be protective against the formation of Kawasaki disease-associated abdominal aortic aneurysm (19). In addition, we identified an up-regulation of *CCR6*, which encodes for a receptor that can mediate the recruitment of immature/mature dendritic cells and other antigen-presenting cells (20). Immune cells that express *CCR6* (such as CCR6+ T cells) have been reported to populate the wall infiltrate in GCA patients and can cause injury to vascular smooth muscle cells (21).

Meanwhile, from the 93 genes down-regulated in inflammatory aortic aneurysm, we identified 206 enriched GO terms (Supplementary Table 8, available on the *Arthritis & Rheumatology* website at <https://onlinelibrary.wiley.com/doi/10.1002/art.42138>). The top 10 of these were mostly associated with neuronal activities (Figure 3C and Supplementary Figures 2D–F), which may possibly reflect an elevated presence of damaged neurons in the aorta resulting from sustained levels of inflammation. Notably, we observed that these top GO terms shared far fewer genes among each other than the top GO terms enriched in the

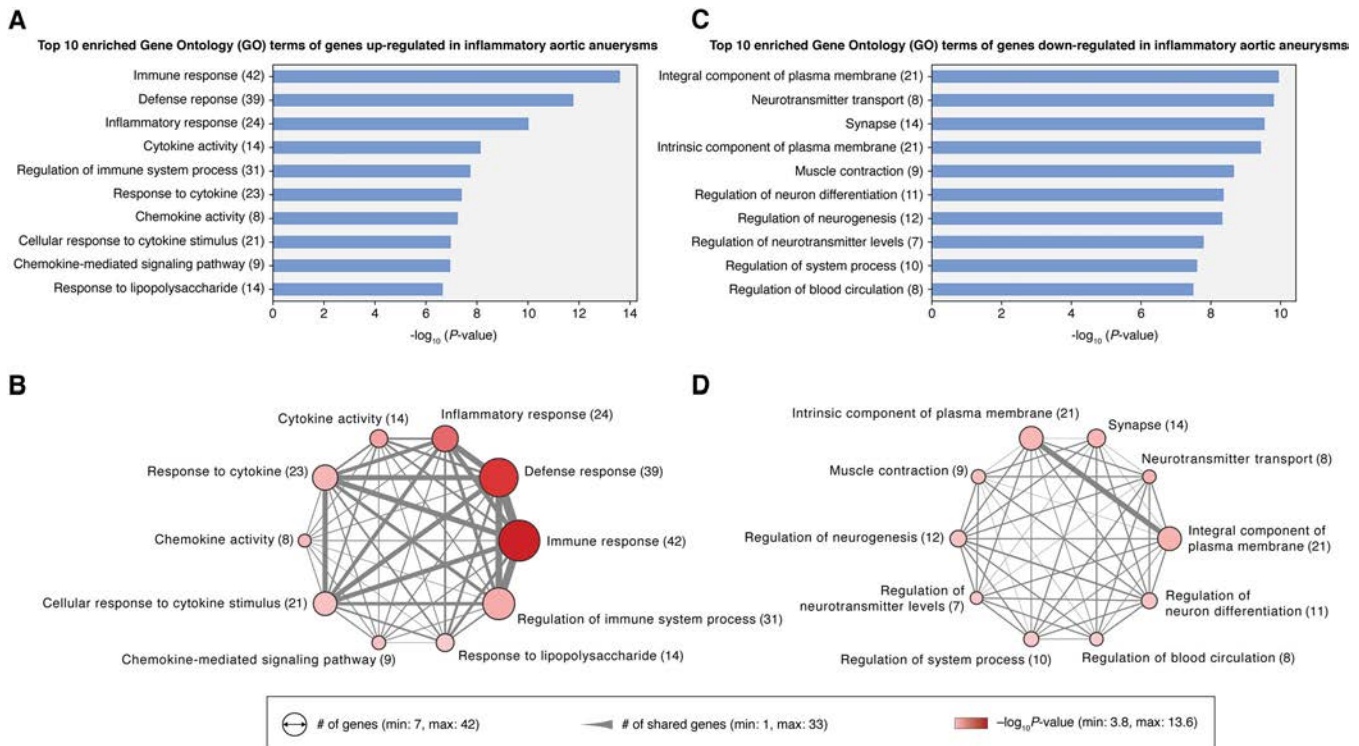


Figure 3. Gene Ontology (GO) enrichment analysis revealed strong up-regulation of immune response and down-regulation of neuronal activity in inflammatory aortic aneurysms. **A** and **B**, Top 10 enriched GO terms of the up-regulated DEGs (n = 159) (**A**) and a network of their gene set similarities (**B**). **C** and **D**, Top 10 enriched GO terms of the down-regulated DEGs (n = 93) (**C**) and a network of their gene set similarities (**D**). The size of nodes in the network corresponds to the number of genes of each GO term. The width of the edge represents the number of genes common to both GO terms. Colors of nodes (pink to red) signify the statistical significance of GO enrichment. Gene set enrichment analysis of GO terms was performed in DAVID (version 6.8).

up-regulated genes (Figure 3D). Moreover, we only identified 1 common gene (*ATP1A2*) across the top 3 GO terms (i.e., “integral component of plasma membrane,” “neurotransmitter transport,” “synapse”), which encodes an $\alpha 2$ -subunit of the sodium/potassium pump primarily found in glial cells (22). To date, the role of *ATP1A2* in inflammatory diseases remains unclear, although it has been suspected that this gene may be involved in neuroinflammatory processes (23).

Differential expression of genes targeted by aortitis treatment drugs. We next investigated known drug targets (i.e., genes) in aortitis. Specifically, we focused on the expression of genes known to be targeted by JAK inhibitors, IL-6 inhibitors, Th1/Th17 inhibitors, prednisone, and methotrexate (Figure 4). Of note, none of these drugs except for prednisone ($n = 1$) were administered to our study population.

Baricitinib, tofacitinib, and ruxolitinib are JAK inhibitors that can target members of the JAK/STAT signaling pathway. Drugs that inhibit the JAK/STAT signaling pathway can potentially suppress vascular inflammation by reducing the activity of vascular dendritic cells and T cells (15,24–26). Interestingly, we identified *JAK1* and *JAK3* to be up-regulated in inflammatory aortic aneurysms, which further supports the utility of JAK inhibitors for the treatment of aortitis. However, *JAK2* was not identified to have differential expression between inflammatory and noninflammatory aortic aneurysms.

The IL-6 inhibitors sirukumab and tocilizumab target the proinflammatory cytokine IL-6 and its receptor (IL-6R), respectively. This blocks the binding of IL-6 to IL-6R and thereby reduces the recruitment of new macrophages (27). The up-regulation of *IL6R* found in our study supports the use of tocilizumab for aortitis treatment (27). On the other hand, we did not identify differences in the expression of *IL6* in resected tissues between inflammatory and noninflammatory aortic aneurysms.

Ustekinumab and abatacept are Th1/Th17 inhibitors that suppress the activation of T cells by blocking proinflammatory cytokines (i.e., IL-12, IL-23) and Th1/Th17 membrane receptors (CD80, CD86). Our study identified genes that encode for the targets of abatacept (*CD80* and *CD86*) to be up-regulated in inflammatory aortic aneurysms. This finding is consistent with the use of abatacept to reduce the activity of T cells by interrupting the communication between Th1/Th17 and antigen-presenting cells in aortitis (28). Likewise, among the proinflammatory cytokines targeted by ustekinumab, *IL23A* was found to be up-regulated in inflammatory aortic aneurysms. Ustekinumab has been evaluated in patients with GCA and appears to be of limited benefit (29).

Last, the known gene targets of prednisone and methotrexate were not found to be differentially expressed in inflammatory aortic aneurysms. This result may help to confirm the relatively limited efficacy of these two drugs reported for aortitis (30,31).

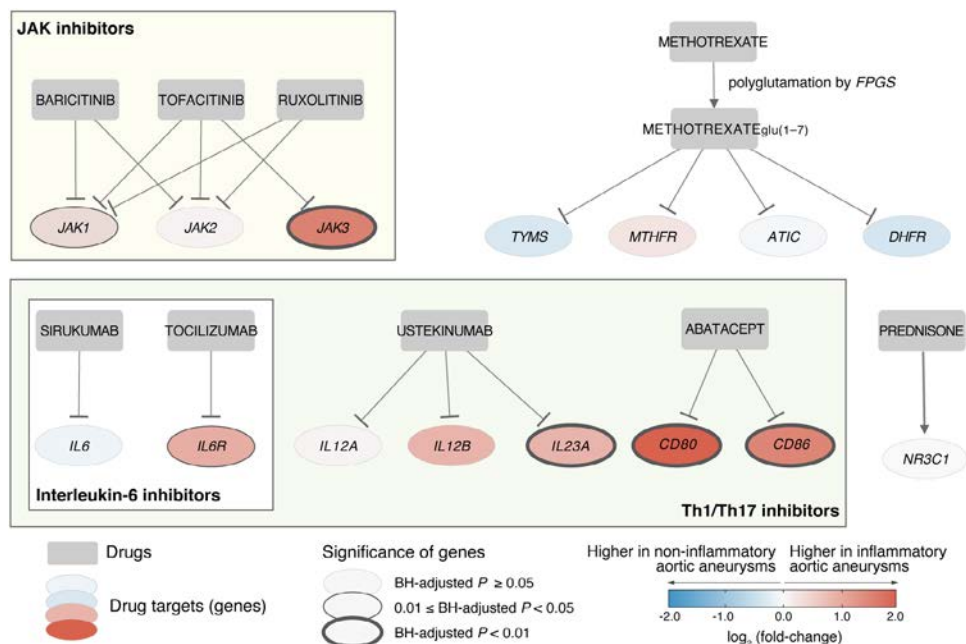


Figure 4. Transcriptomics analysis confirmed higher expression of a subset of known target genes in aortitis. Among the known targets of aortitis immunosuppressive drugs (e.g., JAK inhibitors, interleukin-6 inhibitors, Th1/Th17 inhibitors, prednisone, and methotrexate), 6 genes (*JAK1*, *JAK3*, *IL6R*, *IL23A*, *CD80*, and *CD86*) were found to display differential expression between inflammatory and noninflammatory aortic aneurysms. Square and circle nodes indicate drug names and gene symbols, respectively. Interactions (edges) with a hammerhead indicate inhibition. The color (blue to red) of each node represents gene expression fold change between inflammatory and noninflammatory aortic aneurysms. BH = Benjamini-Hochberg.

Identification of potential drug targets through pharmacogenomic network analysis.

Global transcriptomic profiling has been well demonstrated for drug target discovery (32), and several studies have coupled gene expression profiles with various systematic approaches for drug repurposing or biomarker discovery (32,33). Among various strategies for novel drug target identification, the network-based framework uses curated network topology (e.g., PPI network, metabolic network) to investigate the association across genes (or their products), diseases, and drugs (34). In this sense, we constructed a pharmacogenomic network composed of 36 genes and 92 interactions (representing the LCC; see Supplementary Figure 1, available on the *Arthritis & Rheumatology* website at <https://onlinelibrary.wiley.com/doi/10.1002/art.42138>, for the full interactome network) by integrating

DEGs, a high-confidence PPI network, and drug–gene interactions. Our pharmacogenomic network identified 10 potentially new druggable gene targets in aortitis: *BLK*, *CNR2*, *CR2*, *GZMB*, *IDO1*, *IFNG*, *IL1A*, *CXCL10*, *CXCL13*, and *S1PR5* (Figure 5).

Near the hub of the pharmacogenomic network, we identified up-regulated genes for cytokines (*IL1A*, *IFNG*) and chemokines (*CXCL5*, *CXCL9*, *CXCL10*, *CXCL11*, *CXCL13*, *CCL1*, *CCL7*, *CCL20*) that can be targeted by drugs already known for the treatment of aortitis or other inflammatory diseases. For example, our results suggest that drugs targeting *IFNG* (e.g., methylprednisolone, prednisone, cisplatin) and *CXCL10* (e.g., atropine, zidovudine, atorvastatin) can be potentially used for the treatment of aortitis. Notably, interferon- γ (IFN γ) (product of *IFNG*), which is produced by effector Th1 cells, is considered

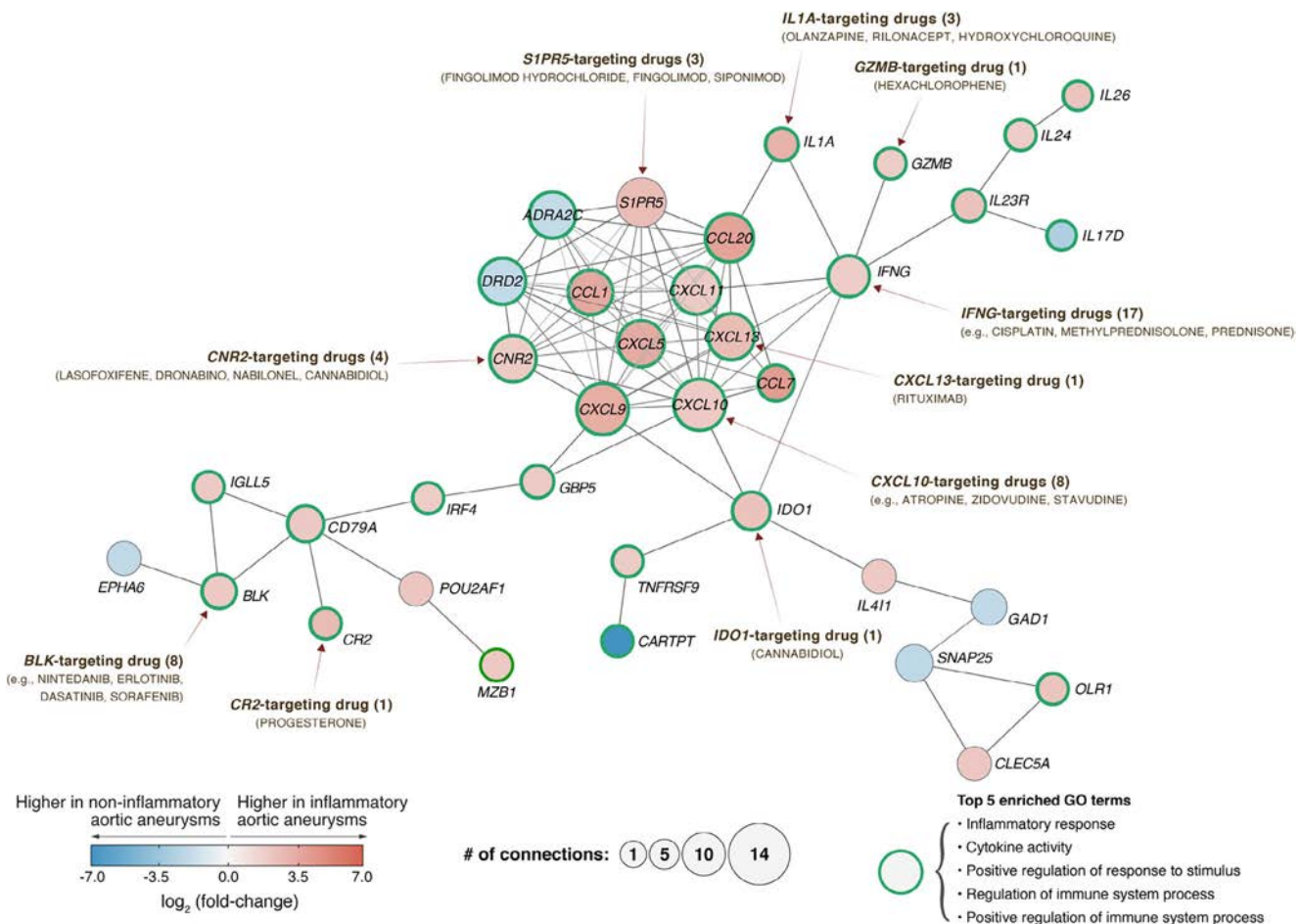


Figure 5. Pharmacogenomic network analysis uncovered the drug–gene interaction landscape in inflammatory aortic aneurysms. The largest connected component in the differentially expressed gene–based protein–protein interaction network is composed of 36 genes (nodes) and 92 interactions (edges). Using pharmacologic information, 10 of the 36 genes were identified as “druggable” (both directly and indirectly) with US Food and Drug Administration–approved pharmaceutical drugs. In the pharmacogenomic network, 29 of the 36 genes are related to the top 5 enriched Gene Ontology (GO) terms. Nodes with green borders represent genes that are related to the top 5 GO terms: “inflammatory response,” “cytokine activity,” “positive regulation of response to stimulus,” “regulation of immune system process,” and “positive regulation of immune system process.” The color (blue to red) of each node represents gene expression differences between inflammatory and noninflammatory aortic aneurysms. The size of each node represents its degree, i.e., number of connections to other nodes. GO enrichment analysis was performed on 36 genes using DAVID (version 6.8). Information on drug target genes was obtained from the Drug Gene Interaction Database (version 4.0).

as one of the key cytokines involved in the pathogenesis of GCA (35). In addition, *CXCL10*, which is an IFN-stimulated gene that responds to different types of IFNs (i.e., IFN α , IFN β , IFN γ , IFN λ), encodes a chemokine that promotes the recruitment of CD8+ and Th1 cells (36).

Of note, Corbera-Bellalta et al performed an ex vivo experiment in cultured GCA arteries showing reduced expression of *CXCL9*, *CXCL10*, and *CXCL11* by blocking endogenous IFN γ with A6-abrogated STAT1 phosphorylation (35). Furthermore, *CXCL13*, which is a chemokine that attracts B cells and contributes to the production of antibodies (37), may be potentially targeted with rituximab in aortitis. Rituximab is an anti-CD20 monoclonal antibody designed to target the surface of B cells and block interactions with effector T cells (38); preliminary studies have demonstrated promising results for rituximab in GCA (39). In summary, our pharmacogenomic network analysis identified promising drug targets for potentially new treatment strategies in aortitis. We summarize all gene-gene and drug-gene interactions found within our pharmacogenomic network in Supplementary Table 9, available on the *Arthritis & Rheumatology* website at <https://onlinelibrary.wiley.com/doi/10.1002/art.42138>. In addition, a comprehensive summary of the enriched functions (GO terms) of all genes in the pharmacogenomic network is provided in Supplementary Table 10.

DISCUSSION

In this study, we performed a genome-wide expression analysis to identify signature genes and biomolecular processes underlying aortitis. First, we compared gene expression profiles between inflammatory and noninflammatory aortic aneurysms. Within inflammatory aortic aneurysms, we compared profiles between GCA/PMR and CIA. Notably, this study revealed for the first time that the transcriptomic signature of CIA is not different from that of aortitis related to GCA/PMR, suggesting that these 2 disease states largely share common pathophysiologic mechanisms. Next, we investigated the functional annotations (i.e., protein class, biological pathway) and enriched GO terms of the DEGs. We found that the up-regulated genes were generally enriched in immune processes, and in particular those in response to microbial agents. In contrast, the down-regulated genes were enriched in neuronal processes. Finally, a pharmacogenomic network-based approach revealed a range of potentially new drug targets (genes) and therapeutics for the multimodal treatment of aortitis. The findings described herein motivate future research using multiomics data or peripheral blood to investigate the broad landscape of biomolecular pathways and networks in aortitis, as well as advancing biomarker discovery (40), as we have demonstrated in another autoimmune disease (41,42).

Interestingly, a subset of the DEGs (Benjamini-Hochberg-adjusted $P < 0.05$) were associated with receptors for

pathogen-associated molecular patterns. It is yet unclear whether infectious agents play a causal role in blood vessel inflammation, and there has been no compelling evidence showing that abating aortitis symptoms are linked to the clearance of infections (43). Nevertheless, our study identified up-regulation of the following: viral single-stranded RNA-specific endosomal pattern recognition receptors (*TLR7*, *TLR8*); other Toll-like receptors (*TLR1*, *TLR2*, *TLR4*, *TLR5*, *TLR6*, *TLR7*, *TLR8*) and nucleotide-binding oligomerization domain-like receptors (*NOD1*, *NOD2*, *NLRC4*); pattern recognition receptor pathways that stimulate type 1 IFN production (*MYD88*, *IRAK4*, *TRAF3*, *IKBKB*, *IRF5*); members of the IFN/JAK/STAT pathway (*IFNAR1*, *IFNAR2*, *IL10RB*, *IFNGR1*, *IFNGR2*, *JAK1*, *TYK2*, *STAT1*, *STAT2*, *IRF9*); IFN regulatory factors (*IRF1*, *IRF2*, *IRF4*, *IRF5*, *IRF8*, *IRF9*); mature dendritic cell markers (*CD80*, *CD83*, *CD86*); and cell surface markers of plasmacytoid dendritic cells (*CLEC4C*, *CCR7*, *LILRB4*, *NRP1*), which are a subtype of dendritic cells that specifically sense viral RNA and DNA (44).

By providing a system-wide view of mechanistic gene (protein) interactions, our pharmacogenomic network analysis can facilitate the design of novel pharmacologic intervention strategies. For example, our analysis identified *CD79A* (immunoglobulin-associated alpha), which encodes a component of B cell antigen receptors, as a putative target in aortitis treatment. The product of *CD79A* is a highly reliable marker for B cells that is present on the cell surface throughout their life cycle (45). Although the efficacy of targeting B cells in aortitis has yet to be clearly and convincingly demonstrated, the role of B cells in aortitis is gradually being revealed (15). For example, van der Geest et al reported changes in the distribution and homeostasis of B cells in GCA (46). Additionally, a B cell-activating factor in GCA patients was shown to directly correlate with disease activity (47). In consideration of these findings, we can hypothesize that B cell suppressors may be beneficial for aortitis patients.

During the preparation of this manuscript, a transcriptomics study in large-vessel GCA was published by Vieira et al (48). The investigators used microarray technology on aortic tissues from patients with GCA ($n = 10$) and controls ($n = 9$). Like our results above, up-regulated gene sets for pathways involving interferons, JAK/STAT signaling, and proinflammatory cytokines and chemokines in GCA (compared to controls) were found. The authors also identified higher expression of members of the JAK/STAT signaling pathway (e.g., *STAT1*, *STAT2*) and type I-specific IFN response genes (e.g., *EPST11*) in inflamed aortic aneurysms in GCA. Therefore, our study using high-resolution transcriptome profiling by RNA-seq demonstrated favorable reproducibility of previous findings by others and enabled novel insights including the discovery of other possible DEGs, the finding that GCA and CIA are not different at the gene expression level, and new (albeit putative) targets of current aortitis treatment drugs (e.g., JAK inhibitors, Th1/Th17 inhibitors) and FDA-approved off-label drugs.

We note a few limitations of this study. First, we acknowledge that 25 cases (inflammatory aortic aneurysms) and 25 controls (noninflammatory aortic aneurysms) are a relatively small number of samples. Nevertheless, we were still able to identify a large number of statistically significant genes even after multiple hypothesis correction; this indicates that despite the limited sample sizes, global gene expression differences between inflammatory and noninflammatory aortic aneurysms are sufficiently robust. Second, RNA-seq only allows us to observe the biomolecular processes within inflammatory aortic aneurysms at the gene expression level. Integrating our current findings with laboratory tests (e.g., real-time quantitative polymerase chain reaction, immunohistochemistry staining) or other omics data, such as metabolomics, proteomics, and single-cell RNA-seq or mass cytometry (CyTOF), in future studies can confirm our results or elucidate additional details of the inherent biological processes in aortitis.

Third, the current protein interactome network may not fully reflect the associations between the identified DEGs during the construction of the pharmacogenomic network. The stringent cutoff used to obtain the high-confidence network may lead to a loss in interactions between genes and therefore missed opportunities to identify additional potential targets of known drugs. Nevertheless, the constructed pharmacogenomic network still identified genes that can be targeted by drugs conventionally prescribed for aortitis (e.g., prednisone) or other inflammatory diseases (e.g., rituximab). Last, our study used only FFPE samples from tissue biopsies but did not investigate immune cells in circulation. Future immunophenotyping studies conducted with patient blood samples are needed to explore how the peripheral immune system is altered during disease onset and progression (49,50).

ACKNOWLEDGMENTS

First and foremost, we thank our dear patients who volunteered for this study. We also thank the Mayo Clinic Genome Analysis Core staff members for making this work possible.

AUTHOR CONTRIBUTIONS

All authors were involved in drafting the article or revising it critically for important intellectual content, and all authors approved the final version to be published. Dr. Sung had full access to all of the data in the study and takes responsibility for the integrity of the data and the accuracy of the data analysis.

Study conception and design. Warrington, Sung.

Acquisition of data. Koster, Jang, Warrington.


Analysis and interpretation of data. Hur, Koster, Jang, Weyand, Warrington, Sung.

REFERENCES

- Bossone E, Pluchinotta FR, Andreas M, Blanc P, Citro R, Limongelli G, et al. Aortitis. *Vascul Pharmacol* 2016;80:1–10.
- Quimson L, Mayer A, Capponi S, Rea B, Rhee RL. Comparison of aortitis versus noninflammatory aortic aneurysms among patients who undergo open aortic aneurysm repair. *Arthritis Rheumatol* 2020;72:1154–9.
- Ladich E, Yahagi K, Romero ME, Virmani R. Vascular diseases: aortitis, aortic aneurysms, and vascular calcification. *Cardiovasc Pathol* 2016;25:432–41.
- Gornik HL, Creager MA. Aortitis. *Circulation* 2008;117:3039–51.
- Byron SA, Van Keuren-Jensen KR, Engelthaler DM, Carpten JD, Craig DW. Translating RNA sequencing into clinical diagnostics: opportunities and challenges. *Nat Rev Genet* 2016;17:257–71.
- Bolger AM, Lohse M, Usadel B. Trimmomatic: a flexible trimmer for Illumina sequence data. *Bioinformatics* 2014;30:2114–20.
- Dobin A, Davis CA, Schlesinger F, Drenkow J, Zaleski C, Jha S, et al. STAR: ultrafast universal RNA-seq aligner. *Bioinformatics* 2013;29:15–21.
- Li B, Dewey CN. RSEM: accurate transcript quantification from RNA-Seq data with or without a reference genome. *BMC Bioinformatics* 2011;12:323.
- Love MI, Huber W, Anders S. Moderated estimation of fold change and dispersion for RNA-seq data with DESeq2. *Genome Biol* 2014;15:550.
- Mi H, Muruganujan A, Ebert D, Huang X, Thomas PD. PANTHER version 14: more genomes, a new PANTHER GO-slim and improvements in enrichment analysis tools. *Nucleic Acids Res* 2019;47:D419–26.
- Jiao X, Sherman BT, Huang DW, Stephens R, Baseler MW, Lane HC, et al. DAVID-WS: a stateful web service to facilitate gene/protein list analysis. *Bioinformatics* 2012;28:1805–6.
- Gene Ontology Consortium. The Gene Ontology resource: enriching a GOLD mine. *Nucleic Acids Res* 2021;49:D325–34.
- Szklarczyk D, Gable AL, Lyon D, Junge A, Wyder S, Huerta-Cepas J, et al. STRING v11: protein-protein association networks with increased coverage, supporting functional discovery in genome-wide experimental datasets. *Nucleic Acids Res* 2019;47:D607–13.
- Griffith M, Griffith OL, Coffman AC, Weible JV, McMichael JF, Spies NC, et al. DGI: mining the druggable genome. *Nat Methods* 2013;10:1209–10.
- Koster MJ, Warrington KJ. Giant cell arteritis: pathogenic mechanisms and new potential therapeutic targets. *BMC Rheumatol* 2017;1:2.
- Cinar I, Wang H, Stone JR. Clinically isolated aortitis: pitfalls, progress, and possibilities. *Cardiovasc Pathol* 2017;29:23–32.
- Duvallet E, Semerano L, Assier E, Falgarone G, Boissier MC. Interleukin-23: a key cytokine in inflammatory diseases. *Ann Med* 2011;43:503–11.
- Di Paolo NC, Shayakhmetov DM. Interleukin 1 α and the inflammatory process. *Nat Immunol* 2016;17:906–13.
- Wakita D, Kurashima Y, Crother TR, Rivas MN, Lee Y, Chen S, et al. Role of interleukin-1 signaling in a mouse model of Kawasaki disease-associated abdominal aortic aneurysm. *Arterioscler Thromb Vasc Biol* 2016;36:886–97.
- Ito T, Carson WF IV, Cavassani KA, Connett JM, Kunkel SL. CCR6 as a mediator of immunity in the lung and gut. *Exp Cell Res* 2011;317:613–9.
- Deng J, Ma-Krupa W, Gewirtz AT, Younge BR, Goronzy JJ, Weyand CM. Toll-like receptors 4 and 5 induce distinct types of vasculitis. *Circ Res* 2009;104:488–95.
- McGrail KM, Phillips JM, Sweadner KJ. Immunofluorescent localization of three Na,K-ATPase isozymes in the rat central nervous system: both neurons and glia can express more than one Na,K-ATPase. *J Neurosci* 1991;11:381–91.
- Kinoshita PF, Yshii LM, Orellana AM, Paixão AG, Vasconcelos AR, Lima LS, et al. Alpha 2 Na⁺,K⁺-ATPase silencing induces loss of

- inflammatory response and ouabain protection in glial cells. *Sci Rep* 2017;7:4894.
24. Sanchez GA, Reinhardt A, Ramsey S, Wittkowski H, Hashkes PJ, Berkun Y, et al. JAK1/2 inhibition with baricitinib in the treatment of autoinflammatory interferonopathies. *J Clin Invest* 2018;128:3041–52.
 25. Heine A, Held SA, Daেকে SN, Wallner S, Yajnanarayana SP, Kurts C, et al. The JAK-inhibitor ruxolitinib impairs dendritic cell function in vitro and in vivo. *Blood* 2013;122:1192–202.
 26. Zhang H, Watanabe R, Berry GJ, Tian L, Goronzy JJ, Weyand CM. Inhibition of JAK-STAT signaling suppresses pathogenic immune responses in medium and large vessel vasculitis. *Circulation* 2018;137:1934–48.
 27. Stone JH, Tuckwell K, Dimonaco S, Klearman M, Aringer M, Blockmans D, et al. Trial of tocilizumab in giant-cell arteritis. *N Engl J Med* 2017;377:317–28.
 28. Langford CA, Cuthbertson D, Ytterberg SR, Khalidi N, Monach PA, Currence S, et al. A randomized, double-blind trial of abatacept (CTLA-4Ig) for the treatment of giant cell arteritis. *Arthritis Rheumatol* 2017;69:837–45.
 29. Matza MA, Fernandes AD, Stone JH, Unizony SH. Ustekinumab for the treatment of giant cell arteritis. *Arthritis Care Res (Hoboken)* 2021;73:893–7.
 30. Hoffman GS, Cid MC, Hellmann DB, Guillemin L, Stone JH, Schousboe J, et al. A multicenter, randomized, double-blind, placebo-controlled trial of adjuvant methotrexate treatment for giant cell arteritis. *Arthritis Rheum* 2002;46:1309–18.
 31. Delecoeuillerie G, Joly P, de Lara AC, Paolaggi JB. Polymyalgia rheumatica and temporal arteritis: a retrospective analysis of prognostic features and different corticosteroid regimens (11 year survey of 210 patients). *Ann Rheum Dis* 1988;47:733–9.
 32. Yang X, Kui L, Tang M, Li D, Wei K, Chen W, et al. High-throughput transcriptome profiling in drug and biomarker discovery. *Front Genet* 2020;11:19.
 33. Feng Y, Wang Q, Wang T. Drug target protein-protein interaction networks: a systematic perspective. *Biomed Res Int* 2017;2017:1289259.
 34. Barabási AL, Gulbahce N, Loscalzo J. Network medicine: a network-based approach to human disease. *Nat Rev Genet* 2011;12:56–68.
 35. Corbera-Bellalta M, Planas-Rigol E, Lozano E, Terrades-García N, Alba MA, Prieto-González S, et al. Blocking interferon γ reduces expression of chemokines CXCL9, CXCL10 and CXCL11 and decreases macrophage infiltration in ex vivo cultured arteries from patients with giant cell arteritis. *Ann Rheum Dis* 2016;75:1177–86.
 36. Peperzak V, Veraar EA, Xiao Y, Babala N, Thiadens K, Brugmans M, et al. CD8+ T cells produce the chemokine CXCL10 in response to CD27/CD70 costimulation to promote generation of the CD8+ effector T cell pool. *J Immunol* 2013;191:3025–36.
 37. Legler DF, Loetscher M, Roos RS, Clark-Lewis I, Baggiolini M, Moser B. B cell-attracting chemokine 1, a human CXC chemokine expressed in lymphoid tissues, selectively attracts B lymphocytes via BLR1/CXCR5. *J Exp Med* 1998;187:655–60.
 38. Taylor RP, Lindorfer MA. Drug insight: the mechanism of action of rituximab in autoimmune disease—the immune complex decoy hypothesis. *Nat Clin Pract Rheumatol* 2007;3:86–95.
 39. Bhatia A, Eli PJ, Edwards JC. Anti-CD20 monoclonal antibody (rituximab) as an adjunct in the treatment of giant cell arteritis. *Ann Rheum Dis* 2005;64:1099–100.
 40. Sung J, Wang Y, Chandrasekaran S, Witten DM, Price ND. Molecular signatures from omics data: from chaos to consensus. *Biotechnol J* 2012;7:946–57.
 41. Hur B, Gupta VK, Huang H, Wright KA, Warrington KJ, Taneja V, et al. Plasma metabolomic profiling in patients with rheumatoid arthritis identifies biochemical features predictive of quantitative disease activity. *Arthritis Res Ther* 2021;23:164.
 42. Gupta VK, Cunningham KY, Hur B, Bakshi U, Huang H, Warrington KJ, et al. Gut microbial determinants of clinically important improvement in patients with rheumatoid arthritis. *Genome Med* 2021;13:149.
 43. Moiseev S, Novikov P, Smitienko I, Shchegoleva E. Giant cell arteritis, infections and biologics. *Ann Rheum Dis* 2017;76:e29.
 44. Li S, Wu J, Zhu S, Liu YJ, Chen J. Disease-associated plasmacytoid dendritic cells. *Front Immunol* 2017;8:1268.
 45. Li R, Wang T, Bird S, Zou J, Dooley H, Secombes CJ. B cell receptor accessory molecule CD79 α : Characterisation and expression analysis in a cartilaginous fish, the spiny dogfish (*Squalus acanthias*). *Fish Shellfish Immunol* 2013;34:1404–15.
 46. Van der Geest KS, Abdulahad WH, Chalan P, Rutgers A, Horst G, Huitema MG, et al. Disturbed B cell homeostasis in newly diagnosed giant cell arteritis and polymyalgia rheumatica. *Arthritis Rheumatol* 2014;66:1927–38.
 47. Van der Geest KS, Abdulahad WH, Rutgers A, Horst G, Bijzet J, Arends S, et al. Serum markers associated with disease activity in giant cell arteritis and polymyalgia rheumatica. *Rheumatology* 2015;54:1397–402.
 48. Vieira M, Régnier P, Maciejewski-Duval A, Le Joncour A, Darasse-Jèze G, Rosenzwaig M, et al. Interferon signature in giant cell arteritis aortitis. *J Autoimmun* 2022;127:102796.
 49. Lee JS, Park S, Jeong HW, Ahn JY, Choi SJ, Lee H, et al. Immunophenotyping of COVID-19 and influenza highlights the role of type I interferons in development of severe COVID-19. *Sci Immunol* 2020;5:eabd1554.
 50. Jang JS, Juran BD, Cunningham KY, Gupta VK, Son YM, Yang JD, et al. Single-cell mass cytometry on peripheral blood identifies immune cell subsets associated with primary biliary cholangitis. *Sci Rep* 2020;10:12584.

Driving Role of Interleukin-2–Related Regulatory CD4+ T Cell Deficiency in the Development of Lung Fibrosis and Vascular Remodeling in a Mouse Model of Systemic Sclerosis

Camelia Frantz,¹  Anne Cauvet,² Aurélie Durand,² Virginie Gonzalez,² Rémi Pierre,² Marcio Do Cruzeiro,² Karine Bailly,² Muriel Andrieu,² Cindy Orvain,² Jérôme Avouac,¹ Mina Ottaviani,³ Raphaël Thuillet,³ Ly Tu,³ Christophe Guignabert,³ Bruno Lucas,² Cédric Auffray,² and Yannick Allanore¹

Objective. Systemic sclerosis (SSc) is a debilitating autoimmune disease characterized by severe lung outcomes resulting in reduced life expectancy. Fra-2–transgenic mice offer the opportunity to decipher the relationships between the immune system and lung fibrosis. This study was undertaken to investigate whether the Fra-2–transgenic mouse lung phenotype may result from an imbalance between the effector and regulatory arms in the CD4+ T cell compartment.

Methods. We first used multicolor flow cytometry to extensively characterize homeostasis and the phenotype of peripheral CD4+ T cells from Fra-2–transgenic mice and control mice. We then tested different treatments for their effectiveness in restoring CD4+ Treg cell homeostasis, including adoptive transfer of Treg cells and treatment with low-dose interleukin-2 (IL-2).

Results. Fra-2–transgenic mice demonstrated a marked decrease in the proportion and absolute number of peripheral Treg cells that preceded accumulation of activated, T helper cell type 2–polarized, CD4+ T cells. This defect in Treg cell homeostasis was derived from a combination of mechanisms including impaired generation of these cells in both the thymus and the periphery. The impaired ability of peripheral conventional CD4+ T cells to produce IL-2 may greatly contribute to Treg cell deficiency in Fra-2–transgenic mice. Notably, adoptive transfer of Treg cells, low-dose IL-2 therapy, or combination therapy changed the phenotype of Fra-2–transgenic mice, resulting in a significant reduction in pulmonary parenchymal fibrosis and vascular remodeling in the lungs.

Conclusion. Immunotherapies for restoring Treg cell homeostasis could be relevant in SSc. An intervention based on low-dose IL-2 injections, as is already proposed in other autoimmune diseases, could be the most suitable treatment modality for restoring Treg cell homeostasis for future research.

INTRODUCTION

Systemic sclerosis (SSc) is a rare and incurable connective tissue disease characterized by microvascular injury, extensive immune abnormalities, and fibrosis of the skin and internal organs (1). SSc is recognized as the most life-threatening rheumatic disease, with pulmonary complications, including interstitial lung

disease and pulmonary hypertension (PH) remaining the greatest causes of mortality (2).

Several inducible and genetic SSc mouse models have been developed, but none of them fully encompass all the features of SSc (3). Fra-2–transgenic mice, which overexpress the activator protein 1 transcription factor Fra-2, encoded by *Fosl2*, develop spontaneous systemic inflammation and fibrosis preferentially

Supported by Société Française de Rhumatologie and Association des Sclérodermiques de France.

Drs. Lucas, Auffray, and Allanore contributed equally to this work.

¹Camelia Frantz, MD, PhD, Jérôme Avouac, MD, PhD, Yannick Allanore, MD, PhD: Université de Paris, Inserm U1016, CNRS UMR 8104, and Cochin Hospital, Paris, France; ²Anne Cauvet, Aurélie Durand, Virginie Gonzalez, Rémi Pierre, Marcio Do Cruzeiro, Karine Bailly, Muriel Andrieu, PhD, Cindy Orvain, PhD, Bruno Lucas, PhD, Cédric Auffray, PhD: Université de Paris, Inserm U1016, CNRS UMR 8104, Paris, France; ³Mina Ottaviani, Raphaël Thuillet, PhD, Ly Tu, PhD, Christophe Guignabert, PhD: INSERM UMR S 999, Hôpital Marie Lannelongue, and Université Paris-Saclay, Paris, France.

Author disclosures are available at <https://onlinelibrary.wiley.com/action/downloadSupplement?doi=10.1002%2Fart.42111&file=art42111-sup-0001-Disclosureform.pdf>.

Address correspondence to Cedric Auffray, PhD, Université Paris Cité, CNRS, INSERM, Cochin Institute, F-75014 Paris, France (email: cedric.auffray@inserm.fr); or to Yannick Allanore, MD, PhD, Service de Rhumatologie, Hôpital Cochin Université de Paris, 27 rue du Faubourg Saint-Jacques, 75014 Paris, France (email: yannick.allanore@inserm.fr).

Submitted for publication September 15, 2021; accepted in revised form March 3, 2022.

occurring in the lungs (4). This overexpression results in an increase in perivascular and peribronchial inflammation that leads to the development of fibrosis and premature death. Prior to the development of pulmonary fibrosis, vascular remodeling occurs in Fra-2-transgenic mice, accompanied by collagen deposition in the vessel wall and increased vessel muscularization leading to pulmonary hypertension (PH) (4). This genetic model is of paramount interest for sequential pathologic events mirroring human disease (5). Indeed, initial vascular injury and subsequent fibrosis of the skin, lung, and heart, are closely modeled.

Although SSc pathogenesis is complex and not fully understood (6), research has confirmed that immune dysfunction is one of the most important components (7). For instance, genetic studies identified haplotype-dependent HLA susceptibility to SSc, as well as non-HLA susceptibility genes related to immunity and inflammation (8). Furthermore, numerous studies have highlighted the detrimental role of the adaptive immune system in SSc onset (9,10). B lymphocytes and T lymphocytes may thus trigger complex biochemical and molecular changes that promote vessel remodeling and tissue fibrosis. In this aberrant immune response, T cells appear to be of particular importance, specifically Th2-polarized effector CD4+ T cells and the profibrotic mediators they release, i.e., interleukin-4 (IL-4), IL-5, and IL-13 (11,12).

Recently, Renoux et al found that Fra-2-transgenic mice develop a strong systemic inflammatory phenotype characterized by leukocyte infiltration of multiple organs and an accumulation of Th2-polarized CD4+ T cells (13). Interestingly, that study also showed that *Fos/2* may affect FoxP3 expression, therefore repressing CD4+ Treg cell development in the thymus and altering homeostasis in the periphery.

Treg cells are the main mediators of peripheral tolerance in physiologic settings (14). In the periphery, Treg cells include cells that have been naturally produced within the thymus (thymic Treg cells) (15) and cells with a similar phenotype and similar functions that are differentiated from naive CD4+ T cells following antigen recognition in secondary lymphoid organs (SLOs) (peripheral Treg cells) (16). All Treg cells express the transcription factor FoxP3 (17), have high surface levels of the α -chain of the IL-2 receptor (CD25), and mainly rely on IL-2 availability for both homeostasis and survival (18).

In the present study, we investigated whether pulmonary fibrosis and vascular remodeling, the main clinical features of SSc, that also develop in Fra-2-transgenic mice, may result from an imbalance between the Th2 effector cell compartment and Treg cell compartment. We first performed a detailed analysis of the homeostasis of peripheral CD4+ T cells in Fra-2-transgenic mice during the disease course. Then, based on our findings, we tested different treatments aimed at restoring Treg cell homeostasis and preventing related lung damage in this mouse model of SSc.

MATERIALS AND METHODS

Additional methods are available in Supplementary Methods (available on the *Arthritis & Rheumatology* website at <http://onlinelibrary.wiley.com/doi/10.1002/art.42111>).

Mice. Fra-2-transgenic, C57BL/6 CD3 $\epsilon^{-/-}$ mice, C57BL/6 CD45.1 mice, C57BL/6 FoxP3-green fluorescent protein (GFP) CD45.2 mice, and CD45.1/2 mice were housed in the Cochin Institute animal facilities under specific and opportunistic pathogen-free conditions. All animals were treated in accordance with the Guide for the Care and Use of Laboratory Animals used by Institut National de la Santé et de la Recherche Médicale, and the study protocol was approved by the Université de Paris ethics committee.

Neonatal adoptive transfer of CD4+ Treg cells.

Neonatal adoptive transfer of Treg cells was performed as previously described (19). A total of 5×10^5 Treg cells were injected intraperitoneally (IP) into 3–5-day-old sex-matched Fra-2-transgenic mice or wild-type (WT) littermate controls. Mice were monitored and then euthanized between ages 16 and 18 weeks for phenotype evaluation.

IL-2 treatment. *Short-term treatment.* In this study, 4-week-old Fra-2-transgenic mice received daily IP injections of 200,000 IU of recombinant human IL-2 (Novartis) for 4 consecutive days, as previously described (20).

Long-term treatment. Additionally, 4-week-old Fra-2-transgenic mice and WT littermates received daily treatment for 10 consecutive days with IP injections of either phosphate buffered saline (PBS) or 50,000 IU of recombinant human IL-2 (Novartis) diluted in PBS. Additional 5-day daily treatment was repeated every 3 weeks, as previously described (21). Mice were euthanized between ages 16 and 18 weeks for phenotype evaluation.

Hemodynamic measurements and assessment of vessel remodeling.

Right ventricular systolic pressure (RVSP) and heart rate were determined in mice receiving isoflurane anesthesia through a face mask, as previously reported. Morphometric analyses were performed using paraffin-embedded lung sections stained with hematoxylin and eosin (H&E) and α -smooth muscle actin, as previously described (22).

Histopathologic assessment of fibrosing alveolitis.

Lung sections were stained with H&E. Fibrosing alveolitis severity was semiquantitatively assessed according to the method described by Ashcroft et al, with 2 examiners blinded with regard to the genotype and treatment (23). All images were obtained using a lamina multilabel slide scanner.

Collagen measurements. Collagen content was measured using Sircol soluble collagen assay (Biocolor). Lung biopsy specimens (right lobes) were used in this assay.

Statistical analysis. All data analyses were performed using GraphPad Prism. Data are presented as the mean \pm SEM and were analyzed using ordinary one-way analysis of variance (ANOVA), two-way ANOVA with Holm-Sidak's multiple comparisons test, standard unpaired *t*-test, two-tailed Student's paired *t*-test, or Wilcoxon's matched pairs signed rank test. *P* values less than 0.05 were considered statistically significant.

RESULTS

Activation of CD4+ T cells in Fra-2-transgenic mice.

We first characterized CD4+ T cells in the SLOs from Fra-2-transgenic mice using flow cytometry phenotyping combined with unsupervised visual implementation of t-distributed stochastic neighbor embedding (t-SNE) analysis. On t-SNE analysis, a phenotype shift in CD4+ T cells was obvious in both 12-week-old Fra-2-transgenic mouse lymph nodes (LNs) (Supplementary Figures 1A and B, <http://onlinelibrary.wiley.com/doi/10.1002/art.42111>) and spleens (Supplementary Figures 2A and B, <http://onlinelibrary.wiley.com/doi/10.1002/art.42111>). This change in the t-SNE plot of Fra-2-transgenic CD4+ T cells was mainly due to enrichment of this compartment in cells with high expression of cell-surface glycoprotein CD44 and low expression of the cell adhesion molecule L-Selectin (CD62L) (Supplementary Figure 2C), a phenotype characterizing effector memory T (Tem) cells (CD44^{high}CD62L⁻ cells).

In agreement, while the total numbers of CD4+ T cells decreased with age (Supplementary Figure 1C, <http://onlinelibrary.wiley.com/doi/10.1002/art.42111>), proportions of both Tem cells and central memory T (Tcm) cells (CD44^{high}CD62L⁺ cells) among conventional CD4+ T cells were significantly increased in 12-week-old Fra-2-transgenic mice compared to their WT littermates (Supplementary Figure 1D, <http://onlinelibrary.wiley.com/doi/10.1002/art.42111>). This increase was far more pronounced in CD4+ Tem cells than in CD4+ Tcm cells. Thus, analysis of the peripheral CD4+ T cell compartment revealed accumulated memory CD4+ T cells within the SLOs of Fra-2-transgenic mice.

Disease-associated accumulation of Th2 cells and cell-intrinsic impairment of the balance between Th1/Th2 cells in Fra-2-transgenic mice.

To further characterize the qualitative changes in the CD4+ T cell compartment in Fra-2-transgenic mice, we next analyzed expression of key markers characterizing Th1 cell lineages (T-bet and CXCR3), Th2 cell lineages (GATA-3 and CCR4), and Th17 cell lineages (retinoic acid receptor-related orphan nuclear receptor γ T and CCR6). The proportion of Th2 cells among CD4+ Tem cells was greatly increased in LNs from Fra-2-transgenic mice as soon

as 6 weeks after birth and was more pronounced at age 12 weeks. The concomitant decrease in Th1 cell percentages among CD4+ Tem cells was even more marked, with an almost complete disappearance of this subset in 12-week-old Fra-2-transgenic mice (Figure 1A). However, corresponding changes in the proportion of interferon- γ (IFN γ)- and IL-13-producing CD4 memory cells occurred later and only became significant at age 12 weeks (Figure 1B). These data were supported by the gradual increase in concentrations of IL-4 and IL-5 in serum from Fra-2-transgenic mice (Figure 1C). Of note, in 16-week-old mice, serum IFN γ levels also increased, although this increase was not of the same magnitude as the observed increase in IL-4 and IL-5 (Figure 1D). With regard to Th17 cell lineage, there was no significant difference between Fra-2-transgenic mice and WT mice concerning the proportion of Th17 cells among CD4+ Tem cells or the concentration of IL-17 in serum (Figures 1A, C, and D).

Overall, our data suggest that, in Fra-2-transgenic mice, alterations in the effector profile of CD4 memory cells begins as soon as 6 weeks after birth, with increased representation of the Th2 effector cell lineage leading to the progressive development of severe, Th2-associated inflammatory disease at age 12 weeks. Consistent with this hypothesis, CD4+ T cell infiltration and eosinophils were already detectable in the lung parenchyma from 9-week-old Fra-2-transgenic mice (Supplementary Figure 3, <http://onlinelibrary.wiley.com/doi/10.1002/art.42111>).

This inverted in vivo ratio between Th1 and Th2 effector cells in young Fra-2-transgenic mice led us to investigate whether this imbalance may result from a cell-intrinsic defect in the ability of CD4+ naive T cells to polarize into Th1 and Th2 effector cells. In vitro polarization assays strongly indicate that this Th1/Th2 imbalance results from a cell-intrinsic defect, as CD4+ naive T cells from Fra-2-transgenic mice were unable to differentiate into IFN γ -producing Th1-like cells in vitro, while their polarization into Th2-like cells revealed their higher sensitivity to convert into IL-13-producing cells at low doses of IL-4 (Figures 1E and F). Consistent with this observation, when stimulated in the absence of specific polarizing cytokines, CD4+ naive T cells from Fra-2-transgenic mice efficiently converted into IL-13-producing cells, compared to only a small proportion of their WT counterparts (Supplementary Figure 4, <http://onlinelibrary.wiley.com/doi/10.1002/art.42111>).

Reduced absolute numbers of CD4+ Treg cells in SLOs from Fra-2-transgenic mice.

Since this accumulation of activated, Th2-polarized CD4+ T cells in Fra-2-transgenic mice indicates the possibility of impaired regulation of the immune system in these mice, we next focused on CD4+ Treg cells.

On t-SNE analysis, the cluster corresponding to Treg cells appeared to be reduced in the SLOs from both 6- and 12-week-old Fra-2-transgenic mice compared to age-matched WT

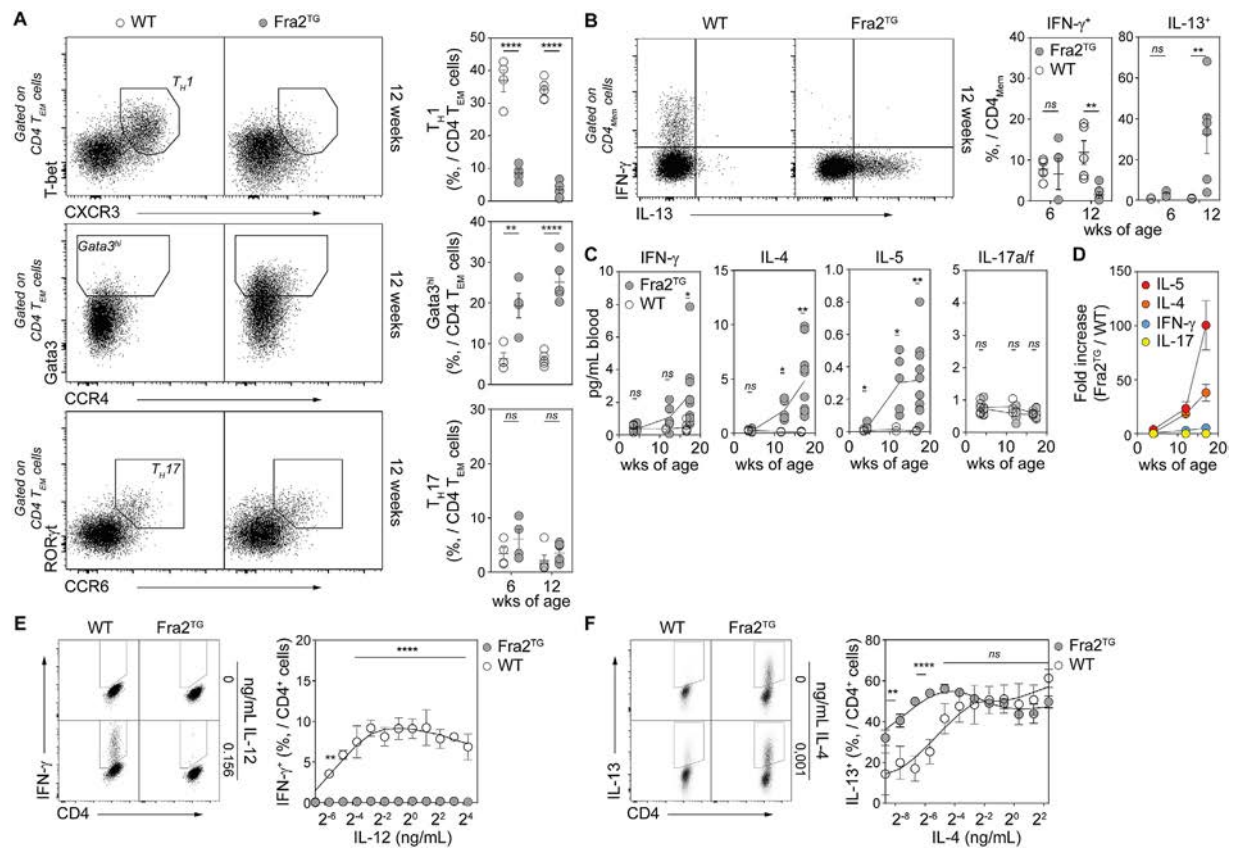


Figure 1. Disease-associated accumulation of Th2 cells and cell-intrinsic Th1/Th2 imbalance in Fra-2-transgenic (Fra-2^{TG}) mice. **A** and **B**, Dot plots showing frequencies of T-bet⁺CXCR3⁺ (Th1), Gata3^{high}CCR4⁺, and retinoic acid receptor γ t-positive (ROR γ t⁺) CCR6⁺ (Th17) cells among CD4⁺ effector memory T (T_{EM}) cells (CD4⁺CD8⁻ T cell receptor β -positive FoxP3⁻CD44^{high}CD62L⁻ T cells) in pooled peripheral lymph nodes (LNs) and mesenteric LNs from 12-week-old Fra-2-transgenic mice and wild-type (WT) littermates (**A**), and frequencies of interferon- γ (IFN γ)⁺ and interleukin-13 (IL-13)⁺-producing cells among CD4⁺ memory T cells (CD4_{Mem}) in pooled peripheral LNs and mesenteric LNs from 6- and 12-week-old Fra-2-transgenic mice and WT littermates (**B**). Data are representative of at least 2 independent experiments (n = 2 mice per group). **C** and **D**, Levels of IFN γ , IL-4, IL-5, and IL-17 in serum from 4-week-old, 10–13-week-old, and 17–18-week-old Fra-2-transgenic mice and age-matched WT littermates (**C**), and fold increase in levels of these cytokines in Fra-2-transgenic mice relative to WT mice (**D**). **E** and **F**, Analysis of flow cytometry–sorted naive CD4⁺ T cells (CD44^{low}CD8b⁻CD11b⁻CD11c⁻CD19⁻CD25⁻NK1.1⁻Ter-119⁻ cells) from Fra-2-transgenic mice and WT littermates for expression of IFN γ (**E**) and IL-13 (**F**) after 4 days of stimulation with coated anti-CD3 and anti-CD28 antibodies (4 μ g/ml) in the presence of IL-4–blocking antibody, IL-2, and graded doses of IL-12 (**E**) or in the presence of IFN γ -blocking antibody and graded doses of IL-4 (**F**). Dot plots show data from representative mice in each group. Data are from 2 independent experiments (n = 2 mice per group). Symbols represent individual mice; bars show the mean \pm SEM. * = $P < 0.05$; ** = $P < 0.01$; **** = $P < 0.0001$, by two-way analysis of variance and Holm-Sidak's multiple comparisons test in **A**, **B**, **E** and **F** or standard unpaired t -test in **C** and **D**. NS = not significant. Color figure can be viewed in the online issue, which is available at <http://onlinelibrary.wiley.com/doi/10.1002/art.42111/abstract>.

littermates (Figure 2A). Accordingly, both the percentage of Treg cells among CD4⁺ T cells and absolute number of Treg cells were dramatically decreased in LNs from Fra-2-transgenic mice compared to control mice (Figure 2B). Neuropilin 1 (Nrp-1) allows for within-SLO differentiation of naturally produced thymic Treg cells (Nrp-1⁺) from peripherally induced Treg cells (Nrp-1⁻) (24). Although percentages of Nrp-1⁻ cells were 2-fold higher among Treg cells from Fra-2-transgenic mice compared to their WT littermates, the absolute number of Nrp-1⁻ Treg cells remained significantly lower in Fra-2-transgenic mice than in WT mice (Figure 2C). Consistent with these results, we observed that CD4⁺ naive T cells from Fra-2-transgenic mice have an impaired ability to differentiate into induced Treg

(iTreg) cells in vitro. Indeed, at the higher tested concentration of transforming growth factor β (TGF β), CD4⁺ naive T cells from Fra-2-transgenic mice lead to a 2-fold lower proportion of iTreg cells compared to WT cell counterparts (43.6% versus 79.4%, respectively), with 3-fold higher TGF β 50% maximum response concentration values (Figure 2D). These results suggest lower cell-intrinsic sensitivity to CD4⁺ naive T cells from Fra-2-transgenic mice to iTreg cell polarization signals, confirmed with an in vivo polarization assay (Supplementary Figure 5, <http://onlinelibrary.wiley.com/doi/10.1002/art.42111>). Indeed, when adoptively transferred into lymphopenic recipient mice, CD4⁺ naive T cells from Fra-2-transgenic mice did not differentiate into peripheral Treg cells, whereas 4–14% of WT CD4⁺ naive

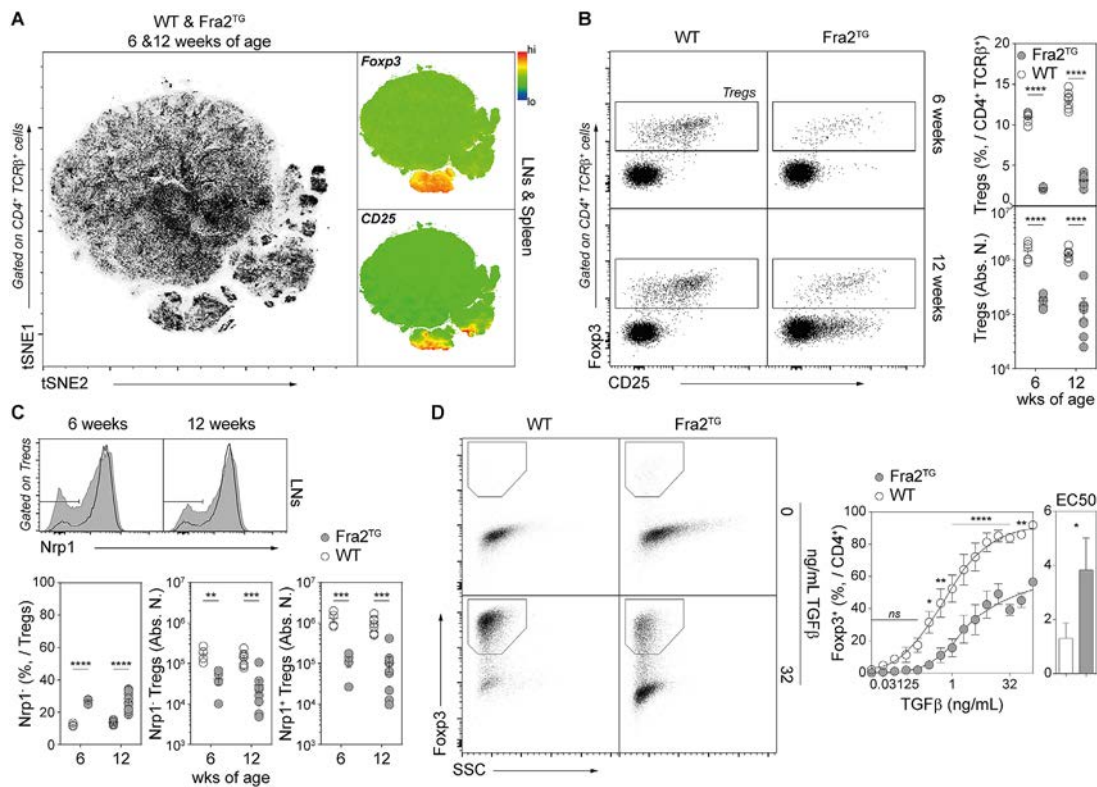


Figure 2. Decrease in absolute number (Abs. N.) of CD4⁺ Treg cells in secondary lymphoid organs from Fra-2-transgenic mice. **A**, Left, Representative t-distributed stochastic neighbor embedding 1 (tSNE1)/tSNE2 plots showing related CD4⁺ T cells from the pooled peripheral LNs and mesenteric LNs and spleens of 6- and 12-week-old Fra-2-transgenic mice and WT littermates. Right, FoxP3 and CD25 expression in LNs and spleens, with color-coded levels ranging from low to high. **B**, CD4⁺ T cell expression in pooled peripheral LNs and mesenteric LNs from 6- and 12-week-old Fra-2-transgenic mice and WT littermates. Left, Representative dot plots show CD25 and FoxP3 expression among gated CD4⁺ T cells in LNs from 6- and 12-week-old Fra-2-transgenic mice and WT littermates. Right, Frequencies and absolute number of Treg cells among CD4⁺ T cells are shown. Data are representative of at least 3 independent experiments ($n = 2$ mice per group). **C**, CD4⁺ Treg cells (CD4⁺CD8⁻TCR β ⁺FoxP3⁺ cells) in pooled peripheral LNs and mesenteric LNs from 6- and 12-week-old Fra-2-transgenic mice and WT littermates analyzed for neuropilin-1 (Nrp-1) expression. Top, Representative histograms showing Nrp-1 expression among gated Treg cells. Bottom, Frequencies and absolute numbers of both Nrp-1⁻ and Nrp-1⁺ cells among CD4⁺ Treg cells in LNs from 6- and 12-week-old Fra-2-transgenic mice and WT littermates. Data are representative of 2 independent experiments ($n = 2$ mice per group). **D**, Analysis of flow cytometry-sorted naive CD4⁺ T cells (CD44^{low}CD8b⁺CD11b⁺CD11c⁺CD19⁺CD25⁺NK1.1⁻Ter-119⁺ cells) from Fra-2-transgenic mice and WT littermates after stimulation with coated anti-CD3 and anti-CD28 antibodies (4 μ g/ml) in the presence of IL-4-blocking antibody, IL-2, and graded doses of transforming growth factor β (TGF β) or in the presence of IFN γ -blocking antibody and graded doses of TGF β . CD4⁺ T cells were analyzed for FoxP3 expression after 4 days of stimulation. Left, Representative dot plots showing proportions of FoxP3⁺CD4⁺ T cells as a function of TGF β concentrations. Data are representative of 3 independent experiments ($n = 2$ mice per group). Right, Concentrations of TGF β 1 needed to obtain 50% of the maximum percentage of induced Treg cell polarization (50% maximum response concentration) in each CD4⁺ naive T cell subset. In **B–D**, symbols represent individual mice; bars show the mean \pm SEM. * = $P < 0.05$; ** = $P < 0.01$; *** = $P < 0.001$; **** = $P < 0.0001$, by two-way analysis of variance with Sidak's multiple comparisons test in **B** and **C** or Wilcoxon's matched pairs signed rank test in **D**. See Figure 1 for other definitions. Color figure can be viewed in the online issue, which is available at <http://onlinelibrary.wiley.com/doi/10.1002/art.42111/abstract>.

T cells differentiated into FoxP3-expressing cells (Supplementary Figure 5).

Impaired generation and maturation of Treg cells in the thymus of Fra-2-transgenic mice. Fra-2-transgenic mice may also exhibit altered production of Treg cells in the thymus. Equivalent numbers of single-positive CD4 (CD4SP) T cell receptor β (TCR β)-positive cells were found in 4–6-week-old Fra-2-transgenic mice and their WT littermates (Figure 3A). Interestingly, while there were comparable percentages of pre-Treg cells in the

thymus from Fra-2-transgenic mice and WT littermates, the proportions and absolute number of Treg cells among CD4SP TCR β ⁺ cells were significantly reduced in Fra-2-transgenic mice compared to WT mice (Figures 3B–D). In WT mice, the absolute number of pre-Treg cells and Treg cells in the thymus were almost perfectly correlated, whereas there was no significant correlation between the absolute number of these cells in Fra-2-transgenic mice (Figure 3D), suggesting impairment of thymic Treg development in Fra-2-transgenic mice, resulting, at least in part, from the defective differentiation of pre-Treg precursor cells into Treg cells.

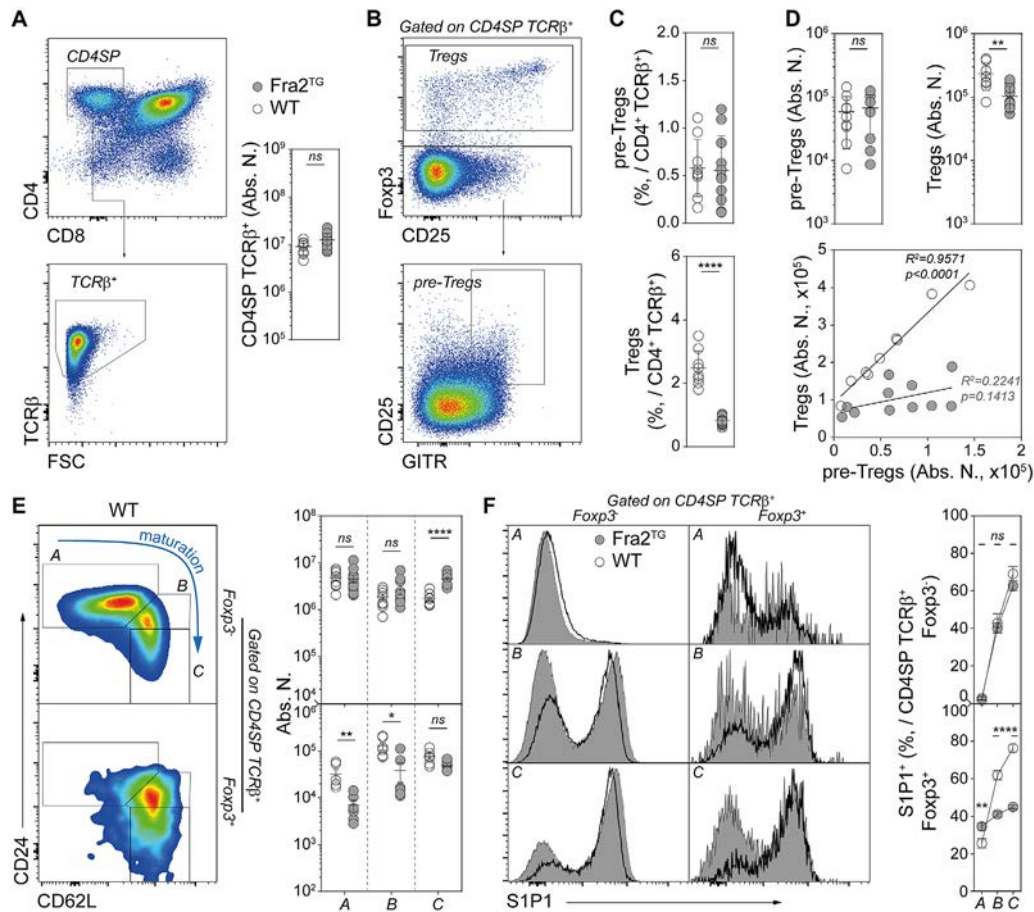


Figure 3. Impaired generation and maturation of Treg cells in thymus tissue from Fra-2-transgenic mice. **A**, Left, Representative dot plots show single-positive CD4 (CD4SP) cell expression among gated live CD4+CD8- T cells and TCR β expression among CD4+ T cells in thymi from 5–6-week-old Fra-2-transgenic mice and WT littermates. Right, Absolute numbers of CD4SP-expressing TCR β + cells are shown. Results are representative of 5 independent experiments ($n =$ at least 2 mice per group). **B**, The same gating strategy was applied to identify CD4+ Treg cells (CD4+CD8-TCR β +FoxP3+ cells) and pre-Treg cells (CD4+CD8-TCR β +FoxP3-GITR^{high}CD25+ cells). **C** and **D**, Frequencies of pre-Treg cells and Treg cells among CD4SP-expressing TCR β + cells (**C**) and absolute number of pre-Treg cells and Treg cells (**D**) are shown. Results are from 5 independent experiments ($n =$ at least 2 mice per group). **D**, Bottom right, Pearson's correlation analyses assessed correlations between the absolute numbers of Treg cells and pre-Treg cells in thymi from Fra-2-transgenic mice and WT littermates. **E**, Left, Representative dot plots show CD24/CD62L expression among gated FoxP3- and FoxP3+ CD4+CD8- T cells (CD4SP cells) from WT mice. Gates for maturation stages A, B, and C (CD24+CD62L-, CD24+CD62L+, and CD24-CD62L+, respectively) are indicated. Right, Absolute numbers of cells at each maturation stage in Fra-2-transgenic mice and WT littermates are shown. Data are from 5 independent experiments ($n =$ at least 2 mice per group). **F**, Left, Representative histograms show sphingosine 1-phosphate receptor 1 (S1P₁) expression among gated FoxP3- and FoxP3+ CD4+CD8- T cells (CD4SP cells) at the C maturation stage in thymi from Fra-2-transgenic mice and WT littermates. Right, Frequencies of S1P₁+ cells at each maturation stage in Fra-2-transgenic mice and WT littermates are shown. Data are from 3 independent experiments ($n =$ at least 2 mice per group). In **C–F**, symbols represent individual mice; bars show the mean \pm SEM. * = $P < 0.05$; ** = $P < 0.01$; **** = $P < 0.0001$, by two-way analysis of variance with Sidak's multiple comparisons test. See Figure 1 for other definitions. Color figure can be viewed in the online issue, which is available at <http://onlinelibrary.wiley.com/doi/10.1002/art.42111/abstract>.

We used CD24 and CD62L to identify 3 maturation stages of SP thymocytes (CD24+CD62L-, CD24+CD62L+, and CD24-CD62L+ in Figures 3E and F). For CD4SP TCR β + FoxP3- cells, we observed an equivalent absolute number of cells in thymi from WT mice and Fra-2-transgenic mice at early stages of maturation. Consistent with the lack of a correlation between the absolute numbers of pre-Treg cells and Treg cells (Figure 3D), the absolute number of FoxP3+ cells was greatly reduced in Fra-2-transgenic mice at earlier maturation stages (Figure 3E). Surprisingly, no significant

difference between Fra-2-transgenic mice and WT mice was observed at the last maturation step. We hypothesized that this could be due to an altered ability of Treg cells from Fra-2-transgenic mice to exit the thymus and therefore due to their accumulation at this late stage of maturation. Analysis of the expression of sphingosine phosphate receptor, which is required for lymphocyte recirculation in the periphery and egress from the thymus, reveals altered up-regulation of this receptor on the surface of Treg cells across maturation stages in Fra-2-transgenic mice (Figure 3F). Overall,

our results suggest that in Fra-2-transgenic mice, pre-Treg cells not transitioning to Treg cells, combined with a blockage of the egress of the few Treg cells that were generated, greatly contributed to the quantitative defect observed in Treg cells from SLOs.

Effect of neonatal adoptive transfer of Treg cells on lung involvement in Fra-2-transgenic mice. Based on our findings, we investigated whether neonatal complementation with WT Treg cells could prevent development of the disease. We adoptively transferred highly purified fluorescence-activated cell-sorted Treg cells from WT FoxP3-GFP mice into Fra-2-transgenic newborn mice or WT newborn mice (Figure 4A).

Survival curves showed longer survival of Fra-2-transgenic mice after Treg cell adoptive transfer compared to PBS-injected Fra-2-transgenic mice (91.7% versus 50% survival at week 18, respectively) (Figure 4B).

We observed increased pulmonary artery wall thickness associated with increased muscularization and perivascular inflammatory infiltrates in the lungs of PBS-injected Fra-2-transgenic mice (Figure 4C). The neonatal adoptive transfer of Treg cells into Fra-2-transgenic mice strongly inhibits vascular remodeling by limiting both the increase in medial wall thickness and muscularization of distal pulmonary arteries observed in PBS-treated Fra-2-transgenic control mice (Figure 4C). Such vascular remodeling of pulmonary arteries led to elevated RVSP in PBS-injected Fra-2-transgenic control mice that was substantially reduced by the neonatal adoptive transfer of Treg cells (Figure 4D).

Fra-2-transgenic mice injected with PBS developed SSc-like histologic features of nonspecific interstitial pneumonia characterized by both diffuse cellular inflammation and collagen deposition. After neonatal adoptive transfer of Treg cells, collagen levels were significantly reduced in the lungs of Fra-2-transgenic mice (Figure 4E). Consistently, lung fibrosis histologic scores (Ashcroft

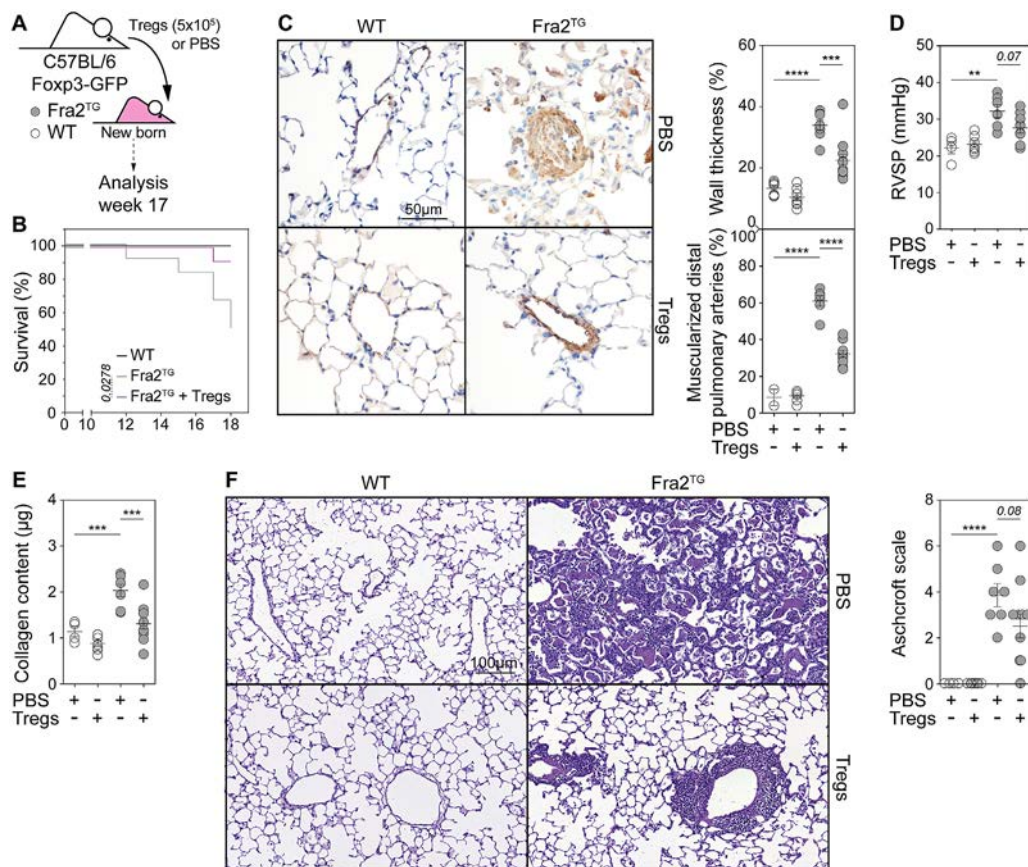


Figure 4. Neonatal adoptive transfer of Treg cells alleviates pulmonary hypertension and lung fibrosis in Fra-2-transgenic mice. **A**, Diagram of the experimental procedure. WT mice and Fra-2-transgenic mice were injected with either phosphate buffered saline (PBS) ($n = 4$ and $n = 12$, respectively) or Treg cells ($n = 7$ and $n = 12$, respectively). **B**, Survival curves. **C**, Representative images showing α -smooth muscle cell actin immunohistochemical staining (left) and quantification of the wall thickness and percentage of muscularized pulmonary arteries (right). **D**, Right ventricular systolic pressure (RVSP). **E**, Collagen content in lung specimens, assessed using Sircol assay. **F**, Left, Representative hematoxylin and eosin-stained lung sections. Right, Lung fibrosis scores (Ashcroft scale). In **D–F**, symbols represent individual mice; bars show the mean \pm SEM. ** = $P < 0.01$; *** = $P < 0.001$; **** = $P < 0.0001$, by ordinary one-sided analysis of variance with Dunnett's multiple comparison test. GFP = green fluorescent protein (see Figure 1 for other definitions). Color figure can be viewed in the online issue, which is available at <http://onlinelibrary.wiley.com/doi/10.1002/art.42111/abstract>.

scale) were reduced in Fra-2-transgenic mice injected with Treg cells compared to Fra-2-transgenic mice receiving PBS, although it was not significant (Figure 4F).

Effect of increasing IL-2 levels on the absolute number of Treg cells in Fra-2-transgenic mice. Usually, the size of the peripheral Treg cell compartment does not solely depend on the extent of thymic production in these cells. Thus, the absolute number of Treg cells in SLOs were indexed to IL-2 peripheral levels and are therefore predominately fixed by the number of conventional CD4+ T cells that produce IL-2 (25). Subsequent studies were therefore carried out to explore the putative causative role of IL-2 in the defect in Treg cells observed in the periphery of Fra-2-transgenic mice. To this end, young mice (4–6-week-old) were used to avoid the skewed effect, due to nascent inflammation in older Fra-2-transgenic mice.

Analysis of Treg cell proliferation, which was mostly dependent on TCR and IL-2 signaling pathways, indicates that there was no proliferative defect in Fra-2-transgenic mice. Indeed, Treg

cells from Fra-2-transgenic mice proliferated slightly more than cells from WT mice counterparts (Figure 5A). Using STAT5 phosphorylation in vivo to quantify proximal IL-2 receptor signaling in Treg cells, we did not detect any defect in Treg cells from Fra-2-transgenic mice (Figure 5B). Overall, the quantitative defect in Treg cells from Fra-2-transgenic mice cannot be attributable to either a proliferative defect or major inability of these cells to respond to IL-2.

We then compared the ability of CD4+ naive T cells from Fra-2-transgenic mice and WT littermates to produce IL-2 in response to stimulation. Lower percentages of IL-2-producing cells were observed in CD4+ T cells from Fra-2-transgenic mice. Furthermore, IL-2-producing cells from Fra-2-transgenic mice produced less IL-2 than cells from WT mouse counterparts (Figure 5C). Accordingly, 4.4 times less IL-2 was measured in the culture supernatant of CD4+ T cells sorted from Fra-2-transgenic mice than in the culture supernatant of CD4+ T cells from WT mice (Figure 5D).

Based on these results, we then investigated whether an increase in IL-2 levels could increase levels of Treg cells in SLOs

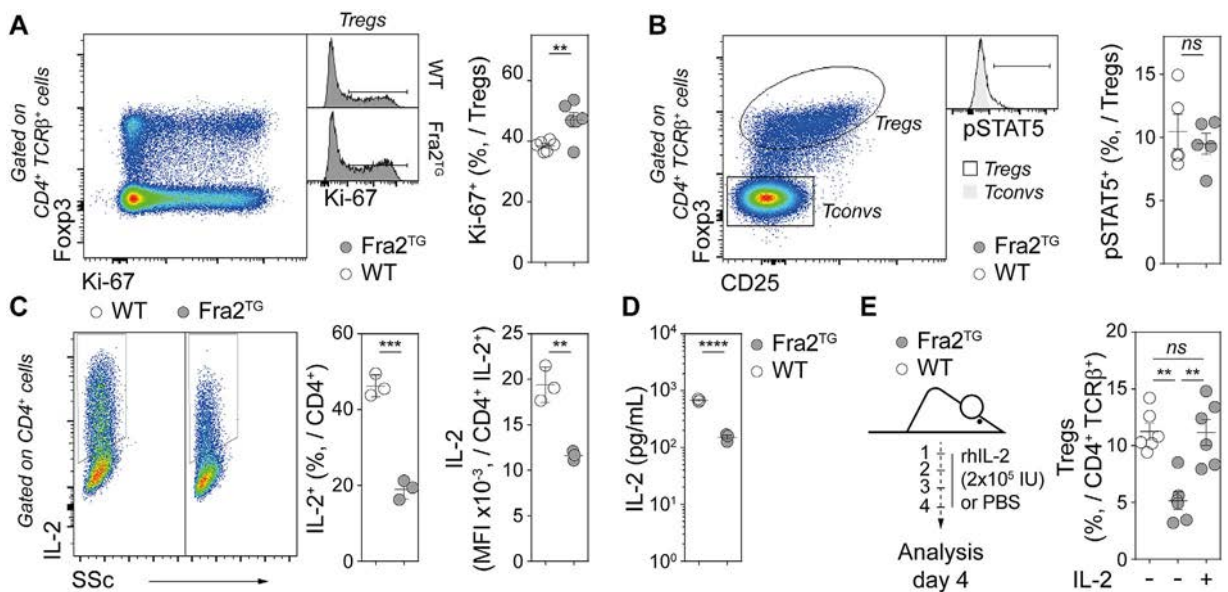


Figure 5. Restoration of normal Treg cell numbers with increasing IL-2 levels in Fra-2-transgenic mice. **A** and **B**, CD4+ T cells in spleens from 6-week-old Fra-2-transgenic mice and WT littermates were analyzed for Ki-67 expression (**A**) and STAT5 phosphorylation (**B**). Representative dot plots show Ki-67 expression among gated CD4+ Treg cells (CD4+CD8–TCRβ+FoxP3+ cells) (**A**, left) and CD25 expression among gated CD4+ Treg cells (CD4+CD8–TCRβ+FoxP3+ cells) and CD4+ conventional T cells (Tconvs) (CD4+CD8–TCRβ+FoxP3– cells) with a pSTAT5 histogram overlay (**B**, left). Right, Data are presented as the frequency of Ki-67+ cells (**A**) or pSTAT5+ cells (**B**) among Treg cells are shown. Data are from 2 independent experiments ($n = 3$ mice [**A**] or $n = 2$ –3 mice per group [**B**]). **C** and **D**, Frequencies and proportions of IL-2+CD4+ T cells and mean fluorescence intensity (MFI) of IL-2 expression among IL-2-producing CD4+ T cells among flow cytometry–sorted CD4+ naive T cells (CD44^{low}CD8b–CD11b–CD11c–CD19–CD25–NK1.1–Ter-119– cells) were analyzed in the serum of Fra-2-transgenic mice and WT littermates. CD4+ T cells were subjected to 18 hours of stimulation with coated anti-CD3 and anti-CD28 antibodies (4 μ g/ml), and IL-2 levels were measured in culture supernatants after stimulation. Representative dot plots are shown in **C**. Data are from 2 independent experiments ($n = 3$ mice per group). **E**, Left, Diagram shows the treatment scheme, in which 4–5-week-old Fra-2-transgenic mice received 2×10^5 IU recombinant human IL-2 (rhIL-2) daily. After 4 days of treatment, CD4+ T cell levels were analyzed in the spleens from untreated and treated Fra-2-transgenic mice and WT littermates. Right, Frequencies of Treg cells (CD4+CD8–TCRβ+FoxP3+ cells) among CD4+ T cells are shown. Data are from 2 independent experiments ($n = 3$ mice per group). Symbols represent individual mice; bars show the mean \pm SEM. ** = $P < 0.01$; *** = $P < 0.001$; **** = $P < 0.0001$, by Mann-Whitney test in **A** and **E** or Student's unpaired 2-tailed t -test in **B**–**D**. See Figure 1 for other definitions. Color figure can be viewed in the online issue, which is available at <http://onlinelibrary.wiley.com/doi/10.1002/art.42111/abstract>.

from Fra-2-transgenic mice. Consistent with the ability of Treg cells from Fra-2-transgenic mice to respond to IL-2, increasing IL-2 levels restored normal Treg cell percentages in splenic CD4+ T cells in these mice (Figure 5E).

Effect of low-dose IL-2 treatment on lung involvement in Fra-2-transgenic mice. We then evaluated the therapeutic potential of IL-2 in Fra-2-transgenic mice. To this end, Fra-2-transgenic mice received successive treatment with low-dose IL-2, with or without neonatal adoptive transfer of Treg cells (Figure 6A).

At week 18, survival rates of Fra-2-transgenic mice receiving treatment with low-dose IL-2 or those receiving combination therapy were 80% and 100%, respectively, whereas the survival rate was 58% for PBS-injected mice (Figure 6B).

Consistent with the increase in Treg cell levels induced by IL-2 in Fra-2-transgenic mice, successive low-dose IL-2 treatment induced similar beneficial effects compared to neonatal adoptive transfer of Treg cells. In particular, vascular remodeling

was greatly reduced by this treatment, with a significant decrease in both the percentages of medial wall thickness and muscularized distal pulmonary arteries compared to PBS-injected mice (Figure 6C). However, there was no additional effect of combination therapy. Similarly, PH was alleviated with limited elevation of RVSP in mice treated with low-dose IL-2 or combination therapy compared to PBS-injected control mice (Figure 6D).

Low-dose IL-2 treatment also ameliorated pulmonary fibrosis, with decreased lung collagen content (Figure 6E) and a consistent reduction in Ashcroft scale scores compared to Fra-2-transgenic mice injected with PBS (Figure 6F). Again, there was no additional effect of the combination therapy.

DISCUSSION

The main finding from our study is that Fra-2-transgenic mice exhibit a marked decrease in the proportion and absolute number of peripheral Treg cells that precedes accumulation of activated, Th2-polarized CD4+ T cells. This inflammatory

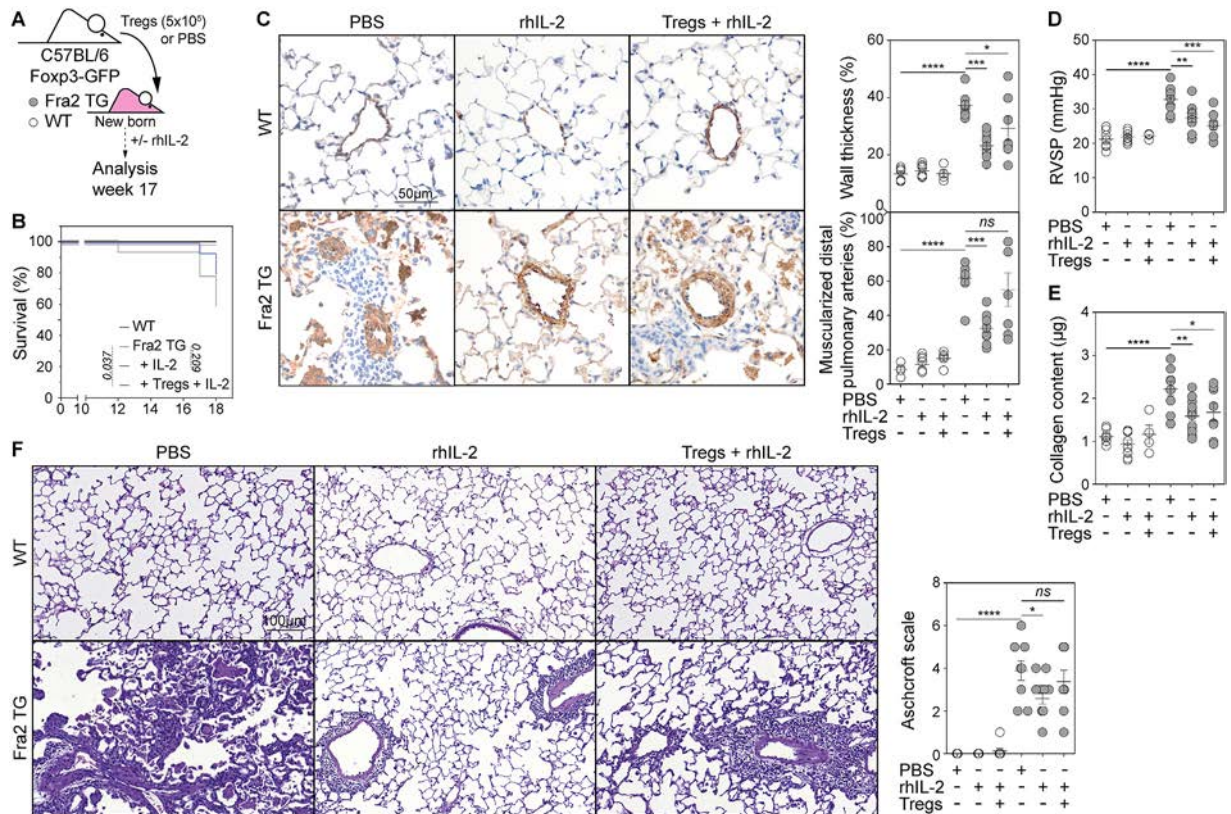


Figure 6. Low-dose IL-2 treatment reverses pulmonary hypertension and lung fibrosis in Fra-2-transgenic mice. **A**, Diagram of the experimental procedure. WT mice and Fra-2-transgenic mice were treated with either phosphate buffered saline (PBS) (n = 7 and n = 13, respectively), recombinant human IL-2 (rhIL-2) (n = 8 and n = 15 respectively), or combination therapy (n = 4 and n = 8, respectively). **B**, Survival curves. **C**, Representative images showing α -smooth muscle cell actin immunohistochemical staining and quantification of the wall thickness and percentage of muscularized pulmonary arteries. **D**, Right ventricular systolic pressure (RVSP). **E**, Collagen content in lung specimens, assessed using Sircol assay. **F**, Left, Representative hematoxylin and eosin staining of lung sections. Right, Lung fibrosis scores (Ashcroft scale). In **C**, **D**, and **F**, symbols represent individual mice; bars show the mean \pm SEM. * = $P < 0.05$; ** = $P < 0.01$; *** = $P < 0.001$; **** = $P < 0.0001$, by ordinary one-sided analysis of variance with Dunnett’s multiple comparison test. GFP = green fluorescent protein (see Figure 1 for other definitions).

phenotype can be reversed by Treg cell adoptive transfer and IL-2 treatment.

In the current study, we showed a notable accumulation of activated, Th2-polarized, CD4⁺ T cells from Fra-2-transgenic mice and a reduced number of Th1 effector CD4⁺ T cells. This biased Th1/Th2 balance results, at least in part, from a cell-intrinsic defect. Indeed, CD4⁺ naive T cells from Fra-2-transgenic mice exhibited an enhanced ability to differentiate into Th2 cells and an inability to differentiate into Th1 cells *in vitro*. This cell-intrinsic bias may result from Fra-2-induced repression of the Th1-specific transcription factor *Tbx21* (26) and Fra-2-induced expression of the Th2 master regulator *Irf-4* (27). Accumulation of Th2 effector cells within SLOs from Fra-2-transgenic mice may also be derived from impairment of Treg cell homeostasis observed in the periphery in Fra-2-transgenic mice. Quantitative or qualitative Treg cell deficiencies have been associated with Th2-mediated diseases (28–31). In particular, a skin homing defect in Treg cells (32) or chronic Treg cell partial depletion in FoxP3-DTR^{+/-} mice cause skin fibrosis (33). Consistent with this hypothesis, the significant decrease in the absolute number of Treg cells in SLOs from Fra-2-transgenic mice precedes accumulation of Th2-polarized CD4⁺ Tem cells. Regarding human SSc, converging data support a role of Th2 cells, but to date there is no direct evidence of their role in damaged tissue, which warrants future specific studies.

The proportion and absolute number of Treg cells are significantly reduced in the thymus of Fra-2-transgenic mice, whereas immediate precursors remain unaffected, suggesting impaired conversion of pre-Treg precursor cells into Treg cells. Interestingly, decreased proportions and absolute numbers of Treg cells were also observed in the thymus of Keratin14-Cre Fli-1^{flx/flx} mice (34), another mouse model of SSc.

Rather than only relying on thymic output, the number of Treg cells in the periphery is also dependent on homeostatic signals. IL-2 has a central role in Treg cell homeostasis, as the absolute number of Treg cells in SLOs relies on IL-2 peripheral resources and is therefore mainly determined by the number of CD4⁺ T cells that produce IL-2 (25). Therefore, within SLOs, Treg cells group around IL-2-producing T cells (35). We thus explored the putative causative role of IL-2 in the defect in Treg cells observed in the periphery in Fra-2-transgenic mice. Whereas the recent findings by Renoux et al (13) suggest that *Fosl-2* overexpression in Fra-2-transgenic mice represses Treg cell generation in the thymus and represses homeostasis in the periphery by decreasing FoxP3 expression through a Treg cell-intrinsic mechanism, we showed that Treg cell deficiency in Fra-2-transgenic mice is also derived from a Treg cell-extrinsic mechanism. We observed impaired ability of peripheral conventional CD4⁺ T cells from Fra-2-transgenic mice to produce IL-2 in response to stimulation. As both the development of Treg cells in the thymus and Treg cell homeostasis in the periphery rely on IL-2 availability (25,36), decreased production of this interleukin by conventional T cells may greatly contribute to

the drastic decrease of the peripheral Treg cell compartment observed in Fra-2-transgenic mice. Consistent with this hypothesis, Treg cell proportions were restored to normal levels by low-dose IL-2 injections. Interestingly, it has been reported that frequencies of IL-2-producing CD4⁺ T cells and CD8⁺ T cells were significantly lower in SSc patients than in healthy controls (37). As in Fra-2-transgenic mice, a quantitative deficit of IL-2-producing conventional T cells could be the cause of altered Treg cell homeostasis in SSc patients.

Evidence of numeric and functional defects in Treg cells in SSc patients has emerged in recent years. Indeed, despite some discrepancies, the majority of studies demonstrated decreased frequencies and/or impaired function of circulating Treg cells in SSc patients compared to healthy controls (38). However, future studies are needed to clarify their role in SSc pathogenesis, and in particular in the development of lung damage. Regarding vascular remodeling, there is growing evidence that abnormal Treg cell functions may be responsible for the immune dysregulation which contributes to the pathobiology of pulmonary arterial hypertension (39–42). In lung tissue, data are still controversial and solely relate to idiopathic pulmonary fibrosis (IPF). Indeed, Treg cells were found to be beneficial or detrimental depending on the IPF models studied, likely influenced by the disease state or the burden of inflammation in different animal models (43).

In the present study, adoptive transfer of Treg cells, low-dose IL-2 therapy, and combination therapy were associated with a significant reduction in pulmonary fibrosis and lung vascular remodeling in Fra-2-transgenic mice. This protective effect of IL-2-induced expansion of Treg cells has recently been demonstrated in the infection-induced exacerbation of pulmonary fibrosis in mice (44). Cell therapy, as exemplified by stem cell therapy, represents significant developments in medicine. With regard to Treg cells, although it might be feasible to isolate and expand Treg cells from a patient for autologous reinjection, as demonstrated in a single lupus patient (45), the bioavailability and biologic effects remain unknown. In contrast, *in vivo* expansion of Treg cells using low-dose IL-2 has already shown promising results in controlling inflammation and restoring immune tolerance in various diseases (46–48) including systemic lupus erythematosus (49), and trials are ongoing in connective tissue diseases including SSc ([ClinicalTrials.gov](https://clinicaltrials.gov/ct2/show/study/NCT01988506) identifier: NCT01988506).

In the current study, therapies were administered in a prophylactic setting. However, this does not preclude the use of IL-2 as a therapeutic option in SSc, as exemplified by recent data on tocilizumab for the prevention of SSc-associated lung fibrosis. Indeed, in a recent phase III study, tocilizumab was able to prevent the progression as well as the development of lung fibrosis in patients with early diffuse SSc (50). This group of patients at an early disease stage likely represent the immunoinflammatory disease phase rather than the advanced fibrotic stage, and this early stage might be a window of opportunity for therapy to preserve lung function. Whether IL-2

therapy may have a place in this therapeutic concept warrants further investigation.

In summary, the significant decrease of the peripheral Treg cell compartment in Fra-2-transgenic mice, combined with an accumulation of activated, Th2-polarized CD4+ T cells, leads to the progressive development of severe, Th2-associated inflammatory fibrotic disease, which can be prevented by the adoptive transfer of Treg cells or low-dose IL-2 therapy. Thus, for SSc patients, IL-2 therapy is promising for Treg cell expansion, restoration of immune tolerance, and consequent reduction in dependence on generalized immunosuppressive medications.

ACKNOWLEDGMENT

We would like to thank Dr. Benoit Salomon for the fruitful discussion and his help with the low-dose IL-2 therapy experiments.

AUTHOR CONTRIBUTIONS

All authors were involved in drafting the article or revising it critically for important intellectual content, and all authors approved the final version to be published. Dr. Frantz had full access to all of the data in the study and takes responsibility for the integrity of the data and the accuracy of the data analysis.

Study conception and design. Lucas, Auffray, Allanore.

Acquisition of data. Frantz, Cauvet, Durand, Gonzalez, Pierre, Do Cruzeiro, Bailly, Andrieu, Orvain, Ottaviani, Thuillet, Tu, Guignabert, Auffray.



Analysis and interpretation of data. Frantz, Avouac, Guignabert, Lucas, Auffray.

REFERENCES

- Elhai M, Avouac J, Kahan A, Allanore Y. Systemic sclerosis: recent insights. *Jt Bone Spine Rev Rhum* 2015;82:148–53.
- Elhai M, Meune C, Avouac J, Kahan A, Allanore Y. Trends in mortality in patients with systemic sclerosis over 40 years: a systematic review and meta-analysis of cohort studies. *Rheumatology (Oxford)* 2012; 51:1017–26.
- Yue X, Yu X, Petersen F, Riemekasten G. Recent advances in mouse models for systemic sclerosis. *Autoimmun Rev* 2018;17:1225–34.
- Elhai M, Avouac J, Hoffmann-Vold AM, Ruzehaji N, Amiar O, Ruiz B, et al. OX40L blockade protects against inflammation-driven fibrosis. *Proc Natl Acad Sci U S A* 2016 05;113:E3901–10.
- Avouac J, Konstantinova I, Guignabert C, Pezet S, Sadoine J, Guilbert T, et al. Pan-PPAR agonist IVA337 is effective in experimental lung fibrosis and pulmonary hypertension. *Ann Rheum Dis* 2017;76: 1931–40.
- Varga J, Trojanowska M, Kuwana M. Pathogenesis of systemic sclerosis: recent insights of molecular and cellular mechanisms and therapeutic opportunities. *J Scleroderma Relat Disord* 2017;2:137–52.
- Brown M, O'Reilly S. The immunopathogenesis of fibrosis in systemic sclerosis [review]. *Clin Exp Immunol* 2018;195:310–21.
- Orvain C, Assassi S, Avouac J, Allanore Y. Systemic sclerosis pathogenesis: contribution of recent advances in genetics [review]. *Curr Opin Rheumatol* 2020;32:505–14.
- Fuschiotti P. T cells and cytokines in systemic sclerosis. *Curr Opin Rheumatol* 2018;30:594–9.
- Yoshizaki A. Pathogenic roles of B lymphocytes in systemic sclerosis. *Immunol Lett* 2018;195:76–82.
- Truchetet ME, Brembilla NC, Montanari E, Allanore Y, Chizzolini C. Increased frequency of circulating Th22 in addition to Th17 and Th2 lymphocytes in systemic sclerosis: association with interstitial lung disease. *Arthritis Res Ther* 2011;13:R166.
- Wynn TA. Fibrotic disease and the T(H)1/T(H)2 paradigm [review]. *Nat Rev Immunol* 2004;4:583–94.
- Renoux F, Stellato M, Haftmann C, Vogetseder A, Huang R, Subramaniam A, et al. The AP1 transcription factor Fosl2 promotes systemic autoimmunity and inflammation by repressing Treg development. *Cell Rep* 2020;31:107826.
- Sakaguchi S, Sakaguchi N, Asano M, Itoh M, Toda M. Immunologic self-tolerance maintained by activated T cells expressing IL-2 receptor α -chains (CD25). Breakdown of a single mechanism of self-tolerance causes various autoimmune diseases. *J Immunol* 1995;155: 1151–64.
- Josefowicz SZ, Lu LF, Rudensky AY. Regulatory T cells: mechanisms of differentiation and function. *Annu Rev Immunol* 2012;30:531–64.
- Weiss JM, Bilate AM, Gobert M, Ding Y, de Lafaille MA, Parkhurst CN, et al. Neuropilin 1 is expressed on thymus-derived natural regulatory T cells, but not mucosa-generated induced Foxp3+ T reg cells. *J Exp Med* 2012;209:1723–42.
- Hori S, Nomura T, Sakaguchi S. Control of regulatory T cell development by the transcription factor Foxp3. *Science* 2003;299:1057–61.
- Amado IF, Berges J, Luther RJ, Mailhé MP, Garcia S, Bandeira A, et al. IL-2 coordinates IL-2-producing and regulatory T cell interplay. *J Exp Med* 2013;210:2707–20.
- Fontenot JD, Gavin MA, Rudensky AY. Foxp3 programs the development and function of CD4+CD25+ regulatory T cells. *Nat Immunol* 2003;4:330–6.
- Delpoux A, Poitrasson-Riviere M, Le Campion A, Pommier A, Yakonowsky P, Jacques S, et al. Foxp3-independent loss of regulatory CD4+ T-cell suppressive capacities induced by self-deprivation. *Eur J Immunol* 2012;42:1237–49.
- Dansokho C, Ahmed DA, Aid S, Toly-Ndour C, Chaigneau T, Calle V, et al. Regulatory T cells delay disease progression in Alzheimer-like pathology. *Brain* 2016;139:1237–51.
- Boletto G, Guignabert C, Pezet S, Cauvet A, Sadoine J, Tu L, et al. T-cell costimulation blockade is effective in experimental digestive and lung tissue fibrosis. *Arthritis Res Ther* 2018;20:197.
- Ashcroft T, Simpson JM, Timbrell V. Simple method of estimating severity of pulmonary fibrosis on a numerical scale. *J Clin Pathol* 1988;41:467–70.
- Yadav M, Louvet C, Davini D, Gardner JM, Martinez-Llordella M, Bailey-Bucktrout S, et al. Neuropilin-1 distinguishes natural and inducible regulatory T cells among regulatory T cell subsets in vivo. *J Exp Med* 2012;209:1713–22.
- Amado IF, Berges J, Luther RJ, Mailhé MP, Garcia S, Bandeira A, et al. IL-2 coordinates IL-2-producing and regulatory T cell interplay. *J Exp Med* 2013;210:2707–20.
- Ciofani M, Madar A, Galan C, Sellars M, Mace K, Pauli F, et al. A validated regulatory network for Th17 cell specification. *Cell* 2012;151: 289–303.
- Ubieta K, Garcia M, Grötsch B, Uebe S, Weber GF, Stein M, et al. Fra-2 regulates B cell development by enhancing IRF4 and Foxo1 transcription. *J Exp Med* 2017;214:2059–71.
- Kim JM, Rasmussen JP, Rudensky AY. Regulatory T cells prevent catastrophic autoimmunity throughout the lifespan of mice. *Nat Immunol* 2007;8:191–7.
- Kanangat S, Blair P, Reddy R, Deheshia M, Godfrey V, Rouse BT, et al. Disease in the scurfy (sf) mouse is associated with overexpression of cytokine genes. *Eur J Immunol* 1996;26:161–5.

30. Zheng Y, Chaudhry A, Kas A, de Roos P, Kim JM, Chu TT, et al. Regulatory T-cell suppressor program co-opts transcription factor IRF4 to control T(H)₂ responses. *Nature* 2009;458:351–6.
31. Rubtsov YP, Rasmussen JP, Chi EY, Fontenot J, Castelli L, Ye X, et al. Regulatory T cell-derived interleukin-10 limits inflammation at environmental interfaces. *Immunity* 2008;28:546–58.
32. Dudda JC, Perdue N, Bachtanian E, Campbell DJ. Foxp3+ regulatory T cells maintain immune homeostasis in the skin. *J Exp Med* 2008;205:1559–65.
33. Kalekar LA, Cohen JN, Prevel N, Sandoval PM, Mathur AN, Moreau JM, et al. Regulatory T cells in skin are uniquely poised to suppress profibrotic immune responses. *Sci Immunol* 2019;4:eaaw2910.
34. Takahashi T, Asano Y, Sugawara K, Yamashita T, Nakamura K, Saigusa R, et al. Epithelial Fli1 deficiency drives systemic autoimmunity and fibrosis: Possible roles in scleroderma. *J Exp Med* 2017;214:1129–51.
35. Liu Z, Gerner MY, Van Panhuys N, Levine AG, Rudensky AY, Germain RN. Immune homeostasis enforced by co-localized effector and regulatory T cells. *Nature* 2015;528:225–30.
36. Hemmers S, Schizas M, Azizi E, Dikiy S, Zhong Y, Feng Y, et al. IL-2 production by self-reactive CD4 thymocytes scales regulatory T cell generation in the thymus. *J Exp Med* 2019;216:2466–78.
37. Tsuji-Yamada J, Nakazawa M, Minami M, Sasaki T. Increased frequency of interleukin 4 producing CD4+ and CD8+ cells in peripheral blood from patients with systemic sclerosis. *J Rheumatol* 2001;28:1252–8.
38. Frantz C, Auffray C, Avouac J, Allanore Y. Regulatory T cells in systemic sclerosis. *Front Immunol* 2018;9:2356.
39. Huertas A, Phan C, Bordenave J, Tu L, Thuillet R, Le Hiress M, et al. Regulatory T cell dysfunction in idiopathic, heritable and connective tissue-associated pulmonary arterial hypertension. *Chest* 2016;149:1482–93.
40. Tamosiuniene R, Manouvakhova O, Mesange P, Saito T, Qian J, Sanyal M, et al. Dominant role for regulatory T cells in protecting females against pulmonary hypertension. *Circ Res* 2018;122:1689–702.
41. Nicolls MR, Voelkel NF. The roles of immunity in the prevention and evolution of pulmonary arterial hypertension. *Am J Respir Crit Care Med* 2017;195:1292–9.
42. Rabinovitch M, Guignabert C, Humbert M, Nicolls MR. Inflammation and immunity in the pathogenesis of pulmonary arterial hypertension. *Circ Res* 2014;115:165–75.
43. Van Geffen C, Deißler A, Quante M, Renz H, Hartl D, Kolahian S. Regulatory immune cells in idiopathic pulmonary fibrosis: friends or foes? *Front Immunol* 2021;12:663203.
44. Moyé S, Bormann T, Maus R, Sparwasser T, Sandrock I, Prinz I, et al. Regulatory T cells limit pneumococcus-induced exacerbation of lung fibrosis in mice. *J Immunol* 2020;204:2429–38.
45. Dall’Era M, Pauli ML, Remedios K, Taravati K, Sandoval PM, Putnam AL, et al. Adoptive Treg cell therapy in a patient with systemic lupus erythematosus. *Arthritis Rheumatol* 2019;71:431–40.
46. Koreth J, Matsuoka K, Kim HT, McDonough SM, Bindra B, Alyea EP, et al. Interleukin-2 and regulatory T cells in graft-versus-host disease. *N Engl J Med* 2011;365:2055–66.
47. Saadoun D, Rosenzweig M, Joly F, Six A, Carrat F, Thibault V, et al. Regulatory T-cell responses to low-dose interleukin-2 in HCV-induced vasculitis. *N Engl J Med* 2011;365:2067–77.
48. Hartemann A, Bensimon G, Payan CA, Jacqueminet S, Bourron O, Nicolas N, et al. Low-dose interleukin 2 in patients with type 1 diabetes: a phase 1/2 randomised, double-blind, placebo-controlled trial. *Lancet Diabetes Endocrinol* 2013;1:295–305.
49. Humrich JY, Riemekasten G. Restoring regulation – IL-2 therapy in systemic lupus erythematosus. *Expert Rev Clin Immunol* 2016;12:1153–60.
50. Roofeh D, Lin CJ, Goldin J, Kim GH, Furst DE, Denton CP, et al. Tocilizumab prevents progression of early systemic sclerosis-associated interstitial lung disease. *Arthritis Rheumatol* 2021;73:1301–10.

A Comparison of International League of Associations for Rheumatology and Pediatric Rheumatology International Trials Organization Classification Systems for Juvenile Idiopathic Arthritis Among Children in a Canadian Arthritis Cohort

Jennifer J. Y. Lee,¹  Simon W. M. Eng,² Jaime Guzman,³  Ciáran M. Duffy,⁴ Lori B. Tucker,³ Kiem Oen,⁵ Rae S. M. Yeung,¹ and Brian M. Feldman,¹ on behalf of the ReACCh-Out Investigators

Objective. The aim of the Paediatric Rheumatology International Trials Organisation (PRINTO) juvenile idiopathic arthritis (JIA) classification criteria, which is still in development, is to identify homogeneous groups of JIA patients. This study was undertaken to compare International League of Associations for Rheumatology (ILAR) JIA classification criteria and PRINTO JIA classification criteria using data from the ReACCh-Out (Research in Arthritis in Canadian Children, Emphasizing Outcomes) cohort.

Methods. We used clinicobiologic data recorded within 7 months of diagnosis to assign a diagnosis of JIA and identify subcategories of JIA among 1,228 patients according to the 2 JIA classification systems. We compared the proportions of patients classified and the alignment of classification categories with clinicobiologic subtypes and adult arthritis types.

Results. The PRINTO criteria classified 244 patients (19.9%) as having early-onset antinuclear antibody–positive JIA, 157 (12.8%) as having enthesitis/spondylitis–related JIA, 38 (3.1%) as having systemic JIA, and 10 (0.8%) as having rheumatoid factor–positive JIA. A total of 12% of patients were unclassifiable using the ILAR criteria, while 63.3% were unclassifiable using the PRINTO criteria (777 with other JIA and 2 with unclassified JIA). In sensitivity analyses, >50% of patients remained unclassifiable using the PRINTO criteria. Compared to the PRINTO criteria, ILAR JIA categories aligned better with clinicobiologic subtypes in 131 patients ($\chi^2 = 44$, $P = 0.005$, versus $\chi^2 = 15$, $P = 0.07$ for PRINTO), and ILAR categories aligned better with adult types of arthritis in 389 evaluable patients.

Conclusion. Currently identified PRINTO disorders can only be used to classify a minority of JIA patients, leaving a large proportion of JIA patients with other disorders requiring further characterization. Current PRINTO JIA classification criteria do not align better with clinicobiologic subtypes or adult forms of arthritis compared with the older ILAR classification system.

INTRODUCTION

Juvenile idiopathic arthritis (JIA) defines a group of heterogeneous conditions characterized by chronic joint inflammation in children (1). Since children with JIA can have varied clinical

presentation, disease trajectories, and outcomes, classification systems have been developed to subdivide patients into well-defined, homogeneous groups (2,3). Classification criteria shared by clinicians and researchers provides common nomenclature and meaningful context for research findings.

Supported by the Fast Foundation and a New Emerging Team research grant from the Canadian Institutes of Health Research (grant QNT 69301).

Drs. Lee and Eng contributed equally to this work. Drs. Yeung and Feldman are co-principal investigators.

¹Jennifer J. Y. Lee, MD, FRCPC, Rae S. M. Yeung, MD, PhD, Brian M. Feldman, MD, MSc, FRCPC: The Hospital for Sick Children (SickKids) and University of Toronto, Toronto, Ontario, Canada; ²Simon W. M. Eng, PhD: The Hospital for Sick Children (SickKids), Toronto, Ontario, Canada; ³Jaime Guzman, MD, MSc, FRCPC, Lori B. Tucker, MD, FRCPC: BC Children's Hospital and University of British Columbia, Vancouver, British Columbia, Canada; ⁴Ciáran M. Duffy, MB, BCh, MSc, FRCPC, FRCPI: Children's Hospital

of Eastern Ontario and University of Ottawa, Ottawa, Ontario, Canada; ⁵Kiem Oen, MD, FRCPC: University of Manitoba, Winnipeg, Manitoba, Canada.

Author disclosures are available at <https://onlinelibrary.wiley.com/action/downloadSupplement?doi=10.1002%2Fart.42113&file=art42113-sup-0001-Disclosureform.pdf>.

Address correspondence to Brian M. Feldman, MD, MSc, FRCPC, The Hospital for Sick Children (SickKids), 555 University Avenue, Toronto, Ontario, Canada M5G 1X8. Email: brian.feldman@sickkids.ca.

Submitted for publication January 21, 2021; accepted in revised form March 9, 2022.

The 2001 International League of Associations for Rheumatology (ILAR) JIA classification criteria were developed through expert consensus and are currently internationally recognized and used almost exclusively (1,4). ILAR JIA criteria stratify patients into 7 mutually exclusive categories: systemic arthritis, oligoarthritis, rheumatoid factor (RF)-negative polyarthritis, RF-positive polyarthritis, psoriatic arthritis (PsA), enthesitis-related arthritis (ERA), and undifferentiated arthritis (UA). Clinical and laboratory features used to define these categories include the number of affected joints, family history, extraarticular manifestations, RF positivity, and HLA-B27 positivity.

Several shortcomings of the ILAR criteria have been identified, including discrepancies between the names of certain JIA categories and their counterparts in adults (which may interfere with the follow-up of children after transition to adult care) (5), significant heterogeneity in epidemiologic characteristics and prognoses of patients assigned to ILAR categories (6–9), and lack of inclusion of relevant biologic markers involved in JIA pathogenesis that may impact treatment decisions and response (10–13).

To address some of these shortcomings, the Pediatric Rheumatology International Trials Organization (PRINTO) proposed a revision of the ILAR JIA criteria (14). Like the ILAR criteria, the initial PRINTO JIA classification criteria were developed through expert consensus and in this criteria set, clinical information together with additional laboratory and imaging data are considered. The goal of this revision is to identify correlating conditions seen both in children and in adults and to distinguish conditions unique to children. Currently 4 PRINTO JIA disorders are defined, 3 with proposed adult counterparts: systemic JIA (adult counterpart being adult-onset Still's disease [AOSD]), RF-positive JIA (adult rheumatoid arthritis [RA]), and enthesitis/spondylitis-related JIA (adult spondyloarthritis [SpA]), as well as 1 disorder unique to the pediatric population: early-onset antinuclear antibody (ANA)-positive JIA. The early-onset ANA-positive subtype is novel and is believed to encompass a homogeneous group of patients within 3 ILAR categories (PsA, RF-negative polyarthritis, and oligoarthritis) (8,9). Two additional categories for unclassifiable patients are included: other JIA (patients who do not fit any defined category) and unclassified JIA (patients who fit ≥ 2 defined categories). Organizing unclassifiable patients into homogeneous groups is pending a prospective validation study (14).

Compared with the ILAR JIA classification criteria, it is unclear whether using the current PRINTO JIA classification criteria results in fewer unclassifiable patients, more homogeneous patient groups, or greater agreement with correlating adult diagnoses. Since both ILAR and PRINTO JIA classification criteria utilize clinical data to classify patients, it is also unclear which better aligns with disease classifications that incorporate biologic features with clinical data (15,16). One such clinicobiologic classification has been explored by Eng et al, who recovered 5 homogeneous patient clusters using a combination of cytokine expression data and clinical characteristics (15).

A formal prospective validation study of the PRINTO JIA classification criteria is underway (14). In the interim, the preliminary PRINTO classification criteria may be applied to previous large cohorts of JIA patients, like the ReACCh-Out (Research in Arthritis in Canadian Children, Emphasizing Outcomes) cohort (see Appendix A for additional members of the ReACCh-Out study), to investigate the uncertainties mentioned previously. ReACCh-Out is a large Canadian prospective inception cohort of patients with newly diagnosed JIA (17). Utilizing data collected from the ReACCh-Out cohort, we compared the performance of the PRINTO JIA criteria and ILAR JIA criteria. Specifically, the objectives of this study were to 1) classify patients according to each set of criteria in silico and evaluate agreement between classified groups, 2) evaluate the alignment of each disease classification with a clinicobiologic classification, and 3) evaluate the alignment of each disease classification with adult arthritis diagnoses.

PATIENTS AND METHODS

Patient cohort. Procedures and the analyses performed are outlined in Supplementary Figure 1 (available on the *Arthritis & Rheumatology* website at <http://onlinelibrary.wiley.com/doi/10.1002/art.42113>). The methods used in the ReACCh-Out cohort study have been described previously (17,18). Briefly, ReACCh-Out is a prospective inception cohort study that recruited patients with newly diagnosed JIA, according to the ILAR definition of JIA, from January 2005 to December 2010 from 16 Canadian pediatric rheumatology centers. Study visits occurred at enrollment, at 6-month intervals for 2 years, and yearly thereafter, for up to 5 years of follow-up. Among other data, the following data were collected at study visits: active joint count, number of joints with limited range of motion, number of enthesitis sites, and extraarticular manifestations, including uveitis. Erythrocyte sedimentation rate (ESR) data, ANA data, RF data, and HLA-B27 data were collected as available. ReACCh-Out was approved by the research ethics boards at each institution and carried out in accordance with the Declaration of Helsinki. Informed consent was obtained from parents or guardians, and assent was obtained from participants as appropriate for their age.

Patients were included in the ReACCh-Out cohort if they were diagnosed as having JIA within 12 months prior to enrollment and their age at diagnosis was < 16 years. Patients enrolled ≤ 6 months after diagnosis were selected for the present study, and data from study visits that occurred up to June 4, 2012 were analyzed. Analyses were conducted using R version 3.5.0 (URL: <https://www.r-project.org>) and Python version 3.7 (URL: <https://www.python.org>). Circos charts were generated using Circos version 0.63 (19).

Handling of missing data. For our primary analyses, criteria directly related to missing measurements were considered unsatisfied and were analyzed as negative when assigning ILAR

JIA categories, PRINTO JIA disorders, or adult diagnoses to individual patients. For example, a patient without an HLA-B27 result was considered HLA-B27 negative. We performed sensitivity analyses to see how our results would change under different simulations of missing data (see below).

ILAR classification of JIA categories. For each patient, the ILAR JIA classification was first assigned by the attending pediatric rheumatologist and then reviewed by 1 investigator (RY) who was blinded with regard to the original assignment, to confirm that the participant fulfilled the ILAR criteria based on submitted study data. In the case of a disagreement, 4 investigators (CD, LT, KO, RY) resolved disagreements by consensus. These procedures produced the validated, physician-assigned ILAR JIA categories.

For this study, a computer algorithm was created to assign computed ILAR categories by applying ILAR JIA classification criteria as strictly as possible to data obtained <6 months after diagnosis (Supplementary Figure 1 and Supplementary Text 1, <http://onlinelibrary.wiley.com/doi/10.1002/art.42113>) (1). This was performed to provide a fair, data-driven comparison between the ILAR and PRINTO classification systems, as physician assignments and additional validation steps had not been performed for the new PRINTO groupings.

Agreements between previously validated physician-assigned and computed ILAR categories were visualized using circo charts and quantified using Fleiss' κ with irr R package version 0.84.1. McNemar's test was used to further validate agreements between physician-assigned and computed ILAR categories.

PRINTO classification of JIA disorders. Patients were also computationally classified according to the PRINTO JIA criteria using data obtained <6 months after diagnosis, which thus yielded the list of computed PRINTO disorders (Supplementary Figure 1 and Supplementary Text 2, <http://onlinelibrary.wiley.com/doi/10.1002/art.42113>). Several adjustments were made when applying PRINTO definitions, since the PRINTO disorders did not exist during original data collection (Supplementary Text 2). There were important deviations from the PRINTO definitions. Since imaging data were not collected, sacroiliitis imaging could not be included as a possible criterion for enthesitis/spondylitis-related JIA. As anti-cyclic citrullinated peptide (anti-CCP) data were unavailable, positive anti-CCP was not used as an alternative to a positive RF finding for RF-positive JIA. Only 1 positive ANA finding was required for our primary analyses, rather than the 2 ANA-positive readings at titers $\geq 1:160$, ≥ 3 months apart, as specified in the PRINTO classification system (see below).

Determination of RF and ANA status. For ILAR and PRINTO classifications, patients were considered RF-positive if

they had ≥ 2 positive RF findings ≥ 91 days apart. However, to account for delays between blood collection and the return of results, we considered results reported <7 months after diagnosis. We accepted ANA results reported as positive or negative in the ReACCh-Out data set for the present analysis. A positive result was defined as an ANA titer of $\geq 1:80$, detected using immunofluorescence assay (20). ANA titers were not explicitly noted on data collection forms. Instead, investigators were instructed to report positive or negative findings according to local laboratory reference values, but a survey of investigators indicated that an ANA titer of $\geq 1:80$ was considered positive at the majority of participating rheumatology centers.

Sensitivity analysis. The ReACCh-Out study was not structured for testing classification criteria and therefore mostly depended on attending rheumatologists to apply ILAR criteria and report serologic results. Since strictly applied definitions for serology may not have been adhered to, sensitivity analyses were conducted by simulating missing data. Missing HLA-B27 data were simulated so that a random 5% of missing results were considered positive. This simulation was repeated at 5% increments, such that a random 10–20% of these results were positive. Missing ANA and RF data were similarly simulated, with positive results ranging between 5% and 30% at 5% increments for ANA and ranging between 1% and 10% at 1% increments for RF.

In each scenario, ILAR and PRINTO classifications of JIA were computed, and 2,000 repeated simulations were conducted. Additionally, in order to reflect clinical practice better, we evaluated how our sensitivity analyses would differ if only 1 RF-positive value was required for the patient to be considered RF positive.

Comparisons between ILAR and PRINTO classification systems. Relationships between ILAR and PRINTO groupings were visualized using circo charts. Distributions were compared using Pearson's chi-square test. If chi-square test values were significant ($P < 0.05$), overrepresented pairs were defined as those with Z scores of 1.96 or more, corresponding to the critical significance threshold of $\alpha = 0.05$ determined by 2-tailed test with normally distributed data.

To determine if early-onset ANA-positive JIA is a homogeneous disorder, we compared demographic and clinical features in patients assigned to different ILAR categories who fulfilled criteria for early-onset ANA-positive JIA. These included age at diagnosis, age at symptom onset, sex, and the number of active joints and joints with limited range of motion at diagnosis. We also compared the risk of uveitis throughout follow-up. Apart from female sex and presence of uveitis, in which case we used univariable logistic regression analysis, univariable linear regression analyses were performed for the remaining variables. Model and coefficient Bonferroni-adjusted P values account for multiple hypothesis testing.

Comparison of the ILAR JIA classification system and PRINTO JIA classification system with a clinicobiologic subtype classification system.

Eng et al previously defined the following 5 clinicobiologic subtypes of JIA by principal components analysis of demographic data, clinical data, biochemical data, and cytokine expression data. These 5 clinicobiologic subtypes are subtype I (children with predominantly older age at onset, very low measures of disease activity, and low levels of circulating proinflammatory cytokines), subtype II (low measures of disease activity and low levels of proinflammatory cytokines), subtype III (increased measures of disease activity and moderate levels of Th1/Th17/macrophage-associated soluble mediators of inflammation), subtype IV (younger age at diagnosis, earlier diagnosis after symptom onset, intermediate measures of disease activity, and intermediate levels of proinflammatory cytokines), and subtype V (older age at diagnosis with low measures of disease activity but very high levels of proinflammatory cytokines) (15). The present study included 131 of Eng et al's original 157 patients. Relationships and associations between clinicobiologic subtypes and ILAR and PRINTO classifications were assessed as described above.

Comparison of the ILAR JIA classification system and PRINTO JIA classification system with adult arthritis classification systems.

Patients were classified in silico according to criteria for 4 adult forms of arthritis: AOSD, PsA, RA, and SpA (21–24) (Supplementary Table 6 and Supplementary Text 3–6, <http://onlinelibrary.wiley.com/doi/10.1002/art.42113>). Several of these adult arthritis classification criteria explicitly contain clauses that prevent co-diagnosis with another form of arthritis. In our study, those clauses were ignored, and individual patients could, in theory, fulfill criteria for multiple conditions. Relationships and associations between ILAR and PRINTO JIA classifications and each diagnosis based on adult arthritis criteria were assessed in the same manner as described above.

RESULTS

Patient population and physician-assigned ILAR classifications of JIA.

The ReACCh-Out study recruited 1,508 patients between January 2005 and December 2010, of whom 1,228 patients were included in this study. Among the excluded patients, 182 were enrolled >6 months after diagnosis, 77 only attended the first study visit, and 21 were re-diagnosed with conditions other than JIA during follow-up (including those with inflammatory bowel disease-related arthritis). Table 1 shows the baseline clinical characteristics of the 1,228 patients and their corresponding physician-assigned ILAR categories. Selected patients were enrolled a median of 0.47 months after diagnosis. Computed ILAR categories were consistent with physician-

Table 1. Baseline demographic and clinical characteristics of 1,228 patients from the ReACCh-Out cohort*

Sex, female	776 (63)
Age at diagnosis, median (IQR) years	9.4 (4–13)
Disease duration from diagnosis to enrollment, median (IQR) months	0.47 (0–2)
Duration of follow-up, median (IQR) months since enrollment	34.6 (21–49)
Active count at enrollment, median (range)	2 (0–63)
Enthesitis count at enrollment, median (range)	0 (0–22)
PhGA, median (IQR) score at enrollment	2.7 (1–5)
ILAR disease category†	
Systemic JIA	76 (6)
Oligoarthritis	489 (40)
RF-negative polyarthritis	247 (20)
RF-positive polyarthritis	47 (4)
Psoriatic arthritis	78 (6)
Enthesitis-related arthritis	169 (14)
Undifferentiated arthritis	122 (10)
ANA	
≥1 positive result	529 (43)
≥2 positive results	59 (5)
Results missing	126 (10)
RF	
≥1 positive result	75 (6)
≥2 positive results	16 (1)
Results missing	170 (14)
HLA-B27	
HLA-B27 positive	112 (9)
Results missing	676 (55)

* Except where indicated otherwise, values are the number (%) of patients. ReACCh-Out = Research in Arthritis in Canadian Children, Emphasizing Outcomes; IQR = interquartile range; PhGA = physician global assessment of disease activity; ILAR = International League of Associations for Rheumatology; JIA = juvenile idiopathic arthritis; RF = rheumatoid factor; ANA = antinuclear antibody.

† Original physician-assigned categories are reported.

assigned categories for 75% of patients ($n = 921$) (McNemar's test $B = 0.15$, $P = 0.17$; Fleiss' $\kappa = 0.67$) (Supplementary Tables 1 and 2 and Supplementary Figure 2, <http://onlinelibrary.wiley.com/doi/10.1002/art.42113>).

PRINTO classification of JIA disorders.

According to the PRINTO classification criteria, 38 of 1,228 patients (3%) fulfilled criteria for systemic JIA, 10 patients (0.8%) fulfilled criteria for RF-positive JIA, 157 patients (13%) fulfilled criteria for enthesitis/spondylitis-related JIA, and 244 patients (20%) fulfilled criteria for early-onset ANA-positive JIA. Nearly 66% of patients could not be classified under these 4 PRINTO disorders, as 777 patients (63%) were assigned other JIA and 2 patients (0.2%) were assigned unclassified JIA.

In total, 529 patients (43%) had ≥1 positive ANA result and 126 (10%) were completely missing ANA results. Of those with no ANA results, 107 patients (85%) were classified as having other JIA, and 45 patients (36%) were age <7 years. Of the 244 patients with early-onset ANA-positive JIA, 38 patients (16%) had at least 2 positive ANA results, and the remaining patients had 1 positive ANA result.

Classifications in the sensitivity analysis. Figure 1 shows the effect of simulating missing HLA-B27, RF, and ANA results. For ILAR classification, as we increased the percentage of HLA-B27 results simulated as positive to 20%, the number of patients classified as having ERA increased from 217 patients to 264 patients, and there was a corresponding decrease in the number of patients classified as having systemic arthritis (36 patients to 26 patients) as well as those having PsA (61 patients to 56 patients) (Figure 1A). Similar simulations of HLA-B27 results affected PRINTO classification less, with the number of enthesitis/spondylitis-related JIA patients increasing from 157 patients to 160 patients (Figure 1D). Increasing the percentage of ANA results simulated as positive to 30% increased the number of early-onset ANA-positive JIA patients from 244 patients to 340 patients and decreased the number of other JIA patients from 777 patients to 678 patients (Figure 1E). As expected, simulating missing ANA results did not affect ILAR categories (Figure 1B). Although the number of affected patients was small, simulating 10% of missing RF data as positive had a large effect on RF-positive categories in both classification systems; the number of patients with RF-positive polyarthritis

increased from 6 to 13 (Figure 1C), and the number of patients with RF-positive JIA increased from 10 to 27 (Figure 1F).

Despite the percentage of missing results simulated as positive increasing to maximal percentages (increasing the rate of HLA-B27 positivity to 20%, ANA positivity to 30%, and RF positivity to 10%), most patients were still classified as having other JIA (62%, 55%, and 62% of patients in the groups classified based on maximal simulated percentages of positivity for HLA-B27, ANA, and RF, respectively). Further, relaxing the definition of RF positivity from 2 to 1 positive result and increasing the percentage of missing RF data simulated as positive from 1% to 10% did not significantly change the number of patients with ILAR or PRINTO JIA classifications (Supplementary Figure 3, <http://onlinelibrary.wiley.com/doi/10.1002/art.42113>).

Discrepancies in classification between PRINTO and ILAR classification systems. Figure 2 and Table 2 map patient classifications from ILAR categories to PRINTO disorders. The 2 classification systems resulted in significantly different groupings ($\chi^2 = 2,533$, $P < 0.001$), with 2 exceptions: all patients with systemic arthritis and RF-positive polyarthritis were categorized identically using PRINTO JIA criteria, and 60% of patients (134 of

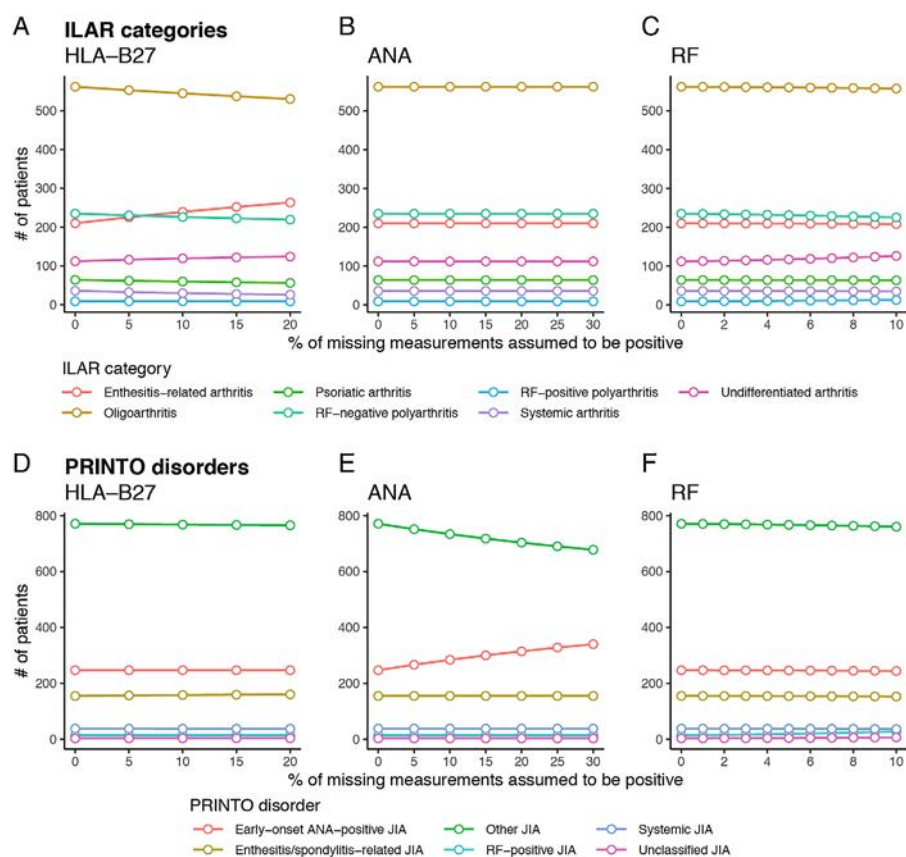


Figure 1. Sensitivity of classification of juvenile idiopathic arthritis (JIA) based on the International League of Associations for Rheumatology (ILAR) classification categories (A–C) and Pediatric Rheumatology International Trials Organization (PRINTO) classification categories (D–F) to increasing percentages of patients with missing laboratory measurements assumed to be positive. The serum measurements included determination of HLA-B27 positivity, as well as positivity for antinuclear antibodies (ANA) and rheumatoid factor (RF).

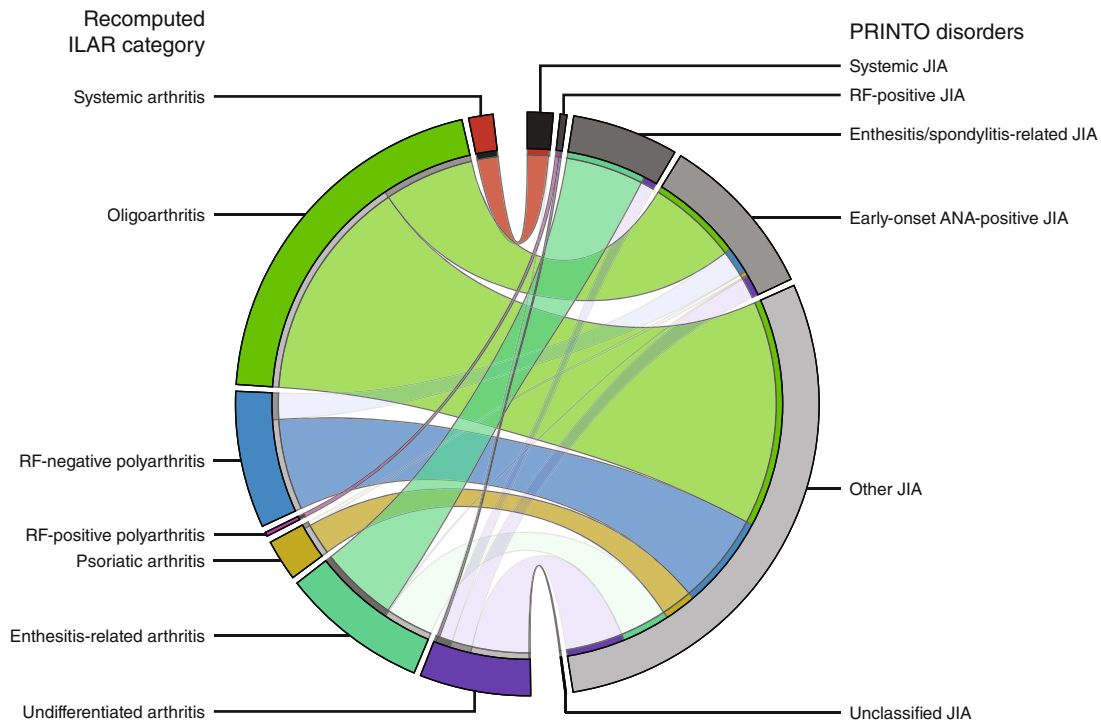


Figure 2. Relationships between classification of JIA according to ILAR JIA categories and classification of JIA according to PRINTO JIA disorders. The segmented circos chart depicts linkages between ILAR JIA categories (colored wedges) and PRINTO-classified JIA disorders (gray wedges). Ribbons indicate shared JIA classifications according to both an ILAR category and PRINTO-defined disorder, with ribbon widths proportional to the number of patients. The more opaque ribbons represent enriched pairs ($\chi^2 = 2,533$, $P < 0.001$). See Figure 1 for definitions.

225) with ERA (according to ILAR criteria) were categorized as having enthesitis/spondylitis-related JIA (according to PRINTO criteria). However, the majority of patients in the remaining ILAR categories were then classified as having other JIA (according to PRINTO criteria), including 71% of patients (387 of 542) with oligoarthritis, 78% of patients (157 of 202) with RF-negative polyarthritis, 89% of patients (54 of 61) with PsA, and 60% of patients (98 of 164) with UA.

Heterogeneity in the features of early-onset ANA-positive JIA based on the PRINTO classification criteria.

The 244 patients with early-onset ANA-positive JIA corresponded to 155 patients with oligoarthritis, 45 patients with RF-negative polyarthritis, 7 patients with PsA, 2 patients with ERA, and 35 patients with UA. Patients in these ILAR categories in the early-onset ANA-positive JIA group were indistinguishable according to age at onset, age at diagnosis, and sex (Supplementary Table 3, <http://onlinelibrary.wiley.com/doi/10.1002/art.42113>), but they differed in the numbers of swollen and tender joints and joints with limited range of motion at enrollment as well as in the development of uveitis throughout the duration of follow-up (Supplementary Tables 4 and 5 and Supplementary Figure 4, <http://onlinelibrary.wiley.com/doi/10.1002/art.42113>). Of those with early-onset ANA-positive JIA, 45 patients developed uveitis ≤ 5 years after their enrollment visits.

Clinicobiologic subtypes associated with ILAR JIA categories, but not PRINTO disorders.

Figure 3 shows the relationships between the 5 clinicobiologic subtypes and the ILAR categories and PRINTO disorders, respectively. We found significant associations between ILAR categories and clinicobiologic subtypes ($\chi^2 = 44$, $P = 0.005$). Clinicobiologic subtype I (characterized by very low levels of circulating proinflammatory cytokines) was associated with ERA ($Z = 2.0$), subtype III (characterized by high disease activity) was associated with RF-negative polyarthritis ($Z = 4.0$) and undifferentiated JIA ($Z = 2.3$), and subtype IV (characterized by younger age at diagnosis and earlier diagnosis following symptom onset) was associated with oligoarthritis ($Z = 3.2$) (Supplementary Table 6, <http://onlinelibrary.wiley.com/doi/10.1002/art.42113>). We did not find any associations with subtype II (low disease activity and cytokine activity) or subtype V (older children with delayed diagnoses, low disease activity, and very high cytokine levels). In contrast to ILAR JIA categories, we found no associations between PRINTO JIA disorders and clinicobiologic subtypes ($\chi^2 = 14$, $P = 0.066$).

Significant mapping from JIA classifications to adult arthritis classifications.

We could only assign adult arthritis classifications to 389 of the 1,228 patients (32%). Figure 4 shows the relationships between PRINTO disorders and ILAR categories, and the projected adult diagnoses. Fifty-eight patients (15%)

Table 2. Relationships between ILAR JIA categories and PRINTO JIA disorders*

ILAR JIA category	PRINTO JIA disorder					
	Systemic	RF-positive	Enthesitis/spondylitis related	Early-onset ANA-positive	Other	Unclassified
Systemic						
No. of patients [†]	36	0	0	0	0	0
ILAR category, % [‡]	100	0	0	0	0	0
PRINTO disorder, % [§]	95	0	0	0	0	0
<i>P</i> , ILAR vs. PRINTO	<0.001	0.58	0.02	0.002	<0.001	0.81
Oligoarthritis						
No. of patients [†]	0	0	0	155	387	0
ILAR category, % [‡]	0	0	0	29	71	0
PRINTO disorder, % [§]	0	0	0	64	50	0
<i>P</i> , ILAR vs. PRINTO	<0.001	0.0048	<0.001	<0.001	<0.001	0.21
RF-negative polyarthritis						
No. of patients [†]	0	0	0	45	157	0
ILAR category, % [‡]	0	0	0	22	78	0
PRINTO disorder, % [§]	0	0	0	18	20	0
<i>P</i> , ILAR vs. PRINTO	0.005	0.16	<0.001	0.35	<0.001	0.53
RF-positive polyarthritis						
No. of patients [†]	0	6	0	0	0	0
ILAR category, % [‡]	0	100	0	0	0	0
PRINTO disorder, % [§]	0	60	0	0	0	0
<i>P</i> , ILAR vs. PRINTO	0.66	<0.001	0.35	0.22	0.0013	0.92
Psoriatic arthritis						
No. of patients [†]	0	0	0	7	54	0
ILAR category, % [‡]	0	0	0	11	89	0
PRINTO disorder, % [§]	0	0	0	2.9	6.9	0
<i>P</i> , ILAR vs. PRINTO	0.15	0.47	0.0022	0.092	<0.001	0.75
Enthesitis-related arthritis						
No. of patients [†]	0	0	134	2	81	0
ILAR category, % [‡]	0	0	62	0.9	37	0
PRINTO disorder, % [§]	0	0	85	0.8	10	0
<i>P</i> , ILAR vs. PRINTO	0.0037	0.14	<0.001	<0.001	<0.001	0.51
Undifferentiated arthritis						
No. of patients [†]	2	4	23	35	98	2
ILAR category, % [‡]	1.2	2.4	14	21	60	1.2
PRINTO disorder, % [§]	5.3	40	15	14	13	100
<i>P</i> , ILAR vs. PRINTO	0.14	0.01	0.61	0.61	0.31	<0.001

* For all standardized statistics, $\chi^2 = 2,533$, $P < 0.001$. RF = rheumatoid factor; ANA = antinuclear antibody.

[†] Refers to the number of patients with juvenile idiopathic arthritis (JIA) fulfilling the International League of Associations for Rheumatology (ILAR) criteria and Pediatric Rheumatology International Trials Organization (PRINTO) criteria.

[‡] Refers to the percentage of patients assigned an ILAR category of JIA who also had the JIA classification according to the PRINTO criteria.

[§] Refers to the percentage of patients with an assigned PRINTO JIA classification who were also assigned the JIA classification according to the ILAR criteria.

assigned adult diagnoses were classified as having undifferentiated JIA (according to ILAR criteria), compared with 216 patients (56%) classified as having other JIA or unclassified JIA (according to PRINTO criteria). Among ILAR categories, AOSD was associated with systemic arthritis ($Z = 24$), adult PsA was associated with PsA ($Z = 27$) and UA ($Z = 4.8$), RA was associated with RF-negative polyarthritis ($Z = 13$) and RF-positive polyarthritis ($Z = 5.0$), and adult SpA was associated with PsA ($Z = 4.3$), ERA ($Z = 13$), and UA ($Z = 3.3$) (Figure 4 and Supplementary Table 7, <http://onlinelibrary.wiley.com/doi/10.1002/art.42113>). Similarly, among PRINTO disorders, AOSD was associated with systemic JIA ($Z = 24$), RA was

associated with RF-positive JIA ($Z = 6.5$), and adult SpA was associated with enthesitis/spondylitis-related JIA ($Z = 15$); however, PsA was only associated with other JIA ($Z = 2.9$) (Figure 4 and Supplementary Table 7, <http://onlinelibrary.wiley.com/doi/10.1002/art.42113>). No adult classification correlated with ILAR oligoarthritis or PRINTO early-onset ANA-positive JIA.

DISCUSSION

Utilizing data from the ReACCh-Out JIA cohort, we compared the performance of current proposed PRINTO JIA

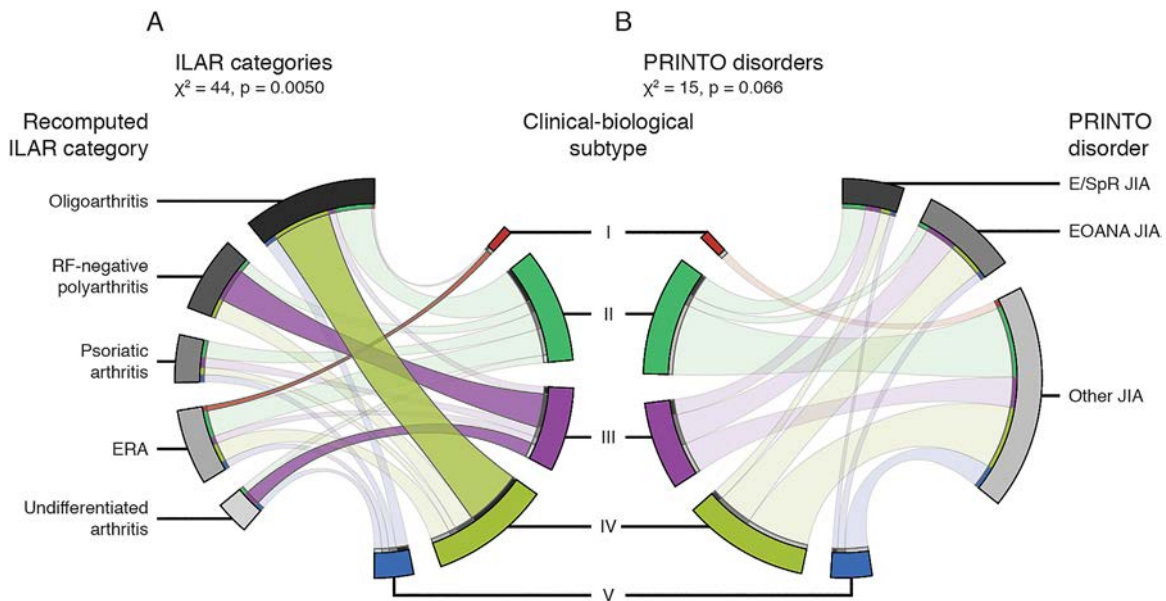


Figure 3. Relationships between ILAR JIA categories and PRINTO JIA disorders and clinicobiologic subtypes. The segmented circos charts show linkage of patient phenotypes from clinical data and cytokine expression measurements (colored wedges) to ILAR JIA categories (gray wedges) (A) and PRINTO-defined disorders (gray wedges) (B). Ribbons indicate shared clinicobiologic subtype pairs and ILAR JIA category or PRINTO disorder, with ribbon widths proportional to the number of patients sharing a clinicobiologic subtype pair and ILAR category or PRINTO disorder. More opaque ribbons represent overrepresented pairs as determined using standardized chi-square test. EOANA = early-onset ANA-positive; ERA = enthesitis-related arthritis; E/SpR = enthesitis-spondylitis/related (see Figure 1 for other definitions).

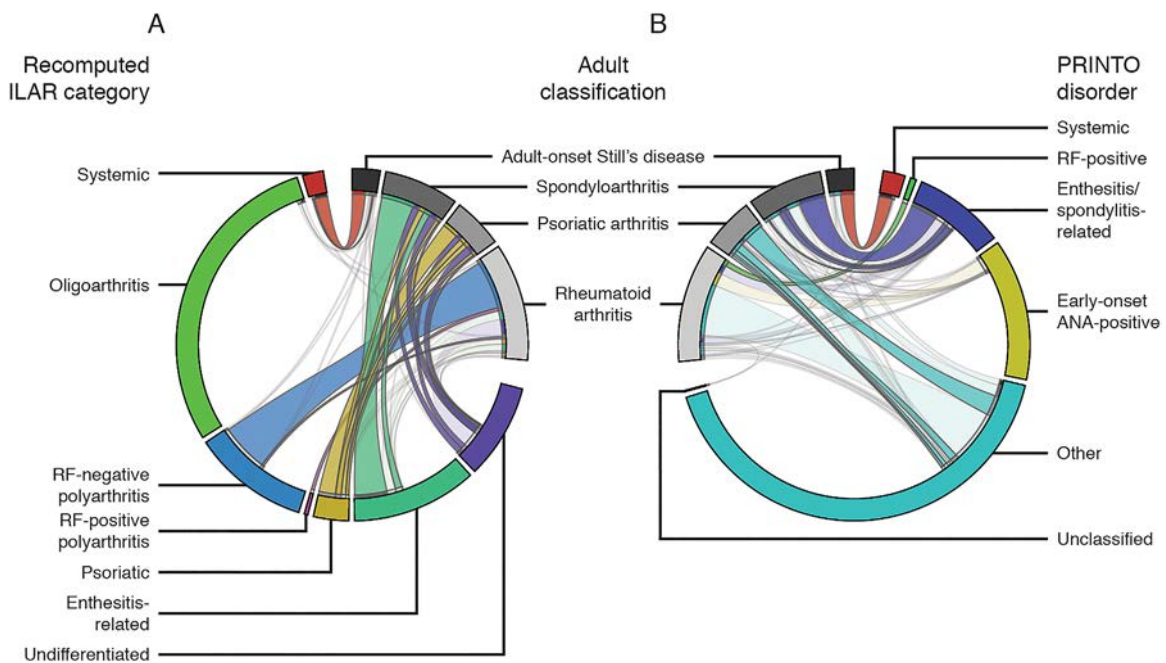


Figure 4. Relationships between ILAR JIA categories, PRINTO JIA disorders, and adult rheumatic disease classifications. The segmented circos charts show linkage of recomputed ILAR JIA categories (colored wedges) (A) or PRINTO disorders (colored wedges) (B) to adult rheumatic disease classifications (grey wedges). Ribbons link shared ILAR JIA categories and adult rheumatic disease classifications. Wider ribbons indicate that more patients share the two classifications, and ribbons that are more opaque represent overrepresented pairings as identified using standardized chi-square test assessing the distributions of ILAR categories in each adult arthritis classification. See Figure 1 for definitions.

classification criteria to the performance of the ILAR classification criteria. Overall, we could not classify ~66% of patients as having JIA among each of the differentiated PRINTO disorders, while 12% of patients were unclassifiable using the ILAR JIA criteria. The PRINTO JIA criteria did not better align with clinicobiologic subtypes or adult arthritis diagnoses.

It is unlikely that lack of data alone explains the low proportion of patients classifiable using the PRINTO JIA criteria. First, we did not exclude patients from being classified as having certain PRINTO disorders based on unavailable information, such as imaging required for enthesitis/spondylitis-related JIA, and we used relaxed definitions for ANA positivity to remain as inclusive as possible. It is important to be aware that ReACCH-Out was planned and executed to be compatible with the standard of care at the time of its conception. Although the majority of patients had 1 ANA test result and 1 RF test result reported at the time of enrollment, additional tests may not have been reported to ReACCH-Out, as they may not have coincided with study visits.

Second, we performed sensitivity analyses to assess the impact of missing ANA, RF, and HLA-B27 serologies on classification. In simulations, we randomly assigned positive values to a percentage of missing results to determine if there was a significant change in the distributions within classification assignments. We varied the simulated percentage of positive missing serologies up to a maximum of 20% for HLA-B27, 30% for ANA, and 10% for RF, since higher prevalence values were unlikely. For example, prevalence rates up to 8% for HLA-B27, 30% for ANA, and 5% for RF have been reported in the general population (24–28). Although the proportion of classifiable patients increased somewhat with ANA simulations, the majority of patients remained unclassifiable using PRINTO JIA criteria.

There is only one other published study evaluating PRINTO JIA classification criteria. Kwon et al retrospectively assigned PRINTO disorders to 262 JIA patients and determined that 27% of their cohort was unclassifiable (25). In contrast, only 7% of their cohort was unclassifiable using ILAR JIA criteria. In most studies, ~10–20% of patients were unclassifiable using ILAR JIA criteria (18,26–30).

The difficulties in classifying a large proportion of our cohort using the PRINTO system may be attributable, in part, to the differences in the composition of patient cohorts. Like other North American JIA registries, the ReACCH-Out cohort is predominantly composed of patients with ILAR-classified oligoarthritis and patients with ILAR-classified RF-negative polyarthritis (31,32). The majority of these patients were reclassified as having other JIA (according to PRINTO criteria) rather than the more restricted early-onset ANA-positive JIA PRINTO disorder. This is in contrast to a European cohort where only 16% of patients with oligoarthritis or RF-negative polyarthritis were not classified as ANA positive and presumably would have been classified as having other JIA (33). These differences suggest that the proportion of

demographic and clinical characteristics in our oligoarthritis and RF-negative polyarthritis patient groups differed, with our cohort containing greater proportions of patients with older age at onset and/or who were ANA negative. Population differences in the distribution of JIA categories have been previously recognized and are possibly attributable to genetic variability (34–36). This highlights the importance of internationally evaluating the performance of the PRINTO system using differing JIA populations.

The development of the early-onset ANA-positive JIA PRINTO disorder was based on evidence of a common phenotype among patients with oligoarthritis, patients with RF-negative polyarthritis, and patients with PsA, consisting of ANA positivity, early age at onset, female predominance, asymmetric arthritis, and higher risk of chronic uveitis (8). We confirmed homogeneity with respect to sex and age at onset among patients with early-onset ANA-positive JIA, but interestingly there are differences in uveitis risk over time, depending on the original ILAR category. The early-onset ANA-positive JIA group did not align well with any of the clinicobiologic subtypes. Our results support that early-onset ANA-positive JIA is a uniquely childhood disorder without an analogous adult rheumatic disease diagnosis. However, the same conclusion applies to the ILAR oligoarthritis category.

Both PRINTO and ILAR classification criteria primarily rely on clinical data to categorize patients. It is possible that including genetic or biologic markers may produce more robust homogeneous classification. We analyzed the correlation between the PRINTO and JIA classifications and the clinicobiologic subtypes developed by Eng et al (15,37). It is important to recognize that the clinical significance of these subtypes is not clear. Nevertheless, our findings suggest that ILAR categories better align with these clinicobiologic subtypes than PRINTO disorders. However, one recent study reported that clinicobiologic subtypes of JIA patients often changed over time, reflecting the dynamic nature of biologic processes and lack of stability when incorporating additional biologic features (38). More research is needed to evaluate whether the inclusion of biologic data improves classification (13).

One rationale for the development of the PRINTO JIA classification system was to identify equivalent adult diagnoses for pediatric JIA groupings to the greatest extent possible (14). This is controversial, as some believe there are advantages of congruity between pediatric and adult classification systems to identify similarities, while others believe pediatric and adult arthritides are different disease entities entirely (5,14). In this study, we could only assign adult diagnoses to ~33% of our cohort. This may be partly due to lack of requisite data, as certain clinical or laboratory variables were not specifically collected or systematically recorded within our cohort and several assumptions were required. Among patients who fulfilled adult RA criteria, only the RF-positive subset was classifiable using PRINTO, while the remainder fulfilled criteria for other PRINTO subtypes. We were able to classify almost all ILAR-classified PsA patients with adult

PsA, but the current PRINTO system does not distinctly classify patients who would have been classified as having adult PsA. Identifying the juvenile equivalent of adult PsA, reflecting the adult joint pattern distribution, spinal involvement, or relevant extraarticular manifestations, would likely improve congruence (39).

Martini et al identified drawbacks of evaluating the PRINTO classification system using existing cohorts like ReACCh-Out because the data lacked specific components of the proposed criteria (14). Indeed, we could not assess the impact of certain criteria e.g., an ANA threshold $\geq 1:160$, anti-CCP as an alternative to RF, and sacroiliitis on imaging. However, we attempted to gauge any uncertainties by performing sensitivity analyses using simulations for missing data. Although an inception cohort study conducted by PRINTO investigators would both validate the proposed criteria and provide data regarding additional disorders, guidelines for criteria development suggest that the final classification criteria should be validated in independent cohorts (40). Thus, despite limitations, large cohorts like ReACCh-Out provide meaningful opportunities to evaluate classification sets without additional participant recruitment or data collection.

In conclusion, our findings suggest that a potentially large proportion of patients have arthritis that may not be classifiable using the proposed PRINTO JIA criteria. In addition to further refinement and the development of additional disorders within the PRINTO JIA classification system, we recommend validation of the criteria in different populations. As the criteria currently stand, the ILAR JIA classification system appears to better align with adult arthritis subtypes and clinicobiologic subtypes than does the PRINTO JIA classification system.

ACKNOWLEDGMENT

We would like to thank all of the families for their generous participation.

AUTHOR CONTRIBUTIONS

All authors were involved in drafting the article or revising it critically for important intellectual content, and all authors approved the final version to be published. Dr. Feldman had full access to all of the data in the study and takes responsibility for the integrity of the data and the accuracy of the data analysis.

Study conception and design. Lee, Eng, Guzman, Yeung, Feldman.

Acquisition of data. Guzman, Duffy, Tucker, Oen, Yeung, Feldman.

Analysis and interpretation of data. Lee, Eng, Guzman, Oen, Yeung, Feldman.

REFERENCES







- Petty RE, Southwood TR, Manners P, Baum J, Glass DN, Goldenberg J, et al. International League of Associations for Rheumatology classification of juvenile idiopathic arthritis: second revision, Edmonton, 2001. *J Rheumatol* 2004;31:390.
- Aggarwal R, Ringold S, Khanna D, Neogi T, Johnson SR, Miller A, et al. Distinctions between diagnostic and classification criteria? [review]. *Arthritis Care Res (Hoboken)* 2015;67:891–7.
- Singh JA, Solomon DH, Dougados M, Felson D, Hawker G, Katz P, et al. Development of classification and response criteria for rheumatic diseases. *Arthritis Rheum* 2006;55:348–52.
- Fink CW. Proposal for the development of classification criteria for idiopathic arthritides of childhood. *J Rheumatol* 1995;22:1566–9.
- Nigrovic PA, Raychaudhuri S, Thompson SD. Genetics and the classification of arthritis in adults and children [review]. *Arthritis Rheumatol* 2018;70:7–17.
- Martini A. Are the number of joints involved or the presence of psoriasis still useful tools to identify homogeneous disease entities in juvenile idiopathic arthritis? *J Rheumatol* 2003;30:1900–3.
- Lovell DJ, Giannini EH, Reiff A, Cawkwell GD, Silverman ED, Nocton JJ, et al. Etanercept in children with polyarticular juvenile rheumatoid arthritis. *N Engl J Med* 2000;342:763–9.
- Ravelli A, Felici E, Magni-Manzoni S, Pistorio A, Novarini C, Bozzola E, et al. Patients with antinuclear antibody-positive juvenile idiopathic arthritis constitute a homogeneous subgroup irrespective of the course of joint disease. *Arthritis Rheum* 2005;52:826–32.
- Greenwald AG, Zakerzadeh A, Laxer RM, Schneider R, Cameron B, Feldman B, et al. Later-onset rheumatoid factor negative polyarticular juvenile idiopathic arthritis (JIA): a unique patient group? *Clin Exp Rheumatol* 2013;31:645–52.
- Van den Ham HJ, de Jager W, Bijlsma JW, Prakken BJ, de Boer RJ. Differential cytokine profiles in juvenile idiopathic arthritis subtypes revealed by cluster analysis. *Rheumatology (Oxford)* 2009;48:899–905.
- De Benedetti F, Brunner HI, Ruperto N, Kenwright A, Wright S, Calvo I, et al. Randomized trial of tocilizumab in systemic juvenile idiopathic arthritis. *N Engl J Med* 2012;367:2385–95.
- Pascual V, Allantaz F, Arce E, Punaro M, Banchereau J. Role of interleukin-1 (IL-1) in the pathogenesis of systemic onset juvenile idiopathic arthritis and clinical response to IL-1 blockade. *J Exp Med* 2005;201:1479–86.
- Nigrovic PA, Colbert RA, Holers VM, Ozen S, Ruperto N, Thompson SD, et al. Biological classification of childhood arthritis: roadmap to a molecular nomenclature [review]. *Nat Rev Rheumatol* 2021;17:257–69.
- Martini A, Ravelli A, Avcin T, Beresford MW, Burgos-Vargas R, Cuttica R, et al. Toward new classification criteria for juvenile idiopathic arthritis: first steps, pediatric rheumatology international trials organization international consensus. *J Rheumatol* 2018;46:190–7.
- Eng SW, Duong TT, Rosenberg AM, Morris Q, Yeung RS, on behalf of the REACCH OUT and BBOP Research Consortia. The biologic basis of clinical heterogeneity in juvenile idiopathic arthritis. *Arthritis Rheumatol* 2014;66:3463–75.
- Thomas E, Barrett JH, Donn RP, Thomson W, Southwood TR, and the British Paediatric Rheumatology Group. Subtyping of juvenile idiopathic arthritis using latent class analysis. *Arthritis Rheum* 2000;43:1496–503.
- Guzman J, Oen K, Tucker LB, Huber AM, Shiff N, Boire G, et al. The outcomes of juvenile idiopathic arthritis in children managed with contemporary treatments: results from the reacch-out cohort. *Ann Rheum Dis* 2015;74:1854–60.
- Oen K, Duffy CM, Tse SM, Ramsey S, Ellsworth J, Chedeville G, et al. Early outcomes and improvement of patients with juvenile idiopathic arthritis enrolled in a canadian multicenter inception cohort. *Arthritis Care Res (Hoboken)* 2010;62:527–36.
- Krzywinski M, Schein J, Birol I, Connors J, Gascoyne R, Horsman D, et al. Circos: an information aesthetic for comparative genomics. *Genome Res* 2009;19:1639–45.
- Lee JJ, Duffy CM, Guzman J, Oen K, Barrowman N, Rosenberg AM, et al. Prospective determination of the incidence and risk factors of new-onset uveitis in juvenile idiopathic arthritis: the research in arthritis

- in canadian children emphasizing outcomes cohort. *Arthritis Care Res (Hoboken)* 2019;71:1436–43.
21. Aletaha D, Neogi T, Silman AJ, Funovits J, Felson DT, Bingham CO III, et al. 2010 rheumatoid arthritis classification criteria: an American College Of Rheumatology/European League Against Rheumatism collaborative initiative. *Arthritis Rheum* 2010;62:2569–81.
 22. Yamaguchi M, Ohta A, Tsunematsu T, Kasukawa R, Mizushima Y, Kashiwagi H, et al. Preliminary criteria for classification of adult still's disease. *J Rheumatol* 1992;19:424–30.
 23. Taylor W, Gladman D, Helliwell P, Marchesoni A, Mease P, Mielants H. Classification criteria for psoriatic arthritis: development of new criteria from a large international study. *Arthritis Rheum* 2006;54:2665–73.
 24. Rudwaleit M, van der Heijde D, Landewé R, Akkoc N, Brandt J, Chou CT, et al. The assessment of spondyloarthritis international society classification criteria for peripheral spondyloarthritis and for spondyloarthritis in general. *Ann Rheum Dis* 2011;70:25–31.
 25. Kwon HJ, Bang MH, Kim KN. New provisional classification of juvenile idiopathic arthritis applying rheumatoid factor and antinuclear antibody. *J Rheum Dis Treat* 2018;25:34–46.
 26. Foeldvari I, Bidde M. Validation of the proposed ILAR classification criteria for juvenile idiopathic arthritis. *International League of Associations for Rheumatology. J Rheumatol* 2000;27:1069–72.
 27. Krumrey-Langkammerer M, Häfner R. Evaluation of the ILAR criteria for juvenile idiopathic arthritis. *J Rheumatol* 2001;28:2544.
 28. Merino R, de Inocencio J, Garcia-Consuegra J. Evaluation of revised International League of Associations For Rheumatology classification criteria for juvenile idiopathic arthritis in Spanish children (Edmonton 2001). *J Rheumatol* 2005;32:559–61.
 29. Glerup M, Rypdal V, Arnstad ED, Ekelund M, Peltoniemi S, Aalto K, et al. Long-term outcomes in juvenile idiopathic arthritis: 18 years of follow-up in the population-based nordic juvenile idiopathic arthritis cohort. *Arthritis Care Res (Hoboken)* 2019;72:507–16.
 30. Hofer MF, Mouy R, Prieur AM. Juvenile idiopathic arthritides evaluated prospectively in a single center according to the durban criteria. *J Rheumatol* 2001;28:1083–90.
 31. McErlane F, Beresford MW, Baildam EM, Chieng SE, Davidson JE, Foster HE, et al. Validity of a three-variable juvenile arthritis disease activity score in children with new-onset juvenile idiopathic arthritis. *Ann Rheum Dis* 2013;72:1983–8.
 32. Beukelman T, Kimura Y, Ilowite NT, Mieszkalski K, Natter MD, Burrell G, et al. The new Childhood Arthritis and Rheumatology Research Alliance (CARRA) registry: design, rationale, and characteristics of patients enrolled in the first 12 months. *Pediatr Rheumatol Online J* 2017;15:30.
 33. Ravelli A, Varnier GC, Oliveira S, Castell E, Arguedas O, Magnani A, et al. Antinuclear antibody-positive patients should be grouped as a separate category in the classification of juvenile idiopathic arthritis. *Arthritis Rheum* 2011;63:267–75.
 34. Prahalad S, Glass DN. A comprehensive review of the genetics of juvenile idiopathic arthritis. *Pediatr Rheumatol Online J* 2008;6:11.
 35. Saurenmann RK, Rose JB, Tyrrell P, Feldman BM, Laxer RM, Schneider R, et al. Epidemiology of juvenile idiopathic arthritis in a multiethnic cohort: ethnicity as a risk factor. *Arthritis Rheum* 2007;56:1974–84.
 36. Macaubas C, Nguyen K, Milojevic D, Park JL, Mellins ED. Oligoarticular and polyarticular JIA: epidemiology and pathogenesis [review]. *Nat Rev Rheumatol* 2009;5:616–26.
 37. Rezaei E, Hogan D, Trost B, Kusalik AJ, Boire G, Cabral DA, et al. Clinical and associated inflammatory biomarker features predictive of short-term outcomes in non-systemic juvenile idiopathic arthritis. *Rheumatology (Oxford)* 2020;59:2402–11.
 38. Rezaei E, Hogan D, Trost B, Kusalik AJ, Boire G, Cabral DA, et al. Associations of clinical and inflammatory biomarker clusters with juvenile idiopathic arthritis categories. *Rheumatology (Oxford)* 2020;59:1066–75.
 39. Gladman DD, Antoni C, Mease P, Clegg DO, Nash P. Psoriatic arthritis: epidemiology, clinical features, course, and outcome [review]. *Ann Rheum Dis* 2005;64 Suppl:ii14–7.
 40. Classification, Response Criteria Subcommittee of The American College Of Rheumatology Committee on Quality Measures. Development of classification and response criteria for rheumatic diseases. *Arthritis Care Res (Hoboken)* 2006;55:348–52.

APPENDIX A: MEMBERS OF THE ReACCh-Out STUDY

Members of the ReACCh-Out study include Roxana Bolaria, David Cabral, Mercedes Chan, Katherine Gross, Kristin Houghton, Kim Morishita, Ross E. Petty, Stuart E. Turvey (British Columbia Children's Hospital and University of British Columbia, Vancouver, British Columbia Canada); Janet Ellsworth, Dax Rumsey (Stollery Children's Hospital and University of Alberta, Edmonton, Alberta, Canada); Susanne Benseler, Nicole Johnson, Paivi Miettunen, Heinrike Schmeling (Alberta Children's Hospital and University of Calgary, Calgary, Alberta, Canada); Alan Rosenberg, Natalie Shiff (Royal University Hospital and University of Saskatchewan, Saskatoon, Saskatchewan, Canada); Kerstin Gerhold, (Children's Hospital and University of Manitoba, Winnipeg, Manitoba, Canada); Roberta A. Berard (Children's Hospital, London Health Science Centre and Western University, London, UK); Maggie Larché (McMaster University, Hamilton, Ontario, Canada); Bonnie Cameron, Ronald M. Laxer, Deborah M. Levy, Rayfel Schneider, Earl Silverman, Lynn Spiegel, Shirley M. L. Tse (Hospital for Sick Children and University of Toronto, Toronto, Ontario, Canada); Michele Gibbon (Children's Hospital of Eastern Ontario, Ottawa, Ontario, Canada, and national ReACCh-Out study coordinator), Roman Jurencak, Johannes Roth, Karen Watanabe-Duffy (Children's Hospital of Eastern Ontario and University of Ottawa, Ottawa, Ontario, Canada); Anne-Laure Chetaille, Jean Dorval (Centre Hospitalier Universitaire de Laval and Université Laval, Quebec City, Quebec, Canada); Gilles Boire, Alessandra Bruns (Centre Hospitalier Universitaire de Sherbrooke and Université de Sherbrooke, Sherbrooke, Quebec, Canada); Sarah Campillo, Gaëlle Chédeville, Claire LeBlanc, Rosie Scuccimarrì (McGill University Health Centre and McGill University, Montreal, Quebec, Canada); Debbie Feldman (Université de Montréal, Montréal, Quebec, Canada); Julie Barsalou, Elié Haddad, Claire St. Cyr (CHU Ste-Justine and Université de Montréal, Montréal, Quebec, Canada); Adam Huber, Bianca Lang, Elizabeth Stringer, Suzanne E. Ramsey (IWK Health Centre and Dalhousie University, Halifax, Nova Scotia, Canada); Paul Dancey (Janeway Children's Health and Rehabilitation Centre and Memorial University, Saint John's, Canada).

Identification of Novel Loci Shared by Juvenile Idiopathic Arthritis Subtypes Through Integrative Genetic Analysis

Jin Li,¹  Yun R. Li,² Joseph T. Glessner,³ Jie Yang,¹ Michael E. March,³ Charly Kao,³ Courtney N. Vaccaro,³ Jonathan P. Bradfield,³ Junyi Li,¹ Frank D. Mentch,³ Hui-Qi Qu,³  Xiaohui Qi,¹ Xiao Chang,³ Cuiping Hou,³ Debra J. Abrams,³ Haijun Qiu,³ Zhi Wei,⁴ John J. Connolly,³ Fengxiang Wang,³ James Snyder,³ Berit Flatø,⁵ Susan D. Thompson,⁶  Carl D. Langefeld,⁷ Benedicte A. Lie,⁵ Jane E. Munro,⁸ Carol Wise,⁹  Patrick M. A. Sleiman,¹⁰  and Hakon Hakonarson¹⁰ 

Objective. Juvenile idiopathic arthritis (JIA) is the most common chronic immune-mediated joint disease among children and encompasses a heterogeneous group of immune-mediated joint disorders classified into 7 subtypes according to clinical presentation. However, phenotype overlap and biologic evidence suggest a shared mechanistic basis between subtypes. This study was undertaken to systematically investigate shared genetic underpinnings of JIA subtypes.

Methods. We performed a heterogeneity-sensitive genome-wide association study encompassing a total of 1,245 JIA cases (classified into 7 subtypes) and 9,250 controls, followed by fine-mapping of candidate causal variants at each genome-wide significant locus, functional annotation, and pathway and network analysis. We further identified candidate drug targets and drug repurposing opportunities by *in silico* analyses.

Results. In addition to the major histocompatibility complex locus, we identified 15 genome-wide significant loci shared between at least 2 JIA subtypes, including 10 novel loci. Functional annotation indicated that candidate genes at these loci were expressed in diverse immune cell types.

Conclusion. This study identified novel genetic loci shared by JIA subtypes. Our findings identified candidate mechanisms underlying JIA subtypes and candidate targets with drug repurposing opportunities for JIA treatment.

INTRODUCTION

Juvenile idiopathic arthritis (JIA), the most common chronic immune-mediated joint disease among children, represents a heterogeneous group of immune-mediated diseases that are difficult to diagnose (1). JIA causes severe joint pain, and delays in therapy can result in joint deformities, prompting the need for early genetic or molecular diagnosis.

More than 30 common variant JIA loci have been identified in genome-wide association studies (GWAS); however, the number of JIA loci is far less than that of other autoimmune diseases. To date, GWAS on JIA have been formally performed in seronegative JIA (2) and systemic JIA (3), while other studies show that the loci implicated in seropositive adult rheumatoid arthritis (RA) are applicable to seropositive polyarticular JIA (4). Due to limited sample sizes, it is difficult to investigate the 7 JIA disease subtypes

Ms. Yang's work was supported by the Ministry of Science and Technology of China (grant 2018YFC1313002). Dr. Yun R. Li's work was supported by the NIH (fellowship awards F30 and F32), and the Children's Hospital of Philadelphia Institute For Translational Medicine and Therapeutics Junior Investigator Pilot Grant Program Pilot Research award. Dr. Hakonarson's work was supported by institutional development funds from the Children's Hospital of Philadelphia, the Children's Hospital of Philadelphia Endowed Chair in Genomic Research, and the National Human Genome Research Institute-sponsored Electronic Medical Records and Genomics Network (grant U01-HG006830).

¹Jin Li, PhD, Jie Yang, MS, Junyi Li, MB, Xiaohui Qi, MB: Department of Cell Biology, the Province and Ministry Co-sponsored Collaborative Innovation Center for Medical Epigenetics, School of Basic Medical Sciences, Tianjin Medical University, Tianjin, China; ²Yun R. Li, MD, PhD: The Children's Hospital of Philadelphia, Philadelphia, Pennsylvania, City of Hope Comprehensive Cancer Center, Duarte, California, and Translational Genomics Research Institute, Phoenix, Arizona; ³Joseph T. Glessner, PhD, Michael E. March, PhD, Charly Kao, PhD, Courtney N. Vaccaro, MS, Jonathan P. Bradfield, PhD, Frank D. Mentch, PhD, Hui-Qi Qu, MD, PhD, Xiao Chang, PhD, Cuiping Hou, MS, Debra J. Abrams, MS, Haijun Qiu, PhD, John J. Connolly, PhD,

Fengxiang Wang, MD, PhD, James Snyder, BS: The Children's Hospital of Philadelphia, Philadelphia, Pennsylvania; ⁴Zhi Wei, PhD: New Jersey Institute of Technology, Newark; ⁵Berit Flatø, MD, PhD, Benedicte A. Lie, PhD: Oslo University Hospital, Rikshospitalet, Oslo, Norway; ⁶Susan D. Thompson, PhD: University of Cincinnati College of Medicine and Cincinnati Children's Hospital Medical Center, Cincinnati, Ohio; ⁷Carl D. Langefeld, PhD: Wake Forest University School of Medicine, Winston-Salem, North Carolina; ⁸Jane E. Munro, MD: Royal Children's Hospital, Parkville, Victoria, Australia; ⁹Carol Wise, PhD: Scottish Rite for Children, Dallas, Texas; ¹⁰Patrick M. A. Sleiman, PhD, Hakon Hakonarson, MD, PhD: The Children's Hospital of Philadelphia and University of Pennsylvania, Philadelphia.

Drs. Jin Li and Yun R. Li contributed equally to this work.

Author disclosures are available at <https://onlinelibrary.wiley.com/action/downloadSupplement?doi=10.1002%2Fart.42129&file=art42129-sup-0001-Disclaimerform.pdf>.

Address correspondence to Hakon Hakonarson, MD, PhD, 1515 Civic Center Boulevard, Philadelphia, PA 19104-4399. Email: hakonarson@email.chop.edu.

Submitted for publication March 21, 2021; accepted in revised form March 25, 2022.

defined using the International League of Associations for Rheumatology (ILAR) criteria: enthesitis-related arthritis (ERA), rheumatoid factor (RF)-negative polyarthritis (PA), RF-positive PA, oligoarthritis, psoriatic arthritis (PsA), systemic arthritis, and undifferentiated arthritis (UA) (5).

Biologic and molecular evidence of serum autoantibodies and other molecular biomarkers of immunologic defects suggest that the existing 7 JIA subtypes are heterogeneous but also have overlapping molecular features (6). The RF-positive PA JIA subtype shares serologic features, such as RF, anti-cyclic citrullinated peptide antibodies, anti-mutated citrullinated vimentin antibodies, and genetic loci, with other autoimmune diseases like RA (4,7), resembling predominantly seropositive autoimmune diseases, while ERA and systemic arthritis findings had more characteristics of autoinflammatory diseases (8,9). A transcriptomic study also identified distinct differentially expressed genes and differentially expressed shared genes between the polyarthritis, oligoarthritis, and systemic arthritis subtypes (10). Therefore, the 7 JIA subtypes are not so distinct from a mechanistic or therapeutic standpoint (1,11). Given that a large number of immune pathway modulators are already approved for use in other rheumatologic and immune-mediated disorders, including RA, understanding the genetic basis of JIA subtypes may allow for the early and rapid introduction of already approved drugs to treat disease according to molecular subtype definitions. Studies focusing on JIA subtypes have started to identify molecular differences and similarities (3,4). However, these studies have not systematically examined all 7 subtypes of JIA in terms of genome-wide variants.

In this subset-sensitive GWAS, we identified 15 genome-wide significant loci shared between certain JIA subtypes. We further identified candidate drug targets with drug repurposing opportunities based on genetic associations. The integrative genetic analysis results presented provide new insight into the biologic differences between JIA subtypes and suggest therapeutic targets.

PATIENTS AND METHODS

Dr. Hakonarson will provide access to data upon reasonable request.

Study population. Subjects were recruited for the JIA cohort in the US, Australia, and Norway and the cohort comprised a total of 1,485 patients with arthritis onset at age <16 years (Supplementary Table 1, available on the *Arthritis & Rheumatology* website at <http://onlinelibrary.wiley.com/doi/10.1002/art.42129>). JIA diagnoses and subtypes were determined according to the revised ILAR criteria (5) and confirmed using the JIA calculator software (12), an algorithm-based tool adapted from the ILAR JIA criteria. Prior to standard quality control procedures and exclusion of patients of non-European ancestry, the JIA cohort was composed of 464 case subjects of self-reported

European ancestry from the Texas Scottish Rite Hospital for Children (Dallas, Texas) and Children's Mercy Kansas City Hospital (Kansas City, Missouri), 296 case subjects from the Children's Hospital of Philadelphia (Philadelphia, Pennsylvania), 221 case subjects from the Murdoch Children's Research Institute at the Royal Children's Hospital (Melbourne, Victoria, Australia), and 504 case subjects from Oslo University Hospital (Oslo, Norway). Age- and sex-matched control subjects were identified from the Children's Hospital of Philadelphia Center for Applied Genomics Biobank, ascertained by the exclusion of any patient with any International Classification of Diseases, Ninth Revision, codes for autoimmune disorders or immunodeficiency disorders. A subset of the current study subjects was described in a previous study (see Supplementary Table 1, <http://onlinelibrary.wiley.com/doi/10.1002/art.42129>) (13). This study did not contain personal medical information about an identifiable living individual.

Ethics statement. Ethics approval for this study was obtained from the Children's Hospital of Philadelphia research ethics Institutional Review Board (approval no. 16-013278) and the ethics boards at other collaborating centers. This study was carried out in accordance with nationally approved guidelines. Written informed assent or consent was obtained from all subjects and/or their legal guardians.

Genotyping. Genomic DNA was extracted from peripheral blood, and we performed sample quality control filtering before and after genotyping using standard methods. In our cohort, all samples were genotyped at the Center for Applied Genomics on HumanHap550 and HumanHap610 BeadChip arrays (Illumina). The single-nucleotide polymorphism (SNP) genotype was defined using BeadStudio (Illumina) with default parameters. To minimize population stratification, only individuals of self-reported European ancestry, further confirmed using principal components analysis, were included in the present study. Details of the principal components analysis are provided below.

Sample and SNP quality control. SNPs with a low genotyping rate (<95%), those with a low minor allele frequency (<0.01), or those with significant departure from the expected Hardy-Weinberg equilibrium ($P < 1 \times 10^{-6}$) were excluded. Samples with a low overall genotyping call rate (<95%) or those determined to be from patients of European ancestry who were considered to be outliers according to principal components analysis (detailed below) were removed. In addition, one of each pair of related individuals, as determined using identity-by-state analysis ($PI_HAT > 0.1875$), was excluded, with cases preferentially retained when possible. We conducted case-case comparison by performing association testing between the case groups in each of the 4 cohorts. Any SNP with an association indicated by $P < 1 \times 10^{-5}$, which suggests significant differences in allele frequency between 2 cohorts, was excluded from further analyses.

(Supplementary Tables 2 and 3, <http://onlinelibrary.wiley.com/doi/10.1002/art.42129>).

Principal components analysis. To assess ethnicity, we combined our SNP data together with the HapMap data set to conduct a principal components analysis. We took the set of SNPs common to both data sets and narrowed them down using Plink command “--indep-pairwise 50 10 0.2.” We conducted principal components analysis on the data set with the narrowed-down SNPs via Plink (14). K-means clustering was used to group subjects into distinct populations of ethnic origin, and subjects of European ancestry were identified. A principal components analysis was similarly conducted among subjects of European ancestry in our data set again to determine within-population structure (Supplementary Figure 1, <http://onlinelibrary.wiley.com/doi/10.1002/art.42129>).

Genome-wide SNP imputation. We used Shapelt (15) for whole-chromosome pre-phasing and IMPUTE2 for imputation of the 1000 Genomes Project reference panel (URL: https://mathgen.stats.ox.ac.uk/impute/impute_v2.html [June 2014 haplotype release]). For both, we used parameters suggested by the software developers and described elsewhere (15,16). Imputation was conducted for each 5-Mb regional chunk across the genome, and data were subsequently merged for association testing. Prior to imputation, all SNPs were filtered using the criteria described above. We filtered out SNPs with an Info score <0.8, Hardy-Weinberg equilibrium test with a significance $P < 1 \times 10^{-6}$, and overall minor allele frequency <0.01.

Association analysis. We performed whole-genome association testing using post-imputation genotype probabilities with the score test implemented in SNPTTEST software version 2.5. In all analyses, we adjusted for both sex and ancestry with conditioning for sex and the first 9 principal components derived from the Plink principal components analysis, which yielded λ_{GC} values within acceptable limits for all disease subtype cohorts. The extent of population stratification was assessed using a quantile–quantile plot of the test statistics and by calculating inflation factor λ_S .

Heterogeneity-sensitive meta-analysis. To identify genetic loci that were associated with multiple JIA subtypes and determine the subtype combination that each locus was most strongly associated with, “h.types” and “h.traits” in the R statistical software package ASSET (17) were applied to an exhaustive disease subtype model search, which has been described in detail in our previous study and in other studies (18,19). Briefly, the different combinations of JIA subtypes were exhaustively enumerated and tested for associations with each locus. The combination that yielded the most significant association statistics was selected as the best disease subtype model. A score test

implemented in R package ASSET was used in the “h.types” approach, with adjustment for covariates in the analysis. In our analyses, the “h.types” and “h.traits” methods yielded similar results. We used the discrete local maximum method of correction for multiple testing across all subtype combinations. The contribution of each non-null study to the shared association was measured using the absolute value of the weighted Z statistics $|\sqrt{\pi_k(S)}Z_k|$, in which $\pi_k(S) = n_k / \sum_{k \in S} n_k$ represented the sample size of k^{th} subtype relative to the total sample size of the subtypes of the most significantly associated subtype combination S.

Fine-mapping. Fine-mapping was performed using FINEMAP version 1.3.1 (20). We used GWAS summary statistics and SNP Pearson’s correlation matrixes calculated from genotyped data from the same individuals as input in FINEMAP. We used the default parameter setting with the maximum number of allowed causal SNPs as 5. Candidate causal SNPs with posterior probability >0.2 and heterogeneity-sensitive GWAS with $P < 10^{-4}$ were selected.

Pathway and protein–protein interaction network analysis. The overrepresentation pathway analysis of the 16 candidate genes at 15 genome-wide significant loci was conducted using a web portal WEB-based gene set analysis toolkit (URL: <http://www.webgestalt.org/>). The protein–protein interaction network visualization analysis and competitive pathway enrichment analysis based on genome-wide, summary-level data were performed using GSA-SNP2 (URL: <https://sites.google.com/view/gsasnp2>). Highly correlated adjoining genes were combined based on linkage disequilibrium in the 1000 Genomes European population. The default setting of GSA-SNP2 was used to define each gene region and gene transcript region 20 kb upstream and downstream. The collection of gene set databases included BioCarta, KEGG, the Reactome database, and Molecular Signatures Database Pathway Interaction Database. We used the STRING database for network construction and visualization. The significance threshold was defined as $q < 0.05$ after correction for multiple testing. Significance, defined as a gene score <0.005 and $q < 0.05$, was chosen for constructing a global visual network.

HLA imputation. SNPs within the HLA region, spanning 29–34 Mb on chromosome 6 of the human (hg19) reference genome, were extracted after SNP array data had been quality control filtered. Data from all JIA subjects and controls were imputed together using SNP2HLA software (URL: <http://www.broadinstitute.org/mpg/snp2hla/>) with the Type 1 Diabetes Genetics Consortium reference panel. We also conducted a case–case comparison of the HLA alleles by performing association testing between the case groups in each of the 4 cohorts. Any HLA alleles with an association indicated by $P < 1 \times 10^{-5}$, which suggested significant differences in allele frequency

between 2 cohorts, were excluded from further analyses. The HLA allele frequencies at a 2-digit level were compared between cases and controls for each JIA subtype, with the odds ratio and *P* value for the association derived from a chi-square test of the 2 × 2 table.

RESULTS

Identification of novel pleiotropic JIA loci through a heterogeneity-sensitive GWAS. Our JIA case–control cohort included 1,485 JIA cases (including all 7 JIA subtypes) and 10,352 controls with no history of any existing autoimmune or immune-mediated disease (Figure 1 and Supplementary Table 1, <http://onlinelibrary.wiley.com/doi/10.1002/art.42129>). A total of 506,520 genotyped SNPs from 1,245 JIA cases and 9,250 controls passed quality control filtering (Supplementary Figure 1, <http://onlinelibrary.wiley.com/doi/10.1002/art.42129>).

To optimize study power, after imputation, we performed a heterogeneity-sensitive GWAS (17) across JIA cases in 7 JIA subtypes and the pool of shared control samples. The heterogeneity-sensitive GWAS approach was used to first test every SNP that passed quality control to identify the most strongly associated disease combinations at each SNP, with the discrete local maximum method applied for adjustment for multiple testing. This approach has been successfully used to assess the complex relationships between pediatric autoimmune diseases (18) and neuropsychiatric disorders (19). We included the first 9 principal components as covariates, and the resulting genomic inflation factor for the final heterogeneity-sensitive GWAS results was 1.01 (Supplementary Figure 2 and Supplementary Table 4, <http://onlinelibrary.wiley.com/doi/10.1002/art.42129>), suggesting that population stratification was well controlled. Our results showed that the majority of the association loci reported in previous studies was replicated in our

study. Among the 120 association signals reported in the GWAS Catalog, including those with marginal genome-wide significance ($5 \times 10^{-8} < P < 1 \times 10^{-6}$), 81.0% were replicated in our study at least at a nominal significance level (Supplementary Data 1, <http://onlinelibrary.wiley.com/doi/10.1002/art.42129>).

We observed 15 loci surpassing the genome-wide significance threshold (Figure 2), in addition to strong association signals at the major histocompatibility complex (MHC) region (the 29–34-Mb region on chromosome 6). Five of the 15 genome-wide significant loci overlapped with previously reported autoimmune disease loci (Supplementary Table 5, <http://onlinelibrary.wiley.com/doi/10.1002/art.42129>), and the remaining 10 were novel JIA loci (Table 1) (for regional association plots, see Figure 3 and Supplementary Figure 3, <http://onlinelibrary.wiley.com/doi/10.1002/art.42129>).

The genome-wide significant association of all 15 loci was attributed to associations at a nominal significance level in 2 or more JIA subtypes (Supplementary Figure 4 and Supplementary Table 6 and 7, <http://onlinelibrary.wiley.com/doi/10.1002/art.42129>), including those shared between systemic arthritis and other JIA subtypes. In addition, we observed 25 SNPs with marginal genome-wide significance in our heterogeneity-sensitive GWAS, with 24 shared between 2 or more JIA subtypes at a nominal significance level (Supplementary Table 8, <http://onlinelibrary.wiley.com/doi/10.1002/art.42129>). Thus, our findings support a common genetic basis among JIA subtypes in addition to distinct clinical and molecular features.

Replication of the novel JIA loci. After examining UK Biobank data sets, we found a significant, genome-wide association between SNP rs7731626 and RA. Interestingly, SNP rs12203592 is strongly associated with an RF level >16 IU/ml, while in our study rs12203592 was more strongly associated with

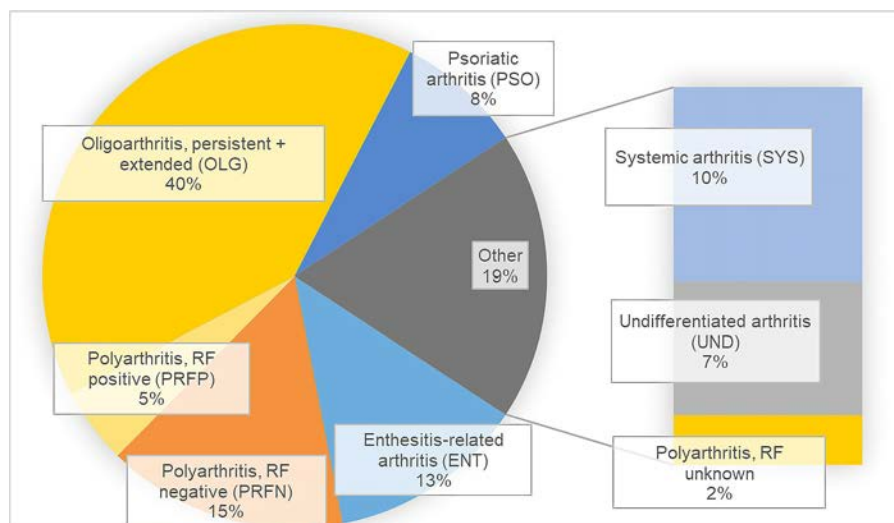


Figure 1. Distribution of juvenile idiopathic arthritis (JIA) subtypes represented in our JIA case–control cohort. RF = rheumatoid factor. Color figure can be viewed in the online issue, which is available at <http://onlinelibrary.wiley.com/doi/10.1002/art.42129/abstract>.

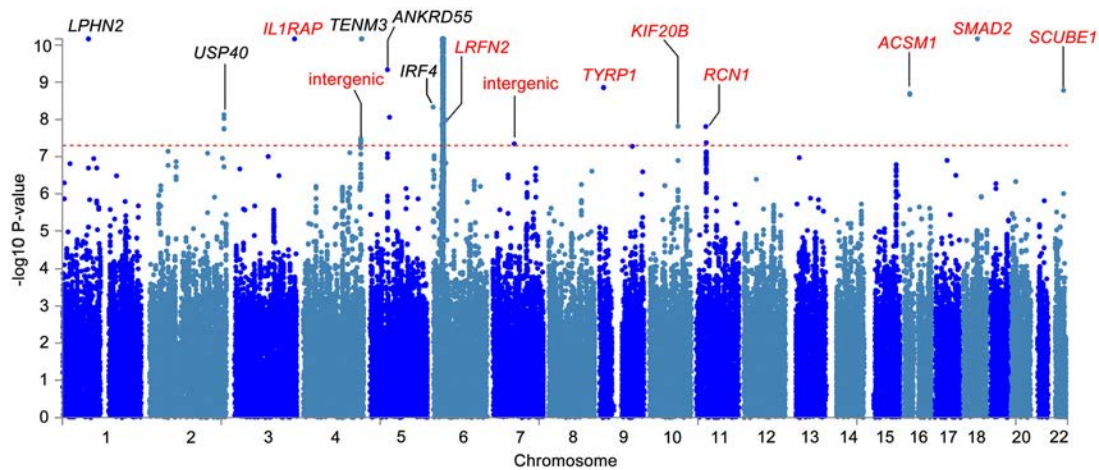


Figure 2. Manhattan plot showing association statistics for the heterogeneity-sensitive genome-wide association study of juvenile idiopathic arthritis subtypes, with adjustment for multiple testing. Candidate gene symbols for genome-wide significant loci are shown, with novel loci indicated in red. Symbols represent individual genes. Color figure can be viewed in the online issue, which is available at <http://onlinelibrary.wiley.com/doi/10.1002/art.42129/abstract>.

RF-negative PA and oligoarthritis than the other JIA subtypes. In addition, a significant, genome-wide association between SNP rs7660520 and psoriasis was shown. In our data set, this SNP was associated with multiple JIA subtypes, including PsA. In the UK Biobank, rs114664970, a novel, genome-wide significant SNP identified in our study, was associated with chronic sinusitis, severe cases of which could be symptomatic of autoimmune diseases (Supplementary Table 9, <http://onlinelibrary.wiley.com/doi/10.1002/art.42129>). The index SNPs at other loci were also associated with established autoimmune or immune-mediated musculoskeletal system conditions. We examined ImmunoChip (IC) data that had previously been reported by Hinks et al (2). At only 2 regions, there were SNPs within 250 kb upstream/downstream of our heterogeneity-sensitive GWAS SNPs rs12203592 and rs7731626 with $r^2 > 0.5$. These SNPs were associated with JIA according to the IC data (Supplementary Table 10, <http://onlinelibrary.wiley.com/doi/10.1002/art.42129>).

Fine-mapping and functional annotation of novel loci.

We conducted fine-mapping for each novel loci. Ten SNPs were identified as candidate causal variants (Supplementary Table 11, <http://onlinelibrary.wiley.com/doi/10.1002/art.42129>). We conducted functional annotation of all index SNPs, candidate causal variants, and leading SNPs at marginally genome-wide significant loci in the Encyclopedia of DNA Elements and Roadmap Epigenomics databases and found overlap between these SNPs/loci and chromatin marks or DNase I-hypersensitive sites, likely playing a role in regulating target gene expression (Supplementary Figure 5, <http://onlinelibrary.wiley.com/doi/10.1002/art.42129>).

We mapped index SNPs to candidate genes according to expression quantitative trait locus (eQTL) data and high-throughput chromosome conformation capture (3C) data (Supplementary Figures 6–8, <http://onlinelibrary.wiley.com/doi/10.1002/art.42129>),

and the most likely candidate genes at genome-wide significant loci are indicated in Figure 2. Highly significant eQTL relationships were observed between heterogeneity-sensitive GWAS SNP gene pairs (rs7731626 and *ANKRD55*, rs7731626 and *IL6ST*, rs12203592 and *IRF4*) in different immune tissue and immune cell types (Supplementary Figures 6 and 7, <http://onlinelibrary.wiley.com/doi/10.1002/art.42129>). A strong eQTL relationship between rs12795402 and *RCN1* was also reported in the Biobank-based Integrative Omics Studies QTL database (21). The candidate gene or genes for other heterogeneity-sensitive GWAS SNPs were determined according to nominally significant eQTL and/or high-throughput 3C interactions (Supplementary Figure 8, <http://onlinelibrary.wiley.com/doi/10.1002/art.42129>). According to data from the Database of Immune Cell Expression, Expression quantitative trait loci and Epigenomics database, 14 candidate genes were expressed in diverse immune cell types at medium-to-high levels (Supplementary Figure 9, <http://onlinelibrary.wiley.com/doi/10.1002/art.42129>), suggesting that both innate immunity and adaptive immunity are involved in JIA pathogenesis.

Association of HLA alleles and JIA subtypes.

According to the SNP genotype at the MHC region, we further imputed classic HLA alleles and examined their association with each JIA subtype after quality control filtering (Supplementary Table 12, <http://onlinelibrary.wiley.com/doi/10.1002/art.42129>). As expected, we found a highly significant association between HLA-B*27 and ERA. Multiple HLA alleles, such as HLA-B*40, HLA-DRB1*04, and HLA-DPB1*02, were significantly associated with >1 JIA subtype (Supplementary Table 13, <http://onlinelibrary.wiley.com/doi/10.1002/art.42129>). Additional HLA alleles were associated with JIA subtypes that surpassed the multiple testing-adjusted significance threshold. We conducted stepwise

Table 1. Summary statistics of the independent, genome-wide significant loci*

SNP	Chromosome	Position†	Candidate gene(s)	A1	MAF	P_{adj}	Associated subtypes
rs2066363	1	82237577	<i>LPHN2</i>	T	0.310	6.82×10^{-11}	ERA, RF-negative PA, RF-positive PA, oligoarthritis, PsA, systemic arthritis, UA
rs144844686	2	234576970	<i>USP40</i>	T	0.029	7.40×10^{-9}	RF-negative PA, oligoarthritis, PsA
rs7636581‡	3	189781195	<i>IL1RAP, CLDN1</i>	A	0.120	6.82×10^{-11}	RF-negative PA, oligoarthritis, PsA
rs13119493‡	4	180911259	Intergenic	G	0.048	3.26×10^{-8}	RF-negative PA, oligoarthritis
rs7660520	4	183745321	<i>DCTD, TENM3</i>	A	0.270	6.82×10^{-11}	ERA, RF-negative PA, RF-positive PA, oligoarthritis, PsA, systemic arthritis, UA
rs7731626	5	55444683	<i>ANKRD55, IL6ST</i>	A	0.380	4.62×10^{-10}	RF-negative PA, oligoarthritis, PsA
rs12203592	6	396321	<i>IRF4</i>	T	0.190	4.62×10^{-9}	ERA, RF-negative PA, oligoarthritis, systemic arthritis, UA
rs114664970‡	6	40127169	<i>LRFN2</i>	C	0.012	1.03×10^{-8}	PsA, systemic arthritis
rs727845‡	7	67607209	Intergenic	G	0.190	4.49×10^{-8}	ERA, RF-negative PA, RF-positive PA, oligoarthritis, UA
rs7042370‡	9	12785073	<i>TYRP1</i>	C	0.440	1.39×10^{-9}	ERA, RF-positive PA, oligoarthritis, PsA, systemic arthritis
rs117572873‡	10	91997663	<i>KIF20B</i>	G	0.011	1.52×10^{-8}	RF-positive PA, oligoarthritis
rs12795402‡	11	32255936	<i>RCN1</i>	C	0.340	4.19×10^{-8}	RF-negative PA, RF-positive PA, oligoarthritis
rs147585949‡	16	20726695	<i>ACSM1</i>	A	0.014	1.98×10^{-9}	ERA, RF-negative PA, PsA
rs11663074‡	18	45023793	<i>SMAD2</i>	C	0.170	6.82×10^{-11}	ERA, RF-negative PA, RF-positive PA, oligoarthritis, PsA, systemic arthritis, UA
rs138816451‡	22	43649657	<i>SCUBE1</i>	A	0.016	1.63×10^{-9}	RF-negative PA, oligoarthritis, PsA, UA

* SNP = single-nucleotide polymorphism; A1 = alternative allele; MAF = minor allele frequency; P_{adj} = adjusted P value; ERA = enthesitis-related arthritis; RF = rheumatoid factor; PA = polyarthritis; PsA = psoriatic arthritis; UA = undifferentiated arthritis.

† Position is measured in bp.

‡ Novel locus.

conditional analyses for each JIA subtype. Similar to results reported by Hink et al (22), we observed >2 independent effects across the MHC region in RF-negative PA and oligoarthritis.

In addition, multiple independent association signals were detected within the HLA-DRB1 gene (Supplementary Table 14, <http://onlinelibrary.wiley.com/doi/10.1002/art.42129>).

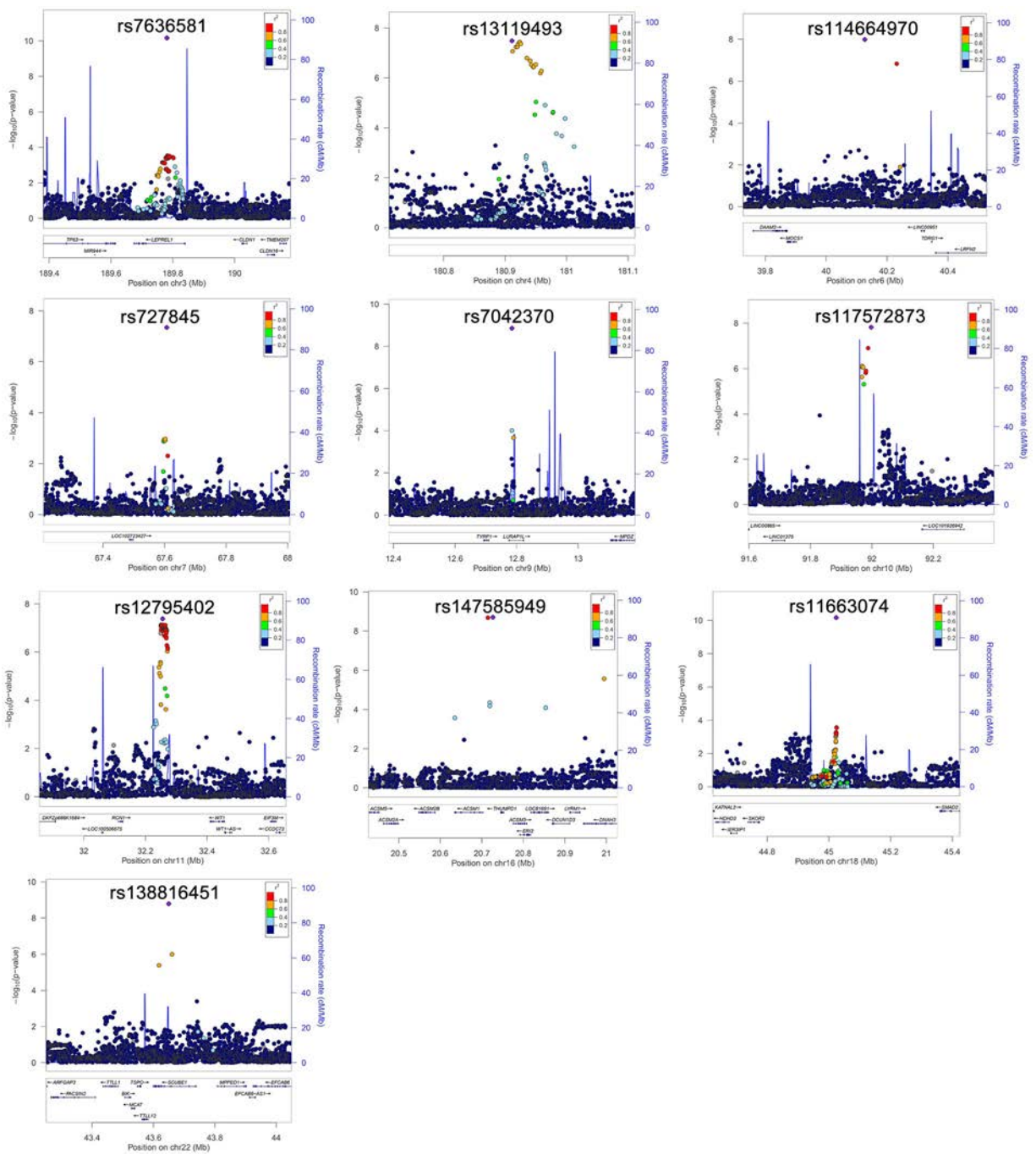


Figure 3. Regional association plots showing novel juvenile idiopathic arthritis genome-wide significant loci. Color-coded symbols represent individual genes showing an association at different thresholds of significance. Color figure can be viewed in the online issue, which is available at <http://onlinelibrary.wiley.com/doi/10.1002/art.42129/abstract>.

Pathway enrichment and network analysis of genome-wide significant loci.

To better understand how these loci may contribute to JIA etiology, we performed pathway enrichment analyses and protein–protein interaction network analysis. We first investigated the most likely candidate genes of the 15 genome-wide significant loci using an overrepresentation analysis. The KEGG Th17 cell differentiation pathway was significantly overrepresented, with 4 candidate genes *SMAD2*, *IRF4*, *IL1RAP*,

and *IL6ST* in this pathway (Supplementary Table 15, <http://onlinelibrary.wiley.com/doi/10.1002/art.42129>). Subsequently, in investigating all the heterogeneity-sensitive GWAS results, we found enrichment of 81 KEGG, BioCarta, and Reactome pathways (Supplementary Data 2, <http://onlinelibrary.wiley.com/doi/10.1002/art.42129>), with pathways related to autoimmune diseases ranking at the top. These top-ranked pathways were mostly driven by the genes at the HLA locus on

chromosome 6. Protein–protein interaction network analysis revealed extensive interaction between immune genes centered on *TNF*, *NOS1*, and HLA genes (Supplementary Figure 10, <http://onlinelibrary.wiley.com/doi/10.1002/art.42129>).

Identification of candidate drug targets with drug repurposing opportunities among JIA-associated loci.

We searched drug target gene databases DrugBank (URL: <https://www.drugbank.ca/>), DrugCentral (URL: <http://drugcentral.org/>), and PharmGKB (URL: <https://www.pharmgkb.org/>) and found that candidate genes at multiple genome-wide significant loci are known targets of existing drugs, including several used for the treatment of arthritis, such as diflunisal, methotrexate, cyclosporine, and diclofenac (Supplementary Table 16, <http://onlinelibrary.wiley.com/doi/10.1002/art.42129>). These target genes of arthritis drugs support the biologic relevance of our study.

In addition, the high-throughput 3C data revealed evidence of chromatin interaction between rs7636581 and *IL1RAP*, suggesting that *IL1RAP* may be a candidate target gene of this locus. With regard to existing therapies, interleukin-1 (IL-1) antagonists (and IL-6 blockade) have been used for treatment of the systemic arthritis subtype and have been transformative in treating this JIA subtype (23). In our analysis, this locus was associated with oligoarthritis and PsA subtypes, suggesting potential application of IL-1 blockade for the treatment of these JIA subtypes in addition to systemic arthritis. Another interesting association was between rs7731626 and *IL6ST*, encoding glycoprotein 130, a coreceptor for many other cytokine receptor complexes besides IL-6 (24). This locus was associated with multiple JIA subtypes, including oligoarthritis, RF-negative PA, and PsA, suggesting that IL-6 blockade may be broadly effective for JIA subtypes. Indeed, tocilizumab is approved by the US Food and Drug Administration for treatment of both systemic arthritis and polyarticular JIA. Patients of both subtypes have shown significant improvements following tocilizumab treatment with confirmed efficacy and safety (25–27).

The association between rs138816451 and *SCUBE1* on chromosome 22 in the JIA subtypes UA, PsA, oligoarthritis, and RF-negative PA was intriguing, as signal peptide, CUB domain, and ECF-like domain containing protein 1 (SCUBE-1) has been implicated in playing a role in angiogenesis and is expressed and bound to the surface of endothelial cells (28). Findings have been reported suggesting that SCUBE-1, SCUBE-3, and vascular endothelial growth factor (VEGF) levels in serum may be a biomarker for angiogenesis (29), which is one of the pathogenic processes involved in psoriasis and arthritis, suggesting that drugs that block angiogenesis may be effective for treating arthritis and psoriasis/PsA (30,31).

DISCUSSION

JIA is a clinically important chronic autoimmune disease among children that causes significant morbidity. However, it

has not been as well studied as many other autoimmune diseases, mostly due to sample size limitations and the clinical heterogeneity of JIA. To address these limitations, we conducted a heterogeneity-sensitive GWAS accounting for phenotypic heterogeneity and identified novel pleiotropic loci shared among multiple JIA subtypes. We genetically illustrated how these loci may have joint or disparate effects on JIA disease subtype susceptibility, which sheds light on JIA pathogenesis and the development of targeted therapeutic approaches.

The significant enrichment of Th17 cell differentiation found in pathway analyses highlight the potential importance of this pathway in JIA etiology. Four candidate genes at genome-wide significant loci (*SMAD2*, *IL1RAP*, *IL6ST*, and *IRF4*) are involved in this pathway. SMAD family member 2 plays critical roles in Th1 cell development and in the generation of Th17 cells that drive the development of autoimmune diseases (32,33). The SNP rs80142631 at the *SMAD2* locus has been reported to be associated with eosinophil counts in the European ancestry patient population (34). IL-1 receptor accessory protein (IL1RAP) belongs to the IL-1 receptor complex. NF- κ B signaling pathway genes and other genes downstream of IL-1 play critical roles in Th17 cell differentiation. *IL6ST* and *IRF4* have both been associated with autoimmune and autoinflammatory diseases in previous studies, including Crohn's disease and RA. Th17 cells are a lineage of CD4+ T cells that secrete cytokines IL-17A and IL-17F, which are involved in the pathogenesis of both autoimmune diseases and inflammatory diseases (35).

Current JIA therapies mainly include disease-modifying antirheumatic drugs and pain therapies. Targeting the underlying causes of JIA may further enhance the effectiveness of therapeutic strategies, particularly for rare JIA subtypes. IL-1 signaling plays an important role in the regulation of proinflammatory reactions that are involved in various autoinflammatory diseases (36). The association between IL1RAP and oligoarthritis and PsA in our analyses suggests that this locus is a potential therapeutic target that might extend to JIA subtypes besides systemic arthritis. In a pilot clinical trial, IL-1 blockade was shown to improve symptoms among adult patients with PsA (37). Similarly, the association between *IL6ST* and multiple JIA subtypes suggests potential repurposing opportunities for anti-IL-6 for several JIA subtypes. In addition to tocilizumab, sarilumab, another antibody to the IL-6 receptor, has undergone testing for polyarticular JIA and systemic arthritis (38). The association between *SCUBE1* and several JIA subtypes (RF-negative PA, oligoarthritis, PsA, and UA) implicates a potential role of angiogenesis in JIA pathogenesis (30,39). Some antiinflammatory drugs, such as anti-tumor necrosis factor and anti-IL-6, have dual roles in blocking both inflammation and angiogenesis (40,41). Drugs that target angiogenesis/vascularization (e.g., anti-VEGF, anti-TIE2, and anti-angiopoietins) may also have a role in these JIA subtypes, but additional experiments and clinical trials should be conducted to clarify this role (42). The identification of associated variants,

candidate genes, and pathways shared between JIA subtypes may lead to the selection of drug repurposing candidates.

There are several limitations of our study. First, the sample size was limited compared to GWAS on complex human diseases and previous GWAS on JIA (2,11). Second, phenotypic heterogeneity may affect study power. Despite these limitations, in this study, we identified several novel loci, likely owing to the strong genetic contribution to pediatric diseases and improved methodology. Compared to GWAS in adult patients, pediatric disease-expressing phenotypes in early life are typically associated with much stronger gene signals than diseases presenting later in life that are often critically impacted by gene–environment interactions. In addition, our study utilized improved methodology (e.g., heterogeneity-sensitive meta-analysis) and integrative genetic analysis. For example, it is plausible that certain SNPs may either be associated with only some disease subtypes or have opposite effects across JIA subtypes. Thus, using a heterogeneity-sensitive GWAS study method considers JIA subtype heterogeneity, boosts study power, and enables the identification of novel loci associated with JIA.

In summary, we identified novel genetic loci with pleiotropic effects across multiple JIA subtypes. Functional annotation indicates that candidate genes at these loci are expressed in diverse immune cell types, which is consistent with their potential role in JIA pathogenesis. In silico analyses suggest that there may be drug repurposing opportunities for rare JIA subtypes, and JIA subtypes may benefit from shared therapeutic approaches according to potential underlying genetic mechanisms.

ACKNOWLEDGMENT

We would like to thank all the patients for their participation in our study.

AUTHOR CONTRIBUTIONS

All authors were involved in drafting the article or revising it critically for important intellectual content, and all authors approved the final version to be published. Dr. Hakonarson had full access to all of the data in the study and takes responsibility for the integrity of the data and the accuracy of the data analysis.

Study conception and design. Jin Li, Y. Li, Hakonarson.

Acquisition of data. Abrams, Connolly, Flatø, Thompson, Langefeld, Lie, Munro, Wise, Hakonarson.


Analysis and interpretation of data. Jin Li, Y. Li, Glessner, Yang, March, Kao, Vaccaro, Bradfield, Junyi Li, Mentch, Qu, Qi, Chang, Hou, Qiu, Wei, Wang, Snyder, Sleiman, Hakonarson.

REFERENCES

- Prakken B, Albani S, Martini A. Juvenile idiopathic arthritis. *Lancet* 2011;377:2138–49.
- Hinks A, Cobb J, Marion MC, Prahalad S, Sudman M, Bowes J, et al. Dense genotyping of immune-related disease regions identifies 14 new susceptibility loci for juvenile idiopathic arthritis. *Nat Genet* 2013;45:664–9.
- Ombrello MJ, Arthur VL, Remmers EF, Hinks A, Tachmazidou I, Grom AA, et al. Genetic architecture distinguishes systemic juvenile idiopathic arthritis from other forms of juvenile idiopathic arthritis: clinical and therapeutic implications. *Ann Rheum Dis* 2017;76:906–13.
- Hinks A, Marion MC, Cobb J, Comeau ME, Sudman M, Ainsworth HC, et al. The genetic profile of rheumatoid factor-positive polyarticular juvenile idiopathic arthritis resembles that of adult rheumatoid arthritis. *Arthritis Rheumatol* 2018;70:957–62.
- Petty RE, Southwood TR, Manners P, Baum J, Glass DN, Goldenberg J, et al. International League of Associations for Rheumatology classification of juvenile idiopathic arthritis: second revision, Edmonton, 2001. *J Rheumatol* 2004;31:390–2.
- Martini A, Ravelli A, Avcin T, Beresford MW, Burgos-Vargas R, Cuttica R, et al. Toward new classification criteria for juvenile idiopathic arthritis: first steps, Pediatric Rheumatology International Trials Organization International Consensus. *J Rheumatol* 2019;46:190–7.
- Zaripova LN, Midgley A, Christmas SE, Beresford MW, Baildam EM, Oldershaw RA. Juvenile idiopathic arthritis: from aetiopathogenesis to therapeutic approaches. *Pediatr Rheumatol Online J* 2021;19:135.
- Mistry RR, Patro P, Agarwal V, Misra DP. Enthesitis-related arthritis: current perspectives. *Open Access Rheumatol* 2019;11:19–31.
- Cimaz R. Systemic-onset juvenile idiopathic arthritis. *Autoimmun Rev* 2016;15:931–4.
- Mo A, Marigorta UM, Arafat D, Chan LH, Ponder L, Jang SR, et al. Disease-specific regulation of gene expression in a comparative analysis of juvenile idiopathic arthritis and inflammatory bowel disease. *Genome Med* 2018;10:48.
- López-Isaac E, Smith SL, Marion MC, Wood A, Sudman M, Yarwood A, et al. Combined genetic analysis of juvenile idiopathic arthritis clinical subtypes identifies novel risk loci, target genes and key regulatory mechanisms. *Ann Rheum Dis* 2020;80:321–8.
- Behrens EM, Beukelman T, Cron RQ. Juvenile idiopathic arthritis classification criteria: loopholes and diagnosis software. *J Rheumatol* 2007;34:234.
- Finkel TH, Li J, Wei Z, Wang W, Zhang H, Behrens EM, et al. Variants in CXCR4 associate with juvenile idiopathic arthritis susceptibility. *BMC Med Genet* 2016;17:24.
- Purcell S, Neale B, Todd-Brown K, Thomas L, Ferreira MA, Bender D, et al. PLINK: a tool set for whole-genome association and population-based linkage analyses. *Am J Hum Genet* 2007;81:559–75.
- Howie BN, Donnelly P, Marchini J. A flexible and accurate genotype imputation method for the next generation of genome-wide association studies. *PLoS Genet* 2009;5:e1000529.
- Delaneau O, Coulonges C, Zagury JF. Shape-IT: new rapid and accurate algorithm for haplotype inference. *BMC Bioinformatics* 2008; 9:540.
- Bhattacharjee S, Rajaraman P, Jacobs KB, Wheeler WA, Melin BS, Hartge P, et al. A subset-based approach improves power and interpretation for the combined analysis of genetic association studies of heterogeneous traits. *Am J Hum Genet* 2012;90:821–35.
- Li YR, Li J, Zhao SD, Bradfield JP, Mentch FD, Maggadottir SM, et al. Meta-analysis of shared genetic architecture across ten pediatric autoimmune diseases. *Nat Med* 2015;21:1018–27.
- Cross-Disorder Group of the Psychiatric Genomics Consortium. Genomic relationships, novel loci, and pleiotropic mechanisms across eight psychiatric disorders. *Cell* 2019;179:1469–82.
- Benner C, Spencer CC, Havulinna AS, Salomaa V, Ripatti S, Pirinen M. FINEMAP: efficient variable selection using summary data from genome-wide association studies. *Bioinformatics* 2016;32: 1493–501.
- Zhernakova DV, Deelen P, Vermaat M, van Iterson M, van Galen M, Arindrarto W, et al. Identification of context-dependent expression quantitative trait loci in whole blood. *Nat Genet* 2017;49:139–45.

22. Hinks A, Bowes J, Cobb J, Ainsworth HC, Marion MC, Comeau ME, et al. Fine-mapping the MHC locus in juvenile idiopathic arthritis (JIA) reveals genetic heterogeneity corresponding to distinct adult inflammatory arthritic diseases. *Ann Rheum Dis* 2017;76:765–72.
23. Dinarello CA, Simon A, van der Meer JW. Treating inflammation by blocking interleukin-1 in a broad spectrum of diseases. *Nat Rev Drug Discov* 2012;11:633–52.
24. Silver JS, Hunter CA. Gp130 at the nexus of inflammation, autoimmunity, and cancer [review]. *J Leukoc Biol* 2010;88:1145–56.
25. Yokota S, Itoh Y, Morio T, Origasa H, Sumitomo N, Tomobe M, et al. Tocilizumab in systemic juvenile idiopathic arthritis in a real-world clinical setting: results from 1 year of postmarketing surveillance follow-up of 417 patients in Japan. *Ann Rheum Dis* 2016;75:1654–60.
26. Yokota S, Imagawa T, Mori M, Miyamae T, Aihara Y, Takei S, et al. Efficacy and safety of tocilizumab in patients with systemic-onset juvenile idiopathic arthritis: a randomised, double-blind, placebo-controlled, withdrawal phase III trial. *Lancet* 2008;371:998–1006.
27. Brunner HI, Ruperto N, Zuber Z, Keane C, Harari O, Kenwright A, et al, for the Paediatric Rheumatology International Trials Organisation (PRINTO) and the Pediatric Rheumatology Collaborative Study Group (PRCSG). Efficacy and safety of tocilizumab in patients with polyarticular-course juvenile idiopathic arthritis: results from a phase 3, randomised, double-blind withdrawal trial. *Ann Rheum Dis* 2015;74:1110–7.
28. Yang RB, Ng CK, Wasserman SM, Colman SD, Shenoy S, Mehraban F, et al. Identification of a novel family of cell-surface proteins expressed in human vascular endothelium. *J Biol Chem* 2002;277:46364–73.
29. Capkin AA, Demir S, Mentese A, Bulut C, Ayar A. Can signal peptide-CUB-EGF domain-containing protein (SCUBE) levels be a marker of angiogenesis in patients with psoriasis? *Arch Dermatol Res* 2017;309:203–7.
30. Elshabrawy HA, Chen Z, Volin MV, Ravella S, Virupannavar S, Shahrara S. The pathogenic role of angiogenesis in rheumatoid arthritis. *Angiogenesis* 2015;18:433–48.
31. Cantatore FP, Maruotti N, Corrado A, Ribatti D. Angiogenesis dysregulation in psoriatic arthritis: molecular mechanisms. *Biomed Res Int* 2017;2017:5312813.
32. Martinez GJ, Zhang Z, Reynolds JM, Tanaka S, Chung Y, Liu T, et al. Smad2 positively regulates the generation of Th17 cells. *J Biol Chem* 2010;285:29039–43.
33. Malhotra N, Kang J. SMAD regulatory networks construct a balanced immune system. *Immunology* 2013;139:1–10.
34. Kichaev G, Bhatia G, Loh PR, Gazal S, Burch K, Freund MK, et al. Leveraging polygenic functional enrichment to improve GWAS power. *Am J Hum Genet* 2019;104:65–75.
35. Maddur MS, Miossec P, Kaveri SV, Bayry J. Th17 cells: biology, pathogenesis of autoimmune and inflammatory diseases, and therapeutic strategies. *Am J Pathol* 2012;181:8–18.
36. Gabay C, Lamacchia C, Palmer G. IL-1 pathways in inflammation and human diseases. *Nat Rev Rheumatol* 2010;6:232–41.
37. Jung N, Hellmann M, Hoheisel R, Lehmann C, Haase I, Perniok A, et al. An open-label pilot study of the efficacy and safety of anakinra in patients with psoriatic arthritis refractory to or intolerant of methotrexate (MTX). *Clin Rheumatol* 2010;29:1169–73.
38. Pelechas E, Voulgari PV, Drosos AA. Clinical evaluation of the safety, efficacy and tolerability of sarilumab in the treatment of moderate to severe rheumatoid arthritis. *Ther Clin Risk Manag* 2019;15:1073–9.
39. Swidrowska-Jaros J, Smolewska E. A fresh look at angiogenesis in juvenile idiopathic arthritis. *Cent Eur J Immunol* 2018;43:325–30.
40. Kim Y, Yi H, Jung H, Rim YA, Park N, Kim J, et al. A dual target-directed agent against interleukin-6 receptor and tumor necrosis factor alpha ameliorates experimental arthritis. *Sci Rep* 2016;6:20150.
41. Cantatore FP, Maruotti N, Corrado A, Ribatti D. Anti-angiogenic effects of biotechnological therapies in rheumatic diseases. *Biologics* 2017;11:123–8.
42. Schonthaler HB, Huggenberger R, Wculek SK, Detmar M, Wagner EF. Systemic anti-VEGF treatment strongly reduces skin inflammation in a mouse model of psoriasis. *Proc Natl Acad Sci U S A* 2009;106:21264–9.

Racial Disparities in Renal Outcomes Over Time Among Hospitalized Children With Systemic Lupus Erythematosus

Joyce C. Chang,¹  Cora Sears,² Veronica Torres,³ and Mary Beth F. Son⁴

Objective. Racial and ethnic minority groups have excess morbidity related to renal disease in pediatric-onset systemic lupus erythematosus (SLE). This study was undertaken to evaluate temporal trends in renal outcomes and racial disparities among hospitalized children with SLE over a period of 14 years.

Methods. We identified patients 21 years old or younger with discharge diagnoses of SLE in the Pediatric Health Information System inpatient database (2006–2019). Adverse renal outcomes included end-stage renal disease (ESRD), dialysis, or transplant, analyzed as a composite and separately. We estimated the odds of adverse renal outcomes at any hospitalization or the first occurrence of an adverse renal outcome, adjusted for calendar period, patient characteristics, and clustering by hospital. We tested whether racial disparities differed by calendar period.

Results. There were 20,893 admissions for 7,434 SLE patients, of which 32%, 16%, 12%, and 8% were Black, Hispanic White, Hispanic Other, and Asian, respectively. Proportions of admissions with adverse renal outcomes decreased over time ($P < 0.01$). Black children remained at the highest risk of adverse renal outcomes at any admission (odds ratio [OR] 2.5 [95% confidence interval (95% CI) 1.8–3.5] versus non-Hispanic White patients). Black and Asian children remained at a higher risk of incident adverse renal outcomes, driven by ESRD among Black children (OR 1.6 [95% CI 1.2–2.1]) and dialysis among Asians (OR 1.7 [95% CI 1.1–2.7]). Relative disparities did not change significantly over time.

Conclusion. Significant reductions in ESRD and dialysis occurred over time for children with SLE across all racial and ethnic groups. The lack of corresponding reductions in racial disparities highlights the need for targeted interventions to achieve greater treatment benefit among higher risk groups.

INTRODUCTION

The burden of pediatric-onset systemic lupus erythematosus (SLE) and its comorbidities falls disproportionately on racial and ethnic minority groups. Children with SLE from historically marginalized groups have a higher incidence of disease, have a younger age of disease onset, and are more likely to have severe renal disease (1–5). As of 2006, Black children accounted for nearly half of all children in the US with end-stage renal disease (ESRD) due to lupus (6). Similarly, in the LUMINA (LUpus in Minorities, NAture versus nurture) cohort, renal damage occurred more frequently among Hispanic and Black individuals (4).

Over the last 2 decades, there have been several advances in the care of children with lupus, including an expansion of

therapeutic options and increasing emphasis on quality metrics that may be associated with improved renal outcomes (7). Mycophenolate mofetil (MMF) has become a mainstay of therapy for pediatric lupus nephritis (8), and the use of B cell–depleting therapies has also become increasingly common (9). Simultaneously, several consensus guidelines for management of pediatric lupus have been released (10,11). It is unclear what impact these advances have made on renal outcomes of pediatric lupus. Moreover, treatment advances have potential to either decrease or exacerbate existing racial inequities. Advances in care that fail to reach underserved groups could result in widening disparities, as previously observed in some pediatric cancers (12). Conversely, targeted treatments have the potential to reduce disparity if, for example, instituting a therapeutic intervention such as MMF

Dr. Chang's work was supported by the National Heart, Lung, and Blood Institute, NIH (grant K23-HL-148539). Dr. Son's work was supported by the Samara Jan Turkel Clinical Center for Pediatric Autoimmune Diseases.

¹Joyce C. Chang, MD, MSCE: Children's Hospital of Philadelphia, Philadelphia, Pennsylvania, Boston Children's Hospital, Boston, Massachusetts, and Harvard Medical School, Cambridge, Massachusetts; ²Cora Sears, MPH: Children's Hospital of Philadelphia, Philadelphia, Pennsylvania; ³Veronica Torres, MPH: Temple University, Philadelphia, Pennsylvania; ⁴Mary Beth F. Son, MD: Boston Children's Hospital and Harvard Medical School, Boston, Massachusetts.

Author disclosures are available at <https://onlinelibrary.wiley.com/action/downloadSupplement?doi=10.1002%2Fart.42127&file=art42127-sup-0001-Disclosureform.pdf>.

Address correspondence to Joyce C. Chang, MD, MSCE, 320 Longwood Avenue, Boston, MA 02115. Email: Joyce.Chang@childrens.harvard.edu.

Submitted for publication November 1, 2021; accepted in revised form March 22, 2022.

conferred greater benefit to racial and ethnic minority groups, as suggested in the Aspreva Lupus Management Study (13).

The objectives of this epidemiologic study included the following: 1) to describe trends in renal outcomes over time from 2006 to 2019 among hospitalized children with SLE, and 2) to determine whether the rate of change in renal outcomes has differed by race or ethnicity. We hypothesized that hospitalizations related to adverse renal outcomes have decreased in the setting of overall advances in pediatric lupus care and that these changes over time may have affected racial and ethnic minority groups differently.

PATIENTS AND METHODS

Data source. The Pediatric Health Information System (PHIS) inpatient database contains de-identified information from 50 free-standing pediatric hospitals in the US, including demographic data, inpatient International Classification of Diseases, Ninth Revision Clinical Modification (ICD-9-CM)/ICD-10-CM diagnosis codes, procedure codes, dates of service, discharge disposition, and indicator variables for certain comorbidities classified by diagnosis groups. For this study, data on inpatient admissions from January 1, 2006 to December 31, 2019 were extracted from the database version as of July 1, 2020. This study was granted an exemption by the Children's Hospital of Philadelphia Institutional Review Board for secondary use of data.

Study population. We identified patients with a primary or secondary ICD-9/ICD-10-CM discharge diagnosis for SLE (710.0, M32.1x, M32.8, M32.9) who were admitted to a PHIS hospital at least once from 2006 to 2019. All patients were between the ages of 5 and 21 years at the time of the index admission, which was defined as the first admission assigned an SLE code at any PHIS hospital during the study period. Admissions with less than a 24-hour length of stay, in addition to those with a code for cyclophosphamide, were excluded.

Study measures. The primary outcome measure was a composite measure of adverse renal outcomes, defined as assignment of an ESRD diagnosis code, a procedure code for dialysis, or renal transplant. ESRD, dialysis, and renal transplant were also each modeled as separate secondary outcomes. The ICD-9 to ICD-10 Procedure Coding System crosswalk for all codes used are provided in Supplementary Table 1, available on the *Arthritis & Rheumatology* website at <https://onlinelibrary.wiley.com/doi/10.1002/art.42127>.

The exposures of interest were calendar period and racial or ethnic category. Due to the presence of interactions between race and Hispanic ethnicity, as well as changes over time in the reporting of race among those of Hispanic ethnicity, the following combined racial and ethnic categories were determined a priori for use in the primary analysis: Asian/Pacific Islander, Black, Hispanic

Other, Hispanic White, Non-Hispanic Other (including a small number of patients reported as American Indian), and Non-Hispanic White (reference group). Race and ethnicity data are submitted by contributing hospitals according to hospital-specific procedures, including self-reported race and ethnicity at the time of patient registration.

Additional covariates tested in the models included the following: sociodemographic factors (age at admission, sex, insurance type, quartile of median household income for zip code derived from 2010 US Census data, census region); disease-related comorbidities including ICD-9-CM diagnosis codes for nephritis, seizure, or stroke, as previously described (14,15), and crosswalked to ICD-10-CM (Supplementary Table 1); mental health disorders classified in the PHIS by the Child and Adolescent Mental Health Disorders Classification System diagnosis groups; the All Patients Refined Diagnosis Related Groups classification of severity of illness; and hospital characteristics (hospital volume of SLE admissions categorized into quartiles).

Statistical analysis. Patient-level demographic and disease characteristics were summarized using standard descriptive statistics. Cuzick's Wilcoxon rank sum test was used to evaluate unadjusted temporal trends in the proportion of all PHIS hospital admissions by patients in the SLE cohort and the proportion of SLE admissions with adverse renal outcomes. For the primary adjusted analysis, we used separate mixed-effects logistic regression models to estimate differences by race in the following: 1) overall burden of adverse renal outcomes, represented by the odds of an ESRD, dialysis, or transplant code at any given hospital admission, and 2) the odds of an SLE patient having their first occurrence of an adverse renal outcome at a PHIS hospital. In the second model, all subsequent admissions after the first hospitalization for an adverse renal outcome were censored for each patient. Based on graphical representations of the raw data, calendar period was incorporated in all models as a categorical indicator variable (2006–2010, 2011–2015, 2016–2019). We used a robust variance estimator to account for heteroscedasticity and included a random intercept to account for correlations within hospitals.

To determine whether rates of improvement over time differed by race, we tested interactions between calendar period and race and ethnicity (on the log odds scale using Wald chi-square tests). We also calculated average adjusted predictions for the probability of each outcome by race and calendar period. Assuming a total sample size of 20,000 admissions and a 5–10% probability of an adverse renal outcome, we had 80% power to detect an odds ratio (OR) of 1.3–1.4 for the smallest minority group (Asian) and an OR of 1.2–1.3 for the largest minority group (Black) compared to the reference group (non-Hispanic White). Assuming a 1.5-fold disparity between 2 groups and a 0.75-fold reduction in renal outcomes between 2 calendar

Table 1. Characteristics of hospitalized children with SLE by race and ethnicity*

	Asian (n = 563)†	Black (n = 2,370)	Hispanic Other (n = 891)	Hispanic White (n = 1,217)	Non-Hispanic Other (n = 1,617)‡	Non-Hispanic White (n = 1,667)
Calendar period						
2006–2010	152 (27)	941 (40)	240 (27)	533 (44)	262 (36)	506 (30)
2011–2015	210 (37)	712 (30)	347 (39)	323 (27)	241 (33)	647 (39)
2016–2019	201 (36)	717 (30)	304 (34)	361 (30)	223 (31)	514 (31)
Age at index admission, mean ± SD years	13.8 ± 3.1	14.6 ± 3.0	13.9 ± 3.4	14.2 ± 3.1	14.2 ± 3.0	14.5 ± 3.1
Female sex	478 (85)	1,993 (84)	717 (80)	990 (81)	601 (83)	1,335 (80)
Insurance type						
Public	245 (44)	1,423 (60)	640 (72)	823 (68)	389 (54)	641 (38)
Private	285 (51)	761 (32)	183 (21)	284 (23)	257 (35)	907 (54)
Other/unknown	33 (6)	186 (8)	68 (8)	110 (9)	80 (11)	119 (7)
Census region						
Midwest	90 (16)	487 (21)	120 (13)	84 (7)	130 (18)	459 (28)
West	283 (50)	226 (10)	473 (53)	594 (49)	244 (34)	374 (22)
Northeast	46 (8)	263 (11)	85 (10)	49 (4)	171 (24)	211 (13)
South	144 (26)	1,394 (59)	213 (24)	490 (40)	181 (25)	623 (37)
Urban area hospital	525 (93)	2,108 (89)	785 (88)	1,078 (89)	649 (89)	1,339 (80)
Income quartile§						
<\$31,061	45 (8)	680 (29)	188 (21)	277 (23)	136 (19)	237 (14)
\$31,061–\$39,625	98 (17)	568 (24)	247 (28)	351 (29)	174 (24)	361 (22)
\$39,626–\$52,223	129 (23)	545 (23)	270 (30)	311 (26)	192 (26)	462 (28)
≥\$52,224	273 (49)	511 (22)	161 (18)	248 (20)	204 (28)	557 (33)
Unknown/missing	18 (3)	66 (3)	25 (3)	30 (2)	20 (3)	50 (3)
Nephritis	359 (64)	1,429 (60)	523 (59)	775 (64)	406 (56)	839 (50)
Seizure	49 (9)	261 (11)	85 (10)	113 (9)	64 (9)	126 (8)
Stroke	24 (4)	130 (5)	41 (5)	53 (4)	41 (6)	56 (3)
Mental health disorder¶	129 (23)	787 (33)	286 (32)	372 (31)	219 (30)	585 (35)

* Except where indicated otherwise, values are the number (%) of patients. SLE = systemic lupus erythematosus.
 † Includes Pacific Islander race (n = 193).
 ‡ Includes Other race (n = 1,117), Unreported race (n = 407), and American Indian race (n = 93).
 § Median household income for zip code.
 ¶ Child and Adolescent Mental Health Disorders Classification System diagnosis groups.

periods, the detectable OR for interactions was 1.7–2.0 for the smallest minority group and 1.5–1.7 for the largest minority group.

We performed several sensitivity analyses. First, we excluded patients whose index year of admission was 2019 to ensure that the observed trends were not due to insufficient follow-up time. Second, we performed a separate subgroup analysis limited to subjects that were ever assigned an inpatient non-ESRD nephritis code to account for potential differences in the incidence of renal involvement. Third, we tested random effects for within-subject correlation instead of within-hospital correlation to account for multiple admissions per subject. We also performed a secondary analysis, in which we disaggregated American Indian race from Other race and Pacific Islander from Asian race, using Hispanic ethnicity as an independent variable, to assess whether the broader racial and ethnic categorizations masked risks specific to minority groups with small sample sizes.

Last, to assess potential ascertainment bias due to differences between the ICD-9 and ICD-10-CM coding systems, we graphically evaluated year-to-year stability of the proportion of SLE admissions over total hospital admissions per year plotted against calendar year and tested for a change point in 2016 using Bayesian change point

analysis. For the SLE patients identified from our institution, we also reviewed their medical records to compare positive predictive values (PPVs) of ICD-9 and ICD-10-CM SLE and ESRD diagnosis codes.

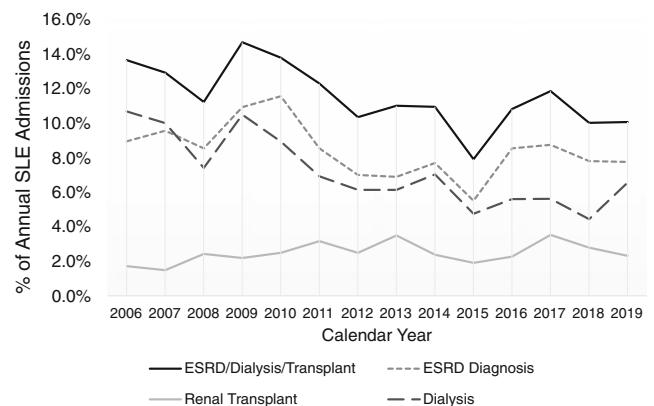


Figure 1. Proportion of yearly systemic lupus erythematosus (SLE) hospital admissions assigned adverse renal outcomes of interest, including an end-stage renal disease (ESRD) diagnosis, a dialysis procedure code, or a renal transplant code, each as separate outcomes and as a composite outcome.

RESULTS

Summary statistics and patient characteristics. We identified 7,434 SLE patients who had a total of 20,893 admissions at 50 hospitals during the study period. There was a median of 1 admission (interquartile range [IQR] 1–3) per individual patient

and a median of 332 admissions per hospital (IQR 195–515). Patient-level characteristics by race and ethnicity are shown in Table 1.

As a proportion of total hospital admission volumes, SLE admissions decreased over time from 0.29% in 2006 to 0.24% in 2019 (*P* for trend = 0.001). There was a decrease over time in

Table 2. Average effects of race, ethnicity, and calendar period on adverse renal outcomes among hospitalized children with SLE*

	Unadjusted fixed effects and no random effects, OR (95% CI)	Adjusted for demographic data and severity fixed effects and no random effects, OR (95% CI)†	Fully adjusted fixed effects and hospital-level random effects, OR (95% CI)‡	Sensitivity analysis fixed effects and hospital-level random effects, OR (95% CI)§
Composite adverse renal outcome at any hospital admission¶				
Race and ethnicity				
Non-Hispanic White	Referent	Referent	Referent	Referent
Asian	1.09 (0.86–1.38)	1.03 (0.80–1.31)	0.95 (0.48–1.89)	0.95 (0.48–1.88)
Black	2.41 (2.10–2.76)#	2.16 (1.87–2.50)#	2.50 (1.77–3.52)#	2.50 (1.75–3.58)#
Hispanic Other	1.12 (0.93–1.34)	1.17 (0.96–1.43)	1.15 (0.62–2.14)	1.13 (0.59–2.15)
Hispanic White	1.21 (1.02–1.43)**	1.04 (0.87–1.26)	1.16 (0.76–1.76)	1.16 (0.76–1.78)
Non-Hispanic Other	1.10 (0.90–1.36)	1.10 (0.88–1.38)	1.24 (0.73–2.10)	1.23 (0.71–2.13)
Calendar period				
2006–2010	Referent	Referent	Referent	Referent
2011–2015	0.81 (0.73–0.89)#	0.60 (0.54–0.67)#	0.60 (0.46–0.79)#	0.60 (0.46–0.79)#
2016–2019	0.81 (0.73–0.90)#	0.51 (0.46–0.58)#	0.54 (0.42–0.68)#	0.57 (0.45–0.73)#
ESRD diagnosis code at any hospital admission				
Race and ethnicity				
Non-Hispanic White	Referent	Referent	Referent	Referent
Asian	0.92 (0.68–1.23)	0.88 (0.64–1.19)	0.82 (0.40–1.69)	0.81 (0.39–1.68)
Black	2.60 (2.22–3.05)#	2.23 (1.89–2.65)#	2.61 (1.85–3.68)#	2.59 (1.81–3.70)#
Hispanic Other	1.17 (0.94–1.45)	1.18 (0.94–1.50)	1.16 (0.56–2.41)	1.16 (0.55–2.43)
Hispanic White	1.38 (1.13–1.67)††	1.16 (0.94–1.44)	1.32 (0.84–2.06)	1.32 (0.84–2.08)
Non-Hispanic Other	1.03 (0.79–1.33)	1.03 (0.79–1.35)	1.19 (0.64–2.23)	1.19 (0.63–2.24)
Calendar period				
2006–2010	Referent	Referent	Referent	Referent
2011–2015	0.73 (0.65–0.83)#	0.56 (0.50–0.64)#	0.56 (0.39–0.80)††	0.56 (0.39–0.80)††
2016–2019	0.84 (0.75–0.95)††	0.56 (0.49–0.64)#	0.59 (0.44–0.80)#	0.64 (0.48–0.86)††
Dialysis procedure code at any hospital admission				
Race and ethnicity				
Non-Hispanic White	Referent	Referent	Referent	Referent
Asian	1.34 (1.02–1.77)**	1.15 (0.86–1.54)	1.07 (0.64–1.80)	1.08 (0.64–1.81)
Black	2.25 (1.90–2.66)#	2.02 (1.68–2.42)#	2.33 (1.69–3.21)#	2.35 (1.68–3.29)#
Hispanic Other	0.96 (0.76–1.22)	0.99 (0.76–1.28)	1.07 (0.61–1.90)	1.06 (0.60–1.89)
Hispanic White	1.22 (0.99–1.50)	1.06 (0.84–1.34)	1.24 (0.84–1.84)	1.24 (0.82–1.87)
Non-Hispanic Other	1.07 (0.82–1.40)	1.02 (0.77–1.34)	1.15 (0.72–1.85)	1.15 (0.71–1.87)
Calendar period				
2006–2010	Referent	Referent	Referent	Referent
2011–2015	0.67 (0.59–0.75)#	0.48 (0.42–0.55)#	0.47 (0.34–0.66)#	0.47 (0.34–0.66)#
2016–2019	0.58 (0.51–0.67)#	0.36 (0.31–0.42)#	0.37 (0.27–0.51)#	0.39 (0.28–0.53)#

* The odds of each renal outcome, expressed as the odds ratio (OR) with 95% confidence interval (95% CI), were evaluated in separate unadjusted (n = 20,893) and adjusted (n = 20,393) mixed-effects logistic regression models. SLE = systemic lupus erythematosus.

† Adjusted for age, census region, insurance type, median household income, the All Patients Refined Diagnosis-Related Groups classification of severity of illness, and seizure diagnosis. Patient sex, urban hospital, hospital volume, stroke diagnosis, and Child and Adolescent Mental Health Disorders Classification System diagnosis groups were tested in the models and did not meet criteria for retention.

‡ Adjusted for all variables included above as fixed effects, and hospital-level clustering as a random effect.

§ Fully adjusted model with hospital-level random effects as in the above footnote, excluding patients whose index admission occurred in 2019 (n = 20,033).

¶ Adverse renal outcomes at any hospital admission were defined as end-stage renal disease (ESRD), dialysis, or renal transplantation.

P < 0.001.

** *P* < 0.05.

†† *P* < 0.01.

the proportion of SLE admissions of Black and Hispanic White patients and a corresponding increase in those reporting as Hispanic Other (P for nonparametric trend <0.001) (Supplementary Figure 1, available on the *Arthritis & Rheumatology* website at <https://onlinelibrary.wiley.com/doi/10.1002/art.42127>).

Descriptive trends in adverse renal outcomes over time. There were 667 unique SLE patients (9%) who had adverse renal outcome during the study period, of which 471 (6%) were assigned ≥ 1 ESRD diagnosis, 566 (8%) had ≥ 1 procedure code for dialysis, and 162 (2%) underwent renal transplant. The median time from the index admission to the first assignment of an ESRD, dialysis, or transplant code was 81 days (IQR 10–666), 43 days (IQR 14–423), or 498 days (IQR 9–1,141), respectively.

There was a significant trend over time toward a decrease in the proportion of SLE admissions per year that were assigned codes for adverse renal outcomes (P for nonparametric trend <0.001) (Figure 1). The proportion of admissions with a first occurrence of an adverse renal outcome for any given SLE patient also decreased over time from 7.0% to 3.1% (P for trend = 0.035), censoring subsequent occurrences.

Change in adverse renal outcomes over time by race and ethnicity. *Burden of all SLE hospitalizations associated with adverse renal outcomes.* On average, across all racial and ethnic groups, the adjusted odds of an adverse renal outcome at any given hospital admission decreased over time by 0.60-fold (95% confidence interval [95% CI] 0.46–0.79) in 2011–2015 and 0.54-fold (95% CI 0.42–0.68) in 2016–2019 compared to 2006–2010 (P for trend <0.001), adjusted for demographic and disease characteristics as well as hospital-level random effects. Similar decreases over time were observed in separate models for ESRD diagnosis and dialysis (Table 2). Despite overall improvements over time in renal outcome rates, Black patients with SLE maintained a persistent 2.5-fold higher adjusted odds (95% CI 1.77–3.52) of an adverse renal outcome at any hospital admission ($P < 0.001$) compared to non-Hispanic White patients. Inclusion of random effects to account for clustering by hospital had a significant impact on the estimates and accounted for 12% of the total variance. There was no significant difference in rates of improvement in adverse renal outcomes over time between any racial or ethnic group (P for interaction = 0.094) and no significant change in the relative Black versus non-Hispanic White disparity over time (P for interaction = 0.728) (Figure 2).

When ESRD and dialysis were modeled as separate outcomes, Asian patients had significantly greater decreases over time in the odds of dialysis compared to Hispanic White patients (OR 0.92 [95% CI 0.47–1.81] in 2006–2010 versus OR 0.27 [95% CI 0.12–0.64] in 2016–2019; P for interaction = 0.023). Asian patients also had statistically non-significant greater decreases over time compared to non-Hispanic White patients

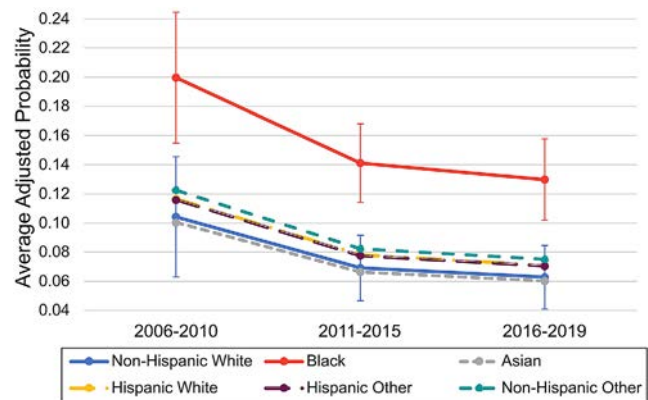


Figure 2. Marginal predictions from a mixed logit model by race and ethnicity and calendar period, representing the average adjusted probability of the composite adverse renal outcome (assignment of end-stage renal disease diagnosis, dialysis procedure code, or renal transplant code) at any given hospital admission. The model was adjusted for age, insurance type, income, census region, All Patient Refined Diagnosis-Related Group classification of illness severity, seizure, and hospital-level random effects. Error bars show 95% confidence intervals for the mean prediction calculated using the Delta method estimates of standard errors and are not shown for racial and ethnic categories that were not significantly different from the reference group (non-Hispanic White) on the log odds scale.

(OR 1.30 [95% CI 0.66–2.6] in 2006–2010 versus OR 0.35 [95% CI 0.16–0.76] in 2016–2019; P for interaction = 0.054). However, there was no significant change over time in the relative disparity between Black and non-Hispanic White patients for either ESRD or dialysis (Supplementary Figure 2, available on the *Arthritis & Rheumatology* website at <https://onlinelibrary.wiley.com/doi/10.1002/art.42127>). There was no significant change in odds of renal transplant by calendar period (OR 0.91 [95% CI 0.51–1.63] in 2016–2019 versus 2006–2010) or by racial and ethnic group.

Among patients with ESRD, Black children had the highest number of admissions associated with ESRD per patient (median 3 [IQR 1–6]; $n = 205$ patients) compared to a median of 2 ESRD admissions for non-Hispanic White children (IQR 1–3; $n = 61$ patients). In contrast, children belonging to Asian and non-Hispanic Other race categories had the lowest number of repeat admissions associated with ESRD (median 1.5 [IQR 1–3]; $n = 28$ patients, and median 1 [IQR 1–5]; $n = 35$ patients, respectively). Similarly, Black children with SLE had the greatest number of hospital admissions requiring dialysis (median 2 [IQR 1–5]) compared to a median of 1 (IQR 1–3) for Hispanic Other patients and a median of 1 (IQR 1–2) for all other race categories.

First occurrence of an adverse renal outcome requiring hospitalization. On average, across all racial and ethnic groups, there was a decrease over time in the odds of a first occurrence of any adverse renal outcome at a PHIS hospital (adjusted OR 0.58 [95% CI 0.47–0.73] in 2011–2015 and OR 0.46 [95% CI 0.36–0.58] in 2016–2019, respectively, compared to 2006–2010; P for trend <0.001) (Table 3). Compared to Non-Hispanic White

Table 3. Average effects of race and ethnicity and calendar period on the odds of an initial hospital admission for an adverse renal outcome*

	Unadjusted fixed effects and no random effects, OR (95% CI)	Adjusted for demographic data and severity fixed effects and no random effects, OR (95% CI)†	Fully adjusted fixed effects and hospital-level random effects, OR (95% CI)‡	Sensitivity analysis fixed effects and hospital-level random effects, OR (95% CI)§
First hospital admission with a composite adverse renal outcome				
Race and ethnicity				
Non-Hispanic White	Referent	Referent	Referent	Referent
Asian	1.56 (1.10–2.21)¶	1.53 (1.05–2.21)¶	1.49 (0.94–2.35)	1.55 (0.99–2.44)
Black	1.44 (1.14–1.82)#	1.37 (1.06–1.76)¶	1.39 (1.08–1.79)¶	1.43 (1.11–1.84)#
Hispanic Other	1.12 (0.83–1.52)	1.27 (0.92–1.77)	1.35 (0.93–1.94)	1.33 (0.91–1.94)
Hispanic White	1.18 (0.90–1.56)	1.07 (0.79–1.46)	1.18 (0.89–1.55)	1.18 (0.90–1.55)
Non-Hispanic Other	1.33 (0.96–1.84)	1.36 (0.96–1.93)	1.40 (0.97–2.04)	1.43 (0.97–2.11)
Calendar period				
2006–2010	Referent	Referent	Referent	Referent
2011–2015	0.83 (0.69–0.99)¶	0.60 (0.49–0.73)**	0.58 (0.47–0.73)**	0.59 (0.47–0.74)**
2016–2019	0.76 (0.62–0.92)#	0.46 (0.37–0.57)**	0.46 (0.36–0.58)**	0.45 (0.36–0.58)**
First hospital admission with ESRD diagnosis				
Race and ethnicity				
Non-Hispanic White	Referent	Referent	Referent	Referent
Asian	1.41 (0.89–2.21)	1.35 (0.84–2.17)	1.27 (0.76–2.14)	1.30 (0.78–2.17)
Black	1.77 (1.33–2.36)**	1.59 (1.17–2.16)#	1.57 (1.16–2.12)#	1.57 (1.15–2.13)#
Hispanic Other	1.38 (0.96–1.99)	1.41 (0.95–2.09)	1.43 (0.94–2.16)	1.41 (0.91–2.18)
Hispanic White	1.55 (1.11–2.16)¶	1.29 (0.90–1.85)	1.38 (0.91–2.08)	1.37 (0.92–2.03)
Non-Hispanic Other	1.29 (0.84–1.96)	1.29 (0.83–2.00)	1.31 (0.76–2.25)	1.31 (0.76–2.24)
Calendar period				
2006–2010	Referent	Referent	Referent	Referent
2011–2015	0.86 (0.69–1.06)	0.67 (0.54–0.85)#	0.66 (0.49–0.90)#	0.66 (0.49–0.90)#
2016–2019	0.81 (0.65–1.02)	0.55 (0.43–0.70)**	0.55 (0.42–0.72)**	0.56 (0.44–0.73)**
First hospital admission with dialysis procedure code				
Race and ethnicity				
Non-Hispanic White	Referent	Referent	Referent	Referent
Asian	1.83 (1.27–2.65)#	1.73 (1.17–2.58)#	1.66 (1.07–2.59)¶	1.73 (1.10–2.71)¶
Black	1.56 (1.20–2.01)#	1.50 (1.14–1.98)#	1.53 (1.14–2.05)#	1.58 (1.17–2.13)#
Hispanic Other	1.18 (0.84–1.65)	1.33 (0.92–1.92)	1.44 (0.96–2.17)	1.44 (0.94–2.19)
Hispanic White	1.30 (0.96–1.76)	1.20 (0.86–1.69)	1.31 (0.94–1.83)	1.31 (0.93–1.83)
Non-Hispanic Other	1.37 (0.96–1.97)	1.42 (0.97–2.08)	1.47 (1.01–2.13)¶	1.50 (1.02–2.21)¶
Calendar period				
2006–2010	Referent	Referent	Referent	Referent
2011–2015	0.85 (0.70–1.03)	0.60 (0.49–0.74)**	0.58 (0.45–0.75)**	0.58 (0.45–0.74)**
2016–2019	0.70 (0.57–0.87)#	0.42 (0.33–0.53)**	0.41 (0.31–0.55)**	0.39 (0.30–0.53)**

* The odds of a first Pediatric Health Information System hospital admission with a composite adverse renal outcome, an ESRD diagnosis, or dialysis, excluding all subsequent admissions, were evaluated in separate unadjusted and adjusted mixed-effects logistic regression models (n = 18,008 in the fully adjusted model of the composite renal outcome). See Table 2 for definitions.

† Adjusted for age, census region, insurance type, median household income, All Patient Refined Diagnosis-Related Group classification of illness severity, and seizure diagnosis. Patient sex, urban hospital, hospital volume, stroke diagnosis, and Child and Adolescent Mental Health Disorders Classification System diagnosis groups were tested in the models and did not meet criteria for retention.

‡ Adjusted for all variables included above as fixed effects, and hospital-level clustering as a random effect.

§ Fully adjusted model with hospital-level random effects as described above excluding patients whose index admission occurred in 2019 (n = 17,204 for composite outcome).

¶ P < 0.05.

P < 0.01.

** P < 0.001.

race, Black race was associated with 1.39-fold higher adjusted odds of a first occurrence of any adverse renal outcome in any calendar period (95% CI 1.08–1.79; P = 0.011) (Table 3). Asian race was also associated with 1.49-fold higher adjusted odds of first occurrence of any adverse renal outcome (95% CI 0.94–2.35; P = 0.087), though this did not reach statistical

significance. There were no significant differences in rates of change in adverse renal outcomes over time according to racial or ethnic group (P for interaction = 0.354) (Figure 3).

Black SLE patients had the highest adjusted odds of a first occurrence of an ESRD diagnosis (OR 1.57 [95% CI 1.16–2.12] compared to non-Hispanic White patients; P < 0.01). There was no

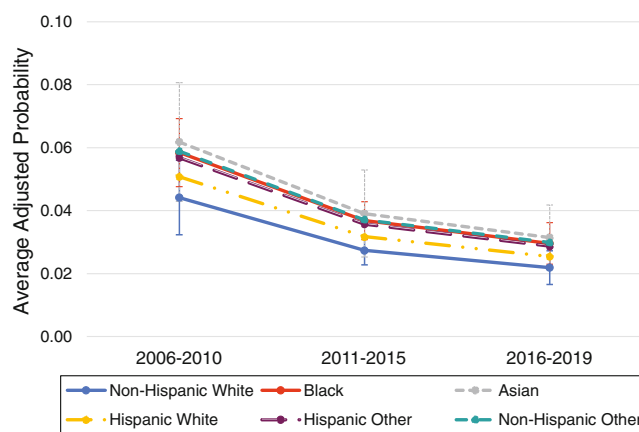


Figure 3. Marginal predictions from a mixed logit model by race and ethnicity and calendar period, representing the average adjusted probability of the first occurrence of any adverse renal outcome at a given hospital admission, excluding all subsequent admissions. The model was adjusted for age, insurance type, income, census region, All Patient Refined Diagnosis-Related Group classification of illness severity, seizure, and hospital-level random effects. Error bars show 95% confidence intervals for the mean prediction calculated using the Delta method estimates of standard errors and are not shown for racial and ethnic categories that were not significantly different from the reference group (non-Hispanic White) on the log odds scale.

significant change in the relative disparity over time (P for interaction = 0.284). With respect to dialysis, Asian, Black, and Non-Hispanic Other SLE patients all had significantly higher adjusted odds of an initial hospital admission for dialysis compared to non-Hispanic White patients (Table 3). These relative disparities also remained unchanged over time, despite overall improvements in rates of dialysis (P for interaction = 0.377) (Supplementary Figure 3, available on the *Arthritis & Rheumatology* website at <https://onlinelibrary.wiley.com/doi/10.1002/art.42127>). There were no significant differences in the odds of an initial renal transplant admission by calendar period or by racial or ethnic group (data not shown).

Sensitivity analyses. The effects of race and calendar period on composite adverse renal outcomes, ESRD, and dialysis were robust with the exclusion of patients whose index date of admission occurred in 2019 (Tables 2 and 3). Adding within-subject random effects resulted in a failure of the models to converge; however, accounting for within-subject random effects alone instead of hospital random effects did not significantly change the magnitude of the estimates. In the subgroup analysis limited to 15,157 admissions assigned any nephritis diagnosis codes, Black SLE patients still had nearly 2-fold increased odds of an adverse renal outcome at any hospital admission compared to non-Hispanic White patients (OR 1.94 [95% CI 1.38–2.75]), with no significant changes in the relative disparity over time. Changing the racial and ethnic categorizations also did not impact our conclusions. There was no significant independent effect of Hispanic ethnicity alone on the primary outcome when modeled separately from race. There were also no significant differences in the

primary outcome identified in Pacific Islander or American Indian race compared to non-Hispanic White race, when disaggregated from Asian and Other race, respectively (Supplementary Table 2, available on the *Arthritis & Rheumatology* website at <https://onlinelibrary.wiley.com/doi/10.1002/art.42127>).

ICD-10 crosswalk. Prior to October 1, 2015, the PPV of an ICD-9-CM discharge diagnosis code for SLE among patients at the Children's Hospital of Philadelphia was 95% (112 of 118 patients reviewed). Similarly, the PPV of an ICD-10-CM discharge diagnosis code after October 1, 2015 was 96% (55 of 57 patients). Of the patients with ESRD ICD-9 and ICD-10-CM diagnosis codes, 91% (10 of 11 patients) and 100% (2 of 2 patients) were confirmed to have ESRD by manual chart review, respectively. The single false-positive result for ESRD occurred in a patient who required dialysis for acute kidney injury. Of the 20 randomly selected SLE patients without ESRD codes (10 with index admission prior to October 1, 2015 and 10 after), none had ESRD according to manual chart review.

DISCUSSION

This US population-based study is the largest to date describing trends in renal outcomes over time among children with lupus, highlighting key findings and future directions pertaining to inequities in pediatric lupus care. Renal outcomes among children with lupus have improved significantly since 2006. At the population level, these improvements have equally benefited racial and ethnic groups, demonstrating progress with regard to treatment and outcomes. However, failure to resolve the Black/White disparity in outcomes emphasizes the critical need for additional health equity initiatives. Furthermore, a significant proportion of variation in renal outcomes is attributable to hospital-level effects, raising the possibility of area-level differences in racial disparities that warrant further exploration at local levels.

From 2006 to 2019, the overall burden of severe renal outcomes associated with pediatric SLE hospitalizations decreased by nearly half. Similar trends in global rates of ESRD were observed at the turn of the century for adults with lupus nephritis amid increased MMF and cyclophosphamide use and decreased severity at presentation due to earlier diagnosis (16,17). Although we cannot determine the definitive reasons for improving trends in pediatric SLE, several contemporary care processes may have contributed. First, MMF became widely adopted for pediatric lupus nephritis after non-inferiority to cyclophosphamide was demonstrated in adults in 2005, and similar efficacy was described in small pediatric studies (18–20). In 2012, the Childhood Arthritis and Rheumatology Research Alliance (CARRA) released a consensus treatment plan solidifying the role of MMF as first-line therapy for proliferative lupus nephritis in children (8).

Use of B cell-depleting therapies also became increasingly common—up to 25% of lupus nephritis patients in the CARRA registry's contemporary pediatric lupus cohort have received

rituximab (9). There have also been several initiatives to develop standards for pediatric lupus care, including international consensus recommendations for quality indicators in 2013 (10), and European guidelines for management of pediatric lupus in 2016 (11,21). It is possible we did not observe corresponding decreases in renal transplantation due to the longer latency between initial SLE hospitalization and the outcome. Of note, improvements in ESRD risk for adults with lupus nephritis largely plateaued from 1990 to 2000 in developed countries (16). Our findings suggest rates of improvement in children may just be beginning to plateau, perhaps reflecting delayed introduction of new therapies in pediatric populations relative to adults (22,23). With increasing adoption of aforementioned practices, as well as recent approvals of newer therapies for lupus nephritis, it is reasonable to anticipate continued progress; however, close monitoring over time and increased efforts to include children and adolescents in clinical trials will be essential.

While renal outcomes improved at the population level, we did not observe the heterogeneous effects needed to achieve reduction of relative Black/White disparities over time. Black children with SLE remained at a significantly higher risk of ESRD or dialysis compared to non-Hispanic White children, and the magnitude of this relative disparity persisted over the study period. Moreover, Black children had more recurrent hospitalizations and assumed the greatest burden of hospital care for adverse renal outcomes. These differences were partially attenuated, but not explained, by median household income or insurance status. The disparity persisted even when limited to patients with nephritis codes and therefore was not due to a higher incidence of renal involvement among Black children. Our findings mirror persistent relative Black/White disparities in care processes across the US, including timely receipt of pre-dialysis nephrology care among adults with chronic kidney disease and insulin pump use among children with type 1 diabetes mellitus, independent of socioeconomic factors (24–27). Standardizing care processes to reduce variability has been proposed as a systems-level approach to address health inequities (28), with varying rates of success (29,30).

Our data suggest that while advances in pediatric lupus care may have reached groups that have been historically marginalized, they have not achieved greater benefit for Black children with lupus. It remains possible, however, that further efforts to improve standardization where treatment variability exists could still preferentially benefit Black children with lupus and reduce disparities. Examples of successful child health interventions include the safe sleep campaigns, which targeted high-risk communities and reduced overall rates of sudden infant death syndrome while narrowing the Black/White disparity in infant mortality (31,32). These efforts can inform targeted approaches for children with chronic diseases such as lupus, as treatment advances alone are insufficient to close the gap.

Regarding other minority groups, Asian patients had the highest probability of a new dialysis requirement during hospitalization compared to any other racial or ethnic group but were not at increased risk of ESRD. Our findings are consistent with a disease trajectory analysis of a Canadian pediatric lupus cohort, which found that Asian children with SLE more commonly present with severe disease but subsequently achieve good long-term outcomes. By comparison, Black children more often experience a refractory, remitting disease course (33). Of note, outcomes among Pacific Islander patients may differ from East Asian and South Asian patients. In one series of Māori children with SLE in New Zealand, 100% developed lupus nephritis and 12 of 15 had proliferative disease (34). In our study, attempting to disaggregate Pacific Islander patients did not reveal differential risk for adverse renal outcomes. However, we advocate for dedicated studies to fully characterize lupus outcomes among children of Pacific Islander descent and greater efforts to report disaggregated results (35).

In contrast to previous studies (36,37), Hispanic ethnicity was not associated with worse outcomes among hospitalized children with SLE. There may be several reasons for this difference, including the use of Hispanic ethnicity as a single construct to represent a heterogeneous and dynamic population. Historical shifts in the composition of the US Hispanic population and how those with Hispanic ethnicity report race present unique challenges in the evaluation of trends over time in health outcomes (38). Between the 2010 and 2020 US Censuses, the proportion of Hispanic individuals who reported Other race rather than White race increased (39,40). Certain countries of origin, younger age, and first-generation immigrant status are associated with increased self-identification with Other race and may confer different risks (38). Furthermore, socioeconomic and health disparities by country of origin are not captured in this database or other national registries (41). Consequently, our findings warrant cautious interpretation and underscore the need for health systems data to reflect the complexities of Hispanic ethnicity, including country of origin and immigration status.

Institutional-level reporting may uncover high-risk populations within hospital catchment areas and differential risks for minority groups between areas. The contribution of hospital-level random effects to the overall variance in adverse renal outcomes suggests there is a smaller subset of patients accounting for a significant burden of renal disease-related admissions. This highlights the importance of local context, because social factors that drive population-level disparities may be systematically concentrated in resource-constrained communities (42). While characteristics of the areas served by each hospital were not available in this study, individual institutions contributing data to the PHIS can leverage their own data to monitor disparities in near real-time and examine local factors that can be targets for intervention. For example, the Colorado Hospital Association mapped hospital claims to social risk scores to track relationships between

social factors and health care utilization (43). Uncovering local factors that drive disparities and directing hospital resources to the highest-risk patients will be an important future direction for pediatric lupus care.

There are several limitations to this study. First, health systems data lack individual and area-level socioeconomic indicators, such as education, area-level poverty, and family structure. Thus, it is unclear how much of the effect of race is mediated by socioeconomic conditions versus structural racism. Second, this data set was limited to inpatient admissions, so we were unable to establish disease duration or follow-up time to estimate ESRD incidence. Similarly, prescription medication data were unavailable, and therefore, we were unable to test associations between changes in medication use and outcomes. Third, the broad categorizations and hospital variation in the quality and completeness of race and ethnicity reporting may result in misclassification. Last, we were unable to fully evaluate trends for the small number of American Indian children in the database, although distinct health inequities have been described for this marginalized group, including earlier age of SLE onset, more frequent vasculitis, and higher disease prevalence (44–46). In our cohort, only 1.25% of children were classified as American Indian, with a high likelihood of underreporting (47). Although they did not appear to have worse renal outcomes than non-Hispanic White children, findings may not be generalizable to American Indian children who live in areas remote from tertiary pediatric hospitals or receive care from the Indian Health Service and rely on interfacility transfer to access subspecialty care (48). Similarly, the generalizability of this study is limited by the low proportion of rural hospitals.

In summary, considerable progress has been made in pediatric lupus care and is reflected in improved renal outcomes. Now more than ever, specific attention is needed to identify what care processes or interventions can preferentially improve renal outcomes among the highest risk groups. Consistent failure to resolve the persistent Black/White health care disparity across many conditions indicates that the same structural barriers are preventing meaningful change. Lessons from successful interventions targeted toward historically marginalized communities will need to be applied to the chronic care model. From a research standpoint, it is also critical for health systems to collect individual and area-level social determinants of health, as well as disaggregated race and ethnicity data to ensure that risks among marginalized groups are not obscured by population averages. This will require coordinated efforts at both local and national levels to systematically evaluate risk and target the root causes of persistent health inequities.

AUTHOR CONTRIBUTIONS

All authors were involved in drafting the article or revising it critically for important intellectual content, and all authors approved the final version to be published. Dr. Chang had full access to all of the data in the

study and takes responsibility for the integrity of the data and the accuracy of the data analysis.

Study conception and design. Chang, Torres.

Acquisition of data. Chang, Sears, Torres.

Analysis and interpretation of data. Chang, Sears, Torres, Son.

REFERENCES

- Hiraki LT, Benseler SM, Tyrrell PN, Harvey E, Hebert D, Silverman ED. Ethnic differences in pediatric systemic lupus erythematosus. *J Rheumatol* 2009;36:2539–46.
- Lim SS, Bayakly AR, Helmick CG, Gordon C, Easley KA, Drenkard C. The incidence and prevalence of systemic lupus erythematosus, 2002–2004: the Georgia Lupus Registry. *Arthritis Rheumatol* 2014;66:357–68.
- Tucker LB, Uribe AG, Fernández M, Vilá LM, McGwin G, Apte M, et al. Adolescent onset of lupus results in more aggressive disease and worse outcomes: results of a nested matched case-control study within LUMINA, a multiethnic US cohort (LUMINA LVII). *Lupus* 2008;17:314–22.
- Alarcón GS, McGwin G, Bartolucci AA, Roseman J, Lisse J, Fessler BJ, et al. Systemic lupus erythematosus in three ethnic groups: IX. Differences in damage accrual. *Arthritis Rheum* 2001;44:2797–806.
- Fernández M, Alarcón GS, Calvo-Alén J, Andrade R, McGwin G, Vilá LM, et al. A multiethnic, multicenter cohort of patients with systemic lupus erythematosus (SLE) as a model for the study of ethnic disparities in SLE. *Arthritis Rheum* 2007;57:576–84.
- Hiraki LT, Lu B, Alexander SR, Shaykevich T, Alarcón GS, Solomon DH, et al. End-stage renal disease due to lupus nephritis among children in the US, 1995–2006. *Arthritis Rheum* 2011;63:1988–97.
- Wenderfer SE, Ruth NM, Brunner HI. Advances in the care of children with lupus nephritis. *Pediatr Res* 2017;81:406–14.
- Mina R, von Scheven E, Ardoin SP, Eberhard BA, Punaro M, Ilowite N, et al. Consensus treatment plans for induction therapy of newly diagnosed proliferative lupus nephritis in juvenile systemic lupus erythematosus. *Arthritis Care Res (Hoboken)* 2012;64:375–83.
- Vazzana KM, Daga A, Goilav B, Ogbu EA, Okamura DM, Park C, et al. Principles of pediatric lupus nephritis in a prospective contemporary multi-center cohort. *Lupus* 2021:096120332110286.
- Hollander MC, Sage JM, Greenler AJ, Pendl J, Avcin T, Espada G, et al. International consensus for provisions of quality-driven care in childhood-onset systemic lupus erythematosus: attainment of international consensus for childhood-onset SLE [review]. *Arthritis Care Res (Hoboken)* 2013;65:1416–23.
- Groot N, de Graeff N, Marks SD, Brogan P, Avcin T, Bader-Meunier B, et al. European evidence-based recommendations for the diagnosis and treatment of childhood-onset lupus nephritis: the SHARE initiative. *Ann Rheum Dis* 2017;76:1965–73.
- Pui CH, Pei D, Pappo AS, Howard SC, Cheng C, Sandlund JT, et al. Treatment outcomes in black and white children with cancer: results from the SEER database and St Jude Children's Research Hospital, 1992 through 2007. *J Clin Oncol* 2012;30:2005–12.
- Appel GB, Contreras G, Dooley MA, Ginzler EM, Isenberg D, Jayne D, et al. Mycophenolate mofetil versus cyclophosphamide for induction treatment of lupus nephritis. *JASN* 2009;20:1103–12.
- Chibnik L, Massarotti E, Costenbader K. Identification and validation of lupus nephritis cases using administrative data. *Lupus* 2010;19:741–3.
- Chang JC, Mandell DS, Knight AM. High health care utilization preceding diagnosis of systemic lupus erythematosus in youth. *Arthritis Care Res (Hoboken)* 2018;70:1303–11.

16. Tektonidou MG, Dasgupta A, Ward MM. Risk of end-stage renal disease in patients with lupus nephritis, 1971-2015: a systematic review and Bayesian meta-analysis: ESRD RISK IN LUPUS NEPHRITIS. *Arthritis Rheumatol* 2016;68:1432-41.
17. Moroni G, Vercelloni PG, Quaglini S, Gatto M, Gianfreda D, Sacchi L, et al. Changing patterns in clinical-histological presentation and renal outcome over the last five decades in a cohort of 499 patients with lupus nephritis. *Ann Rheum Dis* 2018;77:1318-25.
18. Ginzler EM, Dooley MA, Aranow C, Kim MY, Buyon J, Merrill JT, et al. Mycophenolate mofetil or intravenous cyclophosphamide for lupus nephritis. *N Engl J Med* 2005;353:2219-28.
19. Buratti S, Szer IS, Spencer CH, Bartosh S, Reiff A. Mycophenolate mofetil treatment of severe renal disease in pediatric onset systemic lupus erythematosus. *J Rheumatol* 2001;28:2103-8.
20. Falcini F, Capannini S, Martini G, La Torre F, Vitale A, Mangiantini F, et al. Mycophenolate mofetil for the treatment of juvenile onset SLE: a multicenter study. *Lupus* 2009;18:139-43.
21. Groot N, de Graeff N, Avcin T, Bader-Meunier B, Brogan P, Dolezalova P, et al. European evidence-based recommendations for diagnosis and treatment of childhood-onset systemic lupus erythematosus: the SHARE initiative. *Ann Rheum Dis* 2017;76:1788-96.
22. Neel DV, Shulman DS, DuBois SG. Timing of first-in-child trials of FDA-approved oncology drugs. *Eur J Cancer* 2019;112:49-56.
23. Barry E, Walsh JA, Weinrich SL, Beaupre D, Blasi E, Arenson DR, et al. Navigating the regulatory landscape to develop pediatric oncology drugs: expert opinion recommendations. *Pediatr Drugs* 2021; 23:381-94.
24. Purnell TS, Bae S, Luo X, Johnson M, Crews DC, Cooper LA, et al. National trends in the association of race and ethnicity with predialysis nephrology care in the United States from 2005 to 2015. *JAMA Netw Open* 2020;3:e2015003.
25. Lipman TH, Willi SM, Lai CW, Smith JA, Patil O, Hawkes CP. Insulin pump use in children with type 1 diabetes: over a decade of disparities. *J Pediatr Nurs* 2020;55:110-5.
26. Willi SM, Miller KM, DiMeglio LA, Klingensmith GJ, Simmons JH, Tamborlane WV, et al. Racial-ethnic disparities in management and outcomes among children with type 1 diabetes. *Pediatrics* 2015; 135:424-34.
27. Agarwal S, Schechter C, Gonzalez J, Long JA. Racial-ethnic disparities in diabetes technology use among young adults with type 1 diabetes. *Diabetes Technol Ther* 2021;23:306-13.
28. Penner LA, Blair IV, Albrecht TL, Dovidio JF. Reducing racial health care disparities: a social psychological analysis. *Policy Insights Behav Brain Sci* 2014;1:204-12.
29. Norris K, Nissenson AR. Race, gender, and socioeconomic disparities in CKD in the United States. *JASN* 2008;19:1261-70.
30. Chang JC, Xiao R, Burnham JM, Weiss PF. Longitudinal assessment of racial disparities in juvenile idiopathic arthritis disease activity in a treat-to-target intervention. *Pediatr Rheumatol Online J* 2020;18:88.
31. Rasinski KA, Kuby A, Bzdusek SA, Silvestri JM, Weese-Mayer DE. Effect of a sudden infant death syndrome risk reduction education program on risk factor compliance and information sources in primarily black urban communities. *Pediatrics* 2003;111:e347-54.
32. Khan SQ, de Gonzalez AB, Best AF, Chen Y, Haozous EA, Rodriguez EJ, et al. Infant and youth mortality trends by race/ethnicity and cause of death in the United States. *JAMA Pediatrics* 2018;172: e183317.
33. Lim LS, Pullenayegum E, Feldman BM, Lim L, Gladman DD, Silverman ED. From childhood to adulthood: disease activity trajectories in childhood-onset systemic lupus erythematosus. *Arthritis Care Res* 2018;70:750-7.
34. Concannon A, Rudge S, Yan J, Reed P. The incidence, diagnostic clinical manifestations and severity of juvenile systemic lupus erythematosus in New Zealand Maori and Pacific Island children: the Starship experience (2000-2010). *Lupus* 2013;22:1156-61.
35. Shimkhada R, Scheitler AJ, Ponce NA. Capturing racial/ethnic diversity in population-based surveys: data disaggregation of health data for Asian American, Native Hawaiian, and Pacific Islanders (AANHPIs). *Popul Res Policy Rev* 2021;40:81-102.
36. Alarcon GS. Systemic lupus erythematosus in three ethnic groups. XX. Damage as a predictor of further damage. *Rheumatology (Oxford)* 2003;43:202-5.
37. Son MB, Johnson VM, Hersh AO, Lo MS, Costenbader KH. Outcomes in hospitalized pediatric patients with systemic lupus erythematosus. *Pediatrics* 2014;133:e106-13.
38. Cohn D, Brown A, Lopez MH. Black and Hispanic Americans see their origins as central to who they are, less so for White adults. *Pew Research Center* 2021;41. URL: <https://www.pewresearch.org/social-trends/2021/05/14/hispanic-identity-and-immigrant-generations/#fn-31333-6>.
39. United States Census Bureau. Decennial Census P.L. 94-171 Redistricting Data. 2021. URL: <https://www.census.gov/programs-surveys/decennial-census/about/rdo/summary-files.html>.
40. United States Census Bureau. 2020 Census Illuminates Racial and Ethnic Composition of the Country. 2021. URL: <https://www.census.gov/library/stories/2021/08/improved-race-ethnicity-measures-reveal-united-states-population-much-more-multiracial.html>.
41. Mendoza FS. Selected measures of health status for Mexican-American, mainland Puerto Rican, and Cuban-American children. *JAMA* 1991;265:227.
42. Acevedo-Garcia D, Osypuk TL, McArdle N, Williams DR. Toward a policy-relevant analysis of geographic and racial/ethnic disparities in child health. *Health Affairs* 2008;27:321-33.
43. Carrot Health for the Colorado Hospital Association. Mapping the correlation between emergency department utilization and social determinants of health. 2020. URL: <https://info.carrothealth.com/hubfs/Brochures%20and%20Whitepapers/Carrot%20Health%20-%20Mapping%20the%20Correlation%20Between%20Emergency%20Department%20Utilization%20and%20SDoH.pdf>.
44. Kheir JM, Guthridge CJ, Johnston JR, Adams LJ, Rasmussen A, Gross TF, et al. Unique clinical characteristics, autoantibodies and medication use in Native American patients with systemic lupus erythematosus. *Lupus Sci Med* 2018;5:e000247.
45. Peschken CA, Esdaile JM. Systemic lupus erythematosus in North American Indians: a population based study. *J Rheumatol* 2000;27: 1884-91.
46. Ferucci ED, Johnston JM, Gaddy JR, Sumner L, Posever JO, Choromanski TL, et al. Prevalence and incidence of systemic lupus erythematosus in a population-based registry of American Indian and Alaska Native People, 2007-2009: Indian Health Service Lupus Registry. *Arthritis Rheumatol* 2014;66:2494-502.
47. Arias E, Heron M, National Center for Health Statistics, Hakes J, US Census Bureau. The validity of race and Hispanic-origin reporting on death certificates in the United States: an update. *Vital Health Stat* 2016:1-21.
48. Warne D, Frizzell LB. American Indian health policy: historical trends and contemporary issues. *Am J Public Health* 2014;104:S263-7.

Complement C4 Copy Number Variation is Linked to SSA/Ro and SSB/La Autoantibodies in Systemic Inflammatory Autoimmune Diseases

Christian Lundtoft,¹ Pascal Pucholt,¹ Myriam Martin,² Matteo Bianchi,³ Emeli Lundström,⁴ Maija-Leena Eloranta,¹ Johanna K. Sandling,¹ Christopher Sjöwall,⁵ Andreas Jönsen,⁶ Iva Gunnarsson,⁴ Solbritt Rantapää-Dahlqvist,⁷ Anders A. Bengtsson,⁶ Dag Leonard,¹ Eva Baecklund,¹ Roland Jonsson,⁸ Daniel Hammenfors,⁹ Helena Forsblad-d'Elia,¹⁰ Per Eriksson,⁵ Thomas Mandl,² Sara Magnusson Bucher,¹¹ Katrine B. Norheim,¹² Svein Joar Auglænd Johnsen,¹² Roald Omdal,¹² Marika Kvarnström,¹³ Marie Wahren-Herlenius,¹⁴ Antonella Notarnicola,⁴ Helena Andersson,¹⁵ Øyvind Molberg,¹⁵ Louise Pyndt Diederichsen,¹⁶ Jonas Almlöf,¹⁷ Ann-Christine Syvänen,¹⁷ Sergey V. Kozyrev,³ Kerstin Lindblad-Toh,¹⁸ the DISSECT Consortium, the ImmunoArray Development Consortium, Bo Nilsson,¹ Anna M. Blom,² Ingrid E. Lundberg,⁴ Gunnel Nordmark,¹ Lina Marcela Diaz-Gallo,⁴ Elisabet Svenungsson,⁴ and Lars Rönnblom¹

Objective. Copy number variation of the *C4* complement components, *C4A* and *C4B*, has been associated with systemic inflammatory autoimmune diseases. This study was undertaken to investigate whether *C4* copy number variation is connected to the autoimmune repertoire in systemic lupus erythematosus (SLE), primary Sjögren's syndrome (SS), or myositis.

Methods. Using targeted DNA sequencing, we determined the copy number and genetic variants of *C4* in 2,290 well-characterized Scandinavian patients with SLE, primary SS, or myositis and 1,251 healthy controls.

Results. A prominent relationship was observed between *C4A* copy number and the presence of SSA/SSB autoantibodies, which was shared between the 3 diseases. The strongest association was detected in patients with autoantibodies against both SSA and SSB and 0 *C4A* copies when compared to healthy controls (odds ratio [OR] 18.0 [95% confidence interval (95% CI) 10.2–33.3]), whereas a weaker association was seen in patients without SSA/SSB autoantibodies (OR 3.1 [95% CI 1.7–5.5]). The copy number of *C4* correlated positively with *C4* plasma levels. Further, a common loss-of-function variant in *C4A* leading to reduced plasma *C4* was more prevalent in SLE patients with a low copy number of *C4A*. Functionally, we showed that absence of *C4A* reduced the individuals' capacity to deposit *C4b* on immune complexes.

Conclusion. We show that a low *C4A* copy number is more strongly associated with the autoantibody repertoire than with the clinically defined disease entities. These findings may have implications for understanding the etiopathogenic mechanisms of systemic inflammatory autoimmune diseases and for patient stratification when taking the genetic profile into account.

INTRODUCTION

Systemic inflammatory autoimmune diseases are a group of diseases characterized by inflammation in multiple organs and

the presence of antibodies targeting different ubiquitously expressed cytoplasmic or nuclear proteins. Systemic lupus erythematosus (SLE), primary Sjögren's syndrome (SS), and idiopathic inflammatory myopathies (myositis) are all categorized as

This study was supported by grants from the Swedish Research Council for Medicine and Health, the Swedish Rheumatism Association, King Gustav V's 80-Year Foundation, the Swedish Society of Medicine, the Ingegerd Johansson Donation, the Swedish Heart Lung Foundation, ALF funding from Stockholm County, and KID funding from the Karolinska Institutet. Dr. Lindblad-Toh's work was supported by a Wallenberg Scholarship.

¹Christian Lundtoft, PhD, Pascal Pucholt, PhD, Maija-Leena Eloranta, PhD, Johanna K. Sandling, PhD, Dag Leonard, MD, PhD, Eva Baecklund, MD, PhD, Bo Nilsson, MD, PhD, Gunnel Nordmark, MD, PhD, Lars Rönnblom, MD, PhD: Uppsala University, Uppsala, Sweden; ²Myriam Martin, PhD, Thomas Mandl, MD, PhD, Anna M. Blom, PhD: Lund University, Malmö, Sweden;

³Matteo Bianchi, PhD, Sergey V. Kozyrev, PhD: Science for Life Laboratory and Uppsala University, Uppsala, Sweden; ⁴Emeli Lundström, PhD, Iva Gunnarsson, MD, PhD, Antonella Notarnicola, MD, PhD, Ingrid E. Lundberg, MD, PhD, Lina Marcela Diaz-Gallo, PhD, Elisabet Svenungsson, MD, PhD: Karolinska Institutet and Karolinska University Hospital, Stockholm, Sweden; ⁵Christopher Sjöwall, MD, PhD, Per Eriksson, MD, PhD: Linköping University, Linköping, Sweden; ⁶Andreas Jönsen, MD, PhD, Anders A. Bengtsson, MD, PhD: Lund University and Skåne University Hospital, Lund, Sweden; ⁷Solbritt Rantapää-Dahlqvist, MD, PhD: Umeå University, Umeå, Sweden; ⁸Roland Jonsson, DMD, PhD: University of Bergen, Bergen, Norway; ⁹Daniel Hammenfors, MD: Haukeland University Hospital, Bergen, Norway;

systemic inflammatory autoimmune diseases. In SLE, multiple tissues and organs such as the skin, joints, cardiovascular system, and kidneys are commonly affected, whereas a more specific involvement is seen with lacrimal and salivary glands affected in primary SS, and muscle as well as connective tissues in myositis. Despite different patterns of tissue and organ involvement, the 3 diseases share important features, including clinical manifestations, presence of autoantibodies to nuclear antigens, and several genetic loci (1–6).

The complement system plays an important role for clearance of immune complexes and apoptotic cells. Impaired removal of cellular debris may lead to exposure of cellular self-antigens and loss of tolerance (7,8). Although mainly studied in SLE, the complement system has also been shown to play a role in the pathogenesis of primary SS and myositis (9,10). Particularly relevant are the genes in the early classical complement pathway, for which deficiency in any of the genes *C1Q*, *C1R*, *C1S*, *C2*, or *C4* may lead to SLE or lupus-like disease (11). Further, low plasma levels of C3 and C4 are routinely used in the clinical setting as biomarkers for complement activation associated with disease activity and flares in SLE (12,13).

C4 is coded by the paralogous genes *C4A* and *C4B* located between the *HLA* class I and class II regions on chromosome 6. A high level of copy number variation exists for the 2 C4 genes, and while most individuals carry 2 *C4A* copies and 2 *C4B* copies, the number of genes may range from 0 to 5 copies for *C4A* and 0–4 copies for *C4B* (14). By definition, *C4A* and *C4B* differ by 4 amino acids (PCPVLD and LSPVIH, respectively) in exon 26 that also affect the biochemical reactivity toward either amino groups or hydroxyl groups, respectively (15–17).

Previous studies have shown an association between low copy number of *C4A* and systemic inflammatory autoimmune diseases (14,18–20). However, due to the strong linkage disequilibrium (LD) between *C4A* copy number and the extended *C*07:01–B*08:01–DRB1*03:01–DQB1*02:01* risk haplotype, which is associated with SLE, primary SS, and myositis in populations of European origin, it has been difficult to define whether the association is with *HLA* or with the complement system (21). In a recent study, *C4* copy number rather than *HLA* was suggested to be the main risk factor for SLE (22). This conclusion was based on a parallel analysis of *C4* copy number and *HLA* alleles in

patients of European and African American origin, for which the latter population shows low LD between *C4A* copy number and *DRB1*03:01*.

Due to a high homology between the genomic reference sequences of *C4A* and *C4B* (99.91% identical), the 2 genes are generally excluded from variant calling analysis due to ambiguous mapping of sequencing reads. In addition, a diploid state is assumed in variant calling of human autosomes, which is incompatible with the high level of variation in the *C4* copy number ranging from 2 to 8 *C4* copies. Therefore, variation in *C4* genes at nucleotide level and the association to disease remain relatively unexplored.

The purpose of the current study was to perform a focused analysis of *C4* copy number and *C4* nucleotide variation in patients with 3 systemic inflammatory autoimmune diseases and in healthy controls. In parallel, we aimed to evaluate the relation between *HLA* alleles and *C4* copy number variation, for which the combined analysis of 3 cohorts of patients with SLE, primary SS, or myositis allowed the comparison of shared and distinct patterns within and between the diseases.

PATIENTS AND METHODS

Study participants. Patients diagnosed as having SLE, primary SS, or myositis at Scandinavian rheumatology clinics, as well as healthy blood donors/population controls have been previously described in detail (23–25), and basic characteristics are presented in Supplementary Table 1, available on the *Arthritis & Rheumatology* website at <https://onlinelibrary.wiley.com/doi/10.1002/art.42122>. For validation of *C4* copy number calls and *HLA* alleles, we included whole-genome sequencing data from 75 parent/offspring trios, in which offspring were diagnosed as having SLE (26). The individual studies were approved by local ethics committees, and all study participants provided written informed consent.

Targeted sequencing, genotyping, and quality control. The capturing array and the targeted DNA sequencing of patients and healthy controls has previously been described (23–25,27). A detailed description of the sequencing workflow, alignment, genotype calling, and quality control at variant- and individual-based levels can be found in the Supplementary

¹⁰Helena Forsblad-d'Elia, MD, PhD: Sahlgrenska Academy at University of Gothenburg, Gothenburg, Sweden; ¹¹Sara Magnusson Bucher, MD: Örebro University, Örebro, Sweden; ¹²Katrine B. Norheim, MD, PhD, Svein Joar Auglænd Johnsen, MD, PhD, Roald Omdal, MD, PhD: Stavanger University Hospital, Stavanger, Norway; ¹³Marika Kvarnström, MD, PhD: Karolinska Institutet, Karolinska University Hospital, and Stockholm Health Services, Region Stockholm, Stockholm, Sweden; ¹⁴Marie Wahren-Herlenius, MD, PhD: Karolinska Institutet and Karolinska University Hospital Stockholm, Sweden, and University of Bergen, Bergen, Norway; ¹⁵Helena Andersson, MD, PhD, Øyvind Molberg, MD, PhD: Oslo University Hospital, Oslo, Norway; ¹⁶Louise Pyndt Diederichsen, MD, PhD: Copenhagen University Hospital, Rigshospitalet, Copenhagen, Denmark, and Odense University Hospital, Odense, Denmark;

¹⁷Jonas Almlöf, PhD, Ann-Christine Syvänen, PhD: Science for Life Laboratory and Uppsala University, Uppsala, Sweden; ¹⁸Kerstin Lindblad-Toh, PhD: Science for Life Laboratory and Uppsala University, Uppsala, Sweden, and Broad Institute of MIT and Harvard, Cambridge, Massachusetts.

Author disclosures are available at <https://onlinelibrary.wiley.com/action/downloadSupplement?doi=10.1002%2Fart.42122&file=art42122-sup-0001-Disclosureform.pdf>.

Address correspondence to Lars Rönnblom, MD, PhD, Department of Medical Sciences, Rheumatology, Rudbeck Laboratory, Dag Hammarskjölds Väg 20, Uppsala University, 75185 Uppsala, Sweden. Email: lars.ronnblom@medsci.uu.se.

Submitted for publication September 21, 2021; accepted in revised form March 15, 2022.

Information, available on the *Arthritis & Rheumatology* website at <https://onlinelibrary.wiley.com/doi/10.1002/art.42122>.

DNA sequencing and genotyping was performed at the SNP&SEQ Technology Platform in Uppsala, part of the National Genomics Infrastructure Sweden and Science for Life Laboratory. The computations were enabled by resources in projects sens2017142 and sens2020577, provided by the Swedish National Infrastructure for Computing at Uppsala Multidisciplinary Center for Advanced Computational Science.

Estimation of *C4* copy number and calling of *HLA* alleles from targeted sequencing data. The total copy number of *C4* was estimated based on read depth using the GermlineCNVCaller (GATK), and the relative read depths of 5 *C4A/C4B*-specific single-nucleotide variants were used for ascertainment of total number of *C4* copies into copy number of *C4A* and *C4B*. Genetic variants in the *C4A/C4B* genes were called at bp resolution using the HaplotypeCaller (GATK). The human endogenous retrovirus element present in some *C4* genes (28) was not analyzed (Supplementary Information, <https://onlinelibrary.wiley.com/doi/10.1002/art.42122>).

HLA alleles of 6 *HLA* genes (*HLA-A*, *HLA-B*, *HLA-C*, *HLA-DPB1*, *HLA-DQB1*, and *HLA-DRB1*) were called at 4-digit resolution from sequencing data using xHLA (29). A detailed workflow for the analysis of *C4* and *HLA* is available in the Supplementary Information together with method validation using results from previous polymerase chain reaction-based *C4* analyses (30–32).

Plasma *C4* concentration and autoantibody status of patients. Measurement of plasma *C4* in SLE and primary SS patients was performed at local centers as part of clinical routine (33,34). Information about autoantibodies was extracted from medical records, and healthy controls were included as a reference cohort under the assumption that autoantibodies are specific to patients. Nevertheless, a small percentage of the individuals in the general population may be positive for autoantibodies (34), but the impact on this study is considered negligible.

***C4b* deposition on heat-aggregated human IgG.** Serum from healthy individuals carrying only *C4A* genes or only *C4B* genes were incubated with heat-aggregated IgG, and deposition of *C4b* was detected by enzyme-linked immunosorbent assay, as described in the Supplementary Information (<https://onlinelibrary.wiley.com/doi/10.1002/art.42122>).

Statistical analysis. Statistical analyses were performed in R version 4.0.4 (35). Two-tailed *P* values less than 0.05 were considered significant. The statistical tests and covariates that were included (e.g., principal components for genetic population structure) are described in the text and figure legends. Odds ratios (ORs) and 95% confidence intervals (95% CIs) were calculated. For analysis of associations in the *HLA* region, a Bonferroni

correction for 5,000 tests was used, corresponding to a statistical significance threshold of 1×10^{-5} .

Data availability. Raw data for individual figures are available in the Supplementary Information (<https://onlinelibrary.wiley.com/doi/10.1002/art.42122>). Genotype data at the individual level are not publicly available since they contain information that could compromise research participant privacy and consent. Scripts for calling *C4* copy number in GermlineCNVCaller are available upon request. Members of the DISSECT consortium and the ImmunoArray consortium are described in the Supplementary Appendix (<https://onlinelibrary.wiley.com/doi/10.1002/art.42122>).

RESULTS

Association of *C4A* copy number with systemic inflammatory autoimmune diseases. Using targeted sequencing data, we estimated the *C4* copy number in 2,290 patients diagnosed as having SLE, primary SS, or myositis, and in 1,251 healthy controls (Figure 1A). The total *C4* copy number calls ranged from 2 to 8 *C4* copies, but since only 2 individuals had more than 6 *C4* copies (Supplementary Information, <https://onlinelibrary.wiley.com/doi/10.1002/art.42122>), we focused on subjects with 2–6 *C4* copies.

Notably, the pattern in *C4* copy number was relatively similar among the 3 systemic inflammatory autoimmune diseases, and therefore, we performed both joint and separate analyses of the diseases. As previously observed, a low *C4* copy number was associated with an increased risk of all 3 diseases compared to healthy controls (*P* for *C4* = 2×10^{-38}) (Figure 1B and Supplementary Figure 1A, <https://onlinelibrary.wiley.com/doi/10.1002/art.42122>), and this association was almost exclusively explained by the copy number of the *C4A* gene (*P* for *C4A* = 5×10^{-45}) (Figure 1C). We noted a negative correlation between *C4A* copy number and *C4B* copy number ($r_s = -0.50$) (Supplementary Figure 1B), and although the copy number of *C4B* was slightly higher in patients compared to controls, each decrease in *C4B* copy number was modestly associated with an increased risk of systemic inflammatory autoimmune disease when adjusting for the effect of *C4A* (*P* for *C4B* = 6×10^{-4}) (Figure 1C and Supplementary Figure 1A). Based on these results, we concluded that low *C4A* copy number is a strong risk factor for systemic inflammatory autoimmune disease, whereas the effect of *C4B* is limited.

Overlap of association with autoantibodies against SSA and SSB between systemic inflammatory autoimmune diseases. Autoantibodies against nuclear antigens are a common feature and part of the clinical evaluation of SLE, primary SS, and myositis, and therefore, we analyzed whether *C4A* copy number was associated with the autoantibody repertoire in patients. A strong and consistent association was detected

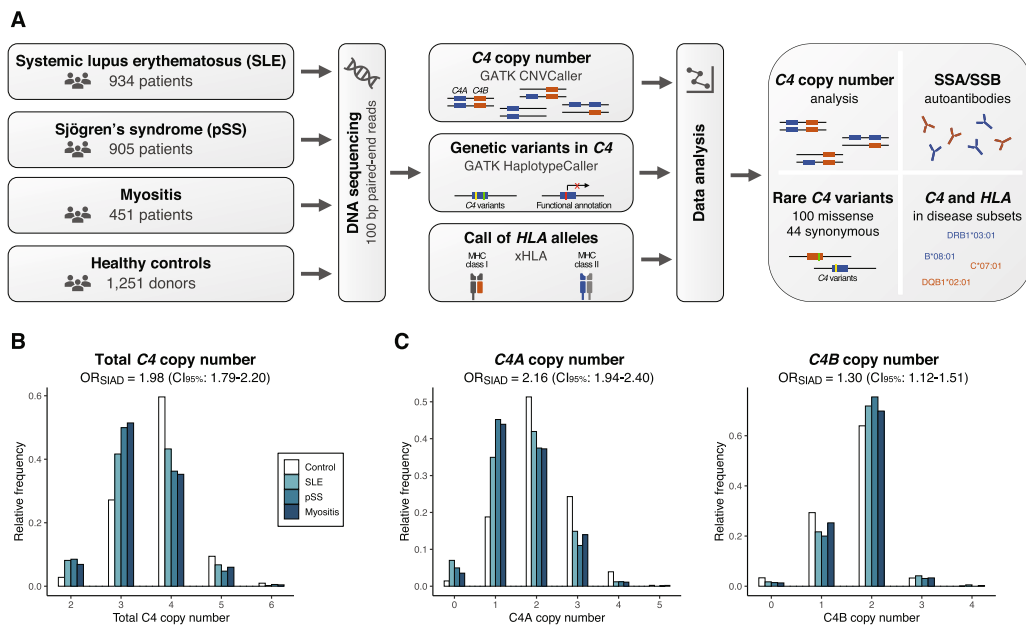


Figure 1. Association between complement *C4* copy number and 3 systemic inflammatory autoimmune diseases (SIADs). **A** Workflow for analysis. Three patient groups with systemic inflammatory autoimmune diseases and 1 reference cohort were analyzed for *HLA* alleles and copy number of the paralogous *C4* genes *C4A* and *C4B*, using targeted sequencing data. Association analysis of *C4* was performed for clinical subsets of the diseases. Additionally, common and rare variants in the *C4* genes were analyzed from the sequencing data. **B**, Total *C4* copy number in healthy controls and patients with systemic lupus erythematosus (SLE), primary Sjögren's syndrome (SS), or myositis ($n = 3,541$). Logistic regression was performed to analyze associations in the combined patient group compared to healthy controls, with adjustment for sex and principal components 1–4 (PC1–PC4). Odds ratios (ORs) represent disease risk in association with each decrease in *C4* copy number. **C**, Copy number of *C4A* and *C4B* in each patient group and healthy controls ($n = 3,520$). Analysis is based on logistic regression with both *C4A* and *C4B* included as additive variables and with adjustment for sex and PC1–PC4. ORs represent disease risk in association with each decrease in *C4A* or *C4B* copy number. MHC = major histocompatibility complex; CI_{95%} = 95% confidence interval.

between low *C4A* copy number and presence of anti-SSA and anti-SSB autoantibodies in all 3 diseases (Supplementary Table 2, <https://onlinelibrary.wiley.com/doi/10.1002/art.42122>). None of the other autoantibodies investigated for all diseases were consistently associated with *C4A* copy number (Supplementary Table 2).

The prevalence of anti-SSA/SSB autoantibodies differed highly among the diseases and was highest in primary SS, with 73% of patients having autoantibodies against SSA and/or SSB (Figure 2A). For myositis, 32% of patients had anti-SSA/SSB autoantibodies with most being against SSA and only 2.4% of patients being positive for both anti-SSA and anti-SSB. In SLE, 41% of patients had autoantibodies against SSA and/or SSB. A few patients (2.4%) had autoantibodies against SSB only, which is in line with the notion that anti-SSA antibodies appear first and may be followed by anti-SSB antibodies due to epitope spreading (36).

Remarkably, we observed a dose–response relationship between *C4A* copy number and the prevalence of autoantibodies against SSA and SSB in all 3 diseases. Each decrease in *C4A* copy number was associated with an increased risk of autoantibodies against both SSA and SSB (OR 5.89 [95% CI 4.83–7.23]), whereas the association with the systemic inflammatory autoimmune diseases without any autoantibodies against SSA/SSB was more modest (OR 1.53 [95% CI 1.36–1.73])

(Figure 2B). Patients with autoantibodies against either SSA or SSB showed a similar intermediate association, and therefore, we combined anti-SSA+SSB– and anti-SSA–SSB+ patients into 1 group (OR 2.37 [95% CI 2.02–2.77]).

Despite slight differences between the diseases, the associations of *C4A* copy number were more specific to the presence of anti-SSA/SSB autoantibodies than to the individual diseases, and thus, we evaluated the prevalence of autoantibodies against number of *C4A* copies collectively for the 3 diseases. This revealed a strong effect of *C4A* copy number on the association with autoantibodies against SSA/SSB, in which the risk of disease with anti-SSA/SSB autoantibodies for individuals with a *C4A* copy number of 0 was ~80 times higher than for individuals with a *C4A* copy number of 3 (Figure 2C). Interestingly, each change in *C4A* copy number was associated with a consistent change in disease risk.

In addition to a genetic association between *C4* copy number and autoantibodies against SSA and SSB, we also identified a functional association linking the two parameters. As previously shown (22,37), plasma C4 levels in patients with primary SS showed higher concentrations with an increasing copy number of *C4A* and *C4B* (Figure 2D). Additionally, we detected lower plasma C4 levels in patients with

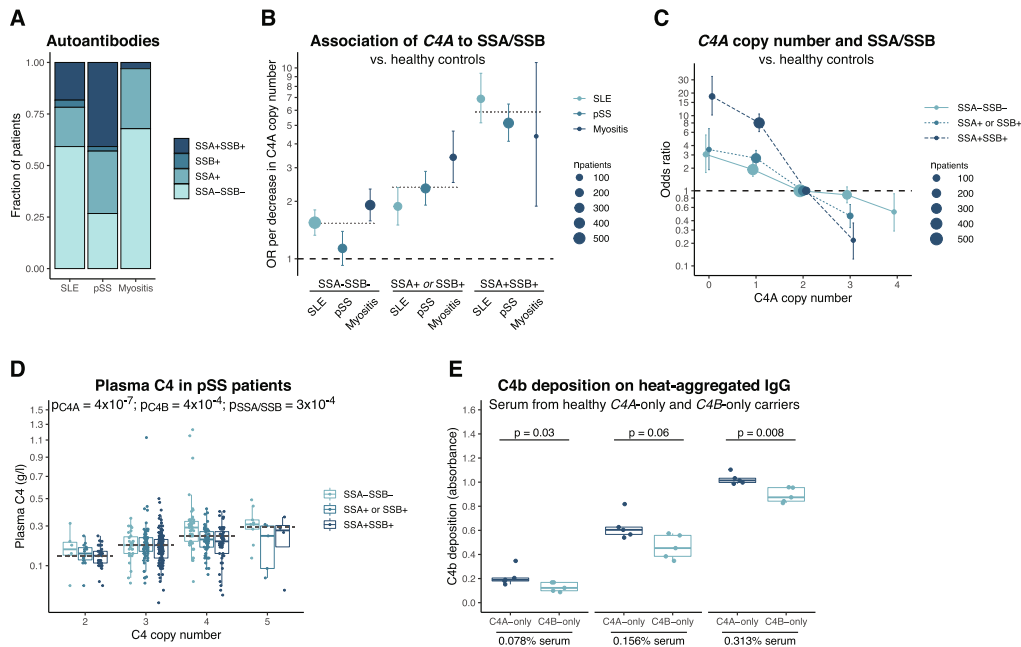


Figure 2. Association between *C4* copy number and anti-SSA/SSB autoantibodies. **A**, Prevalence of anti-SSA/anti-SSB autoantibodies in patients with SLE ($n = 919$), primary SS ($n = 902$), or myositis ($n = 364$). **B**, Logistic regression analysis of association between each decrease in *C4A* copy number and anti-SSA/anti-SSB autoantibody status among each patient group compared to healthy controls. Dotted lines indicate ORs for association in the combined group of 3 diseases. **C**, Logistic regression analysis of association between *C4A* copy number and anti-SSA/anti-SSB autoantibody status in the combined patient group compared to healthy controls. In **B** and **C**, bars represent 95% confidence intervals, and models have been adjusted for presence of *C4B*, sex, and PC1–PC4. **D**, Plasma C4 levels in patients with primary SS. Groups were compared by analysis of variance with square root–transformed values for the C4 concentration, adjusted for sex and cohort ($n = 470$). *C4A* and *C4B* copy number was included in the model; the x-axis shows total *C4* copy number for simplicity. **E**, Deposition of the complement activation product C4b on heat-aggregated human IgG, analyzed with varying concentrations of serum from healthy individuals carrying *C4A* genes only ($n = 5$) or *C4B* genes only ($n = 5$). The samples were analyzed ≥ 3 times, and the mean absorbance for each sample was evaluated using the Mann-Whitney U test. In **D** and **E**, Data are shown as box plots. Each box represents the 25th to 75th percentiles. Lines inside the boxes represent the median, and whiskers extend to 1.5 times the interquartile range. See Figure 1 for other definitions. Color figure can be viewed in the online issue, which is available at <http://onlinelibrary.wiley.com/doi/10.1002/art.42122/abstract>.

primary SS with autoantibodies against SSA/SSB when compared to patients with primary SS without anti-SSA/SSB autoantibodies (Figure 2D), suggesting a direct connection between anti-SSA/SSB autoantibodies and plasma C4. However, a similar association between plasma C4 and anti-SSA/SSB was not found for SLE patients ($P = 0.41$; $n = 411$) (Supplementary Figure 2A, <https://onlinelibrary.wiley.com/doi/10.1002/art.42122>).

By analyzing serum from healthy individuals carrying *C4A* genes only or *C4B* genes only, we detected a higher deposition of the C4 activation product C4b on aggregated human IgG for *C4A* carriers (Figure 2E). These results are consistent with the proposed role of *C4A* being more efficient than *C4B* in clearance of immune complexes and suggest a connection between low *C4A* copy number and impaired removal of immune complexes in systemic inflammatory autoimmune disease.

In summary, we showed a strong association between *C4A* copy number and autoantibodies against SSA and SSB, which to a greater extent represented an association with anti-SSA/SSB autoantibodies rather than with the systemic inflammatory autoimmune diseases themselves.

Higher proportion of SLE patients carrying the *C4A* loss-of-function (LoF) variant rs760602547. We continued by evaluating a common LoF variant (rs760602547) mainly found in *C4A*. The LoF variant results in a CT insertion in exon 29, which introduces a premature stop codon in *C4A* (38).

We called the LoF variant rs760602547 for patients and controls and detected the CT insertion in 7.7% of all individuals. Among the LoF carriers, 98% had 1 LoF variant, and the variant was not found among any of those carrying only *C4B* genes, thus supporting the notion that the CT insertion mainly is found in *C4A* and rarely in *C4B* (39). When analyzing the number of LoF variants in patients with SLE, primary SS, or myositis compared to healthy controls, no enrichment of the variant was seen in patients ($P > 0.10$ by logistic regression). However, logistic regression analysis allowing for interaction between *C4A* copy number and the LoF variant rs760602547 showed that SLE patients with a low *C4A* copy number carried the LoF variant to a greater extent than controls (P for LoF = 0.01; P for interaction = 0.03 [$n = 2,136$]) (Figure 3A), indicating an additional mechanism of impaired *C4A* function in SLE. The increased frequency of the LoF variant among SLE patients with a low *C4A* copy number

was also seen in a focused analysis of SLE patients and healthy controls with 1–2 *C4A* copies ($P = 0.01$ by Fisher’s exact test; $n = 1,559$). For patients with primary SS and those with myositis, no association was found for the LoF variant (P for interaction > 0.10) (Figure 3A). Grouping patients based on anti-SSA/SSB autoantibody status showed a tendency toward an increased frequency of the LoF variant in SSA/SSB-negative patients when compared to healthy controls, whereas no association was seen for the patients with SSA/SSB autoantibodies (Figure 3B).

Analysis of plasma C4 by linear regression showed lower C4 concentrations for carriers of the LoF variant rs760602547 (SLE: $P = 8 \times 10^{-5}$ [$n = 407$]; primary SS: $P = 5 \times 10^{-4}$ [$n = 471$]) (Supplementary Figure 3A, <https://onlinelibrary.wiley.com/doi/10.1002/art.42122>) after accounting for the copy number of *C4A* and *C4B*, demonstrating that the LoF variant directly affects plasma C4 concentration.

To ensure that the enrichment of the LoF variant rs760602547 in SLE patients with a low *C4A* copy number was not caused by an indirect linkage to *DRB1*03:01* or other SLE-associated *HLA* alleles, we analyzed the LD between the LoF

variant and common variants in *C4*, *HLA* alleles, and single-nucleotide polymorphisms (SNPs) in the *HLA* region. We detected multiple SNPs and *C4* variants in high LD with the LoF variant (Supplementary Figure 3B, Supplementary Data). For *HLA* alleles, the strongest LD was seen with *DQB1*06:04* ($R^2 = 0.56$), whereas *C4* copy number or *DRB1*03:01* was not in LD with the LoF variant rs760602547 ($R^2 < 0.10$). Therefore, the association of the LoF variant was independent of SLE-associated *HLA* alleles.

Overall, we detected lower plasma C4 levels in carriers of the LoF variant rs760602547, and the LoF variant was enriched in SLE patients with a low *C4A* copy number, thereby adding another level of complexity in the genetic variation of the complement system.

No enrichment of rare *C4* variants in systemic inflammatory autoimmune diseases. Due to the common variation in *C4* copy number, together with the high sequence homology between *C4A* and *C4B* (99.91% identical), nucleotide variants in the *C4* genes are generally omitted from sequencing-based analyses. By using information about the *C4* copy number for each individual while analyzing *C4* nucleotide variants

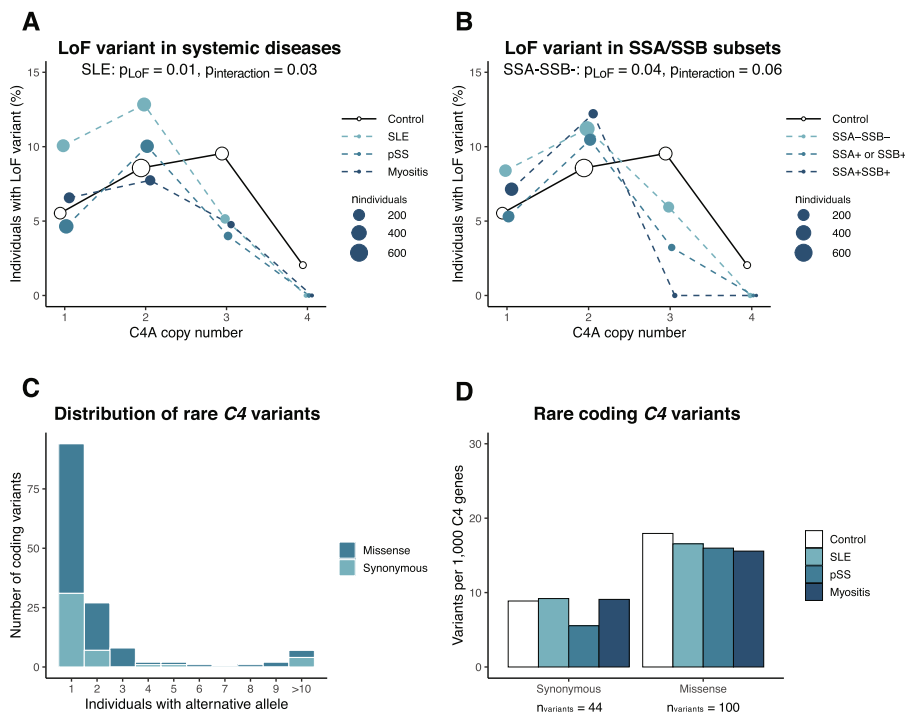


Figure 3. Loss-of-function (LoF) variant in *C4A* and rare variants in *C4* genes. **A**, Proportion of patients and healthy controls carrying the *C4A* LoF variant rs760602547. **B**, Proportion of the LoF variant rs760602547 among SSA/SSB autoantibody subgroups combined across the 3 systemic inflammatory autoimmune diseases and healthy controls. Patients (or SSA/SSB subgroups) and controls were grouped based on *C4A* copy number, and the size of points indicate the total number of individuals in each group with the specific *C4A* copy number. P values are based on logistic regression with interaction between *C4A* copy number and rs760602547. The LoF variant was only present among individuals with 1–4 *C4A* genes. **C**, Number of individuals carrying rare (present among $<0.5\%$ of all individuals) coding variants in ≥ 1 *C4* gene (synonymous, $n = 44$; missense, $n = 100$). Variants present among 10–17 individuals have been combined. **D**, Number of *C4* genes carrying a rare coding variant in each disease cohort. The number of variants in each disease group has been adjusted for total *C4* copy number in order to account for lower copy number of *C4* among patients with systemic inflammatory autoimmune diseases. See Figure 1 for other definitions. Color figure can be viewed in the online issue, which is available at <http://onlinelibrary.wiley.com/doi/10.1002/art.42122/abstract>.

(Supplementary Information, <https://onlinelibrary.wiley.com/doi/10.1002/art.42122>), we called common and rare variants for all study participants, focusing on coding variants. As variants could not be assigned unambiguously to *C4A* or *C4B*, variants were analyzed relative to the total *C4* copy number.

Overall, we detected 144 rare coding variants (present among <0.5% of all study participants). Of these variants, 65% were found in only 1 individual, and 69% of the variants were missense variants (Figure 3C and Supplementary Information). Analysis of rare coding variants in each disease group did not indicate an enrichment of rare synonymous or missense variants in any of the systemic inflammatory autoimmune diseases (Figure 3D). Further, prediction of the effect of missense variants did not show an enrichment of putative benign or deleterious variants in systemic inflammatory autoimmune diseases (Supplementary Figure 3C, <https://onlinelibrary.wiley.com/doi/10.1002/art.42122>), and no difference

was detected for rare *C4* variants in patients grouped based on anti-SSA/SSB autoantibody status (Supplementary Figure 3D).

In summary, we detected 144 rare variants in the coding sequence of *C4*, but no enrichment was observed in *C4* genes of patients with systemic inflammatory autoimmune disease.

Anti-SSA/SSB autoantibody subgroups and association with *HLA* and *C4*. Although the association of *C4A* copy number was more specific to anti-SSA/SSB autoantibody status than to the individual disease entity (Figure 2B), we noted some differences between the 3 systemic inflammatory autoimmune diseases. The most striking difference was observed for patients without anti-SSA/SSB autoantibodies, in which no association was seen between *C4A* copy number and primary SS (OR 1.13, $P = 0.23$), while a strong association was seen for a decrease in *C4A* copy number among myositis patients

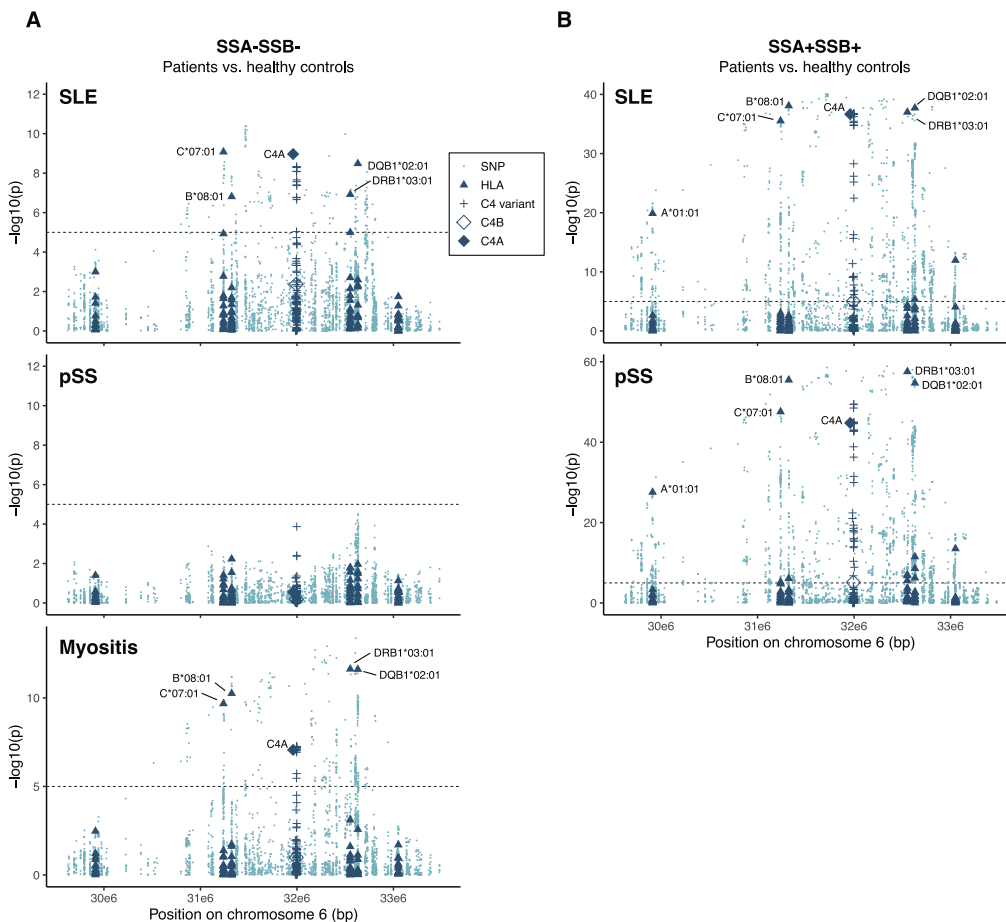


Figure 4. Association of variants in the *HLA* region with anti-SSA/SSB-negative and anti-SSA/SSB-positive patients. **A**, Association of variants in *HLA* region in patients with SLE ($n = 544$), primary SS ($n = 241$), or myositis ($n = 247$) who were negative for autoantibodies against SSA/SSB, as compared to healthy controls ($n = 1,251$). **B**, Regional association plot of *HLA* variants in patients with SLE ($n = 168$) or primary SS ($n = 368$) who were positive for autoantibodies against both SSA and SSB, as compared to healthy controls ($n = 1,251$). Few myositis patients ($n = 11$) had autoantibodies to both SSA and SSB, and therefore the data for these patients were not plotted. *HLA* alleles for 6 genes (*HLA-A*, *HLA-C*, *HLA-B*, *HLA-DRB1*, *HLA-DQB1*, and *HLA-DPB1*) and variants in *C4* present in >1% of individuals were included in the analysis. Groups were analyzed for associations using logistic regression with adjustment for sex and PC1–PC4. Dashed lines represent the Bonferroni-corrected significance threshold ($P = 1 \times 10^{-5}$). Color figure can be viewed in the online issue, which is available at <http://onlinelibrary.wiley.com/doi/10.1002/art.42122/abstract>.

(OR 1.91, $P = 4 \times 10^{-11}$) and to a lesser extent among SLE patients (OR 1.55, $P = 2 \times 10^{-8}$) (Figure 2B).

In order to evaluate whether other variants in the *HLA* region could explain these differences, we analyzed the association of SNPs, *HLA* alleles, *C4* copy number, and common variants in the *C4* genes in relation to the autoantibody status for each of the individual diseases. Global analysis of the *HLA* region generally showed an association with the extended *C*07:01–B*08:01–DRB1*03:01–DQB1*02:01* haplotype together with *C4A* copy number in both SLE and myositis patients without anti-SSA/SSB autoantibodies (Figure 4A). No additional associations were present after conditioning for the *HLA* allele with the strongest association (Supplementary Figure 4, <https://onlinelibrary.wiley.com/doi/10.1002/art.42122>). For patients with primary SS without autoantibodies to SSA/SSB, no association was seen with the *HLA* region (Figure 4A), suggesting at least partially different autoimmune processes among the 3 systemic inflammatory autoimmune diseases for the anti-SSA/SSB–negative subset of patients.

We continued analyzing genetic variation in the *HLA* region for patients with autoantibodies against both SSA and SSB. Due to the low number of anti-SSA/SSB–positive myositis patients ($n = 11$), we focused on SLE and primary SS patients. Again, the extended *C*07:01–B*08:01–DRB1*03:01–DQB1*02:01* haplotype together with *C4A* copy number generally showed a strong association with SLE and primary SS patients with autoantibodies against both SSA and SSB (Figure 4B). After conditioning for *DQB1*02:01* and *C4A* copy number, no additional association with *HLA* alleles was found for SLE (Supplementary Figure 5A, <https://onlinelibrary.wiley.com/doi/10.1002/art.42122>), whereas conditional analysis showed an association with *DRB1*03:01*, *DRB1*15:01*, *DQB1*04:02*, and *B*08:01* in anti-SSA/SSB–positive patients with primary SS patients (Supplementary Figure 5B).

The genomic reference sequence for *C4A* and *C4B* differs at 18 nucleotide positions of which 5 variants in exon 26 are used for defining copy number of *C4A* and *C4B* (Supplementary Information). In addition to the variants differing between *C4A/C4B* reference sequences, we detected 78 variants found in ≥ 1 *C4A/C4B* gene among more than 1% of the individuals. We included all 96 common variants in the analysis of the *HLA* region, using the number of *C4* genes, with alternative alleles for each variant as variables in the analysis. However, the copy number of *C4A* generally explained the largest part of the associations with minimal effect of individual variants in the *C4* genes (Figure 4 and Supplementary Figure 5).

In addition to the analysis of anti-SSA/SSB–negative and anti-SSA/SSB–positive patients against healthy controls, we also performed a pairwise case–case analysis of autoantibody subsets within the individual diseases and for the 3 systemic inflammatory autoimmune diseases combined. Again, the extended *C*07:01–B*08:01–DRB1*03:01–DQB1*02:01* haplotype together with *C4A* copy number explained the main association (Supplementary Figure 6, <https://onlinelibrary.wiley.com/doi/10.1002/art.42122>).

In summary, no association was seen between the *HLA* region and primary SS patients without any autoantibodies against SSA and SSB, in contrast with anti-SSA/SSB–negative SLE and myositis patients. Further, the extended *C*07:01–B*08:01–DRB1*03:01–DQB1*02:01* haplotype together with *C4A* copy number was associated with both anti-SSA/SSB–positive systemic inflammatory autoimmune diseases as well as SLE and myositis without anti-SSA/SSB autoantibodies. In conditional analyses, *C4A* copy number generally followed the extended *HLA* haplotype, and the copy number of *C4A* largely explained the association with *C4* with a minor effect of individual variants in the *C4* genes.

DISCUSSION

In the current study, we demonstrated a strong association between low *C4A* copy number and the presence of anti-SSA/SSB autoantibodies in the 3 systemic inflammatory autoimmune diseases: SLE, primary SS, and myositis. The similarities between the disease associations indicated that a low *C4A* copy number to a higher extent is associated with anti-SSA/SSB autoantibodies rather than to the individual disease entities.

Autoantibodies, such as anti-SSA and anti-SSB, generally appear several years before clinical onset of both SLE (40,41) and primary SS (42,43), indicating a slow progression from asymptomatic autoimmunity to clinical manifestations. Here, we demonstrated that a genetic susceptibility with a low *C4A* copy number is a risk factor for development of anti-SSA/SSB autoantibodies, and when present, the autoantibodies may contribute to systemic inflammatory autoimmune disease in a subset of individuals. Moreover, these observations may explain the partial overlap in clinical manifestations between diseases for a subgroup of patients (e.g., in SLE, in which 25% of patients are affected by secondary SS [44]). However, the low number of myositis patients with autoantibodies against both SSA and SSB limits the conclusions that can be drawn from this subset of patients.

Although the *C4A* copy number was associated with anti-SSA/SSB autoantibodies in a dose-dependent manner, the association between *C4A* copy number and systemic inflammatory autoimmune diseases without anti-SSA/SSB autoantibodies was limited. As described previously, no association with the *HLA* region was found for anti-SSA/SSB–negative patients with primary SS (24,45). In contrast, *C4A* copy number together with the extended *C*07:01–B*08:01–DRB1*03:01–DQB1*02:01* haplotype showed a residual association with anti-SSA/SSB–negative patients with SLE and myositis, which is consistent with earlier reports indicating *DRB1*03:01* as a risk factor in SLE patients without anti-SSA/SSB autoantibodies (46,47). This suggests partly different etiopathogenetic mechanisms for anti-SSA/SSB–negative patients with primary SS compared to patients with SLE or myositis.

We note that the Scandinavian study population in the current analysis is relatively homogenous, which may limit the generalizability of the study. Still, the variation in *C4* copy numbers generally follows the pattern reported in other studies of individuals of European ancestry (14,18,22).

While it is difficult to distinguish the association signal from *C4A* copy number and *DRB1*03:01* in populations of European descent, several lines of evidence support the notion that *C4A* copy number plays a central role in systemic inflammatory autoimmune diseases. Analysis of *C4* copy number in SLE patients of East Asian (48) and African American origin (22)—populations in which the LD between *C4A* copy number and *DRB1*03:01* is low—showed a strong risk with a low *C4* copy number. The importance of the complement system is further supported by the strong risk of SLE and lupus-like symptoms often including anti-SSA autoantibodies in individuals with deficiencies in any of the early classical complement pathway genes *C1Q*, *C1R*, *C1S*, *C4*, and *C2* (10,11).

The higher frequency of the common deleterious *C4A* variant among SLE patients with a low *C4A* copy number adds an additional modulating factor to the variation in *C4A* copy number and plasma levels of *C4* among SLE patients. Previous analyses of the LoF variant did not detect any enrichment in SLE patients (21,49). However, a larger cohort, along with a slightly increased frequency of the LoF variant, may explain the enrichment detected in the current study. Further, the enrichment was only seen when taking the *C4A* copy number into account, which was not done in the previous studies. Nevertheless, no enrichment of the LoF variant was seen in patients with primary SS or myositis, suggesting a higher vulnerability among SLE patients.

Despite a high similarity between the *C4A* and *C4B* proteins, a low copy number of *C4A* explained the major risk for systemic inflammatory autoimmune disease with only a minor effect for the *C4B* copy number. The 4 *C4A/C4B*-defining amino acids in exon 26 of *C4* alter the reactivity of *C4A* and *C4B* toward amino groups and hydroxyl groups, respectively. This is thought to increase the efficiency of *C4A* in the clearance of immune complexes and apoptotic cells, whereas *C4B* is more efficient in targeting microbes (9). We found more extensive depositions of the *C4* activation product *C4b* on aggregated human IgG when adding serum from individuals carrying only the *C4A* gene as compared to serum from individuals carrying only the *C4B* gene, thus indicating that *C4A* has enhanced capability to remove immune complexes. The functional differences between *C4A* and *C4B* were also investigated in a recent study by Simoni et al (50), in which lupus-prone mice were genetically modified to express *C4* with the human *C4A/C4B*-defining amino acids. When compared to mice coding for human *C4B*, mice coding for *C4A* showed enhanced clearance of apoptotic cells, less auto-reactive B cells and lower titers of anti-SSA autoantibodies, overall supporting the notion that *C4A* has a role in prevention of autoantibody generation and autoimmunity.

In conclusion, we demonstrated a strong association between low *C4A* copy numbers and the presence of anti-SSA/SSB autoantibodies in SLE, primary SS, and myositis. Similar relationships between *C4A* copy numbers and autoantibody status were observed in all 3 diseases. Our findings suggest that anti-SSA/SSB autoantibodies are largely dependent on genetic predisposition, and this subset of autoimmune patients may be considered a specific diagnostic entity.

ACKNOWLEDGMENTS

We thank Prof. Chack-Yung Yu for his support in the laboratory-based analysis of *C4* copy number, and Prof. David Pisetsky for critically reviewing the manuscript.

AUTHOR CONTRIBUTIONS

All authors were involved in drafting the article or revising it critically for important intellectual content, and all authors approved the final version to be published. Dr. Lundtoft had full access to all of the data in the study and takes responsibility for the integrity of the data and the accuracy of the data analysis.

Study conception and design. Lundtoft, Pucholt, Martin, Eloranta, Almlöf, Syvänen, Lindblad-Toh, Nilsson, Blom, Diaz-Gallo, Svenungsson, Rönnblom.

Acquisition of data. Lundtoft, Pucholt, Martin, Bianchi, Lundström, Eloranta, Sandling, Sjöwall, Jönsen, Gunnarsson, Rantapää-Dahlqvist, Bengtsson, Leonard, Baecklund, Jonsson, Hammenfors, Forsblad-d'Elia, Eriksson, Mandl, Bucher, Norheim, Johnsen, Omdal, Kvarnström, Wahren-Herlenius, Notarnicola, Andersson, Molberg, Diederichsen, Almlöf, Syvänen, Kozyrev, Lindblad-Toh, Blom, Lundberg, Nordmark, Diaz-Gallo, Svenungsson, Rönnblom.

Analysis and interpretation of data. Lundtoft, Pucholt, Martin, Bianchi, Lundström, Blom, Diaz-Gallo, Svenungsson, Rönnblom.

ADDITIONAL DISCLOSURES

Author Pucholt is currently an employee of Olink Proteomics, but was employed by Uppsala University during the time the study was conducted. Author Mandl is an employee of Novartis.

REFERENCES

1. Bentham J, Morris DL, Graham DS, Pinder CL, Tombleson P, Behrens TW, et al. Genetic association analyses implicate aberrant regulation of innate and adaptive immunity genes in the pathogenesis of systemic lupus erythematosus. *Nat Genet* 2015;47:1457.
2. Langefeld CD, Ainsworth HC, Graham DS, Kelly JA, Comeau ME, Marion MC, et al. Transancestral mapping and genetic load in systemic lupus erythematosus. *Nat Commun* 2017;8:16021.
3. Lessard CJ, Li H, Adrianto I, Ice JA, Rasmussen A, Grundahl KM, et al. Variants at multiple loci implicated in both innate and adaptive immune responses are associated with Sjögren's syndrome. *Nat Genet* 2013;45:1284.
4. Taylor KE, Wong Q, Levine DM, McHugh C, Laurie C, Doherty K, et al. Genome-wide association analysis reveals genetic heterogeneity of Sjögren's syndrome according to ancestry. *Arthritis Rheumatol* 2017;69:1294–305.
5. Miller FW, Chen W, O'Hanlon TP, Cooper RG, Vencovsky J, Rider LG, et al. Genome-wide association study identifies HLA 8.1 ancestral haplotype alleles as major genetic risk factors for myositis phenotypes. *Genes Immun* 2015;16:470–80.

6. Rothwell S, Cooper RG, Lundberg IE, Miller FW, Gregersen PK, Bowes J, et al. Dense genotyping of immune-related loci in idiopathic inflammatory myopathies confirms HLA alleles as the strongest genetic risk factor and suggests different genetic background for major clinical subgroups. *Ann Rheum Dis* 2016;75:1558.
7. Leffler J, Bengtsson AA, Blom AM. The complement system in systemic lupus erythematosus: an update. *Ann Rheum Dis* 2014;73:1601.
8. Thurman JM, Yapa R. Complement therapeutics in autoimmune disease [review]. *Front Immunol* 2019;10:672.
9. Sturfelt G, Truedsson L. Complement in the immunopathogenesis of rheumatic disease [review]. *Nat Rev Rheumatol* 2012;8:458.
10. Lintner KE, Wu YL, Yang Y, Spencer CH, Hauptmann G, Hebert LA, et al. Early components of the complement classical activation pathway in human systemic autoimmune diseases [review]. *Front Immunol* 2016;7:36.
11. Truedsson L. Classical pathway deficiencies—a short analytical review. *Mol Immunol*. 2015;68:14–9.
12. Birmingham DJ, Irshaid F, Nagaraja HN, Zou X, Tsao BP, Wu H, et al. The complex nature of serum C3 and C4 as biomarkers of lupus renal flare. *Lupus* 2010;19:1272–80.
13. Gladman DD, Ibañez D, Urowitz MB. Systemic lupus erythematosus disease activity index 2000. *J Rheumatol* 2002;29:288.
14. Yang Y, Chung EK, Wu YL, Savelli SL, Nagaraja HN, Zhou B, et al. Gene copy-number variation and associated polymorphisms of complement component c4 in human systemic lupus erythematosus (SLE): low copy number is a risk factor and high copy number is a protective factor against SLE susceptibility in European Americans. *Am J Hum Genet* 2007;80:1037–54.
15. Law SK, Dodds AW, Porter RR. A comparison of the properties of two classes, C4A and C4B, of the human complement component C4. *EMBO J* 1984;3:1819–23.
16. Isenman DE, Young JR. The molecular basis for the difference in immune hemolysis activity of the Chido and Rodgers isotypes of human complement component C4. *J Immunol* 1984;132:3019.
17. Yu CY, Belt KT, Giles CM, Campbell RD, Porter RR. Structural basis of the polymorphism of human complement components C4A and C4B: gene size, reactivity and antigenicity. *EMBO J* 1986;5:2873–81.
18. Lintner KE, Patwardhan A, Rider LG, Abdul-Aziz R, Wu YL, Lundström E, et al. Gene copy-number variations (CNVs) of complement C4 and C4A deficiency in genetic risk and pathogenesis of juvenile dermatomyositis. *Ann Rheum Dis* 2016;75:1599.
19. Jüptner M, Flachsbart F, Caliebe A, Lieb W, Schreiber S, Zeuner R, et al. Low copy numbers of complement C4 and homozygous deficiency of C4A may predispose to severe disease and earlier disease onset in patients with systemic lupus erythematosus. *Lupus* 2018;27:600–9.
20. Savelli SL, Roubey RA, Kitzmiller KJ, Zhou D, Nagaraja HN, Mulvihill E, et al. Opposite profiles of complement in antiphospholipid syndrome (APS) and systemic lupus erythematosus (SLE) among patients with antiphospholipid antibodies (aPL). *Front Immunol* 2019;10:885.
21. Boteva L, Morris DL, Cortés-Hernández J, Martin J, Vyse TJ, Fernando MM. Genetically determined partial complement C4 deficiency states are not independent risk factors for SLE in UK and Spanish populations. *Am J Hum Genet* 2012;90:445–56.
22. Kamitaki N, Sekar A, Handsaker RE, de Rivera H, Tooley K, Morris DL, et al. Complement genes contribute sex-biased vulnerability in diverse disorders. *Nature* 2020;582:577–81.
23. Sandling JK, Pucholt P, Rosenberg LH, Farias FH, Kozyrev SV, Eloranta ML, et al. Molecular pathways in patients with systemic lupus erythematosus revealed by gene-centred DNA sequencing. *Ann Rheum Dis* 2021;80:109–17.
24. Thorlacius GE, Hultin-Rosenberg L, Sandling JK, Bianchi M, Imgenberg-Kreuz J, Pucholt P, et al. Genetic and clinical basis for two distinct subtypes of primary Sjögren's syndrome. *Rheumatology (Oxford)* 2021;60:837–48.
25. Bianchi M, Kozyrev SV, Notarnicola A, Rosenberg LH, Karlsson Å, Pucholt P, et al. Contribution of rare genetic variation to disease susceptibility in a large Scandinavian myositis cohort. *Arthritis Rheumatol* 2022;74:342–52.
26. Almlöf JC, Nystedt S, Leonard D, Eloranta ML, Grosso G, Sjöwall C, et al. Whole-genome sequencing identifies complex contributions to genetic risk by variants in genes causing monogenic systemic lupus erythematosus. *Hum Genet* 2019;138:141–50.
27. Eriksson D, Bianchi M, Landegren N, Nordin J, Dalin F, Mathioudaki A, et al. Extended exome sequencing identifies BACH2 as a novel major risk locus for Addison's disease. *J Intern Med* 2016;280:595–608.
28. Dangel AW, Mendoza AR, Menachery CD, Baker BJ, Daniel CM, Carroll MC, et al. The dichotomous size variation of human complement C4 genes is mediated by a novel family of endogenous retroviruses, which also establishes species-specific genomic patterns among Old World primates. *Immunogenetics* 1994;40:425–36.
29. Xie C, Yeo ZX, Wong M, Piper J, Long T, Kirkness EF, et al. Fast and accurate HLA typing from short-read next-generation sequence data with xHLA. *Proc Natl Acad Sci* 2017;114:8059.
30. Wu YL, Savelli SL, Yang Y, Zhou B, Rovin BH, Birmingham DJ, et al. Sensitive and specific real-time polymerase chain reaction assays to accurately determine copy number variations (CNVs) of human complement C4A, C4B, C4-long, C4-short, and RCCX modules: elucidation of C4 CNVs in 50 consanguineous subjects with defined HLA genotypes. *J Immunol* 2007;179:3012.
31. Wu Y, Lundstrom E, Liu CC, Yang Y, Gunnarsson I, Svenungsson E, et al. Low copy-number of complement C4A, the presence of HLA-DR3, and the presence of HLA-DR2 are independent and additive risk factors for human systemic lupus erythematosus (SLE). *J Immunol* 2010;184 Suppl:93.
32. Sekar A, Bialas AR, de Rivera H, Davis A, Hammond TR, Kamitaki N, et al. Schizophrenia risk from complex variation of complement component 4. *Nature* 2016;530:177–83.
33. Enocsson H, Wirestam L, Dahle C, Padyukov L, Jönsen A, Urowitz MB, et al. Soluble urokinase plasminogen activator receptor (suPAR) levels predict damage accrual in patients with recent-onset systemic lupus erythematosus. *J Autoimmun* 2020;106:102340.
34. Svenungsson E, Gustafsson JT, Grosso G, Rossides M, Gunnarsson I, Jensen-Urstad K, et al. Complement deposition, C4d, on platelets is associated with vascular events in systemic lupus erythematosus. *Rheumatology (Oxford)* 2020;59:3264–74.
35. R Core Team. R: a language and environment for statistical computing: R Foundation for Statistical Computing; 2018. URL: <https://www.R-project.org/>.
36. Routsias JG, Tzioufas AG. B-cell epitopes of the intracellular autoantigens Ro/SSA and La/SSB: tools to study the regulation of the autoimmune response. *J Autoimmun* 2010;35:256–64.
37. Yang Y, Chung EK, Zhou B, Blanchong CA, Yu CY, Füst G, et al. Diversity in intrinsic strengths of the human complement system: serum C4 protein concentrations correlate with C4 gene size and polygenic variations, hemolytic activities, and body mass index. *J Immunol* 2003;171:2734.
38. Barba G, Rittner C, Schneider PM. Genetic basis of human complement C4A deficiency. Detection of a point mutation leading to non-expression. *J Clin Invest* 1993;91:1681–6.
39. Lokki ML, Circolo A, Ahokas P, Rupert KL, Yu CY, Colten HR. Deficiency of human complement protein C4 due to identical frame-shift mutations in the C4A and C4B genes. *J Immunol* 1999;162:3687.
40. Arbuckle MR, McClain MT, Rubertone MV, Scofield RH, Dennis GJ, James JA, et al. Development of autoantibodies before the clinical

- onset of systemic lupus erythematosus. *N Engl J Med* 2003;349:1526–33.
41. Eriksson C, Kokkonen H, Johansson M, Hallmans G, Wadell G, Rantapää-Dahlqvist S. Autoantibodies predate the onset of systemic lupus erythematosus in northern Sweden. *Arthritis Res Ther* 2011;13:R30.
 42. Theander E, Jonsson R, Sjöström B, Brokstad K, Olsson P, Henriksson G. Prediction of Sjögren's syndrome years before diagnosis and identification of patients with early onset and severe disease course by autoantibody profiling. *Arthritis Rheumatol* 2015;67:2427–36.
 43. Jonsson R, Theander E, Sjöström B, Brokstad K, Henriksson G. Autoantibodies present before symptom onset in primary Sjögren syndrome. *JAMA* 2013;310:1854–5.
 44. Ruacho G, Kvarnström M, Zickert A, Oke V, Rönnelid J, Eketjäll S, et al. Sjögren syndrome in systemic lupus erythematosus: a subset characterized by a systemic inflammatory state. *J Rheumatol* 2020;47:865.
 45. Gottenberg JE, Busson M, Loiseau P, Cohen-Solal J, Lepage V, Charon D, et al. In primary Sjögren's syndrome, HLA class II is associated exclusively with autoantibody production and spreading of the autoimmune response. *Arthritis Rheum* 2003;48:2240–5.
 46. Morris DL, Fernando MM, Taylor KE, Chung SA, Nititham J, Alarcón-Riquelme ME, et al. MHC associations with clinical and autoantibody manifestations in European SLE. *Gene Immun* 2014;15:210.
 47. Diaz-Gallo LM, Oke V, Lundström E, Elvin K, Wu YL, Eketjäll S, et al. Four systemic lupus erythematosus subgroups, defined by autoantibodies status, differ regarding HLA-DRB1 genotype associations and immunological and clinical manifestations. *ACR Open Rheumatol* 2022;4:27–39.
 48. Chen JY, Wu YL, Mok MY, Wu YJ, Lintner KE, Wang CM, et al. Effects of complement C4 gene copy number variations, size dichotomy, and C4A deficiency on genetic risk and clinical presentation of systemic lupus erythematosus in East Asian populations. *Arthritis Rheumatol* 2016;68:1442–53.
 49. Tsang-A-Sjoe MW, Bultink IE, Korswagen LA, van der Horst A, Rensink I, de Boer M, et al. Comprehensive approach to study complement C4 in systemic lupus erythematosus: gene polymorphisms, protein levels and functional activity. *Mol Immunol* 2017;92:125–31.
 50. Simoni L, Presumey J, van der Poel CE, Castrillon C, Chang SE, Utz PJ, et al. Complement C4A regulates autoreactive B cells in murine lupus. *Cell Rep* 2020;33:108330.

LETTERS

DOI 10.1002/art.42121

On the perils of peeking into the future: comment on the article by Rosenthal et al

To the Editor:

We read with interest the report of the study by Dr. Rosenthal and colleagues (1) in which they examined the effects of biologic treatment for psoriasis on the incidence of psoriatic arthritis (PsA) in a cohort of psoriasis patients compiled using administrative data from Israel. The authors observed a 39% increase in the risk of PsA among psoriasis patients who did not receive biologic disease-modifying antirheumatic drug (bDMARD) treatment compared with those who did receive this treatment (corresponding to a 28% reduction in psoriasis patients who received bDMARD treatment). We have 2 important issues to raise about this study.

The study, in contrast to its title mentioning a nested case–control analysis, uses a cohort design to compare the exposure groups. The basic idea underlying a case–control design is a comparison based on an outcome, where the difference of the sought exposure between the cases and controls quantifies the association between the exposure and the outcome. When a case–control study is undertaken within a cohort (i.e., nested) and the controls are sampled from risk sets of noncases at the time of each case occurrence, the design can be considered equivalent to a cohort and appropriately named as a “quasi-cohort” study (2). Rosenthal and colleagues, however, compared cohorts of exposure categories (ever used bDMARDs versus never used bDMARDs) for the incidence of an outcome (PsA). Thus, their study is a typical cohort study.

The second and more important issue involves exposure classification. Although not explicitly stated in their report, it had occurred to us, after we inspected the Kaplan–Meier curve presented in Figure 2, that the starting point of the time axis for the primary analysis was the date of psoriasis diagnosis. The authors then attempted to balance and further adjust for the time from diagnosis to treatment initiation in the 2 study arms, as well as to adjust for other confounders. Regardless of how appropriate these adjustments are, such splitting of a cohort at baseline based on exposure that has not yet occurred (i.e., peeking into the future) is the primary culprit in immortal time bias (3). In the study by Rosenthal and colleagues, one would expect considerable immortal person-time inserted into the bDMARD arm since bDMARDs are usually initiated when patients do not adequately respond to systemic treatments and/or to psoralen ultraviolet A. Therefore, by design, their study prohibited patients treated with

bDMARDs from developing PsA under systemic treatments that preceded the initiation of bDMARDs, while no such prohibition existed in the non-bDMARD control group. This immortal person-time in the bDMARD arm that was accrued under non-bDMARD treatment by design should have been classified as non-bDMARD systemic treatment and would have reduced the incidence of PsA observed under non-bDMARD treatment. Although we share the contention of the authors that bDMARD treatment in patients with psoriasis might be expected to reduce the risk of developing PsA, we suggest that the hazard ratio reported in this study was exaggerated by the addition of immortal person-time into the bDMARD arm that should have been included in the non-bDMARD arm.

Author disclosures are available at <https://onlinelibrary.wiley.com/action/downloadSupplement?doi=10.1002%2Fart.42121&file=art42121-sup-0001-Disclosureform.pdf>.

Melek Yalcin Mutlu, MD 
Friedrich Alexander University of Erlangen Nuremberg
and Universitätsklinikum Erlangen
Erlangen, Germany
and University of Health Sciences
Basaksehir Cam and Sakura City Hospital
Istanbul, Turkey
Koray Tascilar, MD 
koray.tascilar@uk-erlangen.de
Friedrich Alexander University of Erlangen Nuremberg
and Universitätsklinikum Erlangen
Erlangen, Germany

1. Rosenthal YS, Schwartz N, Sagy I, Pavlovsky L. Incidence of psoriatic arthritis among patients receiving biologic treatments for psoriasis: a nested case–control study. *Arthritis Rheumatol* 2022;74:237–43.
2. Suissa S. The Quasi-cohort approach in pharmacoepidemiology: upgrading the nested case-control. *Epidemiology* 2015;26:242–6.
3. Hudson M, Tascilar K, Suissa S. Comparative effectiveness research with administrative health data in rheumatoid arthritis. *Nat Rev Rheumatol* 2016;12:358–66.

DOI 10.1002/art.42123

Reply

To the Editor:

We thank Drs. Mutlu and Tascilar for their interest in our work and their constructive remarks on our recently published article.

We agree that this work was a cohort study, as mentioned in our article. Unfortunately, and regretfully, while working with the running title, we missed the nested case–control part of the full title.


Regarding the second and more important concern of exposure definition and immortal time bias, we would like to clarify our approach to this study design and the necessity of “peeking into the future.”

The main problem in our study was confounding by indication; namely, there were reasons why some patients were prescribed bDMARDs and others were not (e.g., severity of disease, relative unavailability of biologics in the past, good response to systemic treatments). Those not prescribed bDMARDs thus formed our control group, which was made up of patients treated with 2 systemic medications, as required by local regulations before approval for bDMARDs, and we measured the follow-up time from the psoriasis diagnosis, as time from psoriasis diagnosis is one of the major factors for PsA development. As mentioned by Mutlu and Tascilar, this splitting of a cohort at baseline according to future exposure to bDMARDs implemented an immortality time interval; that is, a time interval passed between the initiation of systemic treatment and the start of bDMARD treatment, but only for the bDMARD treatment group. The authors of the letter suggested that immortal person-time should have been also classified for non-bDMARD (systemic) treatments, which would have reduced the incidence of PsA reported in the non-bDMARD treatment group.

To estimate the influence of this bias, we performed additional analysis in which, as noted by Mutlu and Tascilar, the time axis for the primary analysis started at the point when specific treatment (bDMARD or non-bDMARD) was started. By doing so, patients who developed PsA after initiation of systemic treatment but before initiation of bDMARDs were relocated to the control group, and no immortal time interval existed. Multivariable Cox regression analysis was performed, with adjustment for age, sex, and time to systemic treatment initiation. Under these conditions, our preliminary analysis demonstrated that the adjusted hazard ratio (HR_{adj}) for PsA was lower than originally reported (HR_{adj} 1.28 versus 1.39), as was noted by Mutlu and Tascilar. Nonetheless, the finding of higher risk in the non-bDMARD group is still clinically and statistically significant, and therefore the conclusion of our study is valid. Although immortal time bias can occur in cohort studies and can overestimate the outcome rate in the unexposed group (1), sound efforts at minimizing the influence of more common biases should not be sacrificed to that of immortal time bias (2).

In general, retrospective studies such as ours have inherent limitations, as recently mentioned in a review of retrospective studies on PsA development (3). Therefore larger, multinational studies are needed to clarify this important clinical issue.

Author disclosures are available at <https://onlinelibrary.wiley.com/action/downloadSupplement?doi=10.1002%2Fart.42123&file=art42123-sup-0001-Disclosureform.pdf>.

Yael Shalev Rosenthal, MPH 
 Tel Aviv University
 Tel Aviv, Israel
 Naama Schwartz, PhD
 University of Haifa
 Haifa, Israel
 Iftach Sagy, MD, MPA, PhD
 Soroka University Medical Center
 and Ben-Gurion University of the Negev
 Beer Sheva, Israel
 Lev Pavlovsky, MD, PhD
levp@clalit.org.il
 Tel Aviv University
 and Rabin Medical Center
 Petah Tikva, Israel

1. Suissa S. Immortal time bias in observational studies of drug effects. *Pharmacoepidemiol Drug Saf* 2007;16:241–9.
2. Kiri VA, Mackenzie G. Re: “Immortal time bias in pharmacoepidemiology.” *Am J Epidemiol* 2009;170:667–8.
3. Merola JF, Ogdie A. Does psoriasis treatment affect PsA development? *Nat Rev Rheumatol* 2021;17:708–9.

DOI 10.1002/art.42132

No evidence of leptin mediating the effect of body mass index on hand pain and its duration in the Chingford 1000 Women Study: original research supplementing the study by Gløersen et al

To the Editor:

We read with interest the study by Dr. Gløersen and colleagues (1) investigating the direct and indirect effects of body mass index (BMI), mediated via 21 inflammatory biomarkers, on musculoskeletal pain in a hand osteoarthritis (OA) cohort. Gløersen et al found that log-transformed leptin mediated the BMI effect per 5 units on the intensity of hand pain in 1 of 2 used scales. Some of the limitations they discussed included concerns over the generalizability of the findings, lack of longitudinal evidence, and consideration of structural changes. Thus, to further explore this research question, we investigated the direct and indirect effect of BMI via leptin on hand pain in 1) a population-representative (general) sample of middle-aged women, 2) a subsample of women with radiographic hand OA whose disease progressed over 10 years (structural progression), 3) a subsample of women who developed structural hand OA changes in 10 years (structural incidence), and 4) a subsample of women who had no structural changes or over 10 years who developed these in the hand joints (no structural changes).

We utilized longitudinal data (years 1, 10, and 11) from the Chingford 1000 Women study (year 1, mean \pm SD age 54 \pm 5.9 years and BMI 25.3 \pm 3.9 kg/m²; year 10, mean \pm SD BMI

Table 1. Effects of BMI, direct and indirect via leptin, on hand pain and its duration of hand pain*

Sample and BMI effect	Sample size	Hand pain, OR (95% CI)	Duration of hand pain, OR (95% CI)
Cross-sectional models†			
General sample‡			
Direct	757	1.01 (0.96–1.05)	1.01 (0.98–1.03)
Indirect via leptin		1.00 (0.98–1.03)	1.00 (0.98–1.01)
Structural progression subsample			
Direct	252	0.97 (0.90–1.04)	0.97 (0.93–1.01)
Indirect via leptin		1.00 (0.94–1.04)	1.00 (0.98–1.03)
Structural incidence subsample			
Direct	179	1.03 (0.93–1.14)	1.06 (1.01–1.11)§
Indirect via leptin		0.99 (0.92–1.05)	0.98 (0.95–1.01)
Subsample with no structural changes			
Direct	161	0.96 (0.85–1.08)	0.98 (0.94–1.03)
Indirect via leptin		1.04 (0.97–1.13)	1.02 (0.99–1.04)
Longitudinal models†			
General sample‡			
Direct	763	1.01 (0.97–1.05)	1.01 (0.99–1.03)
Indirect via leptin		1.01 (0.99–1.03)	1.00 (0.99–1.02)
Structural progression subsample			
Direct	255	0.94 (0.87–1.02)	0.97 (0.93–1.02)
Indirect via leptin		1.01 (0.97–1.05)	1.01 (0.99–1.04)
Structural incidence subsample			
Direct	180	1.11 (1.01–1.23)§	1.11 (1.05–1.17)§
Indirect via leptin		0.99 (0.94–1.04)	0.98 (0.96–1.00)
Subsample with no structural changes			
Direct	163	1.00 (0.90–1.11)	0.99 (0.95–1.04)
Indirect via leptin		1.01 (0.95–1.08)	1.00 (0.98–1.03)

* Models were created using ordinary least squares regression models with a binary or ordinal outcome and continuous exposure and mediator. The effect of body mass index (BMI) is considered significant if the 95% bootstrap confidence interval (95% CI) does not include the value of 1.00. OR = odds ratio.

† Cross-sectional models included year 10 BMI (kg/m²) (predictor); year 10 leptin (pg/ml) (mediator); year 10 any hand pain in the last year (yes vs. no) or duration of hand pain in the previous month (0, 1–5, 6–14, ≥15 painful days) (outcome); and age (years), smoking (currently yes vs. no), profession/occupation (manager/administration, skilled/unskilled manual worker, other nonspecified vs. housewife/cleaning), menopause (yes vs. no), any medication use (yes vs. no), major illness/operation (yes vs. no), and Short Form 36 health survey score (confounding factors). Longitudinal models included baseline–year 1 BMI (kg/m²) (predictor); year 10 leptin (pg/ml) (mediator); year 10 any hand pain in the last year (yes vs. no) or duration of hand pain in the previous month (0, 1–5, 6–14, ≥15 painful days) (outcome); and the same confounding variables as for the cross-sectional models except the Short Form 36 health survey score that was not available at baseline, but instead physical activity was available and included (active if walking >5 miles or doing sport >2 hours/week or had job that assumed activity at least half of the working time vs. nonactive).

‡ The general sample included participants from the Chingford 1000 Women Study who attended year 1 (baseline) and year 10 follow-ups, had no leptin outliers, and had no missing values in confounding variables. Hand radiographs were obtained in years 1 and 11 and were used for defining structural subsamples. Structural progression subsample included women who, in year 1, had a Kellgren/Lawrence (K/L) radiographic severity grade of ≥2 in any interphalangeal or carpometacarpal joint and who, in year 11, presented a K/L score of ≥2 in the joint with progression of at ≥1 grade from year 1 to year 11. Structural incidence subsample included women who, in year 1, did not have a K/L score of ≥2 in any interphalangeal or carpometacarpal joint but developed it in ≥1 joint in year 11. Subsample with no structural changes included women who did not have K/L radiographic severity grade of ≥2 in any interphalangeal or carpometacarpal joint in year 1 and year 11. There were 153 women did not have repeated radiographic data and 12 women who had a K/L radiographic severity score of ≥2 in interphalangeal or carpometacarpal joint in year 1 that did not progress in severity by year 11.

§ Statistically significant.

26.7 ± 4.6 kg/m²) (2,3) and made several methodologic changes to the study by Gløersen et al. For our analyses, we used a standard unit-change BMI (kg/m²) scale. Over 19 years, fewer than 20% of women had BMI patterns with a 5-unit change (rare effect), and, for participants in the Chingford study with an average height of 1.60 meters, a 5-unit BMI change corresponded to a 12.8-kg weight difference (large effect) (2,3). We did not log-transform leptin. Instead, given our general sample,


we tested for outliers, as we previously demonstrated their impact (2,4), and reported results without leptin outliers. In the Chingford study, 2 pain outcomes were reported: binary, which was defined as any hand pain in the last year, and ordinal, which was defined as duration of hand pain in the previous month. We showed that BMI and hand pain were unidirectionally related (3). Thus, as the exposure, we used year 1 BMI for longitudinal and year 10 BMI for cross-sectional mediation models, with year

10 leptin as mediator and year 10 hand pain outcomes. Mediation models quantify the indirect effects as the product of the exposure to the mediator and the mediator to the outcome effects (2). The analyses were controlled for the influence of age, smoking, profession/occupation, menopause, major illness/surgery, medication use, physical activity, and overall health (according to Short Form 36 health survey) (2,3).


As shown in Table 1, we found a direct BMI effect on hand pain and its duration in women with incidental structural hand OA, but no significant indirect effect via leptin. Perhaps women with higher BMI used their hands to support themselves when getting up as they aged or put weight on their hands through other ways and thus increased their chance for structural changes and pain.


Concerning indirect effects, Kroon et al (5) found no leptin-mediated effects of BMI in hand OA in a cross-sectional setting. Gløersen et al (1) performed multiple-biomarker testing and explored 2 pain intensity scales in hand OA again in cross-sectional settings and found only a leptin-mediated effect with one but not the other scale. We failed to generalize the indirect leptin effect of BMI on hand pain and its duration in a community-based sample and structural hand OA in cross-sectional and longitudinal settings. We suggest that the evidence on leptin-mediated effects of BMI on hand pain can be considered weak and invite considerations of other pathways of BMI mechanism and leptin's role in hand pain.


Author disclosures are available at <https://onlinelibrary.wiley.com/action/downloadSupplement?doi=10.1002%2Fart.42132&file=art42132-sup-0001-Disclosureform.pdf>.

Romain S. Perera, PhD 
University of Oxford
Oxford, UK


and University of Colombo
Colombo, Sri Lanka

Malvika Gulati, MRCP 


Karishma Shah, PhD 
University of Oxford
Oxford, UK

Deborah J. Hart, PhD 

Tim D. Spector, PhD 
King's College London
London, UK

Nigel K. Arden, MD 

University of Oxford
Oxford, UK
and University of Southampton
Southampton, UK

Maja R. Radojčić, PhD 
maja.radojic@ndorms.ox.ac.uk
University of Oxford
Oxford, UK

mediating role of inflammatory biomarkers in hand osteoarthritis. *Arthritis Rheumatol* 2022;74:810–7.

- Perera RS, Chen L, Hart DJ, Spector TD, Arden NK, Ferreira ML, et al. Effects of body weight and fat mass on back pain - direct mechanical or indirect through inflammatory and metabolic parameters? *Semin Arthritis Rheum* 2022;52:151935.
- Radojčić MR, Perera RS, Chen L, Spector TD, Hart DJ, Ferreira ML, et al. Specific body mass index trajectories were related to musculoskeletal pain and mortality: 19-year follow-up cohort. *J Clin Epidemiol* 2021;141:54–63.
- Radojčić MR, Thudium CS, Henriksen K, Tan K, Karlsten R, Dudley A, et al. Biomarker of extracellular matrix remodelling C1M and proinflammatory cytokine IL-6 are related to synovitis and pain in end-stage knee OA patients. *PAIN* 2017;158:1254–63.
- Kroon FP, Veenbrink AI, de Mutsert R, Visser AW, van Dijk KW, le Cessie S, et al. The role of leptin and adiponectin as mediators in the relationship between adiposity and hand and knee osteoarthritis. *Osteoarthritis Cartilage* 2019;27:1761–7.

DOI 10.1002/art.42130

Reply

To the Editor:

We thank Dr. Perera and colleagues for their interest in our study on associations between BMI and pain and the mediating role of inflammatory biomarkers in hand OA. We appreciate their efforts to replicate our findings in a longitudinal population-based study and have some possible explanations for why our results differ.

In the Nor-Hand study, BMI was associated with hand pain intensity in the previous 24 hours (Numerical Rating Scale [NRS]) and hand pain intensity during rest and during hand activities in the previous 48 hours (Australian/Canadian Osteoarthritis Hand Index [AUSCAN]), with leptin appearing to mediate these associations. In the Chingford 1000 Women study, hand pain outcomes were defined differently as presence of any hand pain and duration of hand pain and with a longer recall period (up to 1 year). The complexity of the pain experience and the different dimensions assessed by these outcomes are possible explanations for the difference in findings. Furthermore, because participants in our study were recruited from a rheumatology clinic, most had hand symptoms with large variations in pain intensity. Perera and colleagues studied a sample of middle-aged women. Although they did not provide information on variation in pain intensity, a community-based sample is likely to have a lower range of pain, which can limit the ability to assess associations with pain.

We agree with Perera et al that false-positive results cannot be completely ruled out due to testing of several inflammatory biomarkers. The relative consistency of the mediating role of leptin

1. Gløersen M, Steen Pettersen P, Neogi T, Jafarzadeh SR, Vistnes M, Thudium CS, et al. Associations of body mass index with pain and the

being statistically significant for AUSCAN and borderline statistically significant for NRS suggests this is unlikely to be a chance finding. Furthermore, the magnitude of effect rather than the statistical significance of the mediating effects should be the focus of our inferences (1); for both hand pain outcomes in our study, the mediating effects of leptin were similar.

Perera and colleagues also used a different approach in their analysis of leptin data by removing outliers. In our original analyses, we log-transformed leptin to reduce skewness and the influence of outliers. We repeated our analyses using untransformed data on leptin levels and with removal of outliers, as was done by Perera and colleagues, and we found that our conclusions remained unchanged (Table 1).

Another difference is that we conducted a causal inference-based mediation analysis. This framework separates the effect definitions from the statistical model used for estimation, making it more widely applicable than the traditional approach to mediation analysis (2). We analyzed exposures, mediators, and outcomes as continuous variables to retain all information in the data. We presented our results per standard deviation increase in BMI (5.0 kg/m²) or waist circumference (13.1 cm) for ease of comparing estimates across models with different explanatory variables. This approach leads to easier interpretability than if we had presented our results per unit increase but has no impact on the ability to identify mediating effects.

We agree with Perera and colleagues that the observations of a mediating effect of leptin on the association between BMI and

hand pain should be replicated in longitudinal studies. Future studies should involve a careful selection of pain outcome measures.

The Nor-Hand study was supported by the Major and Lawyer Eivind Eckbo's Foundation, the South-Eastern Norway Regional Health Authority, Dr. Trygve Gythfeldt and wife's Research Foundation, Pahle's Foundation, and Simon Fougner Hartmann's Family Foundation. Dr. Neogi's work (awards P30-AR-072571 and K24 AR-070892) and Dr. Jafarzadeh's work (awards R03-AG-060272, R21-AR-074578, and P30-AR-072571) were supported by the NIH. We thank the participants, physicians, and research assistants involved in the Nor-Hand study and the project coordinators (Karin Magnusson, Elisabeth Mulrooney, Janicke Magnus). We also thank Siri Beisvåg Rom and Gro Jensen at Diakonhjemmet Hospital, who analyzed the plasma inflammatory biomarkers. Author disclosures are available at <https://onlinelibrary.wiley.com/action/downloadSupplement?doi=10.1002%2Fart.42130&file=art42130-sup-0001-Disclosureform.pdf>.



Marthe Gløersen, MD 
marthe.gl@hotmail.com
 Diakonhjemmet Hospital
 and University of Oslo
 Oslo, Norway
 Tuhina Neogi, MD, PhD 
 S. Reza Jafarzadeh, MPVM, PhD 
 Boston University School of Medicine
 Boston, MA
 Joe Sexton, PhD
 Ida K. Haugen, MD, PhD 
 Diakonhjemmet Hospital
 Oslo, Norway

Table 1. Estimates of the total effect of a 5-unit increase in BMI on hand pain and the corresponding natural direct effects and natural indirect effects mediated by plasma levels of leptin*

	AUSCAN hand pain, effect estimate (95% CI)	NRS hand pain, effect estimate (95% CI)
Parsimonious model†		
Total effect	0.73 (0.25, 1.23)‡	0.54 (0.24, 0.84)‡
Direct effect	0.38 (-0.27, 1.02)	0.30 (-0.08, 0.65)
Indirect effect	0.35 (-0.02, 0.75)	0.25 (0.07, 0.44)‡
Comprehensive model†		
Total effect	0.59 (0.12, 1.07)‡	0.49 (0.22, 0.76)‡
Direct effect	0.22 (-0.36, 0.81)	0.26 (-0.08, 0.59)
Indirect effect	0.37 (0.00, 0.73)‡	0.23 (0.04, 0.43)‡

* The effect estimates and 95% confidence interval (95% CI) represent estimated average increase in the pain outcomes per SD (5.0 kg/m²) increase in body mass index (BMI). AUSCAN = Australian/Canadian Osteoarthritis Hand Index (range 0–20); NRS = Numerical Rating Scale (range 0–10).

† The parsimonious model was adjusted for age, sex, and education; the comprehensive model was adjusted for age, sex, education, physical exercise, sleep, smoking, Hospital Anxiety and Depression Scale score, and Pain Catastrophizing Scale score.

‡ Statistically significant at the 5% level.

1. Greenland S, Senn SJ, Rothman KJ, Carlin JB, Poole C, Goodman SN, et al. Statistical tests, P values, confidence intervals, and power: a guide to misinterpretations. *Eur J Epidemiol* 2016;31:337–50.
2. Nguyen TQ, Schmid I, Stuart EA. Clarifying causal mediation analysis for the applied researcher: defining effects based on what we want to learn. *Psychol Methods* 2021;26:255–71.

DOI 10.1002/art.42136

Very limited data in the Global Burden of Disease Study 2019 to estimate the prevalence of osteoarthritis in 204 countries over 30 years: comment on the article by Long et al

To the Editor:

We read with great interest the article by Dr. Long and colleagues (1) in which prevalence trends of osteoarthritis (OA) at 4 anatomic sites were analyzed at global, regional, and national levels. The estimates were sourced from the Global Burden of Disease (GBD) Study 2019 (2). We would like to note that the prevalence data from the GBD Study 2019 that underpin the study from Long et al are incomplete.

As shown in Appendix 1 (page 1,193) of the GBD Study 2019 (2), only data from 23, 25, 40, and 1 country were available for prevalence of OA at the hip, knee, hand, and other anatomic



sites, respectively. With these limited data sources, Long and colleagues calculated prevalence estimates of OA at all 4 sites for 204 countries over a 30-year period (1990–2019). The gaps in data meant that these estimates were highly uncertain; however, this level of uncertainty was not communicated to the readers as a significant limitation of their study. With a limited data input source, we find the estimated prevalence of OA at other sites to be of special concern.

In their study, Long and colleagues presented the national estimated prevalence of OA at other sites in 2019 (Supplementary Figure 11, <http://onlinelibrary.wiley.com/doi/10.1002/art.42089>), the changes in the absolute number from 1990 to 2019 (Supplementary Figure 12), and the estimated annual prevalence changes from 1990 to 2017 (Supplementary Figure 13). To understand the data underpinning these figures, we searched the GBD 2019 website (3) for the actual prevalence data of OA at other sites using the fields of “Nonfatal Health Outcomes” as component, “Osteoarthritis other” as cause, and “Global” as location. Our search uncovered only 6 years of annual US data in the Truven Health Analytics MarketScan Commercial Claims and Encounters database (from 2000 and 2010–2014). We doubt whether these claimants were truly representative of the US population as a whole, and the use of such US health care claims data may be of minimal value for ascertaining the actual prevalence of OA at various other anatomic sites.

The key problem is that Long and colleagues calculated annual prevalence of OA at other sites in 204 countries over 30 years based on only 6 years of US health care data. These estimates should be considered as highly unreliable and with limited practical implication. The authors stated that the GBD modeling could “fill a gap where actual relevant data for a given disease burden are scarce or unavailable, thus allowing comparisons across regions and over time periods.” However, the absolute amount of incomplete data, especially for OA at other sites, was not explicitly revealed to the readers. We do not understand how modeling can provide accurate estimates for annual prevalence of OA at other sites in 204 countries using 6 years of data from the US, let alone how prevalence changes could be calculated in these countries over a 30-year period.

In our view, we believe that more primary studies are needed to determine the actual prevalence and incidence of OA in the real world and to fill in the gaps in the evidence base that underpins the GBD Study 2019.

Author disclosures are available at <https://onlinelibrary.wiley.com/action/downloadSupplement?doi=10.1002%2Fart.42136&file=art42136-sup-0001-Disclosureform.pdf>.

Qiuzhe Chen, BMed, MPT 
 Christopher G. Maher, PhD 
 Gustavo C. Machado, PhD
gustavo.machado@sydney.edu.au

*Institute for Musculoskeletal Health
 University of Sydney
 and Sydney Local Health District
 Sydney
 New South Wales, Australia*

1. Long H, Liu Q, Yin H, et al. Prevalence trends of site-specific osteoarthritis from 1990 to 2019: findings from the Global Burden of Disease Study 2019. *Arthritis Rheumatol* 2022;74:1172–83.
2. GBD 2019 Diseases and Injuries Collaborators. Global burden of 369 diseases and injuries in 204 countries and territories, 1990–2019: a systematic analysis for the Global Burden of Disease Study 2019 [published correction appears in *Lancet* 2020;396:1562]. *Lancet* 2020;396:1204–22.
3. Global Burden of Disease Collaborative Network. Global Burden of Disease Study 2019 (GBD 2019) Data Input Sources Tool. Institute for Health Metrics and Evaluation. URL: <http://ghdx.healthdata.org/gbd-2019/data-input-sources>.

DOI 10.1002/art.42134

Reply

To the Editor:

We thank Dr. Chen and colleagues for their interest in our study and their comments. We appreciate the opportunity to respond.

The procedure of prevalence estimation of OA is based on statistical modeling within the constraints of available data, and all the prevalence estimates in our study were sourced from the Global Health Data Exchange results tool (1). In general, when data in a specific country or region are sparse or absent, prevalence for that country or region is estimated according to data from the geographic proximity to that country or region and model covariates. As a result, the GBD Study provides internal validation on comparisons across regions and over time periods, and these estimates are not comparable to actual results in the real world. For example, data on prevalence of OA at other joints are lacking from many countries. Indeed, prevalence of OA at other joints in the GBD Study 2019 was obtained from only 1 source, the US Truven Health Analytics MarketScan Commercial Claims and Encounters database (years 2000 and 2010–2014) (2); thus, the prevalence estimates of OA at other joints for other countries and regions are dependent on the accuracy of the predictive model.

However, we believe that the secular trend of prevalence of OA at other joints is likely to follow the secular trend of prevalence of OA at the knee and hip, for which data are available for more countries and regions. In addition, such a trend is also consistent with the prevalence of several important risk factors for OA, such as aging and overweight/obesity. With these considerations, the

gene picture of OA prevalence over time, including for OA at other joints, should be robust.

Author disclosures are available at <https://onlinelibrary.wiley.com/action/downloadSupplement?doi=10.1002/art.42134&file=art42134-sup-0001-Disclosureform.pdf>.

Huibin Long, MD 
 Ai Guo, MD
 Beijing Friendship Hospital
 Capital Medical University
 Beijing, China
 Yuqing Zhang, DSc 
 Massachusetts General Hospital
 Harvard Medical School
 Boston, MA
 Qiang Liu, MD 
 Jianhao Lin, MD 
linjianhao@pkuph.edu.cn
 Peking University People's Hospital
 Peking University
 Beijing, China

1. Global Burden of Disease Collaborative Network. Global Burden of Disease Study 2019 (GBD 2019) Results. Institute for Health Metrics and Evaluation. URL: <http://ghdx.healthdata.org/gbd-results-tool>.
2. Global Burden of Disease Collaborative Network. Global Burden of Disease Study 2019 (GBD 2019) Data Input Sources Tool. Institute for Health Metrics and Evaluation. URL: <http://ghdx.healthdata.org/gbd-2019/data-input-sources>.

DOI 10.1002/art.42135

Report of the American College of Rheumatology Fellows-in-Training Subcommittee: experiences of rheumatology fellows early in the COVID-19 pandemic

To the Editor:

With the rapid spread of COVID-19, rheumatology trainees have faced challenges and uncertainties. Many fellowship programs were forced to rapidly implement innovative methods to educate trainees on COVID-19 while also attempting to safely maintain high-quality patient care during the pandemic (1). How COVID-19 and these changes impacted trainees' well-being and education remain unclear.

To understand how fellowship programs were addressing the training of adult and pediatric rheumatology fellows during the early period of the COVID-19 pandemic, the American College of Rheumatology (ACR) Fellows-in-Training (FIT) Subcommittee members created an anonymous electronic survey. The survey was distributed to adult and pediatric rheumatology fellows via email on June 2, 2020 and closed on June 8, 2020. The rapid distribution and closing of the survey resulted in a snapshot of

how COVID-19 initially impacted fellowship education, as well as topics of discussion for fellow townhalls and ACR sessions. The survey questions assessed how the pandemic affected 3 key areas: learning, patient care, and trainee resiliency. All questions were asked in multiple-choice format, allowing respondents to select all the answer options that apply except for the questions on coping mechanisms and topics for town hall discussion, which were open-ended questions. Return of the survey indicated participant consent.

Of 722 surveys distributed, 132 US rheumatology fellows (18.2%) completed the survey (45% in year 1, 43.6% in year 2, and 9.4% in year 3 of fellowship training). Table 1 shows areas of concern related to the early impact of COVID-19 as reported by rheumatology fellows, with the most common being education, physical health and safety as a clinician, and rheumatology job market. For education, 51.2% of respondents reported that the

Table 1. Areas of concern, effect on fellow education, and format of fellow clinics during the early COVID-19 pandemic period as reported by survey respondents*

	Selected response, % of respondents (n = 132)
Areas of concern	
Education	72.6
Physical health and safety as a clinician	71.8
Impact on the rheumatology job market	69.2
Potential changes to how rheumatologists will practice medicine in the future (telemedicine)	64.1
Emotional health	50.4
Ability to complete research project(s)	48.7
Potential changes to fellowship next year	43.5
Financial stress	22.2
Lack of childcare	18.8
Ethical dilemmas	18.8
Effect on fellow education	
Receiving clinical experience and education entirely through virtual platforms	51.2
Previously used virtual platforms, but resumed in-person training	35.9
No interruption on fellowship responsibilities	13.6
Rheumatology training on hold and currently providing care for patients with COVID-19	4.2
Format of fellow clinics	
Mix of both in-person and virtual	53.8
Completely virtual	37.6
Completely in-person	8.6

* Respondents were adult and pediatric rheumatology fellows who participated in a survey developed by the American College of Rheumatology Fellows-in-Training Subcommittee, which was opened on June 2, 2020 and closed on June 8, 2020.

in-person didactics became completely virtual, and 91.4% of respondents reported that their clinics were changed to telemedicine or a hybrid of telemedicine and in-person.

The most commonly reported coping mechanisms among respondents were exercise, family and colleague support, and reading. For virtual town hall topics, respondents most commonly suggested discussions on how the pandemic is affecting the rheumatology job market with specific concerns on hiring freezes, virtual job interviews, and salary negotiation. The next most requested topic was optimization of telemedicine appointments (i.e., conducting virtual physical examinations, ensuring thorough evaluation, and enhancing the telehealth visit experience for both patients and physicians).

To our knowledge, this is one of the first national reports focusing on experiences of rheumatology fellows early during the COVID-19 pandemic. The survey showed that training of the majority of fellows was interrupted by the pandemic and that main concerns of rheumatology fellows-in-training centered on education and physical health. These results have the potential to meaningfully impact the fellowship training environments by addressing these FIT-specific needs and concerns.

Our survey has several limitations. First, because the response rate was 18.2% and only US fellowship programs were included, findings may not reflect the experience of trainees at large. Next, our results captured the experiences of fellows-in-training during the early stages of the pandemic with a potential response bias. Thus, the survey may not fully reflect the current experiences of all trainees.

Based on the survey results of the early impact of COVID-19, future fellowship programs should maximize their resources to address the education and physical safety concerns of fellows-

in-training. As there was a mixed impact of COVID-19 on fellow education and clinical responsibilities, program leadership can use the fellow concerns to guide and individualize rheumatology didactics and clinics to maximize learning opportunities for fellows. With the uncertainty of respondents on rheumatology practice and hiring of rheumatologists, programs and conferences should have sessions that specifically address best telemedicine practices and job searching during a pandemic. Follow-up studies are crucial to better understand the evolving needs of the rheumatology fellows during these unprecedented times.

Dr. Lin's work (award T32-AR-007611-13) was supported by the National Institute of Arthritis and Musculoskeletal and Skin Diseases. Author disclosures are available at <https://onlinelibrary.wiley.com/action/downloadSupplement?doi=10.1002%2Fart.42135&file=art42135-sup-0001-Disclosureform.pdf>.

ACR Fellows-in-Training Subcommittee

Didem Saygin, MD 

didem.Saygin@uchospitals.edu

University of Chicago

Jean Lin, MD, PhD

Northwestern University

Chicago, IL

Noelle A. Rolle, MD

Piedmont Columbus Regional

Columbus, GA

Mary Mamut, DO

Mercy Clinic

Edmond, OK

1. Lockwood MM, Wallwork RS, Lima K, Dua AB, Seo P, Bolster MB. Telemedicine in adult rheumatology: in practice and in training. *Arthritis Care Res (Hoboken)* 2021. doi: <https://doi.org/10.1002/acr.24569>. E-pub ahead of print.